UNIVERSITI SAINS MALAYSIA

Laporan Akhir Projek Penyelidikan Jangka Pendek

Elucidation or Liquid-Solid Phenomena Involving Immiscible reactants During Porous Solid Acid-Catalyzed Oleochemical Reaction Assisted by Ultrasonic Energy

by
Prof. Dr. Ahmad Zuhairi Abdullah
Assoc. Prof. Dr. Tan Soon Huat
Assoc. Prof. Dr. Vel Murugan Vadivellu

2015

Project Code :
(for RCMO use only)

UNIVERSITI SAINS MALAYSIA

RU GRANT FINAL REPORT FORM

Please email a softcopy of this report to rcmo@usm.my

A PROJECT DETAILS

i	**Title of Research:** **Elucidation of liquid-solid phenomena involving immiscible reactants during porous solid acid-catalyzed oleochemical reaction assisted by ultrasonic energy**
ii	**Account Number:** **1001/PJKIMIA/814144**
iii	**Name of Research Leader:** **Prof Dr Ahmad Zuhairi Abdullah**
iv	**Name of Co-Researcher:** **1. Assoc Prof Dr Tan Soon Huat** **2. Assoc Prof Dr Vel Murugan Vadivellu**
v	**Duration of this research:** **a) Start Date : 15 February 2012** **b) Completion Date : 14 February 2015** **c) Duration : 36 months** **d) Revised Date (*if any*) : 14 August 2015**

B ABSTRACT OF RESEARCH

(An abstract of between 100 and 200 words must be prepared in Bahasa Malaysia and in English. This abstract will be included in the Report of the Research and Innovation Section at a later date as a means of presenting the project findings of the researcher/s to the University and the community at large)

Abstract

Biodiesel is produced through transesterification reaction between vegetable oil or animal fats and alcohol and it faces various problems related to the immiscible nature of the reactants causing poor mass transfer rate. Ultrasonic energy can emulsify the reactants to reduce the catalyst requirement, reaction time and reaction temperature. Ultrasonic energy also neglects the limitations in the use certain feed stocks. Transesterification of crude Jatropha oil in presence of tungstophosphoric acid (TPA) supported on activated carbon (AC) using ultrasound-assisted process was investigated. The generated catalysts were characterized for physical and chemical properties to examine the effects of different TPA loadings (15 %, 20 %, 25 % w/w). The catalysts were then used in the transesterification of Jatropha oil with high free fatty acid content. The catalyst with 20 % TPA loading achieved the best methyl ester yield, achieving 87.33 % in just 40 min. The quality of the feed stock was varied by increasing the water content and FFA content to test the tolerance of

the catalysts towards these parameters separately. The catalyst showed good water tolerance to a limit of 1 % w/w and proven to be insensitive to the increment of FFA in the feed stock. The catalyst was also investigated for possible reusability and TPA leaching under ultrasonic conditions. Four reaction variables including reaction time (10-50 min), reaction molar ratio (5:1-25:1), ultrasonic amplitude (30-90 %) and catalyst amount (2.5-4.5 w/w oil) were next chosen and optimized to generate thorough understanding on the behavior of the system under ultrasonic conditions. Mathematical representation for the biodiesel yield was successfully generated. The maximum reaction yield was about 91 % under the optimum conditions. Moderate ultrasonic amplitude (~60 %) under molar ratio (25:1) with moderate reaction temperature (65 °C) led to short reaction time (~ 40 min). The achieved results were great enhancements in terms of reaction time and temperature compared to conventional process. The significance of the model and the interaction between the reaction variables were validated statistically. The experimental data collected from the central composite design were also used to establish artificial neural network (ANN) model in order to predict the response in the reaction. The models were also optimized to identify the suitable network topology and training method. The results obtained from ANN models were compared with the results of the regression analysis and good agreement was obtained to suggest the good potential of ANN in the FAME yield prediction. Ultrasound-assisted transesterification of waste cooking oil catalyzed by hydrotalcite (HT) catalyst prepared using combustion method was also studied. Two important parameters in the HT synthesis i.e.,calcination temperature (550–850◦C) and fuel type (saccharose, glucose and fructose) were particularly investigated. The HT catalyst pre-pared using saccharose and calcined at 650◦C was the best catalyst to be used in the transesterification reaction. It showed high biodiesel yield (about 76.45%) in just 60 min in the presence of low ultrasound amplitude (~11 kHz). The enhancement effect of ultrasound was successfully demonstrated. The reac-tion only needed short reaction time (about 1 h) to give a biodiesel yield of up to 76.45% compared to conventional stirring method that needed about 5 h to achieve the same yield.

Abstrak

Biodiesel dihasilkan melalui tindakbalas transesterifikasi antara minyak sayuran atau lemak haiwan dan alkohol dan ia menghadapi pelbagai masalah yang berkaitan dengan sifat tak boleh campur bahan tindak balas menyebabkan kadar pemindahan jisim rendah. Tenaga ultrabunyi boleh mengemulsikan lemak bahan tindak balas untuk mengurangkan keperluan pemangkin, masa tindak balas dan suhu tindak balas. Tenaga ultrasonik juga mampu mengatasi penggunaan stok suapan tertentu yang terhad. Transesterifikasi minyak Jatropha mentah dalam kehadiran asid tungstophosphorik (TPA) disokong pada karbon diaktifkan (AC) menggunakan proses berbantukan ultrabunyi telah disiasat. Pemangkin dihasilkan telah dicirikan bagi sifat-sifat fizikal dan kimia untuk mengkaji kesan beban TPA yang berbeza (15%, 20%, 25% w / w). Mangkin kemudiannya digunakan dalam transesterifikasi minyak Jatropha dengan kandungan asid lemak bebas yang tinggi. Mangkin dengan 20% bebanan TPA mencapai hasil metil ester terbaik iaitu 87,33% dalam masa 40 min. Kualiti stok suapan diubah dengan meningkatkan kandungan air dan kandungan FFA untuk menguji toleransi satu mangkin terhadap parameter ini secara berasingan. Mangkin itu menunjukkan toleransi terhadap air yang baik kepada terhad kepada 1% w / w dan terbukti tidak sensitif kepada kenaikan FFA dalam stok suapan. Mangkin itu turut disiasat untuk kebolehan gunasemula dan TPA larut lesap di bawah keadaan ultrabunyi. Empat pembolehubah tindakbalas termasuk masa tindak balas (10-50 min), nisbah molar (5: 1-25: 1), amplitud ultrabunyi (30-90%) dan jumlah mangkin (2,5-4,5 w / w minyak) telah dipilih dan dioptimumkan. Perwakilan matematik untuk hasil biodiesel yang telah berjaya dihasilkan. Hasil tindak balas maksimum adalah kira-kira 91% di bawah keadaan optimum. Amplitud sederhana ultrabunyi (~ 60%) di bawah nisbah molar (25: 1) dengan suhu tindak balas sederhana (65 °C) membawa kepada masa tindak balas yang singkat (~ 40 min). Keputusan ini adalah peningkatan yang besar dari segi masa tindak balas dan suhu berbanding proses konvensional. Kepentingan model dan interaksi di antara pembolehubah tindakbalas telah disahkan secara statistik. Data eksperimen yang dikumpul daripada reka bentuk komposit pusat juga telah digunakan untuk mewujudkan model tiruan rangkaian neural (ANN) untuk meramalkan tindak balas dalam tindak balas. Model ini juga dioptimumkan untuk mengenal pasti topologi rangkaian dan kaedah latihan yang sesuai. Keputusan yang diperolehi daripada model ANN dibandingkan dengan keputusan analisis regresi dan persetujuan yang baik telah diperolehi untuk mencadangkan potensi baik ANN dalam ramalan hasil biodiesel. Transesterification berbantukan ultrabunyi sisa minyak masak bermangkinkan hidrotalsit (HT) pemangkin disediakan dengan menggunakan kaedah pembakaran juga dikaji. Dua parameter penting dalam HT sintesis iaitu suhu pengkalsinan (550-850°C) dan jenis bahan api (sakarosa, glukosa dan fruktosa) telah disiasat. Pemangkin HT yang disediakan menggunakan sakarosa dan kalsin pada 650◦C merupakan yang terbaik untuk digunakan dalam tindak balas transesterification itu. Ia menunjukkan hasil biodiesel tinggi (kira-kira 76.45%) hanya dalam masa 60 min di hadapan amplitud ultrabunyi yang rendah (~ 11 kHz). Kesan peningkatan ultrabunyi telah berjaya ditunjukkan. Masa tindak balas yang pendek (kira-kira 1 h) diperlukan untuk memberikan hasil biodiesel sehingga 76.45% berbanding kaedah pengadukan konvensional yang memerlukan kira-kira 5 h untuk mencapai hasil yang sama.

ii **Research Output**

a) Publications in ISI Web of Science/Scopus

No.	Publication (authors,title,journal,year,volume,pages,etc.)	Status of Publication (published/accepted/ under review)
1	Muhammad Ayoub and Ahmad Zuhairi Abdullah (2012). Critical review on the current scenario and significance of crude glycerol resulting from biodiesel industry towards more sustainable renewable energy industry, *Renewable & Sustainable Energy Reviews,* 16, 2671-2686. (Publisher: Elseview).	Published
2	Ali Sabri Badday, Ahmad Zuhairi Abdullah, Muataz S. Khayoon, Keat-Teong Lee (2012). Intensification of biodiesel production via ultrasonic-assisted process: A critical review on fundamentals and recent development, *Renewable & Sustainable Energy Reviews,* 16, 4574-4587. (Publisher: Elseview).	Published
3	Ali Sabri Badday, Ahmad Zuhairi Abdullah, Keat-Teong Lee (2014). Transesterification of crude Jatropha oil by activated carbon-supported heteropolyacid catalyst in an ultrasound-assisted reactor system, *Renewable Energy,* 62, 10-17. (Publisher: Elseview).	Published
4	Ali Sabri Badday, Ahmad Zuhairi Abdullah, Keat-Teong Lee (2013). Optimization of biodiesel production process from Jatropha oil using supported heteropolyacid catalyst and assisted by ultrasonic energy, *Renewable Energy,* 50, 427-432. (Publisher: Elseview).	Published
5	Ali Sabri Badday, Ahmad Zuhairi Abdullah, Keat Teong Lee (2013). Ultrasound-assisted transesterification of crude Jatropha oil using cesium doped heteropolyacid catalyst: Interactions between process variables,. *Energy* 60, 283-291. (Publisher: Elseview).	Published
6	Ali Sabri Badday, Ahmad Zuhairi Abdullah, Keat-Teong Lee (2014). Artificial neural network approach for modeling of ultrasound-assisted transesterification process of crude Jatropha oil catalyzed by heteropolyacid based catalyst, *Chemical Engineering & Processing: Process Intensification,* 75, 31-37. (Publisher: Elseview).	Published
7	Ali Sabri Badday, Ahmad Zuhairi Abdullah, Keat Teong Lee (2012). Ultrasound-assisted transesterification of crude Jatropha oil using alumina-supported heteropolyacid catalyst, *Applied Energy,* 105, 380-388. (Publisher: Elseview).	Published
8	Mohd Hizami Mohd Yusoff, Ahmad Zuhairi Abdullah, Shazia Sultana, Mushtaq Ahmad (2013). Prospects and current status of B5 biodiesel implementation in Malaysia, *Energy Policy*, 62, 456-462. (Publisher: Elseview).	Published
9	Mohd Razealy Anuar, Ahmad Zuhairi Abdullah (2016). Ultrasound-assisted biodiesel production from waste cooking oil using hydrotalcite prepared by combustion method as catalyst, *Applied Catalysis A: General*, 514, 214-223. (Publisher: Elseview).	Published
10	Zahra Gholami, Ahmad Zuhairi Abdullah, Keat Teong Lee (2015). Catalytic etherification of glycerol to diglycerol over heterogeneous calcium-based mixed oxide catalyst: Reusability and stability, *Chemical Engineering Communications*, 202, 1397-1405. (Publisher: Taylor & Francis).	Published

11	Hamed Mootabadi, Ahmad Zuhairi Abdullah (2015). Response surface methodology for simulation of ultrasonic-assisted biodiesel production catalyze by SrO/Al_2O_3 catalyst, *Energy Sources, Part A: Recovery, Utilization, and Environmental Effects* 37, 1747-1755. (Publisher: Taylor & Francis).	Published

b) Publications in Other Journals

No.	**Publication** (authors,title,journal,year,volume,pages,etc.)	**Status of Publication** (published/accepted/ under review)

c) Other Publications
(book,chapters in book,monograph,magazine,etc.)

No.	**Publication** (authors,title,journal,year,volume,pages,etc.)	**Status of Publication** (published/accepted/ under review)
1	Ali Sabri Badday, Ahmad Zuhairi Abdullah, Keat Teong Lee (2013). Application of heteropolyacid-based heterogeneous catalysts for conversion of oleochemical into renewable fuels and other value-added products, Rajesh J. Tayade and Ajay Bansal (Editors), *Engineering Applications of Nanoscience and Nanomaterials*, vol. 757, pp. 1-24. (Trans Tech Publications, Switzerland).	Published

d) Conference Proceeding

No.	**Conference** (conference name,date,place)	**Title of Abstract/Article**	**Level** (International/National)

 # Please attach a full copy of the publication/proceeding listed above

iii **Other Research Ouput/Impact From This Project**
(patent, products, awards, copyright, external grant, networking, etc.)

1. 1 Post-doctoral Fellow, **Dr Shazia Sultana** from Quaid-i-Azam University, Pakistan.
2. Networking with Quaid-i-Azam University researchers, Pakistan with a number of research papers co-published subsequently.

   i. **Shazia Sultana**, Aneela Khalid, Mushtaq Ahmad, Ahmad Zuhairi Abdullah, Lee Keat Teong, Muhammad Zafar, Fayyaz ul Hassan (2014). Production, optimization and characterization of biodiesel from a novel source: Sinapis alba L, *International Journal of Green Energy*, 11, 280-291. (Publisher: Taylor & Francis).
   ii. Kifayat Ullah, Mushtaq Ahmad, **Shazia Sultana**, Lee Keat Teong, Vinod Kumar Sharma, Ahmad Zuhairi Abdullah, Muhammad Zafar, Zahid Ullah (2014). Experimental analysis of di-functional magnetic oxide catalyst and its performance in the hemp plant biodiesel production, *Applied Energy*, 113, 660-669. (Publisher: Elsevier).

iii. Mushtaq Ahmad, Lee Keat Teong, **Shazia Sultana**, Inam Ullah Khan, Ahmad Zuhairi Abdullah, Muhammad Zafar & Fayyaz -ul Hassan (2015). Optimization of biodiesel production from Carthamus tinctorius L. cv. Thori 78: A novel cultivar of safflower crop, *International Journal of Green Energy*, 12, 447-452. (Publisher: Taylor & Francis).

iv. Haleema Sadia, Mushtaq Ahmad, **Shazia Sultana**, Ahmad Zuhairi Abdullah, Lee Keat Teong, Muhammad Zafar (2014). Nutrient and mineral assessment of edible wild fig and mulberry fruits, *Fruits*, 69 (2), 1-8. (Publisher: Cambridge University Press, UK).

v. Mushtaq Ahmad, **Shazia Sultana**, Lee Keat Teong, Ahmad Zuhairi Abdullah, Haleema Sadia, Muhammad Zafar, Taibi ben Hadda, Muhammad Aqeel Ashraf & Rasool Bakhsh Tareen (2015). Distaff thistle oil: A possible new non-edible feedstock for bioenergy, *International Journal of Green Energy*, 12, 1066-1075. (Publisher: Taylor & Francis).

3. A Trans-Disiplinary Research Grant Scheme (TRGS 203/PJKIMIA/6762001) from the Ministry of Higher Education (Fasa 2/2014). Program Title: Production of valuable chemicals from crude glycerol using catalytic and biochemical methods. Project Title: Mesoporous composite catalyst for conversion of purified crude glycerol to lactic acid. 1 February 2015-31 January 2018.

E HUMAN CAPITAL DEVELOPMENT

a) Graduated Human Capital

Student	Nationality (No.)		Name
	National	International	
PhD	1	1	1. Ali Sabry Badday (Completed in 2013) 2. Mohd Razealy Anuar (Thesis submitted in May 2016)
MSc			1. 2.
Undergraduate			1. 2.

b) On-going Human Capital

Student	Nationality (No.)		Name
	National	International	
PhD	-	-	1. 2.
MSc	-	-	1. 2.
Undergraduate	-	-	1. 2.

c) Others Human Capital

Student	Nationality (No.)		Name
	National	International	
Post Doctoral Fellow		1	1. Dr Shazia Sultana 2.
Research Officer			1. 2.
Research Assistant	4	1	1. Nur Fatin Amalina Muhammad Sanusi 2. Helmi Amanullah

				3. Khozema Ahmed Ali 4. Nur Azimah Jamaluddin 5. Zahra Gholami (Iranian)
	Others (.....)			1. 2.

F	COMPREHENSIVE TECHNICAL REPORT
	Applicants are required to prepare a comprehensive technical report explaining the project. The following format should be used (this report must be attached separately): • Introduction • Objectives • Methods • Results • Discussion • Conclusion and Suggestion • Acknowledgements • References (Please see the attached comprehensive technical report)

G	PROBLEMS/CONSTRAINTS/CHALLENGES IF ANY
	(Please provide issues arising from the project and how they were resolved) 1. The ultrasonic processor was sent for repair for few months in 2013 to cause some delay in research work.

H	RECOMMENDATION
	(Please provide recommendations that can be used to improve the delivery of information, grant management, guidelines and policy, etc.) i. To continue with a single line budget policy for internal grants. ii. To encourage inclusion of external researcher in the proposal iii. Successful projects should receive higher priority to secure next grant for continuation of the work.

Project Leader's Signature:

.....

Name : Prof Ahmad Zuhairi Abdullah

Date : 30 June 2016

PROFESSOR DR AHMAD ZUHAIRI ABDULLAH
School of Chemical Engineering,
Universiti Sains Malaysia, Engineering Campus,
Nibong Tebal, Penang, Malaysia.

1.	**COMMENTS, IF ANY/ENDORSEMENT BY PTJ'S RESEARCH COMMITTEE**

Excellent output in terms of publications.

HQD - 2 Students.

18/2/16

Signature and Stamp of Chairperson of PTJ's Evaluation Committee

Name : PROFESOR AZLINA HARUN @ KAMARUDDIN
Dekan
Pusat Pengajian Kejuruteraan Kimia
Kampus Kejuruteraan
Date : Universiti Sains Malaysia, Seri Ampangan
14300 Nibong Tebal, Seberang Perai Selatan
Pulau Pinang.

18/2/16

Signature and Stamp of Dean/ Director of PTJ

Name : PROFESOR AZLINA HARUN @ KAMARUDDIN
Dekan
Pusat Pengajian Kejuruteraan Kimia
Kampus Kejuruteraan
Date : Universiti Sains Malaysia, Seri Ampangan
14300 Nibong Tebal, Seberang Perai Selatan
Pulau Pinang.

UNIVERSITI SAINS MALAYSIA

RU GRANT
FINAL REPORT CHECKLIST

Please use this checklist to self-assess your report before submitting to RCMO.
Checklist should accompany the report.

NO.	ITEM	PLEASE CHECK (✓)		
		PI	JKPTJ	RCMO
1	Completed Final Report Form	√		✓
2	Project Financial Account Statement (e-Statement)	√		✓
3	Asset/Inventory Return Form *(Borang Penyerahan Aset/Inventori)*	√		✓
4	A copy of the publications/proceedings listed in Section D(ii) (Research Output)	√		✓
5	Comprehensive Technical Report	√		✓
6	Other supporting documents, if any	√		
7	Project Leader's Signature	√		✓
8	Endorsement of PTJ's Evaluation Committee	√		✓
9	Endorsement of Dean/ Director of PTJ's	√		✓

Appendix 1

UNIVERSITI SAINS MALAYSIA

BORANG PENYERAHAN ASET / INVENTORI

==========

A. BUTIR PENYELIDIK

1. NAMA PENYELIDIK :PROF DR AHMAD ZUHAIRI ABDULLAH
2. NO STAF :0424/14
3. PTJ :PP KEJURUTERAAN KIMIA
4. KOD PROJEK :1001/PJKIMIA/814144
5. TARIKH TAMAT PENYELIDIKAN :14 OGOS 2015

B. MAKLUMAT ASET / INVENTORI

BIL	KETERANGAN ASET	NO HARTA	NO. SIRI	HARGA (RM)
1	Digital ultrasonic processor set – rosak tiada bateri.	3AK00006361PJKIMIA	DBV-120434034	19,918
2	pH meter – rosak - ada dicas	3AK00006362 PJKIMIA	11460880	3,750
3	Scanspeed 416 centrifuge – elok - tak siap.	3AK00006373PJKIMIA	G122511040208	7,990
4				

C. PERAKUAN PENYERAHAN

Saya dengan ini menyerahkan aset/ inventori seperti butiran B di atas kepada pihak Universiti:

PROFESSOR DR AHMAD ZUHAIRI ABDULLAH
School of Chemical Engineering,
Universiti Sains Malaysia, Engineering Campus,
Nibong Tebal, Penang, Malaysia

Tarikh: 20/06/2016

D. PERAKUAN PENERIMAAN

Saya telah memeriksa dan menyemak setiap alatan dan didapati :

☑ Lengkap
☑ Rosak - Lupus
☐ Hilang : Nyatakan.....
☐ Lain-lain : Nyatakan .....

Diperakukan Oleh :

.....
Tandatangan
Pegawai Aset PTJ

Nama : MOHD YUSOF BIN ISMAIL
Penolong Jurutera
Pusat Pengajian Kejuruteraan Kimia
Kampus Kejuruteraan
Universiti Sains Malaysia
Tarikh : 13/7/2016

***Nota :** Sesalinan borang yang telah lengkap perlulah dikemukakan kepada Unit Pengurusan Harta, Jabatan Bendahari dan Pejabat RCMO untuk tujuan rekod.

Purchase Requisition | Purchase Order | Suppliers | Maintenance | Financials | Coda Info | Reports | Admin

UserCode: NORMIE / USMKCTLIVE / PJKIMIA | Program Code: Votebook9100 | Current Program : Votebook (Header)

Current Date : 24/06/2016 4:32:02 PM | Version: 15.124, Last Updated at 10/06/2016 | DB: 13.00, 9/18/2010 VB: 13.01, 3/14/2011 | Switch Language : English /Malay

Wildcard : eg. Like 100%, Like 10%1, Like %1

Element 1: % Element 2: % Element 4: PJKIMIA

Element 5: 814144 Year: 2016 Search Export to Excel

Detail	Excel	Budget Rule	Budget Control	Account Description	Budget Account Code	Roll over	Budget	Cash Received	Advanced	Commit	Actual	Available	Percentage
Detail	Excel	46	T	Projek Kumpulan Wang Uni Penyelidikan	1001.111.0.PJKIMIA.814144	15,313.26	0.00	0.00	0.00	0.00	0.00	15,313.26	0.00%
		46	T	SubTotal		15,313.26	0.00	0.00	0.00	0.00	0.00	15,313.26	0.00%
Detail	Excel	47	T	Projek Kumpulan Wang Uni Penyelidikan	1001.221.0.PJKIMIA.814144	11,244.20	0.00	0.00	0.00	0.00	0.00	11,244.20	0.00%
Detail	Excel	47	T	Projek Kumpulan Wang Uni Penyelidikan	1001.224.0.PJKIMIA.814144	-4,679.25	0.00	0.00	0.00	0.00	0.00	-4,679.25	0.00%
Detail	Excel	47	T	Projek Kumpulan Wang Uni Penyelidikan	1001.227.0.PJKIMIA.814144	-769.44	0.00	0.00	0.00	3,196.00	0.00	-3,965.44	0.00%
Detail	Excel	47	T	Projek Kumpulan Wang Uni Penyelidikan	1001.228.0.PJKIMIA.814144	-1,840.00	0.00	0.00	0.00	0.00	0.00	-1,840.00	0.00%
Detail	Excel	47	T	Projek Kumpulan Wang Uni Penyelidikan	1001.229.0.PJKIMIA.814144	-12,662.91	0.00	0.00	0.00	1,000.00	1,850.00	-15,512.91	0.00%
		47	T	SubTotal		-8,707.40	0.00	0.00	0.00	4,196.00	1,850.00	-14,753.40	0.00%
Detail	Excel	48	T	Projek Kumpulan Wang Uni Penyelidikan	1001.335.0.PJKIMIA.814144	842.00	0.00	0.00	0.00	0.00	0.00	842.00	0.00%
		48	T	SubTotal		842.00	0.00	0.00	0.00	0.00	0.00	842.00	0.00%
Detail	Excel	50	T	Projek Kumpulan Wang Uni Penyelidikan	1001.552.0.PJKIMIA.814144	-37.63	0.00	0.00	0.00	0.00	0.00	-37.63	0.00%
		50	T	SubTotal		-37.63	0.00	0.00	0.00	0.00	0.00	-37.63	0.00%
		9999		GrandTotal		7,410.23	0.00	0.00	0.00	4,196.00	1,850.00	1,364.23	0.00%

COMPREHENSIVE TECHNICAL REPORT

1. Introduction

1.1 General overview

Oleochemicals are of significant substances for various industrial applications such as in food, pharmaceutical, cosmetics as well as fuel industries [1-3]. As Malaysia is one of the leading players in palm oil production in the world, investigation of oleochemicals will significant towards the development and sustainability of its oil palm industry [4]. In a very recent application, vegetable oils are converted through transesterification process to fatty acid methyl esters that can be used as an alternative fuel beside other applications [5]. Due to its significance and nature of reaction which is commont to some other oleochemical reactions, transesterification reaction is selected to be the model reaction in this research work.

The transformation of vegetable oil or animal fats into fatty acid methyl esters by transesterification is among chemical reactions that draw interest of many researchers [6-9]. Special interest is focused on the production technique while the other interest is for the catalyst that involved in the reaction [5]. Transesterification is the organic reaction of exchanging the organic group of an ester with the organic group of an alcohol producing mixture of fatty acids esters and glycerol as the main co-product. This reaction is commonly catalyzed by acid catalyst, base catalyst or by enzymatic catalyst (biocatalysts) especially lipases [10]. Oleochemical reactions of this type often suffer from the main drawback of immicibility between the reactants to result in low mass transfer leading to low reaction rate. Current trend in this catalysis is to replace homogeneous with heteroggeneous (solid) catalyst. In this respect, base catalysts are more active. However, due to limition involving the side reaction to form soap when oils with high content of free fatty acid (FFA), base catalysts should be replaced with acid catalysts. This reaction and other similar oleochemical reactions will be more economically interesting if the reaction rate can be accelerated.

Ultrasonic technology is new, attractive and effective procedure to solve the problems that are related to immiscibility between reactants. The use of ultrasonic irradiation can enhance mass transfer rate between the immiscible reactants due to larger superficial area between them. As a result, the reaction rate will be significantly accelerated so that high reactant conversion can be achieved in shorter time. Ultrasonic technology has been invested in wide range of chemical processes causing significant reduction in reaction time and improvement in production yield [11]. However, this research area is still at immature state and fundamental understandings on topics related to it is yet to be established.

Oleochemical reactions assisted by ultrasonic energy provides vast potential as various phenomena can be examined. Unfortunately, the ultrasonic-assisted acid catalytic process for the transesterification reaction of vegetable oil is an immature research area and no report is available so far in the literature. Despite some interesting demonstrations made on the

application of homogenous acid catalysts for this reaction [12, 13], the satisfactory address on the fundamental aspects of the heterogeneous catalytic process under ultrasonc field is yet to be made. In this regards, the roles and behaviors of different active (acid) sites of varying strengths in the course of reaction of oil transesterification reaction under ultrasonication are largely unknown[14].

Thus, this work aims at the elucidation of these aspects of the ultrasonic-assisted solid acid catalyzed reaction so that recommendations on the most suitable catalyst system and experimental operation conditions to strategize future research works in the area of oleochemical reactions can be made.

1.2 Application of ultrasound

Ultrasound (US) is simply sound pitched above human hearing ability, usually above 20 kHz. It has plenty of application in our daily life [15]. The use of ultrasound as a source of energy is common these days and recently it is used to provide large assistant to great number of industries. The frequencies beyond 20 kHz till 100 kHz are used in industries but the range of industrial frequencies can be extended to 2 MHz according to the required power [16]. In the recent years, ultrasonic irradiation attracted the researchers to be applied in many areas such as manufacturing of nanostructured materials [16, 17], food industry [18-20] sonodynamic therapy [21-23], processing of biomass [24, 25] and sonochemical degradation of pollutants materials and hazardous chemicals [26-28].

A low frequency ultrasonic-assisted system can be used to produce emulsions from immiscible liquids [29-31]. Since the reactants of oleochemical reactions such as the transesterification reaction are immiscible, ultrasonication could be beneficial for for the acceleration of the reaction rate [32]. Intensification of oleochemical reactions through the application of ultrasonic energy would mean a significant reduction in reaction time, catalyst amount, energy input and elimination of reaction pathways leading to undesired products [33]. Early sucess has been demonstrated [28, 29] but thorought understanding and elucidation of important phenomena during such reaction is now targeted using transesterification process as a model oleochemical reaction.

1.3 Problem Statement

In many oleochemical reactions such as transesterification of triglycerides with alcohols, serious problems and limitations can be noticed and identified. First of all, it is due to the immiscible nature of the reactants involved coupled with the variation in viscosity and density. These are the main reasons for the low contact between the reactants. They resul in poor mass transfer rate, reduction in reaction rate and increasing reaction time [11]. The reaction between two immiscible fluids makes it look like heterogeneous transport phenomenon (heat, mass and fluid) that caused by the lag in the film between them. The mass transefer could be accelerated by applying ultrasonic energy on the reaction mixture to create cavitations phenomena that is

generated by ultrasonic power. These cavitations cause an emulsification between the reactants as well as a local increase in temperature near the boundary layer between the reactants. This increment leads to modify the reaction of transesterfication that cancels the requirement of heating in the production process. On the other hand, the formation of micro jets inside the fluids eliminates the need of mechanical agitation [34]. Early succees in accelerating the reaction rate has been demonstrated [28, 29]. However, for the purpose of manipulating the positive effects of ultrasonication, fundamental understanding on important phenomena occuring during the reaction is indispensable.

The transesterification of triglicerides to methyl esters can be done in two ways, with or without catalyst. The catalyzed reaction can be divided into homogenous and heterogeneous reactions. Homogenous base catalyst recorded high yield [35, 36]. The drawback of using this type of catalyst is the limitation towards the use of many oil feed stocks because of its sensitivity to the presence of free fatty acids. Amounts of FFA larger than 1% wt can react with the catalyst consuming it and forming soap [6]. The behaviors could be significantly different in the presenceof ultrasonic energy. Therefore, it is of interest to characterize and elucidate the behaviors during such reaction.

Investigations of homogenous acid catalysts showed that it have no sensitivity towards FFA but the reaction must maintained at high temperature and the yield of the methyl esters be low [37]. Besides that, acidic catalyst is corrosive and destructive to the reactors and other equipments involved in the process. Other significant disadvantage of homogenous catalyst is that the catalyst cannot be reutilized as it is consumed in the reaction [38]. Recently, heterogeneous catalysts that can promote the reaction with the same efficiency to homogenous catalysts has been investigated [39, 29]. This field seems to be attractive because the needs to reuse the catalyst after the reaction. Some phenomena including internal diffusion between the reactants, mechanism of reaction, reaction kinetics and the mode of catalyst deactivation under the ultrasonic irradiation mixing needs to be further investigated to assist a good scientific foundation for this field of catalysts.

The deactivation of the heterogeneous catalyst in the ultrasonic transesterification reaction is generally a scarcely reported area in the recent published works. In this liquid reaction, the properties of the reactant and the ultrasonic waves could post significant effect on the characteristics of the catalysts [40]. Shear forces by the liquid and the extreme mixing of the ultrasonic field are likely to break some catalyst particles leading to the formation of smaller particles so that the internal diffusion effects would be limited [41]. However, it will also affect the acid site distribution and a reduction in surface area to some catalysts [42]. These changes are likely to influence the catalytic activity and the course of the reaction.

Study on the fundamental aspects of the solid acid-catalyzed transesterification reaction in the presenceof ultrasonic irradiation is still scarce [33]. Most of the research works simply address the applied sides of the process without proper understanding on the fundamental aspects such as the nature and behavior of acid sites, internal diffusion limitation regime with various catalyst systems, reliable reaction mechanisms and the limiting steps as well as the mechanisms

leading to the deterioration of catalysts during the reaction and its consequent effects. These remaining problems are actually the motivation for our research team to investigate and innovate more on transesterification reaction. Ultimately, the findings in this work could of great contribution to the intensification of olechemical reactions of similar nature in the future.

1.4 Hypothesis and research questions

Different types and strength of acid sites would result in different catalytic behaviors in this reaction [33]. Therefore, it is of great interest to characterize the role of each type of acid site on the course of the reaction. In the first place, the types and strength of acid sites must be studied with the help of appropriate characterization methods before the catalytic activity in the reaction is investigated. In this respect, the distribution of acid sites, extent of chemisorption that occurs and reaction rate will provide some information on the correlations between the acidity and the catalytic behaviors.

To elucidate the roles of ultrasonic irradiation on the transesterification reaction, the selected catalysts will be tested under different reaction conditions to generate overall understandings on the important phenomena during the reaction. Studing of the parameters that related to the ultrasonic field such as ultrasonic power and ultrasonic exposure time is importent to eucidate the different roles of ultrasonic energy in accelerating the reaction while at the same time characterizing the liquid-solid-liquid phenomena involved.

The occurence of internal diffusion is governed by many factors such as the fluid conditions, reaction rate, size and shape of internal pores, reactant and product molecules etc. [38]. This phenomenon occurs in various conditions as the ultrasonic mixing would have effects on the rate of diffusion, rate of reaction, kinetic energy of the molecules and interaction between the the reactants [8]. The regions in which significant internal diffusion limitation occurs should be clearly identified as such a condition would result in erroneous and misleading results when an experiment on the catalytic activity is carried out. Different catalysts will catalyze the reaction following specific pathway leading to specific product distribution. Often, one particular product is desirable from the reaction and the intensification in its formation is needed [10]. Therefore, the reaction mechanism must be fully understood.

2. Objectives

i. To synthesize and fully characterized the properties of various supported heteropoly acid and sulfated metal catalysts for ultrasonic-assisted transesterification reaction between used vegetable/non-edible oil and methanol.

ii. To establish understanding on liquid phenomena and correlations between the characteristics of the catalyst used and the reaction fundamentals including mechanisms, diffusion phenomena and kinetics.

iii. To elucidate the interplay between reaction variables and the apparent reaction rate, system equilibrium, limiting reactant conversion and yield of fatty acid methyl esters.

iv. To establish understanding on dominant mechanisms leading to activity decay of the catalysts with the corresponding effects on the reaction phenomena.
v. To establish an intrinsic kinetic model to represent the behaviors of the reaction system for easy manipulation towards the desired effects in the reaction.

3. Methods

3.1 Reagents and materials

Tungstophosphoric acid ($H_3PW_{12}O_{40}$) active component, abbreviated as TPA in this work was purchased from Merck (Malaysia) while activated carbon (AC) support was purchased from Galcon Carbon Corporation (USA). Gamma alumina support were purchased from Merck (Malaysia). The AC was first ground to mean particle sizes between 250-500 μm. Crude Jatropha oil as the source of triglyceride in this study was supplied by Telaga Madu Resources (Malaysia). The properties of the crude Jatropha oil, FFA content and water content are given in Table 3.1. Methanol that was used in the transesterification reaction was supplied by Thermo Fisher Scientific Inc. (USA). Ethanol (for catalyst preparation) and n-hexane (for product analysis) were purchased from Merck (Malaysia). Meanwhile, reference fatty acid methyl ester (FAME) standards were supplied by NuChek Prep. Inc. (Australia).

Table 3.1. Properties of Jatropha oil used in this study.

Property	Value
Density (kg/m^3)	921
Viscosity (cSt)	38.12
Molecular weight	870
Water content (w %)	0.161
FFA content (w %)	10.5

2.2 Catalyst preparation

In order to prepare the supported catalyst, a pretreatment was first conducted by washing the support with 0.1 M NaOH solution, followed by the second treatment with 0.1 M HCl. They were performed to remove any soluble alkaline and acidic impurities from the AC [29]. The supported catalysts were prepared by dissolving the desired amounts of TPA in a mixture of deionized water and ethanol solution (50:50 v/v). Wet impregnation method was then adopted by contacting the support with the solution (4 ml/g support) for 72 h under constant shaking. Then, excess solution was removed by means of a rotary evaporator and the catalyst was subsequently washed excessively with deionized water followed by drying over night. The dry catalyst was then calcined at 453 K in air for 4 h [30].

The alumina based catalysts were synthesized by dissolving the desired amounts of TPA in (50:50 v/v) deionized water and ethanol solution. Wet impregnation method was adopted by contacting the support with the solution (4 ml/g support) for 20 h under constant stirring. Excess solution was then removed using a rotary evaporator and the catalyst was washed with deionized water followed by drying for 2 h. The dry catalysts were then calcined at 400 °C in an air flow for 4 h.

2.3 Catalyst characterization

The surface properties of AC and other catalysts were examined by means of a Micrometrics ASAP 2020 surface analyzer. FT-IR spectra of the supported TPA-AC catalysts were obtained using a Perkin-Elmer FTIR spectrophotometer. The surface morphology and TPA distribution over the carbon support was observed using an SEM unit (Oxford INCA/ENERGY-350) equipped with an energy dispersive X-ray analysis (EDAX) system. Surface acidity of the AC and the immobilized catalysts was determined using an acid-base titration [31].

2.4 Ultrasound-assisted transesterification process

The ultrasound-assisted transesterification process was conducted in a three-neck glass batch reactor placed in a water bath to maintain the reaction temperature. A condenser was attached to the reactor to contain the evaporated methanol and condense it back to the reaction vessel. Ultrasonication was achieved by means of an ultrasonic processor with a probe type transducer. The ultrasonic energy was supplied using a Branson (USA) ultrasonic processor capable of generating a frequency of 20 kHz with a highest power of 400 W.

Blank experimental runs were first carried out in the absence of catalyst or ultrasonic irradiation. The absence of catalyst was tested by providing ultrasonic irradiation at 75 % of the maximum power with a methanol/oil ratio of 20 for 60 min. The same conditions were used in the presence of activated carbon at a loading of 4 %. An experimental run under mechanical stirring was also performed under the same reaction conditions in the presence of catalyst.

In a typical experimental run, the desired amount of oil was transferred to the reactor and placed in the water bath until it reached the desired reaction temperature. Then, a required pre-heated amount of methanol was added to the oil at a molar ratio 20:1 followed by the desired amount of catalyst (4 % wt/wt oil). At this point, ultrasonification was started and the condenser attached to recover the evaporated methanol. Ultrasonic energy was supplied in a discrete pattern with 10 s on and 3 s off with the ultrasonic amplitude set at 75 % of the maximum power. After the desired reaction time (60 min), the reaction mixture was quenched and the excess methanol was distilled out. The reaction mixture was then separated into two layers by centrifugation at 3,000 rpm for 20 min. The upper FAME layer was then collected for GC analysis.

For studying the effect of reaction time, the same previous procedure was conducted at different time intervals between 30 min to 120 min. The effects of water content in Jatropha oil was studied by adding the desired amount of water to the oil at various weight ratios (1 %, 2 %, 3 %, 4 % w H_2O/w oil). Meanwhile, testing of FFA effects was conducted by adding the desired amounts of FFA to the Jatropha oil under heating and continuous stirring. For all experimental runs, the water bath temperature was fixed at about 56 ^{o}C. Due to heat energy that was also generated by the ultrasonic wave, the reaction temperature was steadily maintained at 65 ± 1 ^{o}C.

In order to study the leaching of $PW_{12}O_{40}^{3-}$ heteropoly anion into the polar reaction mixture and to examine the effect of ultrasonic irradiation on the catalyst stability, an experiment similar to the "hot-filtration experiment" was conducted [19, 21]. The catalyst was first mixed with methanol and ultrasonically treated under the reaction conditions. After the desired reaction time, the solid catalyst was filtered out and a desired amount of oil was added to the methanol. The reaction was then performed without the use of any catalyst for the optimum reaction time and the product was collected for analysis. All the experiments were carried out in the presence of air under atmospheric pressure.

2.6 Product analysis

A gas chromatograph (Agilent tech 7890 A GC systems) equipped with a capillary column (Agilent Technologies, Inc. 19091 J-413 hp-5) were used for product analysis. The system was equipped with a flame ionization detector (FID) and helium was used as the carrier gas. The analysis of FAME for each reaction mixture was carried out by dissolving the sample in n-hexane according to the desired dilution factor and 1 µl of the mixture was then injected into the GC.

2.7 Catalyst leaching and stability

In order to study the leaching of Kiggin anion from the supported catalyst and to examine the influence of ultrasonic waves on the catalyst stability, an experiment similar to the "hot-filtration experiment" was conducted [13-14]. The catalyst was added to methanol and then subjected to ultrasonication under the optimum reaction conditions. After the desired reaction time, the solid catalyst was filtered out and the desired amount of oil was added to this methanol. The reaction was then carried out without the presence of catalyst at the optimum reaction conditions in order to examine the contribution of the leached anion on the reaction.

The catalyst reusability was tested by running the same batch of catalyst for several successive runs. First, the desired amount of catalyst was used at optimum reaction conditions of the transesterification process followed by filtration and washing. A filtration system with 0.45 micrometer membrane filter and a vacuum pump were used to extract the catalyst using n-hexane as solvent. Successive washing with n-hexane followed by washing with ethanol were performed to ensure the removal of any polar and non-polar components that were attached to the catalyst. The solid catalyst was then dried at 100 °C for 2 h before reuse.

2.8 Experimental design

Four zero levels (center levels) were selected and applied in a central composite design (CCD) in order to establish the experimental design matrix. Reaction time (X_1), methanol to oil ratio (X_2), ultrasonic amplitude (X_3) and catalyst amount (X_4) were chosen with center values of 30 min, 15, 60 % and 3.5 wt/wt oil, respectively (Table 3.2). For the ultrasonic amplitude, 60 % of the total power was selected as the central level as early observations suggested that levels lower than 30 % were too low to create any positive effect. Meanwhile, 100 % was also avoided due to the very intense cavitation effect. Reaction time center level was selected based on the results of the reaction time effect tests while zero levels of other variables were selected based on the most suitable levels reported for acid catalyzed transesterification [23]. Design Expert 6.0.6 software was employed for constructing the design and the production yield was taken as the response.

Table 3.2. Coded and actual reaction variables used in the experimental design.

Real Variables	Coded Variables	Level		
		-1	0	+1
Reaction time (min)	X_1	10	30	50

Molar ratio	X_2	5:1	15:1	25:1
Ultrasonic amplitude (%)	X_3	30	60	90
Catalyst amount (w/w %)	X_4	2.5	3.5	4.5

4. Results and Discussion

4.1 Characteristics of TPA-AC catalyst

Surface characteristics of AC and the TPA-AC catalysts combined with the surface acidity data are summarized in Table 4.1. Tungstophosphoric acid itself is a non-porous material and the surface area is reported to be only about 1–2 m^2/g [30]. The BET surface area of the AC support used in this research was 750 m^2/g and the area contributed by micropores was about 73 % of the total surface area. It is noted from the table that immobilization of TPA on AC resulted in slight reductions in surface area, microporous volume and total porous volume. The magnitude of reduction was found to increase with increasing amount of TPA in the catalyst. This could be attributed to the partial blockage of pores by the active species. As a highly porous material, AC could accommodate high loading of TPA without experiencing significant drop in its porosity. A reduction in surface area after tungstophosphoric acid incorporation into an activated carbon was also observed Oball et al. [30].

The calculated values of surface acidity as shown in Table 2 reveal that AC was a material with low surface acidity and the catalysts showed significantly higher acidity with the increasing loading of TPA. As significant drop in the surface area was not observed, the acid sites were deemed accessible for reactants during the reaction which could bring about the desirable effect on the reaction rate. These results concluded that loading of TPA into the catalyst successfully introduced significant number of strong acid sites on the surface of the support material to act as good solid acid catalysts.

Table 4.1 Physical properties of AC and TPA catalysts.

Sample	Surface area (m^2/g)		Pore volume (cm^3/g)		Surface Acidity ($\mu mol/g_{cat}$)
	BET	Micropore	Total	Micropore	
AC	750	547	0.47	0.29	520
TPA15-AC	651	491	0.41	0.26	1530
TPA20-AC	621	467	0.39	0.25	1570
TPA25-AC	612	462	0.38	0.24	1690

The FT-IR spectra for supported TPA-AC catalysts are shown in Fig. 4.1. The spectra of pure TPA showed four major bands. These bands are attributed to the stretching modes of oxygen to phosphorous and tungsten in the adsorption mode of the Keggin ion $(PW_{12}O_{40})^{-3}$. Bands at 800 cm^{-1} (W-O-W at the edge), 890 cm^{-1} (W-O-W at the corner), 980 cm^{-1} (W=O) and at 1080 cm^{-1} (P-O) can be detected for the Keggin ion which were in agreement with the results of Ferreira et al. [21]. Based on Fig. 1, no characteristic band could be detected for AC while for the immobilized catalysts, three major bands could be detected with increasing intensity with the amount of TPA loaded. For these bands, some shifts in their positions were noticed due to the new interactions that occurred between AC and TPA. The achieved results showed good

agreements with those reported by Oball et al. [30] and Ferreira et al. [21]. These results suggested the successful synthesis of TPA-AC catalysts without excessive loading of active component that could subsequently affect the activity.

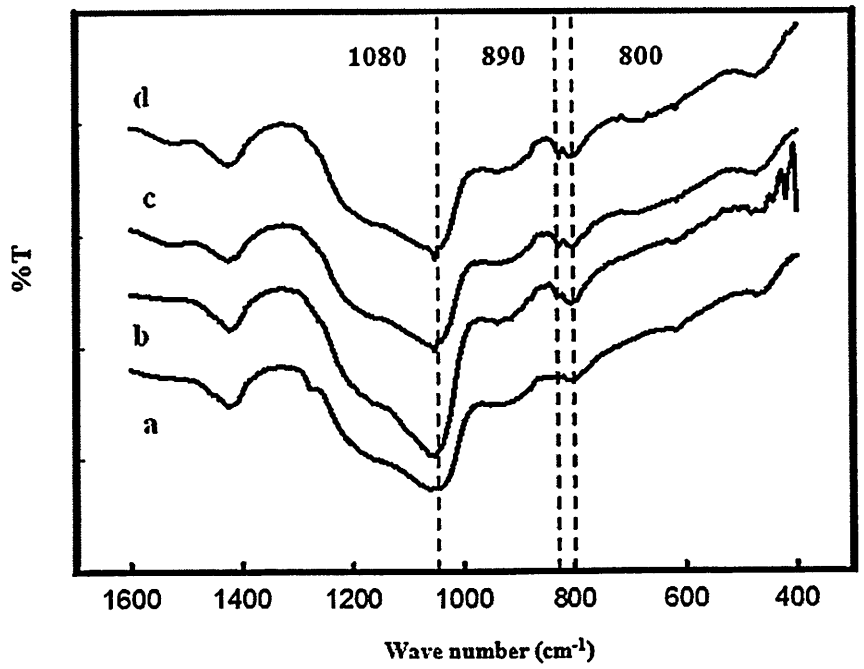

Fig. 4.1. FT-IR spectra for (a) AC (b) TPA15-AC (c) TPA20-AC (d) TPA25-AC.

The SEM images of AC and the supported catalysts are shown in Fig. 4.2. The micro images of the catalysts were obtained using the fresh catalysts before being used in the transesterification reaction. The acid functionalized catalysts showed irregular distributions of the TPA on the AC surface. The deposition of TPA on the surface of AC not only responsible for the partial reduction on the surface area as the amount of the TPA increased but also resulted in the activity increase for the catalysts.

The EDAX results for the support and the immobilized catalysts can be seen in Fig. 4.3. These results prove that the existence of metallic materials attached to AC surface. EDAX result for AC correctly gave only carbon element while for the other catalysts, the presence of the Keggin anion $(PW_{12}O_{40})^{-3}$ can be detected. It can be concluded from these results that the amount of tungsten, oxygen and phosphorous increased with the increasing loading of TPA on AC. This, in turn, increased the catalyst activity in the transesterification of Jatropha oil.

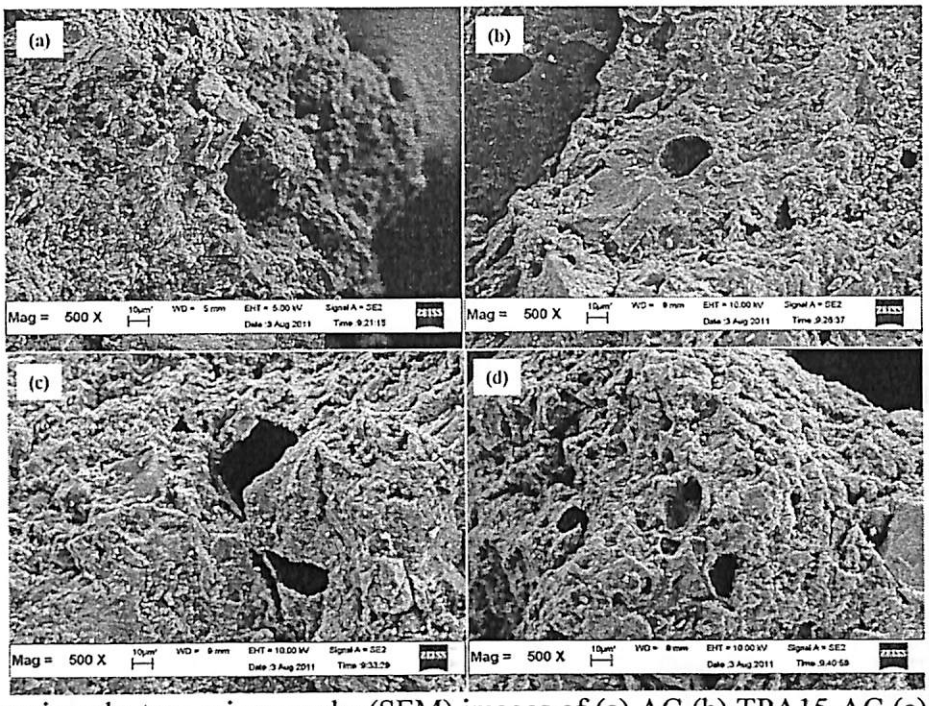

Fig. 4.2. Scanning electron micrographs (SEM) images of (a) AC (b) TPA15-AC (c) TPA20-AC (d) TPA25-AC.

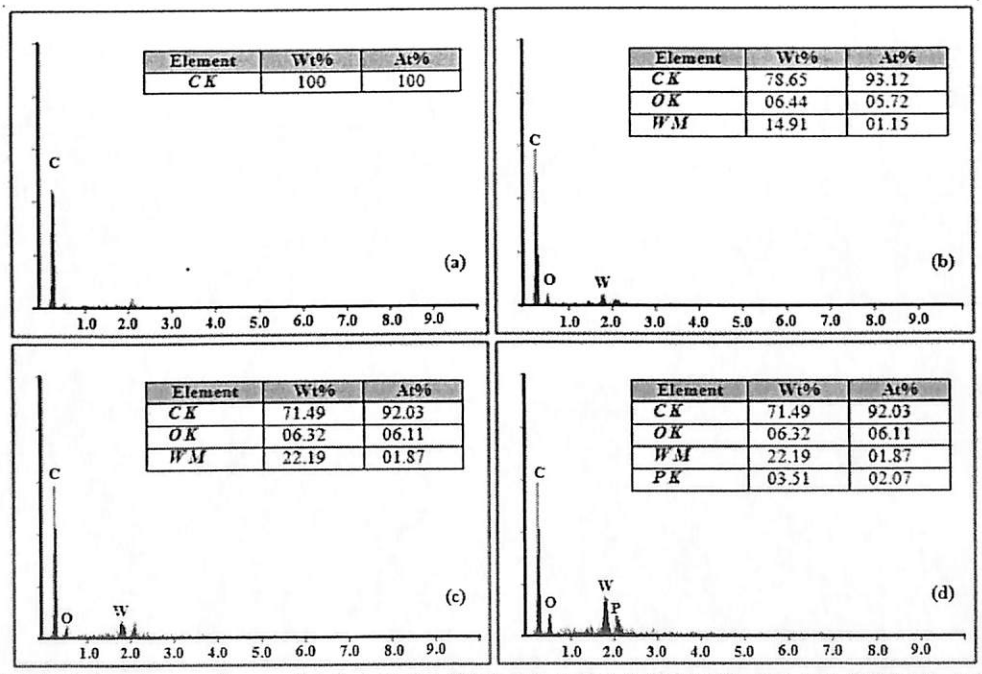

Fig. 4.3. EDAX for the surface of (a) AC (b) TPA15-AC (c) TPA20-AC (d) TPA25-AC.

4.2.1 Blank experiments

The results of blank experimental runs revealed that transesterification reaction did not significantly occur within a short reaction time of 60 min with the presence of AC only or

without the use of any catalyst (Fig. 4.4). This was mainly due to the absence of acid active sites to catalyze the reaction. It also led to the conclusion that a suitable catalyst was indeed essential to achieve significant reaction. However, it is inaccurate to conclude that ultrasonic irradiation could activate the catalyst. Actually, this external energy could accelerate the reaction by improving mass transfer between the two immiscible reactants. Conducting the reaction without the use of ultrasound (mechanically stirred) also resulted in negligible reaction due to the short reaction time coupled with the poor catalytic activity of the solid acid catalysts. It has been reported that conventional acid catalyzed reactions requires long reaction time (5-6 h) due to the slow reaction rate [5]. Meanwhile, base-catalyzed process could be carried out with relatively shorter reaction times (2-3 h) [4, 32].

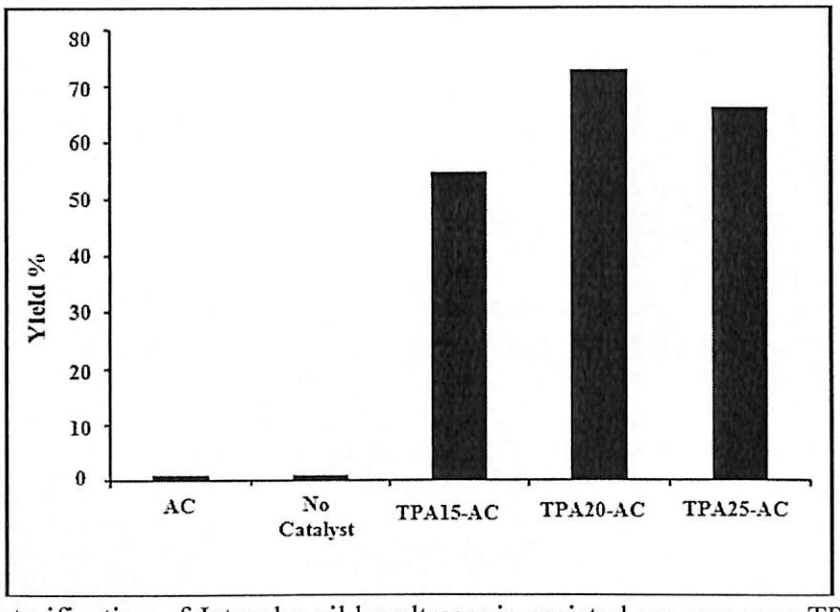

Fig. 4.4. Transesterification of Jatropha oil by ultrasonic-assisted process over TPA immobilized on AC (reaction time 60 min, methanol/oil molar ratio 20:1, catalyst amount 4% (w/w), and ultrasonic power 75%).

It has been generally reported that higher molar ratio of methanol to oil can be used in order to prevent backward reaction to achieve higher biodiesel yield [3, 5, 15]. However, the methanol to oil ratio used in this study was already high i.e. at 20:1. High ratio also means that the concentration of Jatropha oil as the limiting reactant in the system is low to bring about undesired effect as far as the reaction rate is concerned. As such, certain suitable level of this ratio should be used. In this study, effect of reactants' ratio was beyond the main scopes to be investigated. However, it is agreeable that this variable could also affect certain behaviors of the reaction but discussion on this matter will be reported separately.

The activity of the AC-based TPA catalysts was found to be slightly better than that reported previously using alumina-based TPA catalysts [33]. For comparison, 20 wt. % TPA loading in alumina led to a FAME yield of about 50 % in 60 min while the yield simply exceeded 70 % in this study. Differences in the activity could be associated with the significantly higher surface area of the AC-based catalyst used in the present study (93 m^2/g versus 621 m^2/g). Thus, surface area could play a major role in the activity of the catalyst in this ultrasound-assisted reaction.

4.2.2 The effect of HPA loading

The results of catalytic experiments for FAME production yield from Jatropha oil under ultrasonic irradiation for different catalyst loadings are presented in Fig. 4.4. The reaction yield increased as the TPA content in the catalyst was increased and reached its highest level with TPA20-AC. Meanwhile, the catalyst with higher TPA amount did not show better yield as expected. At low TPA content, the presence of active sites on the surface of the support promoted the conversion of the reactants and drove the system towards forward reaction. Excessive amount of TPA in TPA25-AC led to a slight decrease in the reaction yield mainly due to a reduction in the catalyst surface area accessible by the reactants. This behavior was caused by partial blockage of the pores by the active sites leading to internal diffusion limitation for the reactants. Deposition of TPA particles on the pore mouths could cause the surface area within the pores to be unavailable for the reaction. Low accessibility of the reactants to the active sites in the internal pores resulted in negative effect on the reaction yield. Based on these results, TPA amounts above 20 % w/w loading were not recommended due to the decrease in pore volume and surface area due to pore plugging.

In any supported catalyst system, the impregnation of excessive amount of active component will usually lead to loss of surface area and pore volume as observed in this study. As impregnation method was used to prepare the catalyst, the deposition of TPA on the external surface could not be totally avoided. The support material used was also known to contain irregular pore shapes and sizes [15]. As such, it is understandable that if the deposition of the active component occurs at pore mouths, internal diffusion resistance could result. Thus, decreases in these surface properties could affect the catalytic activity in this heterogeneous reaction system. In this respect, SEM images could not clearly show pore mouth blockage as it could also occur at internal narrow areas of the pores.

4.2.3. Effect of reaction time

Effect of reaction time on the methyl ester yield under ultrasonic condition can be seen in Fig. 4.5 for both TPA20-AC and TPA25-AC catalysts. For a low reaction time of 20 min, insufficient contact time between the reactants led to low reaction yield. The yield increased with increasing reaction time, reaching its maximum levels in 40 min for both catalysts. The highest reaction yields were 87.33 % and 71.19 % for TPA20-AC and TPA25-AC, respectively. The behavior of the reaction between 30-50 min in the presence of heterogeneous catalyst can be explained based on the role of ultrasonic mixing in achieving emulsifying effects between the reactants. The ultrafine mixing provided a dispersion effect to the catalyst particles through the reaction media that facilitated the reactants molecules to spread and reach the active sites on the surface of the catalyst. The role of ultrasonic irradiation in enhancing the reaction rate for heterogeneous biodiesel production system has been highlighted by Salamatinia et al. [34] and Mootabadi et al. [35]. In these studies, the reaction times to reach yields exceeding 90 % in a base-catalyzed transesterification of palm oil were about ~50 min and 60 min, respectively. The results were significantly lower than those generally reported for non-ultrasonic reaction systems.

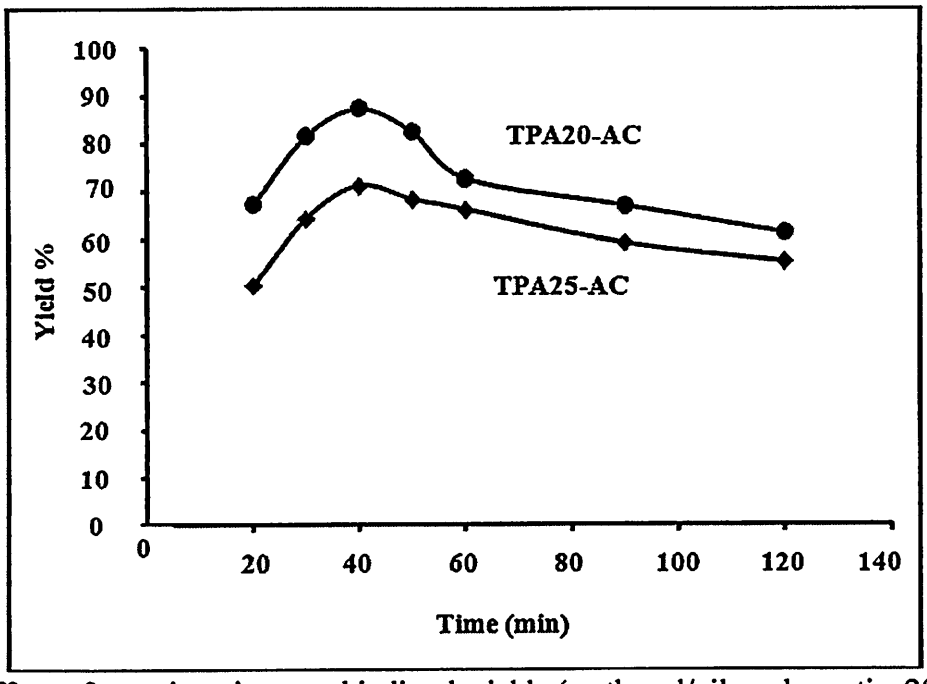

Fig. 4.5. Effect of reaction time on biodiesel yield. (methanol/oil molar ratio 20:1, catalyst amount 4 % (w/w), and ultrasonic power 75 %).

Although the use of ultrasonic irradiation managed to shorten the reaction time, decreases in FAME yields for both catalysts were observed after 60 min. It has been reported for ultrasound-assisted transesterification system that monoglycerides content was high at times beyond 60 min due to the slow reaction rate to convert it to glycerol and FAME [36]. Thus, in the current investigated system, the reaction mixture could contain sufficient amounts of monoglycerides at high reaction time that could enhance the solubility of FAME in the glycerol to result in FAME glycerolysis. Besides that, side (esterification) reactions between FFA and glycerol led to the formation of monoglycerides, diglycerides and finally triglycerides that would negatively affect the reaction yield [15]. Esterification reaction is known to be an acid-catalyzed reaction.

Transesterification process of vegetable oil and methanol is widely reported to be catalyzed by either acid or base catalyst. The reaction rate is influenced by many factors such as the reaction temperature, type of catalyst, ratio of reactants, concentration of the limiting reactant etc. [13, 14]. In this study, high concentration of FAME was expected after a certain duration of time, especially when the FAME yield exceeded about 70 %. At this stage, FAME glycerolysis could occur at a significantly high rate leading to lower FAME yield. At the same time, the formation of FAME through transesterification between the oil and methanol occurred simultaneously but at low rate due to the low concentration oil as the limiting reactant. As such, with progressing reaction time, more FAME could have been used in the glycerolysis compared to that formed through the transesterification reaction.

Cao et al. [37] reported that by using $H_3PW_{12}O_{40}$-$6H_2O$ as the catalyst, the highest transesterification yield of 87 % could be achieved with high reactants' molar ratio of 70:1 and long reaction time of 14 h under mechanical stirring. On the other hand, with the use of immobilized form of HPA (zirconia-supported HPA catalyst), Sunita et al. [23] recorded that the optimum reaction time under conventional process to achieve 97 % of biodiesel yield at 200 °C

was 5 h. Thus, the ultrasonic-assisted reactor system significantly reduced the requirement for a very high methanol to oil ratio for the acid catalyzed process. In addition, significant reductions in reaction time and reaction temperature were achieved. Thus, the reaction could be carried out in a more cost efficient manner.

4.3.4. Effect of water and FFA content

The effect of feed stock water content on FAME yield for both catalysts can be seen in Fig. 4.6. It is noted that by increasing the content of water in Jatropha oil to 1 % (w H_2O/w oil), only a slight decrease in the yields for both catalysts resulted. The results revealed the tolerance of the catalysts towards water. For TPA20-AC, the amount of water beyond 1 % led to a sharp decrease in the biodiesel yield while lower yield was recorded for the higher water content (4 %). In the case of TPA-25AC catalyst, increasing water content gradually decreased the methyl ester yield. However, water contents beyond 2 % did not result in significant decrease in the yield. It could be due to the excess amount of TPA loaded onto the AC.

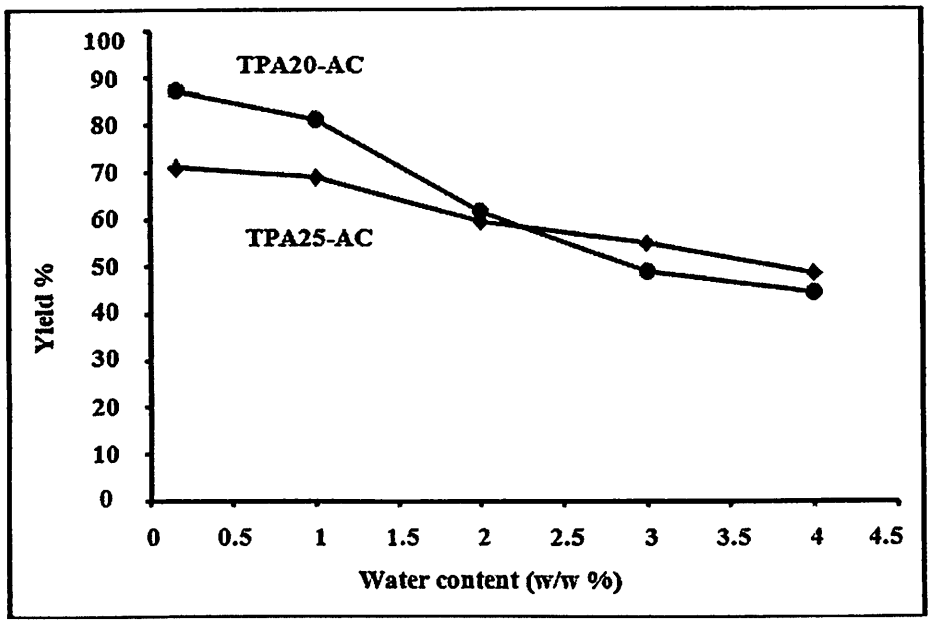

Fig. 4.6. Effect of water content on biodiesel yield. (Reaction time 40 min, methanol/oil molar ratio 20:1, catalyst amount 4 % (w/w), and ultrasonic power 75 %).

As a conclusion, a decrease in reaction yield with increasing of water content could be attributed to the hydrolysis of the esters at high water content. The presence of large amount of water could negatively affect the strength of Brönsted acid sites presented in the catalyst. The hydration of these acid sites could reduce the catalyst activity that in turn, resulted in negative effects on the reaction yield. Nakajima et al. [38] reported the same behavior for carbon based acid catalyst used in the presence of high water content. Good tolerance to high water content as demonstrated by TPA25-AC catalyst could be related to the higher number of active sites that reduced the effects of acid sites hydration.

The effect of FFA % content in the crude vegetable oil on the reaction yield is presented in Fig. 4.7 for TPA20-AC and TPA25-AC catalysts. It can be concluded that both catalysts were

insensitive to the presence of FFA. Beyond 17.5 FFA %, slight reductions in the reaction yields for both of catalysts were noticed. This could be attributed to the effect of high amount of water generated during the esterification reaction due to the high FFA content. The presence of water can affect negatively on the production yield as it can hydrolyze the esters. Meanwhile, the studied catalysts showed good water and FFA tolerance which would enable the use of low grade, cheap price and non-edible vegetable oils for biodiesel production.

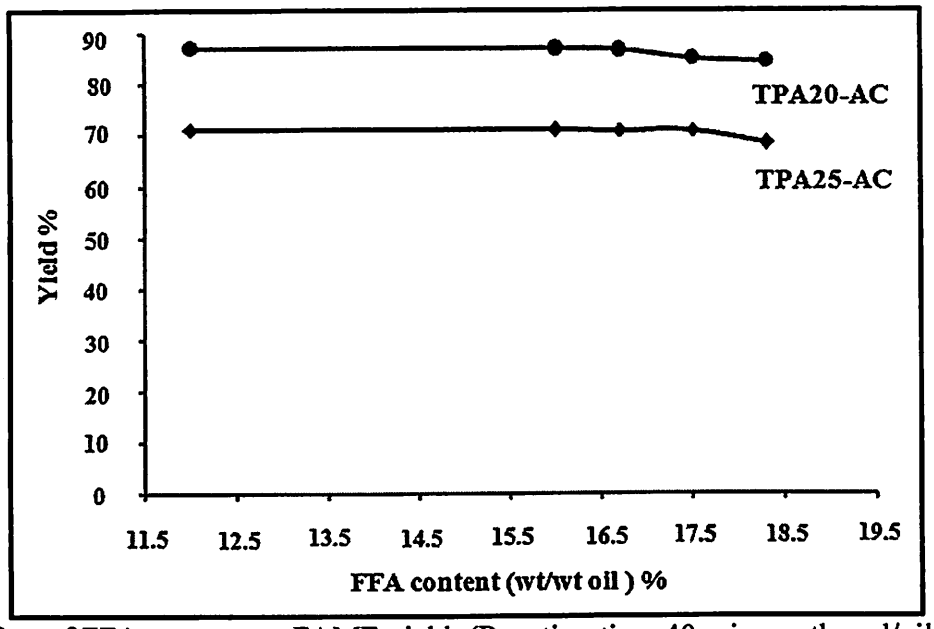

Fig. 4.7. Effect of FFA content on FAME yield. (Reaction time 40 min, methanol/oil molar ratio 20:1, catalyst amount 4 % (w/w), and ultrasonic power 75 %).

4.3.5 Catalyst reusability and stability

In order to study the catalyst reusability under the ultrasonic conditions, consecutive reaction runs were carried out using the same catalyst. After the first experimental run, the TPA20-AC catalyst was filtered and washed several times with ethanol to remove any polar impurities followed by washing with n-hexane to eliminate any non-polar components. The washed catalyst was dried at 100 ^{o}C for 2 h and reused again for the transesterification reaction. Fig. 4.8 shows the catalyst activity for up to three times of use at 75 % of ultrasonic amplitude, 40 min of reaction time and reactants' molar ratio of 20. The results revealed that a drop in the catalytic activity as indicated by a decrement in the reaction yield was noticed. For the first run, 77 % of the original activity was achieved. The reduction in activity could be attributed to the catalyst deactivation, leaching and the loss during washing process between the reuse cycles. A small portion of the solid catalyst was collected as soot in the filtration step during the study. These small carbon particles were formed as a result of the impact of ultrasonic irradiation on the porous solid particles. If the small loss of unrecovered catalyst were to be considered, small drop in the activity from the first run to the third reuse cycle could indicate the stability of the catalyst for repeated use in the process.

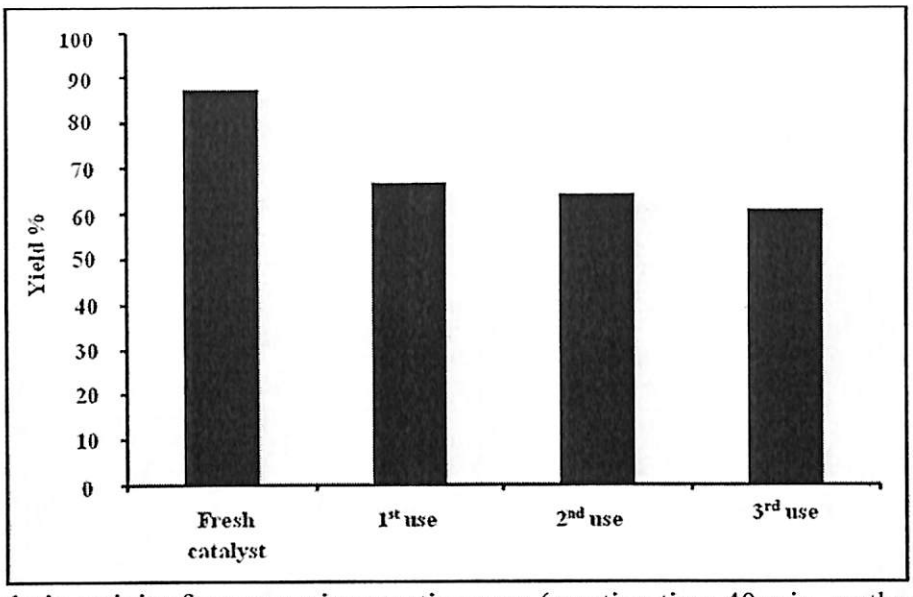

Fig. 4.8. Catalytic activity for successive reaction runs (reaction time 40 min, methanol/oil molar ratio 20:1, catalyst amount 4 % (w/w), and ultrasonic power 75 %).

The stability of the AC-based TPA catalysts was found to be slightly lower than that reported previously using alumina-based TPA catalysts [33]. For comparison, 20 wt. % TPA loading in AC showed about 27 % drop FAME yield after the 3rd cycle of reuse while it was only about 12 % in the case of the alumina-based TPA catalyst. Differences in the activity could be associated with the higher structural stability of the alumina-based catalyst. Thus, structural stability could play a major role in the activity of the catalyst in this ultrasound-assisted reaction. Due to higher porosity of AC-based catalyst, its structural stability was expected to be significantly lower compared to that of alumina-based catalyst.

4.3.6 Catalyst leaching

Investigation on the catalyst stability under the ultrasonic reaction conditions revealed that 12 % of the reaction yield was achieved due to the $PW_{12}O_{40}^{3-}$ anion which leached out from the heterogeneous catalyst. The result showed that major part of the reaction yield was achieved through heterogeneous catalysis. Leaching of active sites from the catalyst occurred due to the good solubility of TPA in the polar reaction mixture and the exposure of the solid catalyst to direct ultrasonic irradiation. However, significant solubilization of TPA did not occur as it was strongly fixed on the surface through calcination and the small pore sizes of the AC support.

Compared with other immobilized forms of HPA on different supports such as zirconia and silica [39], HPA supported on AC used in the current study showed minimal leaching due to the strong fixation of HPA over the surface of activated carbon. Some TPA particles were trapped inside the small pores of the support due to textural porous properties of the support material. Strong electrostatic attraction between TPA species and AC could also happen due to the existence of specific functional groups on the surface of AC [39]. The same behavior of HPA immobilized on AC catalyst was reported for other polar reaction mixtures such as acetylation of glycerol with acetic acid [21] and liquid phase esterification of acetic acid with butanol [40].

4.2 Alumina based catalyst

4.2.1 Characteristics of alumina based catalyst

Surface characteristics of Al and the TPA-Al catalysts are shown in Table 4.2. It can be observed that the surface area, total pore volume and pore diameter decreased with increasing TPA loading. The diameter of the TPA molecule is about 12 Å [24] to suggest its possible inclusion inside the mesopores of the support. Similar observation was recorded upon 20 wt. % TPA loading into alumina [25]. The possibility of TPA multilayer formation on the support surface at high loadings (30 and 35 wt. %) could not be ruled out. The partial blockage of the pores by the multilayer TPA deposition led to a decrease in the surface area [26].

Table 4.2. Physical properties of Al and the TPA catalysts.

Sample	BET Surface area (m^2/g)	Total pore volume (cm^3/g)	Average pore diameter (Å)
Al	109.4	0.23	82.6
TPA25-Al	93.3	0.13	54.9
TPA30-Al	83.4	0.10	52.0
TPA35-Al	71.9	0.09	49.8

Fig. 4.9 shows the FT-IR spectra for Al and the supported catalysts. For a pure TPA, it has been reported that four major bonds are attributed to the stretching modes of oxygen to phosphorous and tungsten of the adsorption mode of the Keggin ion $(PW_{12}O_{40})^{-3}$. Bands at 800 cm^{-1} (W-O-W in the edge), 890 cm^{-1} (W-O-W in the corner), 980 cm^{-1} (W=O) and at 1,080 cm^{-1} (P-O) can be detected for the Keggin anion [14]. For the supported catalysts, a shoulder at 910 cm^{-1} was attributed to the symmetric stretching of (W=O) bond. The difference between the anion area (1.1 nm^2) and the surface area of the support (109 m^2) suggested the high dispersion on the surface [27]. The existence of Keggin anion was not evident for TPA loadings on alumina below 40 wt. %.

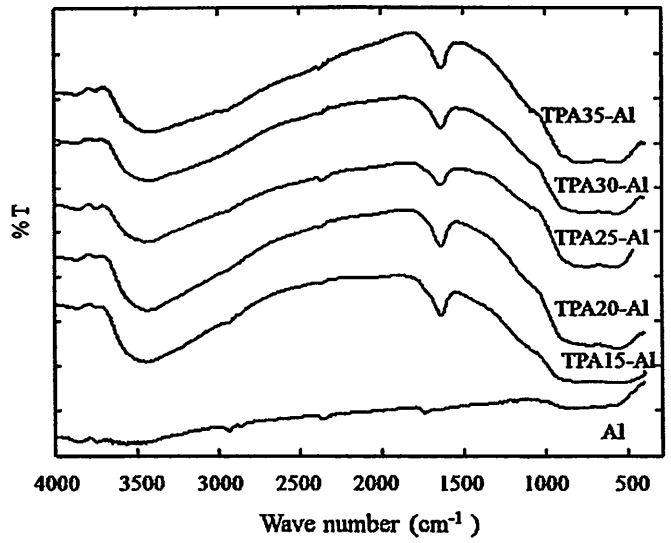

Fig. 4.9. The FT-IR spectra of Al and the supported catalysts.

Analysis done on the TEM images revealed some information about the dispersion of the active species (Fig. 4.10). A wormhole-like mesostructure of Al sample can be observed in Fig. 2(a). The images of the loaded catalysts revealed the presence of the Kiggin anion as small round particles that were distributed over the support. The difference in the diameters between the TPA and the mesopores in the support provided the opportunity for TPA anions to be trapped inside the pores. This was substantiated by the presence of dark particles (Fig. 4.10 (b, c, d)).

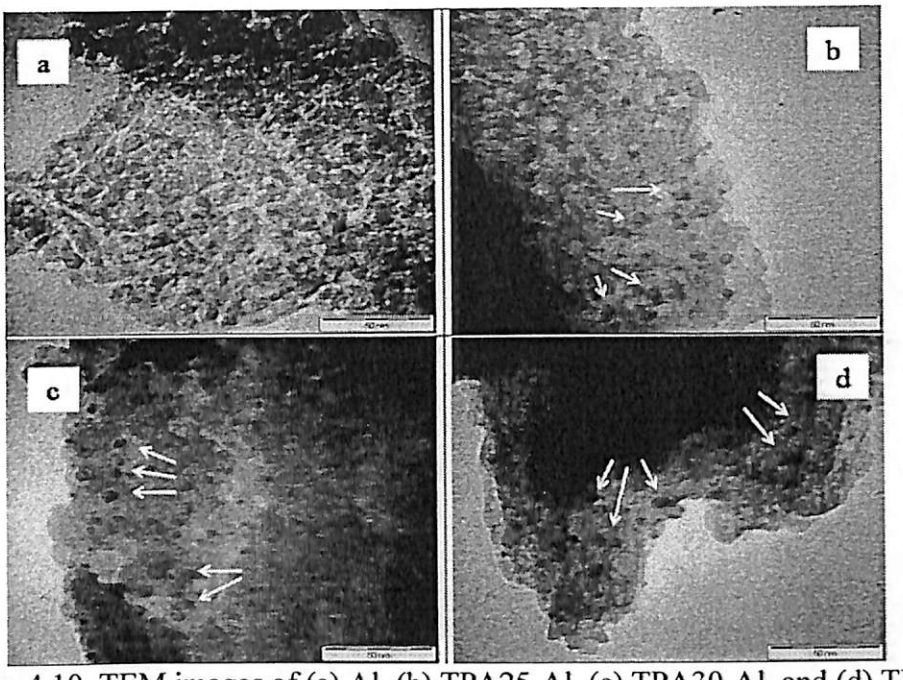

Fig. 4.10. TEM images of (a) Al, (b) TPA25-Al, (c) TPA30-Al, and (d) TPA35-Al catalysts.

It is noted that reductions in diffraction peaks of the support and the magnitude of these reductions increased with the increasing TPA loading (Fig. 4.11). None of the catalysts showed peaks that could be assigned to the active phase which indicated good dispersion of TPA on the support. Similar behavior has been noticed for TPA supported on alumina [25-26], silica, zirconia and activated carbon [25] and for different HPAs immobilized on alumina [11]. This good dispersion could be related to the difference in the mean pore diameter of the supports (about 80 Å) and the diameter of the HPA molecule which allowed more uniform distribution of TPA on the surface [25].

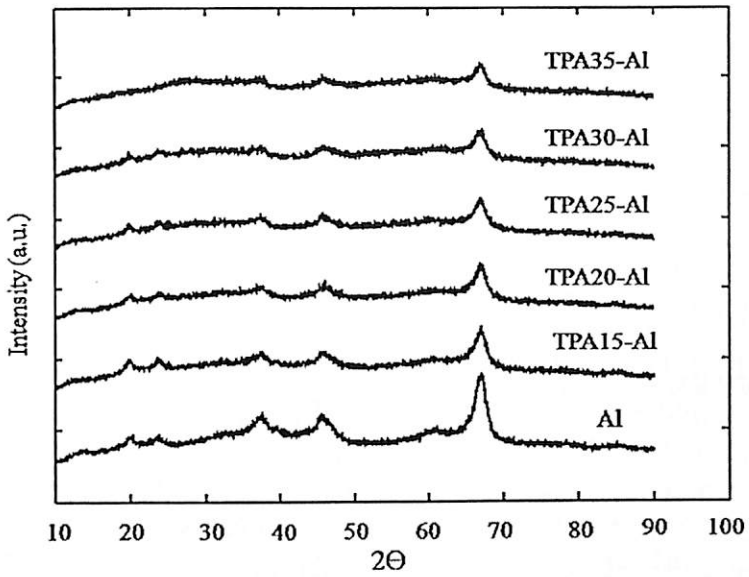

Fig. 4.11. XRD patterns of Al and the supported catalysts.

4.2.2 Preliminary study

The results of blank runs revealed that significant reaction did not occur with the presence of alumina only or without the use of catalyst (reactants alone) (Fig. 4.12). This was mainly due to the absence of acidic i.e. active sites to catalyze the reaction. The run without the use of ultrasound (mechanically stirred) also resulted in no significant reaction. Conventional acid catalyzed reactions require long reaction time (5-6 h) due to the slow reaction rate [4] compared to base-catalyzed ones (2-3 h) [8]. However, base catalysts are not suitable in this study due to high FFA content in the oil.

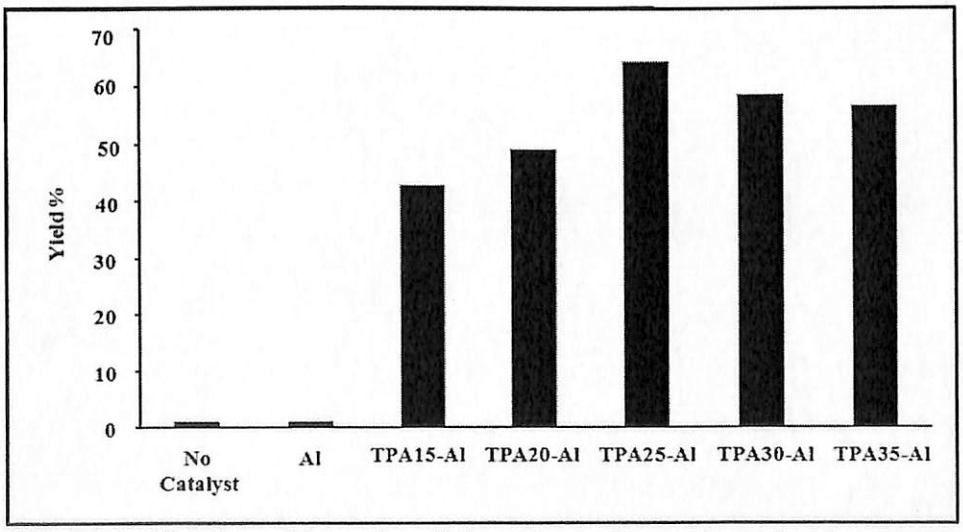

Fig. 4.12. Transesterification of Jatropha oil through an ultrasonic-assisted process over TPA immobilized on alumina (reaction time 60 min, methanol/oil molar ratio 20:1, catalyst amount 4 % (w/w), and ultrasonic power 75 %).

The reaction yield increased with increasing TPA content in the catalyst and reached the highest value with TPA25-Al (Fig. 4). The presence of active sites on the catalyst promoted the reactants' conversion and promoted the forward reaction. High TPA loadings (above 25 wt. %) led to a decrease in the reaction yield due to the reduction in the accessibility of the reactants to the active sites. This was caused by the blockage of the catalyst pores by the active sites leading to internal diffusion limitation. Low accessibility of the reactants to the active sites resulted in negative effects on the reaction yield.

Changes in FAME yield with reaction time can be seen in Fig. 4.13 for both TPA25-Al and TPA30-Al catalysts under ultrasonic condition. For short reaction time, insufficient contact time between the reactants led to low reaction yield. The yields increased with increasing reaction time, reaching their maximum levels in about 60 min for both catalysts. The highest reaction yields were 64.3 % and 56.6 % for TPA25-Al and TPA30-Al, respectively. Meanwhile, FAME yield decreased for both catalysts after 60 min probably due to FAME glycerolysis and other side reactions. It has been reported that beyond 60 min for the ultrasound-assisted transesterification, monoglycerides content was high due to the slow reaction rate to convert it to glycerol and FAME [28]. Sufficient amounts of monoglycerides accumulated in the reaction mixture could lead to enhancement in the solubility of FAME in the glycerol. Side reaction between FFA and glycerol, mono-and glycerides could also result in triglycerides that negatively affected the yield [29].

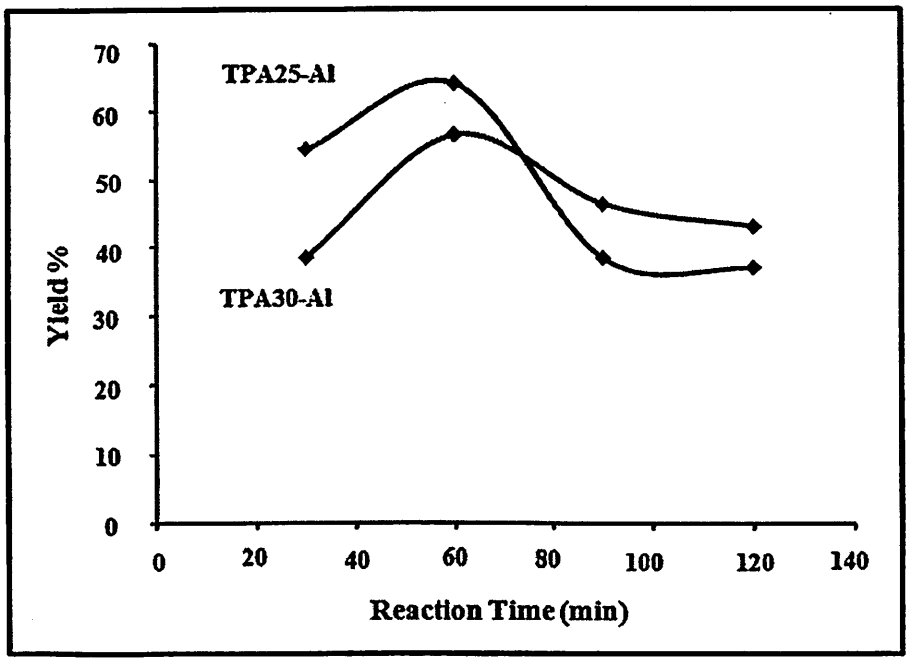

Fig. 4.13. Effect of reaction time on FAME yield. (methanol/oil molar ratio 20:1, catalyst amount 4 % (w/w), and ultrasonic power 75 %).

4.2.3 Statistical analysis

Without the use of any statistical method, a wide range of experimental runs would be required to characterize the interaction between the variables [16]. Different design models such as full factorial design, Taguchi's algorithm and response surface methodology have been

established for optimizing the data. The experimental design matrix including the un-coded values, point types and the experimental responses values is presented in Table 4.3. It consisted of 30 experiments according to 2^k+2k+6, where k is the number of independent variables [30]. Twenty four experiments were improved by six replications at the center points to evaluate the pure error. The third order polynomial equation based on the coded values obtained using multiple regression analysis of the experimental data is;

Table 4.3. Central composite design matrix of four variables and the respective responses.

Run	Point type	Real Variables				Yield (%)
		Time (min)	M/O[a]	Amplitude (%)	Catalyst Amount (w/w %)	
1	Fact	40	20	45	3.0	60.49
2	Fact	20	10	45	4.0	37.55
3	Fact	20	20	75	4.0	53.27
4	Fact	40	10	75	4.0	35.16
5	Fact	20	10	45	3.0	38.16
6	Fact	20	20	75	3.0	49.34
7	Fact	40	10	75	3.0	43.74
8	Fact	20	20	45	4.0	58.45
9	Fact	40	20	75	3.0	61.22
10	Fact	40	10	45	3.0	45.40
11	Fact	40	10	45	4.0	41.55
12	Fact	40	20	75	4.0	84.16
13	Fact	20	20	45	3.0	51.89
14	Fact	40	20	45	4.0	61.15
15	Fact	20	10	75	4.0	36.03
16	Fact	20	10	75	3.0	37.70
17	Axial	30	25	60	3.5	83.74
18	Axial	30	15	60	4.5	66.52
19	Axial	30	15	90	3.5	68.78
20	Axial	10	15	60	3.5	48.33
21	Axial	30	5	60	3.5	33.57
22	Axial	50	15	60	3.5	54.18
23	Axial	30	15	30	3.5	42.67
24	Axial	30	15	60	2.5	46.05
25	Center	30	15	60	3.5	55.47
26	Center	30	15	60	3.5	62.95
27	Center	30	15	60	3.5	60.94
28	Center	30	15	60	3.5	57.31
29	Center	30	15	60	3.5	59.44
30	Center	30	15	60	3.5	51.38

[a] Methanol to oil ratio.

$$Y = 67.99 + 1.82\,X_1 + 0.85\,X_2 - 3.11\,X_3 - 13.27\,X_4 + 0.1\,X_3^2 - 0.14\,X_1X_2 - 0.04\,X_1X_3 - 0.07\,X_2X_3 + 1.22\,X_2X_4 - 7.19 \times 10^{-4}\,X_3^3 - 3.13 \times 10^{-3}\,X_1X_2X_3 \quad (1)$$

Here, Y is the response (FAME yield) while X_1, X_2, X_3 and X_4 are the coded forms of the studied variables. The choice of a cubical polynomial equation to describe the design was made on the basis of the high value of determination coefficient (R^2) that was achieved.

The ANOVA statistical analysis (Table 4.4) shows high significance of the cubical equation to represent the experimental data as expressed by the Fisher F-test value (13.44) combined with a very small probability value (Prop.>F <0.0001). Based on an R^2 value of 89.69 %, the effect on the FAME yield could be attributed to the variation in the independent variables while the remaining (10.31 %) could be explained by residues.

Table 5. Analysis of variance (ANOVA) for the cubic model representing the ultrasound-assisted biodiesel production process.

Sources of variations	Sum of squares	Degrees of freedom	Mean square	F-value	Prob.>F
Model	4198.29	11	381.66	13.44	<0.0001
Residual	482.62	17	28.39	-	-
Lack of fit	396.74	12	33.06	1.92	0.2428
Pure error	82.88	5	17.18	-	-
Total	4680.91	28			

R^2=0.8969, Adj. R^2=0.8302, C.V.=10.18, Std. Div=5.33

Table 4.5. Results of regression analysis for the full second-order polynomial model and the estimated coefficients.

Model Parameters	F-value	Prob.>F
X_1	9.91	0.0059
X_2	103.08	< 0.0001
X_3	1.48	0.2411
X_4	5.34	0.0336
X_3^2	11.68	0.0033
$X_1 X_2$	3.12	0.0952
$X_1 X_3$	1.42	0.2497
$X_2 X_3$	1.49	0.2385
X_2X_4	5.24	0.0351
X_3^3	2.49	0.1328
$X_1 X_2 X_3$	3.10	0.0961

4.2.4 Interaction between parameters

Generally, larger F-value and smaller the Prob.>F value indicate more significant the corresponding variable [31]. It is noted in Table 4.5 that reaction time, molar ratio and catalyst amount had significant effects on the yield while ultrasonic amplitude mostly had its influence in its square value. Two interactions between the molar ratio with reaction time and catalyst amount as well as the triple interaction between the reaction time, molar ratio and the ultrasonic amplitude showed significant effects on the response. The other interactions and the cubical form of the ultrasonic amplitude (Table 4.6) were also considered to establish a historical design based on the experimental data.

Table 4.6. Predicted and experimental results under the optimum conditions for model validation.

Run	Reaction Conditions				Predicted Yield (%)	Experimental Yield (%)	Error (%)
	Time (min)	Molar ratio	Amplitude (%)	Catalyst amount (w/w)			
1	37.00	22.69	72.12	4.26	87.54	89.32	2.04
2	47.17	19.05	64.32	4.44	86.19	83.63	2.97
3	48.13	23.41	46.86	4.44	85.56	88.14	3.01

The possible interactions between the reaction variables should be more observable if 3D surfaces are established from the experimental data. Fig. 4.14(a) shows the interaction between reaction time and molar ratio while the other parameters are kept at their center values. It can be concluded that an increase in reactants' molar ratio had positive effects on the reaction yield for both low and high reaction times, while increasing the reaction time had its positive influence only at high molar ratio. Insufficient amounts of methanol to drive the forward reaction at low molar ratio of 5:1 resulted in low yield. Subjecting the reaction mixture to ultrasonic irradiation for the maximum reaction time in the presence of low methanol amounts led to a decrease in the yield. This could be attributed to severe mixing effects between the small FAME amounts (produced by low methanol amount) with the by-product (glycerol). For high reaction times and high molar ratios, the FAME yields showed maximum values due to the sufficient reaction time and adequate methanol amounts to support the reaction.

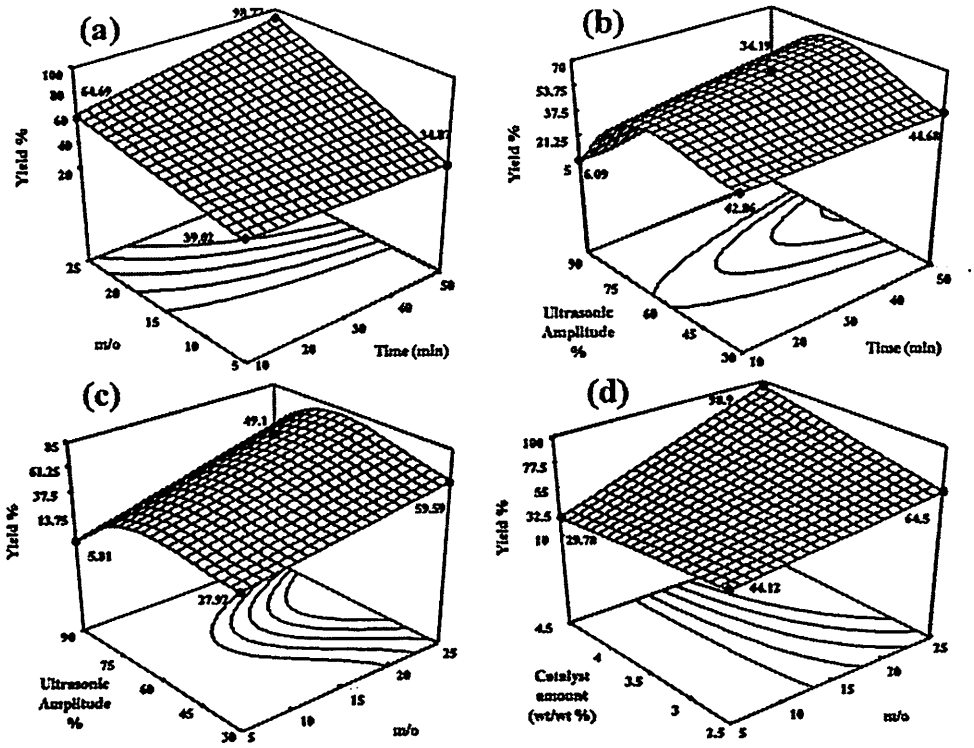

Fig. 4.14. The interactions between the reaction parameters, (a) between the reaction time and the methanol/oil ratio, (b) between the reaction time and the ultrasonic amplitude, (c) between the methanol/oil ratio and the ultrasonic amplitude, and (d) between the molar ratio and the catalyst amount.

The inter-dependence between ultrasonic amplitude, reaction time and reactants' molar ratio are presented in Fig. 6(b) and 6(c), respectively. For low and high reaction times and molar ratios, the reaction yield was found to increase with increasing ultrasonic amplitude and it reached the maximum values at moderate levels (~60-70 %). For all reaction times and molar ratio values, the reaction yields showed a decreasing trend at high ultrasonic amplitudes due to the formation of large number of cavitation bubbles in the liquid. The combination of these bubbles forming larger and more stable bubbles could create a barrier to the acoustic energy transmission through the reaction mixture leading to poor mixing effects between the two immiscible layers. Similar behaviors of ultrasonic-assisted biodiesel production systems at high ultrasonic energy have been reported [22, 32]. In Fig. 4.15(c), increasing molar ratio improved the reaction yield at the minimum and maximum ultrasonic amplitude levels due to the increase in the number of cavitation bubbles that would collapse to form an emulsion between the two layers.

It can be observed in Fig. 4.14(d) that increasing catalyst amount with the presence of low methanol amount negatively affected the yield but it showed an increasing trend in the yield when high methanol amounts were used. Thus, increasing the catalyst amount led to an increase in the available active sites for the reactants to undergo the chemical reaction.

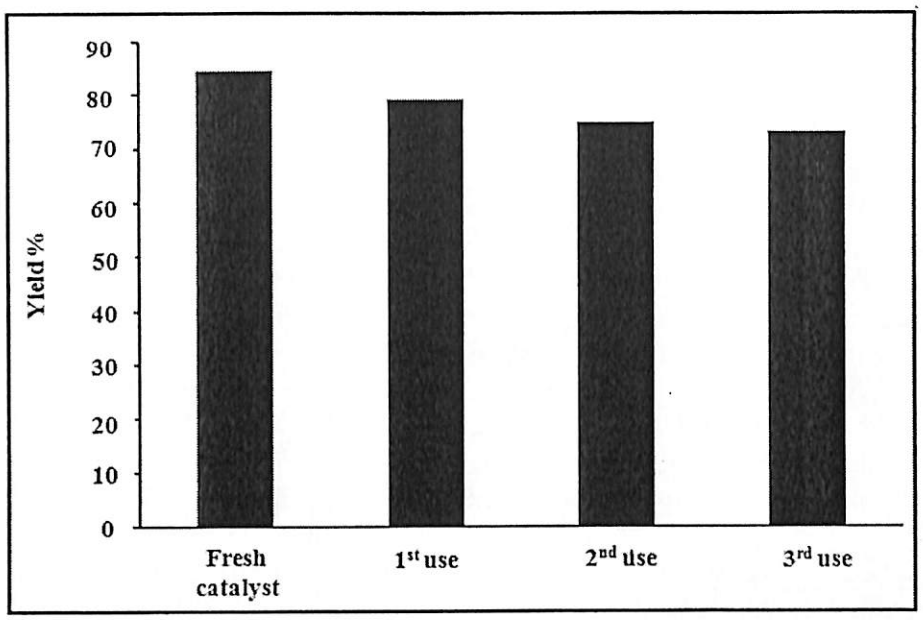

Fig. 4.15. Catalytic activity of TPA25-Al in successive reaction runs under the optimum reaction conditions.

4.2.5 Process optimization

Optimization of the reaction variables by fitting the experimental data to the historical design using the Design Expert 6.0.6 software was also attempted. The software suggested 10 possible solutions according to the order of suitability. Table 7 presents three selected solutions and the corresponding values of the experimental yield to validate the proposed reaction conditions. The experimental results showed good agreement with the predicted ones within 3 % error.

It can be concluded that the reaction time for the ultrasound-assisted process below 50 min achieved ~85 % of FAME yield in the presence of the solid acid catalyst. This observation suggested the contribution of ultrasonic energy in enhancing the reaction rate compared to other conventional transesterification processes that require relatively longer reaction time. The use of TPA either homogenously [33] or supported on a support material [34] recorded high reaction yield of ~90 % within 5 h. Another enhancement in terms of reactant molar ratio achieved in this reaction system was seen based on the methanol to oil ratio of ~22 compared to 70:1 as reported for a conventional stirring reactor system using the same type of catalyst [33-34]. Low acid value crude Jatropha oil was transesterified using an ultrasound-assisted process in the presence of Na/SiO_2 catalyst and the system achieved 98 % yield with a molar ratio of 9:1 [22]. The significant contribution of the solid acid catalyst in converting crude oil with high FFA and water content could be observed in this work.

The significant role of ultrasound in decreasing the required reaction temperature due to the generated heat during the collapse of the cavitation bubbles was also proven. Acid catalyzed biodiesel processes generally require high reaction temperature to reduce the viscosity of the reactants to achieve an acceptable level of mixing due to the slow reaction rate [35]. Without the need for extra heating in the current study, significant saving in the energy input of the process could be achieved. Significant reduction in the energy input requirement for the process due to low reaction time and reaction temperature is critical to the process.

4.2.6 Catalyst stability

Investigation on the stability of the catalyst under the ultrasonic reaction conditions in polar reaction mixture revealed that 9.6 % of the FAME yield was achieved under the optimum conditions due to the minimal leaching of $PW_{12}O_{40}^{3-}$ anion. Thus, the reaction was mostly heterogeneous in nature. Leaching of the active component from the catalyst occurred due to the partial dissolution of TPA in the polar reaction mixture and the exposure of the solid catalyst to direct ultrasonic effects. Compared with other immobilized TPA catalysts on different supports such as zirconia and silica [15], this catalyst showed minimal leaching attributed to the strong absorption of TPA on the alumina. The TPA catalyst stability towards leaching has also been demonstrated for the esterification of n-butanol with different alcohols [36] and alkylation of phenol [37].

The yields achieved in the successive reaction runs to investigate the potential for catalyst reusability are shown in Fig. 4.15. It can be concluded that a reduction of about 6.6 % of the optimum reaction yield was recorded for the first reuse. Second reuse of the catalyst showed 5.3 % a reduction in yield while almost similar reaction yields were achieved between the second and the third reaction runs. This reduction in activity could be attributed to the heteropoly anion leaching, bearing in mind that a washing step was conducted between the reuse cycles.

4.3 Cs based catalyst

4.3.1 Characteristics of Cs based catalyst

The FT-IR spectra of the synthesized catalysts are presented in Fig. 16. The spectrum of the parent TPA shows major bands attributed to the vibration of oxygen attached to phosphorous and tungsten of the adsorption mode of the Keggin ion $(PW_{12}O_{40})^{3-}$. In Fig. 1, four major bands at 800 cm^{-1} (W-O-W in the edge), 890 cm^{-1} (W-O-W in the corner), 980 cm^{-1} (W=O) and at 1,080 cm^{-1} (P-O) can be detected for the Keggin anion. Thus, the presence of Keggin anion could be confirmed as the obtained spectra could be clearly assigned to the typical vibrations of the parent TPA. The FT-IR results revealed that a good Keggin structure retention was achieved after the incorporation of cesium into the heteropoly cage structure.

The XRD patterns of the prepared catalysts and that of the parent TPA are presented in Fig. 17. For pure TPA, diffraction peaks at 18°, 23°, 25°, 30°, 35° and 38° attributed to the triclinic phase of TPA can be detected. Even though the crystalline nature can be observed for all catalyst samples, the diffraction peaks become significantly weaker and broader with increasing Cs^+ content in the prepared catalysts. The shifts of the peaks toward higher angles in the $Cs_xH_{3-x}PW_{12}O_{40}$ samples are consistent with the presence of the body-centered cubic structure of the alkaline salts. This gave the indication for the reduction of the triclinic crystallites size of TPA and the shrinkage of the lattice cell due to the incorporation of Cs^+ ion replacing $H^+(H_2O)_{n/3}$ in the parent TPA [18].

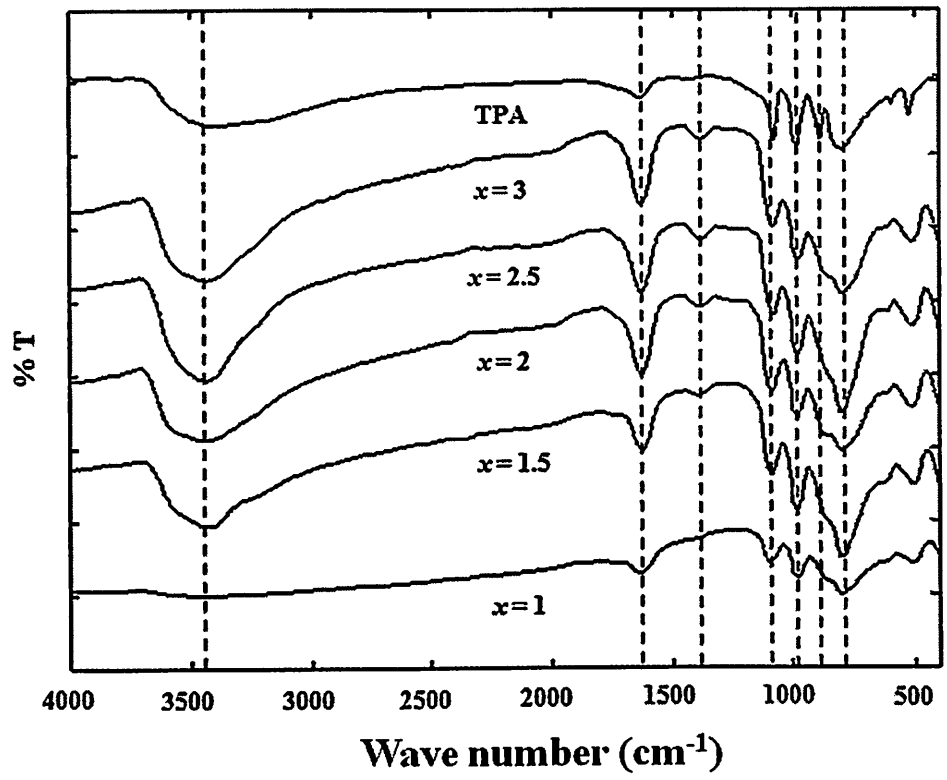

Fig. 4.16. FT-IR spectra of TPA and $Cs_xH_{1-x}PW_{12}O_{40}$ catalysts with different Cs to TPA ionic ratios.

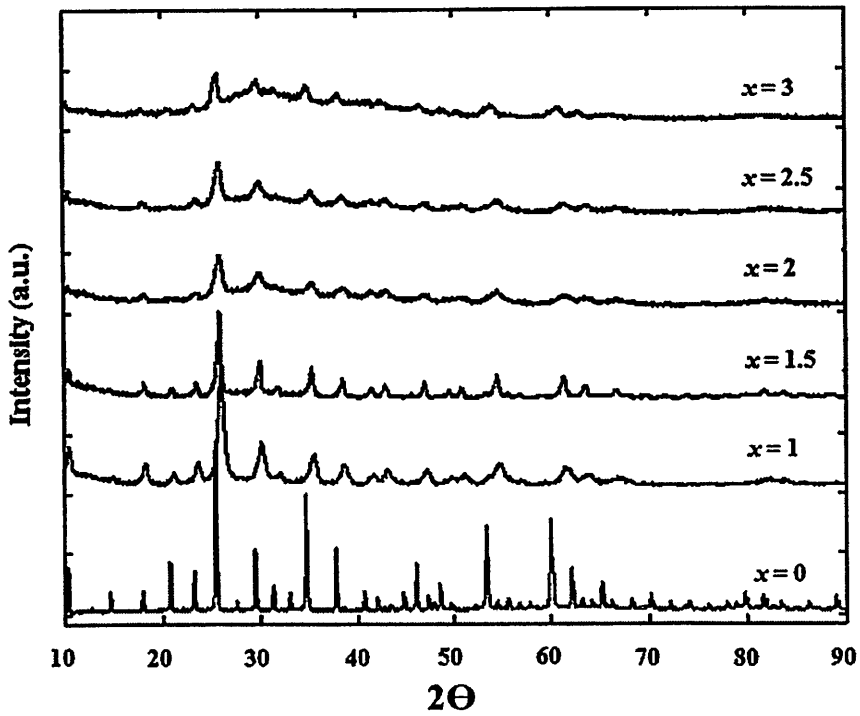

Fig. 4.17. XRD patterns of TPA and $Cs_xH_{1-x}PW_{12}O_{40}$ catalysts with different Cs to TPA ionic ratios.

The surface characteristics of the synthesized catalysts as well as the surface acidity are shown in Table 4.7. Tungstophosphoric acid itself has low surface area of about 1-2 m^2/g [19]. The surface area of the catalyst samples increased as the cesium content was increased for 'x' values larger than 2. This increment was ascribed to the changes in the morphology due to the aggregation of nanoparticles in the structure and voids that were formed between the aggregates. As the cesium amount was increased, the aggregates became denser and negatively affected the porous structure between the nanoparticles. Thus, a reduction in the specific surface area occurred. It could be concluded that the total pore volume of the prepared catalysts increased as the cesium content in the samples was increased. The increase in the pore volume could be attributed to increases in the voids that existed within the nanoparticles of the cesium doped catalysts.

Table 4.7. Surface properties and acidity of $Cs_xH_{1-x}PW_{12}O_{40}$ catalysts.

Sample	BET Surface area (m^2/g)	Total pore volume (cm^3/g)	Average pore diameter (Å)	Surface acidity (μmol/g)
$x = 1.0$	16.96	0.034	80.9	1850
$x = 1.5$	32.72	0.087	106.9	1760
$x = 2.0$	110.73	0.170	63.1	1680
$x = 2.5$	95.83	0.180	76.8	1290
$x = 3.0$	64.50	0.100	65.5	1180

Further information about the surface morphology of the prepared $Cs_xH_{3-x}PW_{12}O_{40}$ catalysts can be obtained from the SEM micrographs as presented in Fig. 4.18. The morphology of the catalysts was found to change as cesium ions successfully exchanged for hydrogen ion at an increasing ratio from 1 to 3. For an 'x' value of 1, the catalyst surface texture was more compact and smoother in its structure. As the cesium content was increased, the surface structure gradually changed to rather rough morphologies consisting of larger nanoparticles. A more porous structure was observed on the surface due to the aggregation of nanoparticles. As the Cs ratio was increased to ratios exceeding 2, these nanoparticles became denser leading to increasing surface roughness. Enormous amount aggregates were formed with less voids and pores between them.

The mechanism of aggregates formation could consist of three successive steps i.e.: the nucleation of the nanoparticles due to the interaction between Cs^{1+} and $PW_{12}O_{40}^{3-}$ free ions, the formation of aggregates as a result of the combination of these nanoparticles, and the growth of the aggregates due to the agglumeration of different nanoparticles [20]. Thus, increasing the Cs content doped into TPA led to an increase the aggregation in the structure as it increased the nucleation activity of nanoparticles which affected its crystallinity nature as observed in XRD results. Besides that, the agglomeration of the massive number of aggregates reduced the amount of voids and pores on the structure to result in a decrease in the specific surface area as observed in Table 3.

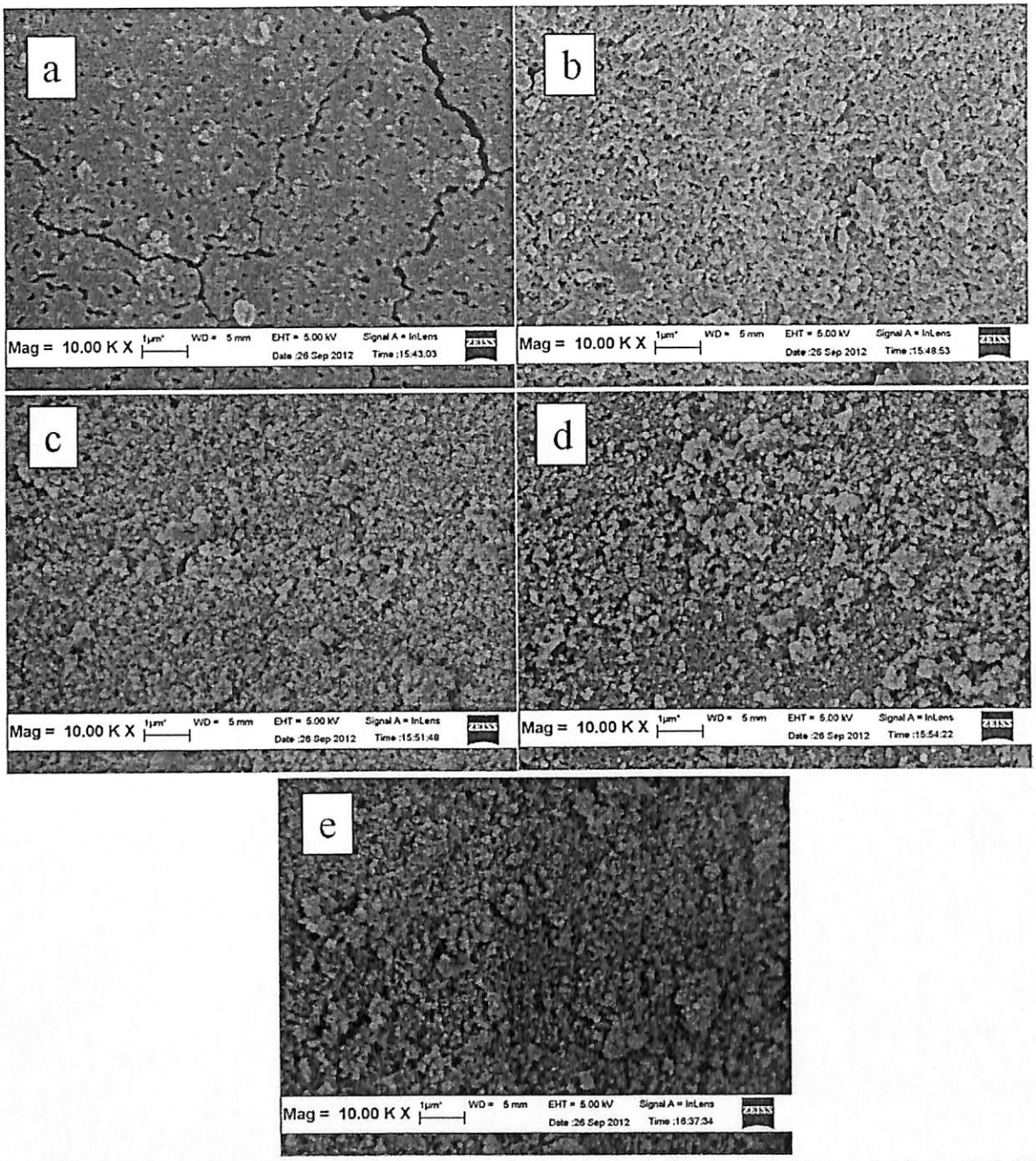

Fig. 4.18. SEM images of $Cs_xH_{1-x}PW_{12}O_{40}$ catalysts (a) $x = 1$ (b) $x = 1.5$ (c) $x = 2$ (d) $x = 2.5$ (e) $x = 3$.

The elemental compositions of the synthesized catalysts observed under EDAX are presented in Table 4.8 and the results proved the successful incorporation of Cs^{1+} ion into TPA structure. Discrepancies were also noticed between the stoichiometric tungsten to cesium ratio and the measured ratios. Nevertheless, the differences between the ratios were within an error range of ~6 % which indicated good agreement between the experimental and calculated ratios.

Table 4.8. Elemental compositions of $Cs_xH_{3-x}PW_{12}O_{40}$ catalysts used in this study.

Sample	Elemental analysis (wt. %)					
	Cs	W	P	O	W/Cs Calc.[a]	W/Cs Measured
$x = 1.0$	6.98	78.69	3.09	11.24	12.0	11.27
$x = 1.5$	9.31	75.50	5.14	10.04	8.0	8.11
$x = 2.0$	12.72	73.03	5.64	8.60	6.0	5.74
$x = 2.5$	16.74	71.27	5.88	6.11	4.8	4.59
$x = 3.0$	18.47	70.46	5.36	5.70	4.0	3.81

[a] Calculated tungsten to cesium ratio according to the stoichiometry.

4.3.2 Preliminary study

Blank experiments were carried out in order to investigate the effects of the absence of catalyst and the influence of ultrasonic irradiation on the reaction. The results revealed that for an ultrasound-assisted process without the presence of catalyst, significant transesterification reaction did not occur due to the absence of the catalytic active sites required. Besides that, no significant result was achieved with the presence of the solid acid catalyst under conventional stirring process due to short reaction time. It was recorded that for this acid catalyzed transesterification process, reaction times of up to 5-6 h were required to achieve significantly high yield due to low reaction rate [21].

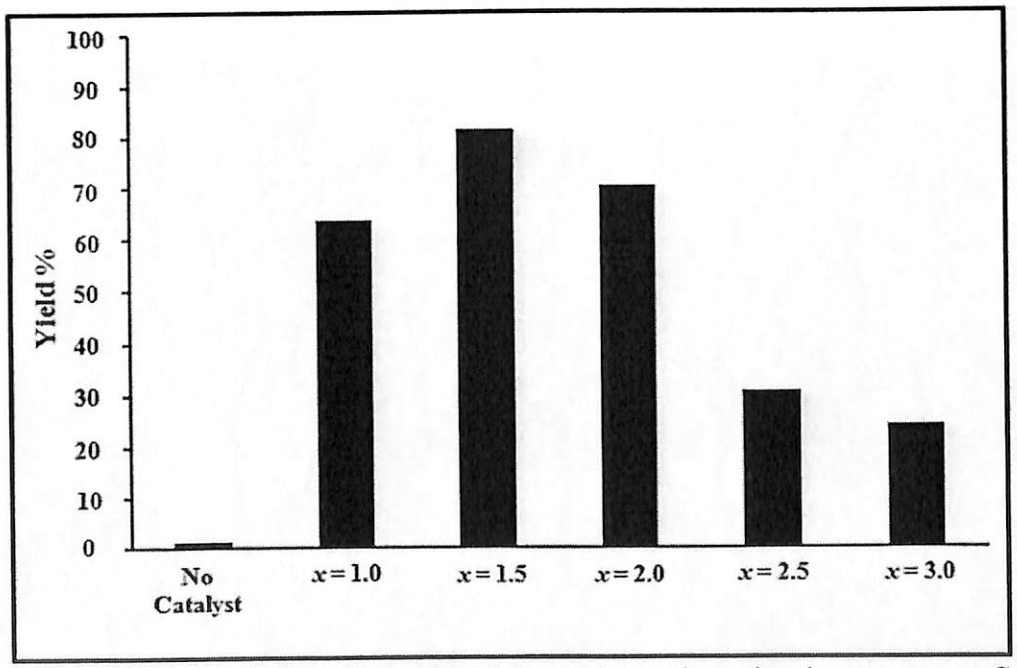

Fig. 4.19. Transesterification of Jatropha oil in an ultrasonic-assisted process over $Cs_xH_{3-x}PW_{12}O_{40}$ catalysts (reaction time 60 min, methanol/oil molar ratio 20:1, catalyst amount 4 % (w/w) and ultrasonic power of 75 %).

The effect of different Cs amounts doped into TPA on the transesterification yield under the preliminary reaction conditions are presented in Fig. 4.19. It can be observed that for Cs

ratios lower than 2, the catalytic activity showed higher values compared with when $x > 2$. This could be attributed to high surface acidity of the catalysts due to the presence of less Cs amounts and the absence of available protons in the catalyst in the case of higher Cs content catalysts. Catalyst with x=1.5 showed the best catalytic activity compared a catalyst with higher surface area when x=2 and higher acidity with lower surface area catalyst when x=1. The results revealed that the surface acidity played a more dominant role in the transesterification reaction rather than the catalyst surface area. For the catalyst with x=1.5, both the catalyst acidity and the surface area contributed in the high catalytic activity so that the catalyst was chosen for further investigations.

4.3.3 Statistical analysis

The experimental design matrix including the un-coded values, point types and the experimental response values is presented in Table 4.9. The design consisted of 30 experiments according to 2^k+2k+6, where k is the number of independent variables [22]. Twenty four experiments were improved by six replications at the center points to evaluate the pure error. Third order polynomial equation based on the coded values was obtained using multiple regression analysis of the experimental data. The choice of a cubical polynomial equation to describe the design was attributed to the high value of determination coefficient (R^2) that was achieved. The polynomial equation describing the system is given as follows;

Table 4.9. Central composite design matrix of four variables and respective responses.

Run	Point type	Real Variables				Yield (%)
		Time (min)	M/O[a]	Amplitude (%)	Catalyst Amount (w/w %)	
1	Fact	40	20	45	3.0	60.94
2	Fact	20	10	45	4.0	26.43
3	Fact	20	20	75	4.0	64.43
4	Fact	40	10	75	4.0	12.95
5	Fact	20	10	45	3.0	20.67
6	Fact	20	20	75	3.0	66.96
7	Fact	40	10	75	3.0	23.21
8	Fact	20	20	45	4.0	56.09
9	Fact	40	20	75	3.0	75.15
10	Fact	40	10	45	3.0	23.14
11	Fact	40	10	45	4.0	19.13
12	Fact	40	20	75	4.0	44.26
13	Fact	20	20	45	3.0	61.14
14	Fact	40	20	45	4.0	65.06
15	Fact	20	10	75	4.0	24.70
16	Fact	20	10	75	3.0	18.27
17	Axial	30	25	60	3.5	87.89
18	Axial	30	15	60	4.5	54.96
19	Axial	30	15	90	3.5	36.50
20	Axial	10	15	60	3.5	30.07
21	Axial	30	5	60	3.5	23.37
22	Axial	50	15	60	3.5	58.18
23	Axial	30	15	30	3.5	37.09
24	Axial	30	15	60	2.5	42.88
25	Center	30	15	60	3.5	41.68
26	Center	30	15	60	3.5	49.04
27	Center	30	15	60	3.5	42.38
28	Center	30	15	60	3.5	46.18
29	Center	30	15	60	3.5	44.13
30	Center	30	15	60	3.5	38.68

[a] Methanol to oil ratio.

$$Y = -609.89 + 2.24\,X_1 + 3.79\,X_2 - 0.94\,X_3 + 477.65\,X_4 - 0.25\,X_1^2 + 0.01\,X_3^2 - 147.92\,X_4^2 + 0.12\,X_1X_3 + 1.65\,X_1X_4 + 0.79\,X_3X_4 + 2.65 \times 10^{-3}\,X_1^3 + 14.13\,X_3^3 - 0.04\,X_1X_3X_4$$

Where, Y is the response (yield of FAME), and X_1, X_2, X_3 and X_4 are the values in the coded form of the studied variables.

The Fisher F-test value of 18.49 combined with very small probability value (Prop.>F <0.0001) as evaluated by the ANOVA statistical analysis of the design indicate high significance of the cubical equation to represent the experimental data as presented in Table. 4.10. It can be concluded from the determination coefficient (R^2 = 93.76 %) that the effect on the FAME yield could be mainly attributed to the variation in the independent variables and the remaining 6.24 % could be explained as residues.

Table 4.10. Analysis of variance (ANOVA) for the cubic model representing the ultrasound-assisted biodiesel production process.

Sources of variations	Sum of squares	Degrees of freedom	Mean square	F-value	Prob.>F
Model	9816.23	13	755.09	18.49	<0.0001
Residual	653.56	16	40.85	-	-
Lack of fit	562.92	11	51.17	2.82	0.1309
Pure error	90.64	5	18.13	-	-
otal	10469.78	29	-	-	-

R^2=0.9376, Adj. R^2=0.8869, C.V.=14.78, Std. Div=6.39

The significance of the reaction variables and interactions between them are summarized in Table 4.11. By virtue of experience, the larger the F-value and the smaller the Prob.>F, the more significant the corresponding variable was [23]. It can be observed that the molar ratio and catalyst amount had their significant effects on the reaction yield while the reaction time mostly had its influence in its single value. For a reversible reaction with low reaction rate such as the transesterification reaction, the presence of sufficient amounts of reactant had its noticeable influence on the reaction yield.

Table 4.11. Results of regression analysis for the third-order polynomial model and the estimated coefficients.

Model Parameters	F-value	Prob.>F
X_1	2.51	0.1328
X_2	210.79	<0.0001
X_3	0.015	0.9039
X_4	3.20	0.0925
X_1^2	0.82	0.3778
X_3^2	5.88	0.0275
X_4^2	0.0073	0.9331
X_1X_3	0.79	0.3873
X_1X_4	3.19	0.0931
X_3X_4	2.22	0.1558
X_1^3	8.26	0.0110
X_4^3	3.66	0.0737
$X_1X_3X_4$	3.02	0.1012

Molar ratio is the practical expression of the presence of reactants and in this study, it had significant influence on the studied design response. The catalyst amount was deemed to have a significant role in the current system as the presence of acid catalyst is generally required to drive the forward reaction, especially in the case of feed stocks with high FFA content. The interactions between reaction time and catalyst amount, between ultrasonic amplitude and catalyst amount as well as the triple interaction between the three variables had their significance influences. Besides that, the cubical forms of reaction time and catalyst amount showed positive

influence on the reaction yield. The other interactions and the square forms as presented in Table 7 were also considered to establish the historical design for the experimental data.

4.3.4 Interaction between reaction parameters

Three dimension response surfaces for the representation of the FAME yield combined with the interaction of the reaction variables are represented in Fig. 4.20. The interaction between the reaction time and the molar ratio while the other variables kept at their center values is presented in Fig. 5(a). It can be concluded that increasing the reaction time had its positive effects for all molar ratio values and vice versa. Low reaction yields with the presence of low methanol ratio for all reaction times were attributed to the insufficient methanol amount in the system to drive the forward reaction. For high reaction time and high molar ratios, the FAME yields showed maximum values attributed to the sufficient reaction time and adequate methanol amounts to support the reaction.

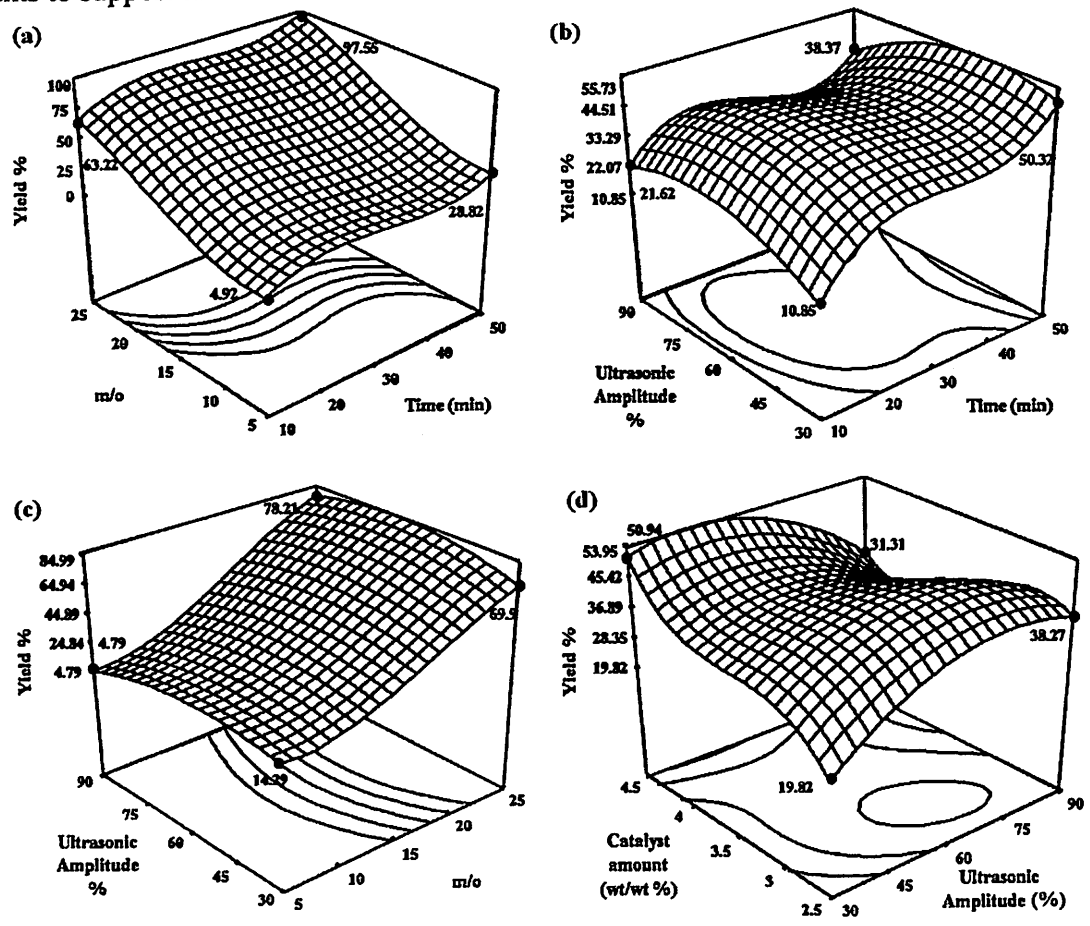

Fig. 4.20. Interactions between the reaction parameters. (a) between the reaction time and the methanol/oil ratio, (b) between the reaction time and the ultrasonic amplitude, (c) between the methanol/oil ratio and the ultrasonic amplitude, and (d) between the ultrasonic amplitude and the catalyst amount.

Unlike the response behavior at high reaction time, Fig. 4.20(b) shows a reduction in reaction response as ultrasonic amplitude was increased for high time values. It can be concluded

that at low reaction time, increasing ultrasonic amplitude led to an increase in the yield. It was attributed to the positive ultrasonic mixing effects in enhancing the contact between the reactants at the initial stages of reaction time. Meanwhile, increasing amplitude under high reaction time levels led to a decrease in the yield after a certain level of amplitude (~60 %). Subjecting the reacting mixture to high acoustic energy led to larger and stable cavitation bubbles which could act as barriers to the transfer of ultrasonic energy throughout the reaction mixture. So, poor mixing effects between the two immiscible layers resulted in low emulsification effects. Then, the transesterification reaction would take place at the boundary between the two layers. Similar behavior of ultrasound-assisted biodiesel production systems could be observed at high ultrasonic energy as reported in our previous work for an activated carbon-supported TPA catalyst [16]. Kumar et al. [24] and Stavarache et al. [25] also reported similar behavior for different ultrasound-assisted systems catalyzed by homogeneous catalysts.

The interaction between ultrasonic amplitude and the molar ratio presented in Fig. 5(c) indicates that for low reactant molar ratio, increasing the ultrasonic amplitude had negative effects on the response. This could be caused by severe mixing effect between the small FAME amounts (generated by low methanol amount) with the side product (glycerol). Meanwhile, slight increase in the reaction yield was observed when the ultrasonic amplitude was increased at high molar ratio. It was clear that at amplitude of ~ 60 %, the reaction yield reached its maximum level with the presence of high methanol ratio. This could be explained on the basis of increment in the sizes and numbers of the droplets which led to an increase the available interface area between the reactants [25].

Increasing ultrasonic amplitude had its positive effects on the reaction yield for all catalyst amounts to a level of 50-60 %. However, negative effects were observed beyond these levels as can be observed in Fig. 5(d). For catalyst amounts above 3.5 %, a decrease in the reaction yield was obtained when the ultrasonic amplitude was set beyond 60 % level. The increasing trend in the reaction yield under low to moderate ultrasonic amplitude could be attributed to the enhancement in the heterogeneous catalyst reactivity due to the ultrasonic dispersion of the reactants on the catalytic active sites of the catalyst. As the crucial factor of any heterogeneous catalyzed system is the contact between the reactants and the catalyst, the cavitational shear force generated by the ultrasonic irradiation created much smaller reactant droplets to improve the interaction between the reactants and the catalyst. This, in turn, increased the available surface area for the reactants and led to the enhancement in the reaction yield. The role of moderate ultrasonic amplitude was also reported for different ultrasound-assisted catalytic processes [24-26]. In contrast, for high ultrasonic amplitude, the effects of large, long lived and stable cavitational bubbles had dominant negative influence on the emulsification process regardless of the presence of higher number of acid active sites in the catalyst system.

4.3.5 Process optimization

In order to identify the optimum reaction conditions and to investigate the validity of the proposed design, Design expert 6.0.6 software was used to fit the experimental data to the historical design. 10 possible solutions for the design were generated according to the order of suitability relating the proposed reaction variables value with the expected transesterification yield. Three solutions were chosen and the corresponding experimental runs were conducted as presented in Table 4.12. The experimental results were in good agreement with the predicted yields within ~ 4 % of error.

Table 4.12. Predicted and experimental results at the optimum conditions for model validation.

Run	Reaction conditions				Predicted yield (%)	Experimental Yield (%)	Error (%)
	Time (min)	Molar ratio	Amplitude (%)	Catalyst loading (w/w)			
1	40	24.98	73	2.64	89.51	91.43	2.15
2	33.14	25	67	2.94	87.06	90.46	3.90
3	49.44	24.13	56	3	95.56	93.06	2.62

It could be observed that the effect of catalyst combined with the ultrasonic mixing improved the transesterification for high FFA content crude Jatropha oil. $Cs_{1.5}H_{1.5}PW_{12}O_{40}$ solid acid catalyst powered by moderate ultrasonic amplitude of 67 % was deemed to have its good influence on an acid catalyzed system to achieve 90.46 % of FAME yield in just ~34 min of reaction. $Cs_{2.3}H_{0.7}PW_{12}O_{40}$ has been used for the esterification of palmitic acid and transesterification of tributyrin conducted at 6 h of reaction time under conventional process to achieve conversions of 100 % and 50.2 %, respectively [27]. In a related case, esterification of rice bran fatty acids conducted by Srilatha et al. [28] achieved 92 % conversion using $Cs_1H_2PW_{12}O_{40}$ within 200 min of reaction. Low reaction yields were reported by Zieba et al. [29] for the transesterification of castor oil with methanol conducted for 180 min at a molar ratio 29:1 using $Cs_2H_1PW_{12}O_{40}$ and $K_2H_1PW_{12}O_{40}$ catalysts.

The significant role of ultrasound in allowing the transesterification reaction to be carried out at relatively low reaction temperature was also due to the generated heat during the collapses of the cavitation bubbles. Acid-catalyzed biodiesel production generally requires high reaction temperature to reduce the viscosity of the reactants in order to obtain an acceptable level of mixing due to the slow reaction rate [6]. Significant saving in the energy input of the process could be achieved as extra heating requirement was not needed in the current study. Significant reduction in the energy input requirements for the process was achieved due to short reaction time and low reaction temperature needed for the process.

4.3.6 Catalyst stability and reusability

The catalyst stability towards leaching is associated by the dissolution of the active component of the catalysts due to the contact with polar reaction mixture. The test revealed that 9.2 % of reaction yield was obtained by the leached $PW_{12}O_{40}^{3-}$ anion from the catalyst structure. Shin et al. [30] reported different leaching levels for Cs doped TPA catalysts under super critical methanol process. Catalyst stability was also verified by Narasimharao et al. [27] who performed leaching tests in hot methanol. The results revealed that low Cs content catalysts showed higher tendency toward leaching while materials with higher Cs content were more stable which confirmed their heterogeneous mode of reaction. Low leaching amount of Cs salt of TPA in water was also reported by Yuan et al. [31].

Fig. 4.20 shows the FAME yields of successive reaction runs to reveal the potential for catalyst reusability. It can be concluded that only 3.8 % of the catalytic activity was lost in the

first run. For the second and third runs, 2.7 % and 1.6 % drops were observed, respectively. These reductions could be attributed to the heteropoly anion leaching and the washing process that was conducted between the cycles. Thus, under ultrasonic irradiation conditions and in polar reaction mixture, $Cs_{1.5}H_{1.5}PW_{12}O_{40}$ demonstrated good catalytic stability and low leaching behavior.

5. Conclusions and Suggestions

Ultrasound-assisted transesterification of crude Jatropha oil in the presence of TPA based catalysts was successfully studied. The catalysts were tested for their activity in FAME production from non edible oil feed stock with high FFA content of 10.5 % w/w oil. TPA immobilized on activated carbon, gamma-alumina or in the form of cesium salt were used in this study. Different TPA loadings on the supported catalysts and different cesium doped TPA ratios were characterized to evaluate the presence of the heteropoly anion in the prepared catalysts.

Effects of PW12O403- anion inclusion in the mesopouros structure of the supported catalysts were seen as a reduction in the supports surface areas i.e. reduction of 18.4 % in the case of activated carbon supported catalyst and 34 % in the case of gamma-alumina supported catalyst. Changes in the specific surface areas for different Cs to heteropoly anion ratios were noticed for Cs salt catalysts and attributed to the changes in the catalysts morphology. The presence of the Keggin anion on the supports and within the salt structure was further proven using Raman spectra which showed characteristic bands attributed to the symmetric stretching of the heteropoly anion bands. Further characterization techniques i.e. XRD, FT-IR and ICP were also conducted to elucidate further useful information on the characteristics of the prepared catalysts.

Testing different TPA loadings and cesium molar ratios for transesterification of crude Jatropha oil under preliminary ultrasound-assisted process conditions was conducted. The results revealed that TPA20-AC, TPA25-Al and Cs1.5HPW catalysts recorded the FAME yields of 72.62%, 64.34% and 81.33 %, respectively. According to these results, the mentioned catalysts were used for the following studies. The optimization of the reaction conditions were successfully conducted by applying CCD design with the ranges of variables of 10-50 min for reaction time, methanol to oil ratio of 5:1-25:1, ultrasonic amplitude of 30-90 %, and catalyst amount of 2.5-4.5 w/w oil. The optimization study revealed that the optimum reaction conditions were different for each catalyst. TPA20-AC catalyst achieved the highest FAME yield of 91.34 % within 38 min of reaction time, while Cs1.5HPW achieved 90.46 % of FAME yield within the shortest reaction time of 34 min. While TPA25-Al was able to produce FAME yield of 83.63 % within 47 min of reaction time with 19:1 for the reactants molar ratio.

Investigating the catalysts stability and reusability potential against the exposure to the direct ultrasonic irradiation and the contact with polar reaction mixture was also studied. The results revealed that Cs1.5HPW catalyst showed the highest reusability potential with minimal leaching tendency. This was attributed to its structure where the Cs was successfully inserted within the heteropoly anion structure providing more stability to the catalyst. Reasonable results were achieved with TPA25-Al catalyst while the lowest reusability potential and highest leaching were recorded by TPA20-AC catalyst.

The influence of the variation in the water and FFA contents in the crude Jatropha oil used in this study was investigated for the catalysts each under its optimum reaction conditions.

The FFA contents were increased as 16, 16.7, 17.5 and 18.3 w % while the water contents were varied at a range of 0.5, 1 1.5 and 2 w %. The results revealed that Cs1.5HPW showed the least sensitivity towards increasing FFA or water contents in the feed stock and the activity was the highest in catalyzing simultaneous esterification and transesterification reactions.

The catalysts were also investigated for other types of non-edible vegetable oils i.e. batch with 38 % FFA content Jatropha oil, crude palm oil and waste cooking palm oil. The results revealed that the synthesized catalysts were able to provide promising transesterification reactions with relatively high FAME yields for the case of waste and crude palm oils. In the case of very high FFA content Jatropha oil, the reaction yields were relatively low because of the generation of high amount of water due to the significant esterification reaction.

Ultrasonic irradiation was proven to be a successful technique used to enhance the emulsification between the reactants increasing the mass transfer rate during the reaction. This enhancement was materialized in the current study by the relatively short reaction time (less than 50 min) compared to conventional production process which required few hours. Reductions in catalyst amount, methanol to oil ratio and reaction as well as reaction temperature (which was 65 OC) were also achieved. The ultrasonic energy provided significant heat amount due to the local hotspots generated in the reaction mixture. This modified the course of the transesterification reaction that consequently eliminated the requirement for external heating in the production process. Thus, a significant improvement in the production economics could be resulted.

Mathematical modeling and kinetic studies were also accomplished in the current study for the three catalysts each under its optimum reaction conditions. The rate of the reaction was determined through the kinetics study for each catalytic system. The activation energy was then estimated taking into consideration the presence of methanol as significant parameter in the process kinetics approach.

A few recommendations can be made for future research work in the research area based on the current research findings:

i) Other types of heteropolyacid based catalyst can be investigated in the ultrasound-assisted transesterification process such as H3PMo12O40, H4SiW12O40 and H4SiMo12O40 immobilized on activated carbon or gamma-alumina to investigate the role of other types of heteropoly anions in the reaction.

ii) Other types of support materials i.e. SPA15, SiO2 and ZrO2 are also suggested to host the TPA active component and used in the reaction to investigate the strength of interaction between the acid sites and the supports as well as the effects of the polar nature of the reaction mixture and the ultrasonic impact on the catalysts.

iii) Ions such as Ba2+, Ag1+ and NH41+ are proposed to be exchanged into TPA to produce other types of doped catalysts to be used in the ultrasound-assisted transesterification reaction.

iv) As ultrasonic irradiation enhances the transesterification reaction in terms of reaction time and reaction temperature, thus, continuous ultrasound-assisted process catalyzed by heteropolyacid based catalysts is suggested for further study.

v) A simple purification process was attempted on the produced FAME mixture in the current study. A study on further purification processes is proposed to be conducted on the product to eliminate the residual methanol and FFA from the product mixture.

6. Acknowledgements

A Research Universiti grant (814144) to support this research work is gratefully acknowwledged.

7. References

[1] Kumar D, Kumar G, Poonam, Singh CP. Ultrason Sonochem. (2013);17:839-44.
[2] Sharma YC, Singh B, Upadhyay SN. Fuel. (2012);87:2355-73.
[3] Thangavadivel K, Megharaj M, Smart RSC, Lesniewski PJ, Naidu R.. J Hazard Mater. (2014);168:1380-6.
[4] Leung DYC, Wu X, Leung MKH. Appl Energ. (2015);87:1083-95.
[5] Marchetti JM, Miguel VU, Errazu AF. Renew Sust Energ Rev. (2013);11:1300-11.
[6] A.Z. Abdullah, A.H. Kamaruddin, N. Razali, H. Abdullah and S. Bhatia, (2007) Sci Technol Adv Mater 8, pp. 249-256.
[7] Vyas AP, Verma JL, Subrahmanyam N. Fuel. (2014);89:1-9.
[8] Santos FFP, Malveira JQ, Cruz MGA, Fernandes FAN. Fuel. (2013);89:275-9.
[9] Jokanovic V, Spasic AM, Uskokovic D. J Colloid and Interf Sci. (2014);278:342-52.
[10] Ahmad Zuhairi Abdullah, Salamatinia B, Mootabadi H, Bhatia S. Energy Policy. (2009);37:5440-8.
[11] Hanh HD, Dong NT, Okitsu K, Maeda Y, Nishimura R. Jpn J Appl Phys, Part 1: Regular Papers and Short Notes and Review Papers. (2012);46:4771-4.
[12] Leung DYC, Guo Y. Fuel Proces Technol. (2012);87:883-90.
[13] Prokhorov VM, Blank VD, Pivovarov GI. Physics Procedia. (2015);3:63-8.
[14] Nikolic S, Mojovic L, Rakin M, Pejin D, Pejin J. Food Chem. (2013);122:216-22.
[15] Ahmad Zuhairi Abdullah, N. Razali, H. Mootabadi B. Salamatinia, (2007) Envir Res Lett, 2, pp. 1-6.
[16] Colucci JA, Borrero EE, Alape F. J Am Oil Chem Soc. (2015);82:525-30.
[17] Deshmane VG, Gogate PR, Pandit AB. Ind Eng Chem Res. (2009);48:7923-7.
[18] Bowman, D. Hilligoss, S. Rasmussen, R. Thomas, Hydrocarbon Processing, Feb 2006.
[19] Ji J, Wang J, Li Y, Yu Y, Xu Z. Ultrasonics. 2006;44:e411-e4.
[20] Tang W, Liu Q, Wang X, Wang P, Zhang J, Cao B. Ultrasonics. (2013);49:786-93.
[21] Tachibana K, Feril Jr LB, Ikeda-Dantsuji Y. Ultrasonics. (2015);48:253-9.
[22] Virot M, Tomao V, Le Bourvellec C, Renard CMCG, Chemat F. Ultrason Sonochem. (2012);17:1066-74.
[23] de la Fuente-Blanco S, Riera-Franco de Sarabia E, Acosta-Aparicio VM, Blanco-Blanco A, Gallego-Juárez JA. Ultrasonics. (2015);44:e523-e7.
[24] Chemat F, Grondin I, Shum Cheong Sing A, Smadja J. Ultrason Sonochem. (2004);11:13-5.
[25] Ashokkumar M, Sunartio D, Kentish S, Mawson R, Simons L, Vilkhu K, et al. Innov Food Sci Emerg. (2012);9:155-60.
[26] Rosenthal I, Sostaric JZ, Riesz P. Ultrason Sonochem. (2016);11:349-63.
[27] Mason TJ. Prog Biophys Mol Bio.(2007) 93:166-75.

[28] Babak Salamatinia, Hamed Mootabadi, Subhash Bhatia, Ahmad Zuhairi Abdullah, (2010) Fuel Proces Technol, 91(5), 441-448.
[29] Hamed Mootabadi, Babak Salamatinia, Subhash Bhatia, Ahmad Zuhairi Abdullah. (2010) Fuel, 89 (8), 1818-1825.
[30] Ahmad Zuhairi Abdullah, Razali N, Lee KT. (2009) Fuel Process Technol.90:958-64.
[31] Lam MK, Lee KT, Mohamed AR. Biotechnol Adv.(2014) 28:500-18.
[32] Sekiguchi K, Sasaki C, Sakamoto K. Ultrason Sonochem. (2011);18:158-63.
[33] Zabeti M, Wan Daud WMA, Aroua MK. Fuel Process Technol. (2009);90:770-7.
[34] J.A. Melero, G. Vicente, G. Morales, M. Paniagua, J.M. Moreno, R. Rolda´n, A. Ezquerro, C. Pe´rez (2015). Applied Catalysis A: General, 32, 556-563.
[35] Vicente G, Martínez M, Aracil J. Bioresour Technol. (2007);98:1724-33.
[36] Kian Fei Yee, Keat Teong Lee, Riccardo Ceccato, Ahmad Zuhairi Abdullah, (2011) Bioresour Technol, 102 (5), 4285-4289.
[37] Ahmad Zuhairi Abdullah, Mohamad Zailani Abu Bakar , Subhash Bhatia, (2006), J Ind. Technol, 15 (2), 77-89.
[38] Georgogianni KG, Kontominas MG, Pomonis PJ, Avlonitis D, Gergis V. Fuel Process Technol. (2012);89:503-9.
[39] Wang Y, Ou S, Liu P, Xue F, Tang S. J Mol Catal A-Chem. (2012);252:107-12.
[40] Stavarache C, Vinatoru M, Nishimura R, Maeda Y. Ultrason Sonochem. (2015);12:367-72.
[41] Ferella F, Mazziotti Di Celso G, De Michelis I, Stanisci V, Vegliò F. Fuel. (2012);89:36-42.

oooOOOooo

Renewable and Sustainable Energy Reviews 16 (2012) 2671–2686

Contents lists available at SciVerse ScienceDirect

Renewable and Sustainable Energy Reviews

journal homepage: www.elsevier.com/locate/rser

Critical review on the current scenario and significance of crude glycerol resulting from biodiesel industry towards more sustainable renewable energy industry

Muhammad Ayoub, Ahmad Zuhairi Abdullah*

School of Chemical Engineering, Universiti Sains Malaysia, Engineering Campus, 14300 Nibong Tebal, Penang, Malaysia

ARTICLE INFO

Article history:
Received 22 April 2011
Received in revised form 12 January 2012
Accepted 14 January 2012

Keywords:
Crude glycerol
Biodiesel industry
Purification processes
Market value
Supply and demand
Outlook

ABSTRACT

Biodiesel production through transesterification of vegetable oils and animal fats is rapidly increasing due to strong governmental policies and incentives. However, corresponding increase in the production of crude glycerol causes mixed effects. Sustainable biodiesel production requires optimization of its production process and drastic increase in the utilization of glycerol. High biodiesel yields and low environmental impacts, with respect to needless waste streams are mandatory. As such, upgrading of crude glycerol to highly pure glycerol and subsequent utilization of the product in producing value-added products are emerging research areas. International crude glycerol market is still at an early and very unstable stage. Globally, future conditions for an international market will largely be decided by supply and demand of glycerol for its utilization in conventional and newly developed industries. This paper highlights the current scenario on glycerol production from biodiesel industry, its global market and its new emerging outlets as commodity chemicals.

Contents

* Corresponding author. Tel.: +60 4 599 6411; fax: +60 4 594 1013.
E-mail addresses: chzuhairi@eng.usm.my, azuhairi@yahoo.com (A.Z. Abdullah).

1364-0321/$ – see front matter © 2012 Elsevier Ltd. All rights reserved.
doi:10.1016/j.rser.2012.01.054

1. Introduction

The unexceptional opportunities have created in recent decades to replace petroleum derived materials with bio-based alternatives due to rapid depletion of fossil of fuels and its escalating prices. Petroleum is a non-regenerative source of energy and it is also an important resource of the modern society for its requirement in applications other than power like household products, clothing, agriculture, as a basic materials for synthetic materials and chemicals. Nowadays, fuel crisis has globally flounced the economy in every region, particularly the oil consuming countries due to the rapidly decreasing available global stocks. Due to this serious situation, biodiesel which comes from 100% renewable resources provides an alternative fuel option for future.

The annual biodiesel consumption in the United States was 15 billion liters in 2006. It has been growing at a rate of 30–50% per year to achieve an annual target of 30 billion liters at the end of year 2012 [1]. According to the same report by National Biodiesel Board, there were 105 biodiesel production facilities operating in the United States in 2007, and 77 other facilities were in the planning or construction stage. If all of these facilities are realized, the estimated US biodiesel production capacity will exceed 9.5 billion liters. This level of production will yield nearly 1.2 million metric tons of crude glycerol, the primary co-product of the biodiesel production process.

Purification of crude glycerol to a chemically pure substance results in a valuable industrial chemical. However, purification is costly and the glycerol market is already saturated. Thus, the price of crude glycerol continues to decline and directly affect on biodiesel production cost. This trend will continue as more biodiesel production facilities begin production. According to a report [2], the biodiesel production cost ranges from $0.17 to $0.42 per liter over the last decade. Today, plenty of glycerol stock is available in the world market and its price is declining day by day. The price of pure glycerol varied from $0.50 to $1.50/lb and crude glycerol from $0.04/kg to $0.33/kg over the past few years [3]. The price of glycerol in the market will continue to drop in such an over saturated market. Currently, the main supply of glycerol coming into the market is from the rapidly growing biodiesel industry.

Basically, the continuously high prices of glycerol make it worthwhile for users to be reformulated to some alternative materials such as sorbitol and synthetic glycerol. Meanwhile, sustained low prices encouraged its use in other applications. The impact of the additional huge quantity of glycerol on its prices is not clear. However, it is likely that if new uses for glycerol are not found, the glycerol price may drop to a level that even justify its use as a burner fuel, which cost is usually about 5 cents/lb. This also implies that the overproduction of low grade glycerol would impact the viability and overall economy of biodiesel production [4], market price stability of current crude glycerol as well as environmental concerns due to improper disposal of glycerol [5]. The high biofuel prices and historically low glycerol prices are two main factors that drive researchers to discover new applications of glycerol and provide an ideal platform for chemical and pharmaceutical industries.

The objective of this work is to provide a critical review on the formation and current scenario of crude glycerol resulting from biodiesel production and to provide an insight into the impact of this crude glycerol over the biodiesel production cost itself. The study also provides a view of glycerol market and its new outlets at present and future with respect to the production of glycerol-based value-added products.

2. Properties of glycerol

Glycerol, commonly known as glycerin is a major by-product of biodiesel manufacturing process. Generally, approximately 4.53 kg of crude glycerol is created for every 45.3 kg of biodiesel produced [6]. Glycerol is a material of outstanding utility with many areas of application. A unique combination of physical and chemical properties of glycerol makes it technically versatile product which is readily compatible with many other substances and easy to handle. Glycerol is also virtually nontoxic to human health and also to environment [7]. Physically, glycerol is a water-soluble, clear, almost colorless, odorless, viscous, hygroscopic liquid with a high boiling point. Chemically, glycerol is a trihydric alcohol, capable of reacting as an alcohol, yet stable under most conditions. A list of physical and chemical properties which are important for its applications is shown in Table 1 [8]. Glycerol finds application in a broad diversity of end users.

A glycerol molecule has three hydrophilic hydroxyl groups that are responsible for its solubility in water and its hygroscopic nature. Therefore, it is actually has multipurpose substance in many applications. Glycerol can be used as a renewable source for biodegradable products and also find applications in green refinery process. It may have a great environmental value demanded by modern society who favors the non-dependence on depleting sources of petroleum and fossil fuel feedstock.

Table 1
Physical and chemical properties of glycerol [8].

Properties	Values	
Chemical formula	$CH_2OH–CHOH–CH_2OH$	
Formula weight	92.09	
Form and color	Colorless and liquid	
Specific gravity	$1.260^{50/4}$	
Melting point	17.9 °C	
Boiling point	290 °C	
Solubility in 100 parts		
Water	Infinity	
Alcohol	Infinity	
Ether	Insoluble	
Heat of fusion at 18.07 °C	47.49 cal/g	
Viscosity of liquid glycerol		
At 100% purity	10 cP	
At 50% purity	25 cP	
Diffusivity in	(DL × 10^5 sq cm/s)	
i-Amyl alcohol	0.12	
Ethanol	0.56	
Water	0.94	
Specific heat in aqueous solution (mol%)	15 °C (cal/g °C)	30 °C (cal/g °C)
2.12	0.961	0.960
4.66	0.929	0.924
11.5	0.851	0.841
43.9	0.670	0.672
100	0.555	0.576

Table 2
Typical elemental analysis result of crude glycerol from biodiesel industry [9].

Elements	Weight%	Standard deviation
Carbon (C)	52.77	1.703
Hydrogen (H)	11.08	0.051
Nitrogen (N)	<0.0001	<0.0001
Sulfur (S)	–	–
Balance oxygen (O)	36.15	–

Table 3
Quality parameter of different categories of glycerol [11].

Parameter	Crude glycerol	Purified glycerol	Refined/ commercial glycerol[a]
Glycerol content (%)	60–80	99.1–99.8	99.2–99.98
Moisture contents (%)	1.5–6.5	0.11–0.8.	0.14–0.29
Ash (%)	1.5–2.5	0.054	<0.002
Soap (%)	3.0–5.0	0.56	N/A
Acidity (pH)	0.7–1.3	0.10–0.16	0.04–0.07
Chloride(ppm)	ND	1.0	0.6–9.5
Color (APHA)	Dark	34–45	1.8–10.3

[a] Ref. [12].

2.1. Characteristics of glycerol

Glycerol is a material of choice mainly because of its physical characteristics, while some other uses rely on its chemical properties. Table 2 shows the typical elemental analysis of crude glycerol generated by biodiesel industry indicating that the major elemental contents of this material are C, H, and O. The high value of the carbon content (52.77%) in glycerol make it renewable energy source for various applications while second high value of oxygen content (36.15%) suggests that it is indeed a valuable compound.

The word 'glycerin' generally applies to purified commercial products containing more than 95% of glycerol while the word 'glycerol' often specifically refers to the chemical compound of 1,2,3-propanetriol and to the anhydrous content in a glycerin product or in a formulation. Concentration is usually by weight and is normally obtained by conversion from specific gravity measurements made at either 20/20 °C or 25/25 °C [10]. In addition, glycerol can be categorized into three main types, i.e. crude glycerol, purified/refined glycerol and commercially synthesized glycerol. The major differences between these three types of glycerol from biodiesel industry can be explained by their properties as shown in Table 3. It is clear from this table that differences between purified and commercial glycerol are minor while major differences can be found between crude glycerol and purified glycerol. Actually, the purified or refined glycerol is often prepared close to the quality of commercial synthesized glycerol due to its use in sensitive materials like medicine, food and cosmetic products. It is also noted in Table 2 that crude glycerol is of 60–80% purity compared with purified or synthesis glycerol which is generally close to 100% pure [11]. Similarly, moisture, ash and soap contents are present at higher quantity in crude glycerol. The acidic value of crude glycerol is slightly higher than others and color is also dark which may due to the presence of these impurities along with some other minor impurities.

A purified or refined glycerol from crude glycerol from biodiesel industry is generally sold as 99.5–99.7% pure in the market. The common purified glycerol available in the market is manufactured to meet the requirements of the United States Pharmacopeia (USP) and the Food Chemicals Codex (FCC). However, technical grades of glycerin that are not certified as USP or FCC are also available in the market. Therefore, the quality of purified glycerol can be identified by its grade. This type of glycerol can be divided into three basic grades on the basis of purity and potential end-uses as shown in Table 4. This table also provides the basic source of each divided glycerol category and application fields for each category of glycerol.

Table 4
Commercially available basic grade of purified glycerol [13].

Grade	Type of glycerol	Preparation and usage
Grade-I	Technical grade ~99.5%	Prepared by synthetic process and used as a building block for various chemicals but not applicable to food or drug formulation
Grade-II	USP grade 96–99.5%	Prepared from animal fat or plant oil sources, suitable for food products, pharmaceuticals and cosmetics
Grade-III	Kosher or USP/FCC grade 99.5–99.7%	Prepared from plant oil sources, suitable for use in kosher foods and drinks

As a matter of fact, the cheap production of biodiesel would entail surplus glycerol production (80–88% purity) that does not meet the purity of crude glycerin of industrial grade (98% purity) [14]. Crude glycerol originating from biodiesel industry is expensive to be purified to above 99% for use in food, pharmaceuticals, or cosmetics industries. The refined glycerol market looks strong as compare to crude glycerin market and it may be due to its new feed and chemical applications.

It can be concluded that in the current scenario of glycerol market, there are different types of glycerol available in open market. The types of glycerol depend on the purity that will directly affect the end uses like food, pharmaceutical, cosmetics or chemical components preparation. It is also a notable point that majority of purified glycerol products are currently based on crude glycerol resulting from biodiesel production.

2.2. Glycerol formation from biodiesel production process

Traditionally, glycerol is obtained from four different processes, i.e. soap manufacture, fatty acid production, fatty ester production and microbial fermentation [15,16]. However, it can also be synthesized from propylene oxide [15]. The reactions for the direct transformation of vegetable oils and animal fats into methyl esters and glycerol have been known for over a century. Transesterification of triglycerides such as rapeseed, palm, soybean and sunflower oils has gained significance for the role in the manufacture of high quality biodiesel fuel [17,18]. Several other chemical and enzymatic processes to produce fatty acid methyl esters from vegetable oil are now commercially available [19].

Actually, glycerol is widely available and is rich in functionalists. Glycerol is found naturally in the form of fatty acid esters. It is also an important intermediate in the metabolism process of living organisms [15]. The most common way to produce biodiesel is to transesterify triacylglycerols in vegetable oil or animal fats with an alcohol in the presence of alkali or acid catalyst [20]. Methanol is the most commonly used alcohol for this process due to its low cost. This process involves the removal of the glycerin from vegetable oil or fat. During this process, methyl esters are separated as the desired product while glycerin is left behind as the by-product. Crude glycerol is normally generated at the rate of one mol of glycerol for every three mol of methyl esters synthesized. Approximately, it constitutes about 10 wt.% of the total product during the biofuel production [21].

Fig. 1 shows the basic formation of crude glycerol during the transesterification process [17]. Generally, 3 mol of methanol reacts in three steps with glycerides in the presence of catalyst to form methyl esters and glycerol. In first step methanol reacts with triglycerides to form diglycerides and methyl ester and then methanol reacts again with diglycerides to form monoglyrides and methyl ester. These monoglycerides then react again with

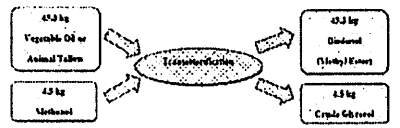

$$\text{Triglycerides} + CH_3OH \rightleftharpoons \text{Diglycerides} + R_1COOCH_3$$
$$\text{Diglycerides} + CH_3OH \rightleftharpoons \text{Monoglycerides} + R_2COOCH_3$$
$$\text{Monoglycerides} + CH_3OH \rightleftharpoons \text{Glycerol} + R_3COOCH_3$$
(Biodiesel)

$$\text{Triglycerides} + 3\,CH_3OH \rightleftharpoons \text{Glycerol} + \text{Methyl Esters (Biodiesel)}$$

* Where R_1, R_2, R_3 are hydrocarbon chain containing 15 to 21 carbon atoms

Fig. 1. Formation of crude glycerol during transesterification process [17].

methanol to form finally glycerol and methyl esters. It is also clear in the process scheme that glycerol is produced with biodiesel at a ratio of 1:10, i.e. for every 45.3 kg of biodiesel, 4.53 kg of crude glycerol is produced. Worldwide biodiesel industry's expansion is practically limited by high capital costs for glycerol refinery. The low value crude glycerol generally has 80–88% purity and needs further purification steps to meet the purity of industrial grade glycerol (99% purity).

It can be concluded that the planned massive increase in the production of biodiesel may inevitably lead to a large oversupply of crude glycerol. Some producers of synthetic glycerol have already responded to this by closing their units which may not compete under these market pressures. If the production of biodiesel continues with this trend rapidity, it might be possible that the potential annual glycerol surplus will touch its peak within the next few years.

2.3. Impurities in crude glycerol from biodiesel industry

Crude glycerol has low economic value due to the presence of various impurities. Common impurities in crude glycerol resulting from biodiesel industry are such as moisture, ash, soap and chloride contents. These impurities along with acidity and color intensity are also shown in Table 3. Sometimes, these impurities also include residual methanol especially when the alcohol is used in excess to drive chemical transesterification and total recovery of entire methanol is not achieved. On the other hand, some free fatty acids present in the initial feedstock can react with alkalis to form soaps, which are soluble in the glycerol layer.

According to a report, crude glycerol from biodiesel industry contains carbon content at an average of about 25% and a small quantity of metals like Na, Ca, K, Mg, Na, P, and S could also present. The quantities of these metals except Na usually present in the range of 4–163 ppm while sodium content could exceed 1%. Other than metals, crude glycerol from the transesterification process also contains proteins (0.06–0.44%), fats (1–13%) and carbohydrates (75–83%) [22]. It generally consists of about 65–80% glycerol. Some biodiesel plants are reported to produce crude glycerol which consists of more than 80% glycerol, depending on specific manufacturing processes. Refined glycerol has about 99.5% purity, after undergoing a highly energy intensive refining process [23]. Gonzaler-Pajuelo et al. [24] and Mu et al. [25] also reported that glycerol could made up anywhere from 65% to 85% (w/w) of the crude glycerol streams.

The process of refining glycerin involves the removal of residual non-glycerol organic matters, water, salt and odors and the operation can directly affect the cost of refined form. Then, this refined glycerin obtained from crude glycerol is used by many industries, including food, cosmetic and pharmaceutical industries. The remaining weight in the crude glycerol streams is mainly due to methanol and soap [26]. Glycerol purity value may depend upon its purification methods used by its processers and different initial feed stocks used in the biodiesel production. Thompson and He [22] reported that mustard seed feed stocks had a low purity level of glycerol (62%), soy oil feed stock had slightly high purity of glycerol (67.8%) while waste vegetable had high level of glycerol purity (76.6%). Simple reason for this difference may be due to different concentrations of elements present in crude glycerol.

Consequently, if glycerol is used for the formation of consumer products like food or drug, it must be refined well beyond the purity at which it comes out of a biodiesel plant. For crude glycerol, it might be easier to be directly used for chemical component preparation rather than for food or drugs preparation that require high purity. Therefore, the present work is mostly concerned with biodiesel based crude glycerol originating from biodiesel industry and its importance for upgrading into higher-value compounds, thereby allowing the biodiesel production to become more cost-effective. Hence, much emphasis is given on the importance of crude glycerol and conversion of this low-value by product to value-added compounds so that a better production–consumption balance can be achieved in the crude glycerol market.

3. Global status of glycerol production

The biodiesel production is increasing worldwide in recent years because of its environmental benefits and the fact that it is made from renewable biological sources [27,28]. This is the basic reason for increasing quantity of glycerol in the market. Crude glycerol was also obtained as by-product from soap and fatty acid production in past years. Currently, most of glycerol is produced from biodiesel production process. Therefore, the price of glycerol is determined by the demand and production of biodiesel instead of soap and fatty acid.

3.1. Current glycerol production

Biodiesel industry continuously produces huge amount of crude glycerol as a co-product. It is predicted that if the production of biodiesel is sustained at the same pace in future, glycerol may create handling problem for industrialists. Therefore, responsible authorities in biodiesel producing countries should take necessary proactive actions to stop subsidies for its production in order to reduce the surfeit of crude glycerol.

The glycerol production worldwide remained relatively stable and very low level from the late 1990s to 2003. Then biodiesel production slightly increased to bring about corresponding increase in the quantity of crude glycerol in 2004. After that, biodiesel production drastically increased with corresponding huge production of crude glycerin. Fig. 2 clearly shows the increasing trend of crude glycerol production due to increasing production of biodiesel during the period of 2004–2006 [29]. It is clear from the figure that glycerol production increased by an approximately a factor of four times from 62 million lbs to 213 million lbs in a mere 1 year from 2005 to 2006. The increasing quantity of glycerol was obviously due to high production of biodiesel from 75 gallons to 250 gallons during 2005–2006.

The National Biodiesel Board [30] reported an annual production of 450 million gallons of biodiesel in 2007, which was a sharp increase from less than 100 million gallons in 2005. The production of crude glycerol was very low until 2005. Basically, glycerol was produced at under 0.5 billion pounds by European Nations only

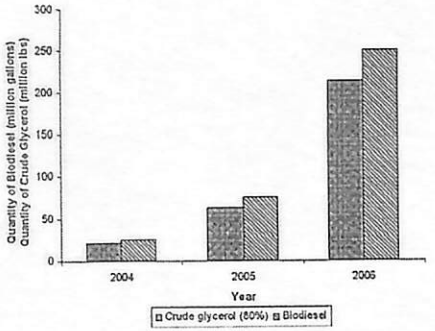

Fig. 2. Production of biodiesel and crude glycerol during 2004–2006 [29].

before 2006. After that, some other countries like USA, Malaysia, Indonesia, India and China that were involved in the production of biodiesel during 2006–2007 sharply increased the production of crude glycerol. After 2007, the production of crude glycerol rapidly increased due to huge production of biodiesel by all these countries. In addition, the federal government of Canada aims to produce 500 million liter/year of biodiesel by the year 2010 to meet the Kyoto protocol [31]. According to the BBI International's Engineering and Consulting team [32], biodiesel manufacturers created 187,000 tons of crude glycerin in 2007. In addition, there was a great slump in imports of US crude glycerol during the recent years of 2008 and 2009.

The overall crude glycerol market in the United State was depressed in these years. This was due to Southeast Asia and Europe, which were exporting glycerin to the United States in large volume and at low cost. This was a direct consequence of an increase in the biodiesel production in Southeast Asia and Europe. At the same time, the glycerol market also experienced a drop in its demand in Asian market due to a new Argentine biodiesel market that was established in this zone.

3.2. Projected glycerol production

Actually, glycerin market is comparatively small on a global basis. Current global production of glycerin is about two billion pounds and is valued at one billion dollar annually [33]. The main regions where crude glycerol is produced in bulk are the European Union, the United States and South East Asian countries. Obviously, the glycerol market is worldwide and vulnerable to shocks in international market even though it is just a small market. Presently, new renewable fuels policies are going to be implemented in developed and developing regions like European Union, United States, South East Asia, Canada and South America. Successful implementation of the policies will ensure that the glycerol market will increase well [34]. The United States and European Union currently dominate the biodiesel and glycerol markets. However, significant growth is underway in South East Asia and China. Furthermore, the United States has a relative advantage over the EU due to the difference in exchange rates.

Fig. 3 shows the clear estimated crude glycerol production resulting from biodiesel production in different countries [35]. It is clear from this figure that the estimated production of glycerol would reach 5.8 billion pounds in 2020. This is due to demand of biodiesel that is projected at 8 billion gallons in 2020. It is also clear from this figure that glycerol production was very low, i.e. less than one billion lbs before 2006 and mostly produced by the European Union. After 2006, the production of glycerol rapidly increased and many other countries like USA, Indonesia, Malaysia, China and India started to produce glycerol. The production of glycerol after 2006 was so rapid and continued so that its production reached above 2 billion lbs in 2009. The projected data suggest that the glycerol production will attain 4 billion lbs in 2015 if its production increases at the same pace. The estimated quantity will touch to 6 billion lbs

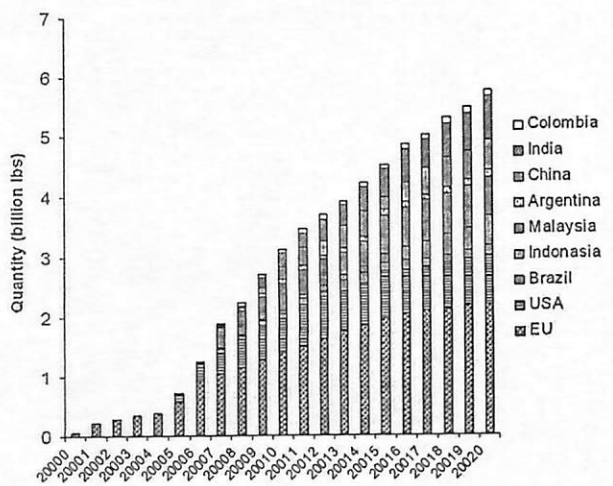

Fig. 3. Estimated production of crude glycerol in different countries [35].

Table 5
Sources of glycerol during 1992–2008 and in estimated year 2010 [37].

Glycerol sources	World glycerol production ($\times 10^3$ metric tons/year)							
	1992	1995	1999	2003	2005	2006	2008	2010
Soaps	208	208	198	188	167	146	125	83
Fatty acids	271	292	313	333	396	438	479	521
Biodiesel	0	42	42	167	375	521	1125	1583
Fatty alcohol	83	104	125	104	125	167	250	250
Synthetic	83	83	63	63	21	0	0	0
Others	0	0	42	63	42	0	21	21
Total production	646	729	781	917	1125	1271	2000	2458

after 2020. The major portion of projected glycerol quantity in 2020 belongs to EU and then USA. The other countries those will boost glycerol production in future are Malaysia, India, China, Indonesia, Brazil, Argentina and Colombia.

In Malaysia, the total combined capacity of biodiesel plants was about 1.5 million tons before 2007. In 2008, biodiesel output increased by only 5% due to the high prices of feedstock. According to a report [36], the figure is expected to show a 30% increase in 2009 as companies are cranking up their machines when the margins started to appear during the latter half of 2008. It is also mentioned in this report that another four plants with a combined capacity of 190,000 tons are going to install for a commercial production by the end of 2009. According to this data, the production of biodiesel in Malaysia may increase by more to 2 million tons at the end of 2010. Ultimately, crude glycerol production will increase in Malaysia.

Consequently, it can be concluded that the production of crude glycerol resulting from biodiesel is rapidly increasing in different religions of the world. Hence, new uses of crude glycerol are required to absorb the problem of glycerol glut in near future and researchers should study in depth to find out possible means for the utilization of glycerol in economical ways for further defraying the cost of biodiesel production.

4. Glycerol supply drivers

4.1. Types of supply drivers involved in glycerol production

An enormous change was observed between supply drivers of glycerol in the last 10 years. Changes in glycerol drivers became prominent after 2003 that saw rapid increase and overcome as a big source in 2008 and may become the strongest source in future as summarized in Table 5 [37]. It can be concluded from this table that fatty acid industry was a strong source of glycerol until year 2003. After that, the contribution of this source slowly decreased and in 2008, biodiesel became the main source of glycerol production. The reason behind this increasing trend of glycerol production was the consumption and production of biodiesel in last few years.

Another notable point in this table is that the overall production of glycerol resulting from different sources slowly increased from 646,000 MT/year to 1,271,000 MT/year during 1992–2006. The sharp increase in glycerol production was observed (2,000,000 MT/year and above) after 2006 and onwards. In addition, the production of synthetic glycerol was only observed during 1992–2005. After this period, its production became virtually zero. This is may be due to high economical production of glycerol by other sources, especially from biodiesel source.

It can be summarized that quick changes in supply drivers and production of glycerol after 2006 was attributed to biodiesel industry. The increasing quantity of crude glycerol may go to useful purpose or just a waste. It means that the utilization of glycerol in the world should increase and new uses of glycerol should be identified to open new markets of glycerol in near future.

4.2. Comparison of supply drivers for glycerol production

The source of glycerol was shifted from one of the most popular supply drivers, i.e. the fatty acids industry to biodiesel industry in past 10 years as shown in Fig. 4 [38]. It is also clear from this figure that fatty acids and soap manufacturing were two main sources for glycerol production before biodiesel industry boosted up during past few years. In 1999, the sources for production of glycerol were fatty acids, soap manufacturing process, fatty alcohols process and biodiesel process. The production ratio for these sources was at 47%, 24%, 12% and 9%, respectively. In 2009, these sources of glycerol were completely changed and they at 21%, 6%, 8% and 64%, respectively. Hence, biodiesel industry jumped up for biggest change in glycerol supply driver from 9% to 64% and fatty acid dropped from 47% to 21% during the same period.

The increasing population of the world might be a factor that urges to increase the consumption of fuel energy, i.e. increase the demand of fuel. Therefore, fuel energy is shifting from petroleum to biofuel to overcome these energy crises. Hence, biodiesel production is increasing day by day and become the biggest driver of glycerol in the last few years.

4.3. Influence of supply drivers on fatty acid and soap industry

Soap industry has conventionally provided most of the glycerin for a domestic market in developed countries like USA. Most industrialists of soap manufacturing in Europe and the Unites States have limited glycerol refining capacity. The depressed price of glycerol is another factor that prevents the construction of new refineries. Due to these problems, global crude glycerol oversupply crisis is continuously rising. Basically, biodiesel manufacturers have cut into the vegetable oil supply and driven up prices across the board and animal fats are expected to be a significant source of biodiesel in the future. Thus, natural input supplies for soap manufacturing will be

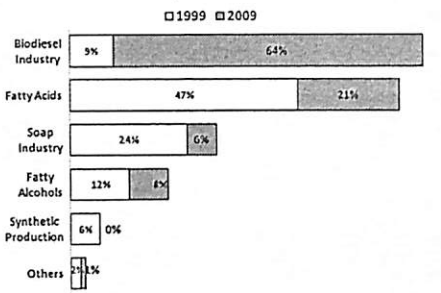

Fig. 4. Glycerol supply driver trend change [38].

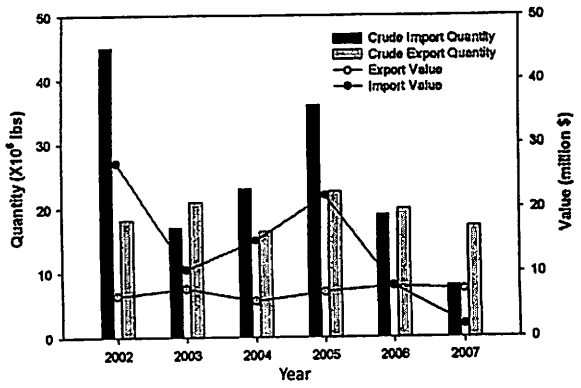

Fig. 5. The import and export of crude glycerol by USA during 2002–2007 [41].

more difficult and more expensive if biodiesel goes through major sustainable growth. Soap manufacturing industrialists are already dealing with a shortage of beef tallow. The short term remedy for soap manufacturers in the US and European countries is by importing palm oil from Malaysia or using petrochemical (synthetic) stock [39]. If these manufacturers are unable to get cheap inputs for soap manufacturing, the production will move from these countries to some other countries in foreign for cheaper labor and inputs.

Ultimately, the recent surge in biodiesel production may be alarming for soap manufacturers due to its impact on the input cost and revenue of soap manufacturing industry. According to current scenario, the dramatic increase in biodiesel production may drive up the price of fatty acid inputs and further reduce the price of glycerol in the near future. The development of some new and alternative uses of glycerol may promise the soap producers some relief from sagging glycerol prices in the future.

5. Global market of crude glycerol

According to a current scenario, it is important to know that there are two different types of glycerol markets: crude and refined. Recently, the market for crude glycerol has been relatively depressed due to a larger supply of crude than the ability to turn it into a refined product while the market for refined glycerol is still reasonably good. As the biodiesel production skyrockets, the market is being flooded with crude glycerol. The American crude glycerol supply may be distorted after a period of stable glycerol prices and a sharp fluctuation during the commodity bubble in 2008. This may cause to pull more glycerol out from already stiffening European glycerol market. It is estimated that the potential annual glycerol surplus will reach around 1.2 metric tons as targeted by the European Union and US to be achieve at the end of 2010 [35].

5.1. Import and export

As a by-product, the image of glycerin shows a poor visual image towards viability and economy of biodiesel production [40]. As fuel consumption is increasing globally day by day that has directly effected on biodiesel production and indirectly has linked with the production of crude glycerol. Fig. 5 shows the import and export quantity of crude glycerol and its value in USA during the period of 2002–2007 [41]. It is clear from this figure that import and export fluctuated over this period. The fluctuation in import was higher compare with that in export. The trend of imported crude glycerol quantity and its value fell and touched zero in 2007. However, the value of crude glycerin export was slightly stable during this period 2002–2007. Actually, after 2005, the USA biodiesel production increased, which produced enough crude glycerol. It might result in a decrease in the import of glycerol after 2005.

On the other hand, the volume of refined glycerol exports was increased during the same period which caused a decrease in the export of crude glycerol from USA. According to a European report [42], refine glycerol market is described as being strong and stable while crude glycerol market is described as week in Europe. The crude glycerin market moves at low levels due to its purity (50–90%) due to water and residual methanol contents.

Germany and Malaysia are the two largest suppliers of glycerol in the world (Table 6). It also shows the import of crude and refined glycerol by USA from these two countries (Germany and Malaysia) and rest of the world [35]. Clearly, the import of crude glycerol from Germany, Malaysia and rest of the world decreased steadily over time 2002–2007. The import of refine glycerol was seem to be stable compared with crude glycerol at the same period except from Malaysia where its import increased from 28 to 50 million kg during 2002–2004 and then decreased to 46 million kg at the end of 2007. The fluctuation in the import of crude glycerol may be due to the high shipping cost of crude glycerol from different countries to the United States. Some time shipping cost is rather high so that it does not meet the market price for crude glycerol. The import of crude glycerol from Malaysia also decreased in the same period, but it is covered by the import of refine glycerol from Malaysia during 2002–2007. It can be concluded that the overall crude glycerol import decreased but refine glycerol import increased during 2002–2007 period. Moreover, Malaysia played an important role for import of both types of glycerol during this period.

Palm oil industry of Malaysia has historically made the country a major player in the fatty acids for biodiesel production that directly influence glycerol market. It means that the country will produce more glycerol in future due to flourishing biodiesel production from palm oil. Therefore, in future, Malaysia might become the biggest exporter of crude glycerol in the world. It can also be predicted that the demand of refine glycerol may increase in future not just in the US but all over the world due to opening of new outlet of glycerol.

Table 6
The imported quantity of refine and crude glycerol by USA [35].

	USA import glycerol from countries				
	Year	Germany ($\times 10^6$ kg)	Malaysia ($\times 10^6$ kg)	Rest of the world ($\times 10^6$ kg)	Total quantity ($\times 10^6$ kg)
Crude glycerol	2002	14.5	24.5	6	45
	2003	4	6	4	14
	2004	9.5	1.5	12.5	23.5
	2005	1	11	24.5	36.5
	2006	6.5	5	7.5	19
	2007	0	3	3.5	6.5
Refine glycerol	2002	14	28	14	56
	2003	14	26	20	60
	2004	16	50	27	93
	2005	25	48	16	89
	2006	25	37	15	77
	2007	18	46	20	84

It is also a notable point that refined glycerol may capture more attention in future market compare with crude glycerol due to its utilization and demand. Therefore, crude glycerol may need to be refined locally prior to its export.

5.2. Supply and demand

In previous decades, glycerol was produced as a by-product during the manufacturing or refining of several chemicals such as petroleum, soap and biodiesel. Currently supply and demand of glycerol totally change due to the shifting of supply derivers from soap and fatty acids to mostly biodiesel process. The glycerol prices can adjust to dealing with the global supply. According to previously published reports [29,43], crude glycerol prices dropped from 25 cents/lb in 2004 to 2.5–5 cents/lb in 2006 because the U.S. demand for glycerol was not large enough for all of this excess glycerol in 2007. In another report [44], it is stated that traffic fuels should contain at least 5.75% of renewable bio-components at the end of 2010. European biodiesel demand could increase to 10 million tons yearly by the end of 2010, which will produce about 1 million tons of glycerol as a by-product, if the target of this directive is to be achieved [45]. On the other hand if the United States replaces 2% of the on-road diesel with biodiesel in a B2 policy by 2012, almost 362.872 million kg of new glycerol would be added to the market [46]. This will badly affect the demand and supply of crude glycerol in USA as well as in the EU countries.

Fig. 6 shows the supply and demand of crude glycerol during 2009 in different regions where crude glycerol played a vital role to their economy [38]. It is clear from figure that demand was high in US, Europe and China during 2009 compared with other countries where demand of crude glycerol was not so high during this time. One reason for increasing demand may be due to increasing consumers of personal care products in these markets. Presently, China is going to become a large industry for personal care products because increasing Asian people going for cosmetics and other personal care products. It can be seen in this figure that China has high demand of glycerol after the US and Europe.

It is clear from this figure that the glycerol supply during 2009 mostly originated from Europe, ASEAN, US and Latin America. In the same year, the supply of glycerol from these countries was 4 times less than its demand in China. It might be possible that the fluctuation in demand and supply is due to development of some new industries in ASAEN regions. These new industries are mostly related to personal care, new chemicals, food products and cosmetics.

According to this scenario and viewing other factors like glycerol market value that directly involved for costing of overall biodiesel production cost, it can be concluded that biodiesel may not be economically feasible any more under these circumstances. Therefore,

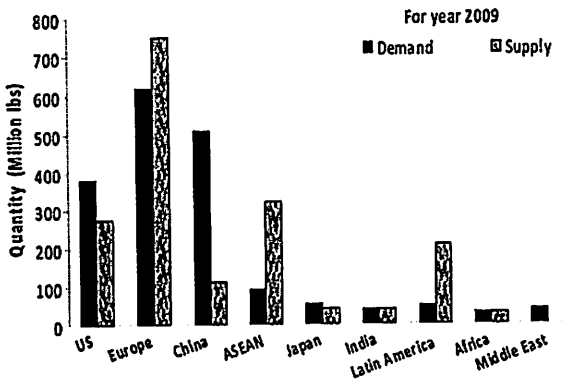

Fig. 6. Supply and demand of crude glycerol in different regions during 2009 [38].

Table 7
Annual glycerol price from 2001 to 2009 [3].

Type of glycerol	Glycerol price (cent per pound)								
	2001	2002	2003	2004	2005	2006	2007	2008	2009
Synthetic	72	73	90	85	85	–	–	–	–
Refined	60	58	65	55	45	35	70.5	55	41
Crude	15	12	12	10	5	2	10	5	6

more research and technological development will be needed in future to letdown the cost of biodiesel production. Hence, utilization of glycerol in new industries on its transformation toward more value-added products with high demand may be one of the best solutions to overcome this problem.

6. Impact of glycerol price on biodiesel cost

6.1. Relationship between biodiesel production cost and glycerol price

A major obstacle in the commercialization of biodiesel is its high cost of manufacturing, particularly with respect to the raw material cost. Biodiesel usually costs over US$0.5/L and its cost is approximately 1.5 times that of petroleum-based diesel depending upon feedstock oils [47,48]. According to Nelson et al. [49], the significant factors that affected the cost of biodiesel were feedstock cost, plant size, and value of the glycerin by-product. You et al. [9] reported that among the system variables of the plant examined, plant capacity, price of feedstock oil, and yields of glycerol and biodiesel were found to be the most significant variables affecting the economic viability of biodiesel production process. According to Zhang et al. [50], the glycerol credit could lead to approximately 13–14% reduction in total production costs of biodiesel fuel.

Consequently, it is concluded that the fluctuation in cost of oil feedstock and glycerol credit will affect the increase or decrease in the capacity of the biodiesel plants as well as production cost of biodiesel. Therefore, it can be assumed that biodiesel total production cost is directly proportional to the cost of oil feedstock and inversely proportional to glycerol credit.

6.2. Unstable price of glycerol

Currently, biodiesel production results in a rapid increase in the availability of crude glycerol worldwide and now refineries have hit the limits of their capacity. The prices for crude glycerol have fallen through the floor, falling down to zero and even negative as producers of glycerol (especially biodiesel) are forced to pay to have it taken away from their plants and incinerated [51]. On the other hand, the prices for refined glycerol have not varied inversely with biodiesel production, as might be expected. Instead, prices halved between 2003 and 2006, while growing by 69% between July 2007 and July 2008 due to other exogenous factors such as its demand in ASEAN [52]. From the 1970s until the last few years, high purity natural glycerol had a fairly stable price from about $1200 per ton to $1800 per ton [51]. This was based on stable markets and production. In 2000 onwards, the glycerol market became tight due to increasing production of crude glycerol. This oversupply of glycerol has significantly affected its price. Table 7 shows the price of different glycerol categories from 2001 to 2009 [3]. It is clear from this table that there is a decreasing trend in refined and crude glycerol prices during 2001–2007. In 2007, the price of both type of glycerol was found to increase to very high levels only to witness significant decreases in the following years.

The price trends of different types of glycerol during 2005–2009 are shown with better detail in Fig. 7 [38]. It can be seen that price trends of all type of glycerol even refine glycerol decreased from 2005 to first quarter of 2007. Then an increase was noted in the middle of year 2007 that continued at the end of 2007. These prices of glycerol were skyrocketing at the start of year 2008. After that prices started to decline sharply till the end of year 2008 and then again became stable at their lowest prices in year 2009. The reason

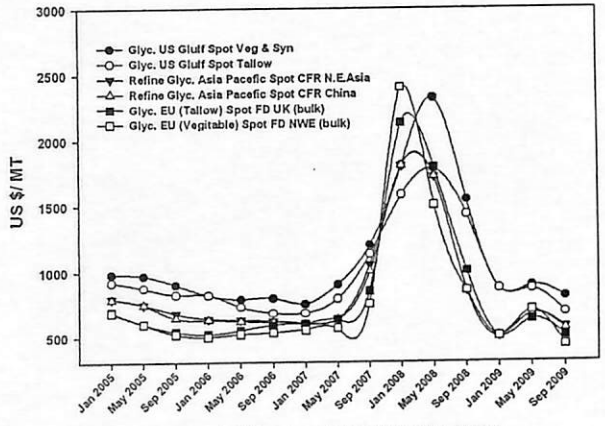

Fig. 7. The price trend of different types of glycerol during 2005–2009 [38].

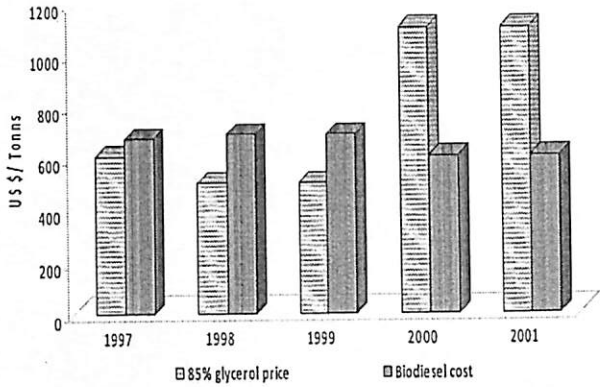

Fig. 8. Impact of glycerol price on the cost of biodiesel fuel during 1997–2001 [50].

behind increasing these prices of glycerol during 2007–2008 was the glycerol supply that began to decline rapidly during 2007–2008. The glycerol supply was disturbed due to escalating prices of seed oils during that period which directly affected the prices of glycerol [3].

According to Erik Groen's report on glycerol price in Europe [53], it is possible that glycerol price might increase in near future after start up of renewable propylene glycol (PG) plant by Archer Daniels Midland Company. It will potentially take 125,000 tons/year out of the crude glycerin market. The tighter market will increase prices even more.

It is concluded that fluctuation in glycerol pricing is due to oversupply of glycerol resulting from biodiesel production process. The fluctuation in price of glycerol from 1995 to 2006 may primarily be attributed to the slowly increasing production of biodiesel. The increasing price of glycerol during 2007–2008 was due to an imbalance between supply and demand of glycerol in global market while the drop in prices after 2008 was due to oversupply of glycerol. This may also be caused by the global economic recession and the excess production of biodiesel in those years (Table 7).

6.3. Effect of glycerol price instability on biodiesel production cost

In the context of biodiesel market, the low value of glycerol plays a vital role because it is a major by-product in the formation of biodiesel. Previous studies [25,54,55], stated that the production cost of biodiesel was found to vary inversely and linearly with variations in the market value of glycerol. A report from WOOC (2007) [56] indicates that the price trend of glycerol was decreasing over the last decade while production of glycerol was increasing due to the increase in biodiesel production. According to Fan et al. [57], biodiesel production cost could be reduced by 25% by increasing value of crude glycerol as its feedstock.

The impact of glycerol price on biodiesel production cost during 1997–2001 is shown in Fig. 8 [50]. It is clear from this figure that biodiesel cost correlate with the glycerol market price. Although, this impact was not very high, it was considerable on the total cost of biodiesel manufacturing. This figure suggests that biodiesel manufacturing cost increased to above 600 US$/ton during 1998–1999 due to a decrease in glycerol price from 600 to 500 USD/ton. This cost then decreased to below 600 USD/ton when glycerol market price increased to above USD 1000/ton during 2000–2001 period. Actually, the import of glycerol increased during 2000–2001 in the United States and Europe due to increased consumption. This directly affected the price of glycerol and caused a price increasing during this period as also reported by Singhabhandhu and Tezuka [58].

The sharp increase in the price of glycerol during 2007–2008 might be due to increasing demand of glycerol for new outlook. Similarly, cost of crude glycerol can be directly correlated with biodiesel price as shown in Fig. 9 [59]. It is clear from the figure that offsets price of a biodiesel increases with increasing crude glycerol price. There is a linear correlation between glycerol price and biodiesel manufacturing cost. Actually, by opening new outlets of crude glycerol, an increase in its demand which is directly linked to the overall cost of production of biodiesel could be achieved. According to another report [60], the cost of biodiesel looked very high at the start of biodiesel production due to a formation of crude glycerol. This cost of biodiesel could decrease with increasing utilization of crude glycerol to produce value-added products.

These results indicate that the amount of produced crude glycerol as a by-product has a significant effect on the net value of the total manufacturing cost of biodiesel. This cost varies inversely with variations of glycerol price in the market. Thus, the seemingly large fluctuation in glycerol price has a considerable impact

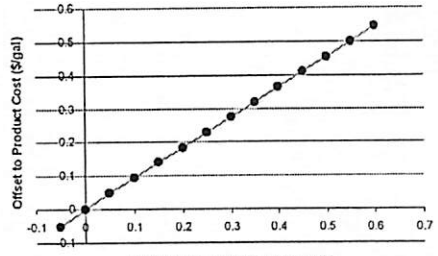

Fig. 9. Crude glycerol impact on the cost of biodiesel [59].

Table 8
List of currently available and predicted outlets for crude glycerol.

Field of application	New applications of glycerol	Remarks
Chemical industry	Textile industry, plastic industry, explosives industry, polymer industry	For formation of a stain-resistant chemical and use for lubricating, sizing and softening to yarn and fabric [69] and as a substitute for petroleum-based polypropelene in a textile [70]. In the formation of nitroglycerin compound which is commonly used in all types of explosives [71]. Use as a component to produce polyglycerol ester (surfactants and lubricants), polyglycerol methacrylates (improve wood stability), polyester polyols/polyurethanes (applied as coatings, foams, and sprays) [72].
Commodity chemicals	Natural organic building blocks	For formation of natural organic building blocks [73] especially for formation of acrolein, dichloropropanol, epichlorohydrin, 1,3-propanediol, 1,2-propanediol, glycerol carbonate, DAG, MG, oxygenate fuels, glyceric acid, tartronic acid, and mesoxalic acid [74–76]. For formation of monoglyceride [77,78]. In antifogging and antistatic additives, lubricants, or plasticizers as di and tri-glycerol (polyglycerols) [79,80].
Pharmaceutical and oral care	Additive in drugs, heart disease drugs, love potion, health supplements, cosmetics, tanning agent	As an additive use in cough syrup, toothpaste, skin care, hair care medicated soap and many others drugs like expectorants, ointments, plasticizers for medicine capsules, ear infection medicines, anesthetics, lozenges, gargles, and as a carrier for antibiotics and antiseptics. Also as an ingredient in laxatives in the form of liquid enema, elixirs and expectorants [81]. Use in cosmetics for improving smoothness and as a humectant where moisturization is desired. Formation of tanning agent like dihydroxyacetone [82].
Food	Safe sweeteners, preservation, thickening agent	As a thickening agent and an ester in shortenings and margarine [83]. As an artificial sweetener, especially in low-fat foods, since it is better for blood pressure than sugar and more useful for sugar patients [84].
Livestock feed	Cow and other animals feed, pigs diet, poultry feed	Use as dairy cows feed in order to prevent ketosis [85]. As feed of pigs due to metabolizable-to-digestible energy ratio of glycerol is similar to corn or soybean oil [86] and as a feed of broiler chickens [87].
Energy as fossil fuel substitution and biogas	Liquid fuel, conversion into ethanol or hydrogen, burning as fuel pellets, combustion in incinerators, combustion as boiler fuel	Form of glycerol blend for biomass conversion to liquid fuel [88].Trying to convert glycerol into ethanol in an anaerobic environment [89]. Aqueous phase reforming transforms glycerol into hydrogen [89,90]. Glycerol fuel pellets can use as fuel instead of coal [68]. To increase the biogas production of anaerobic digesters [70,91]. Combustion in incinerators for heat or dispose off [41]. Use as boiler fuel due to heating value is roughly 9000 BTU/lbs [61]. One ton of glycerol can be produced 600 m^3 of biogas [92]. Suitable for blending agent in gasoline, biodiesel and diesel fuels [93].
Biotechnology	Organic acid, Omega-3, succinic acid by fementation, EPA by fungus	Formation of citric acid by by the yeast *Yarrowia lipolytica* [94], acetic acid, butyric acid and lactic acid by anaerobic fermentation [61], Omega-3 polyunsaturated fatty acids by developing algal fermentation [95], Eicosapentaenoic Acid (EPA) formation by the fungus *Pythium irregular* [26]. Feedstock in *Anaerobiospirillum succiniciproducens* for the production of succinic acid [96].
Miscellaneous	Basic materials, hydraulic and fire-resistant fluid, de-icing aircraft, thermo-chemical products	As a substitute for petroleum-based polypropylene, a textile, and in both rigid and flexible industrial foams [70]. It can be formulated into composites, adhesives, laminates, powder and UV-cured coatings, mouldings, novel aliphatic polyesters, co-polyesters, solvents, anti-freeze and other end uses [74,97,98]. In hydraulic fluids and fire-resistant fluids comprising glycerol-containing [99]. Use as an ingredient in products for de-icing aircraft [100]. Thermochemically conversion into propylene glycol, acetol, or a variety of other products [101,102].

on the biodiesel price. However, glycerol is indeed a valuable by-product with much potential as a feedstock to various value-added products. As such, successful utilization for non-conventional applications could add an appreciable credit to reduce the total manufacturing cost of biodiesel fuel.

7. Global utilization of glycerol

A crude glycerol glut is created due to rapidly expanding biodiesel industry. Therefore, biodiesel producers are seeking alternative methods for its utilization or disposal. Various methods for disposal and utilization of this crude glycerol have been attempted, including combustion, composting, anaerobic digestion, animal feeds, and thermo-chemical or biological conversions to value-added products (Table 8). Crude glycerol is usually sold to large refineries for upgrading. In recent years, however, with the rapid expansion of biodiesel industry, the market is flooded with excessive crude glycerol. As a result, biodiesel producers only receive 2.5–5 cents/lb for this glycerol [61].

7.1. Conventional and current glycerol usages

A comparison between important applications of glycerol during 1995 [62] and 2006 [63] is shown in Fig. 10. This figure contains a complete breakdown of current and previous glycerol consumption according to its end uses. In the figure, clearly the top category belongs to the usage in personal care and pharmaceutical industries. The demand of this category increased from 26% to 34% during 1995–2006. Actually, glycerol is an ideal ingredient in many personal care products, mostly helping to prevent moisture loss. In pharmaceuticals, it provides lubrication and smoothness to many cough syrups and elixirs.

For oral care products, glycerol is commonly found in toothpaste, mouthwash and sugar free gum giving a sweet taste without contributing to tooth decay as well as in cosmetics to hold moisture against the skin to prevent dryness [64]. According to statistics of glycerol application in 2005, glycerol resale was the second big category (17%) as shown in Fig. 9. The resale of glycerol may decrease slowly or distributed into some other glycerol based products like increasing trend of cosmetic or may be due to development of some new outlet during that period. Therefore, there was no opportunity for resale of glycerol in 2006.

It can be seen in the figure that the usage of glycerol in paper industry is replaced by detergent production in 2006. Glycerol is also a source of carbohydrates and gives a sweet taste but it does not cause an insulin secretion during the digestion process. Glycerol is also used as humectants in food products which helps to preserve food and keep it fresh for long times. Therefore glycerol demand is increasing in food industry. According to the statistics on glycerol usages, 11% of overall glycerol was used in food industry and 6% in tobacco in 2006 compared to 8% and 4% in 2005. In the manufacturing of tobacco, glycerin is used as a humectant and

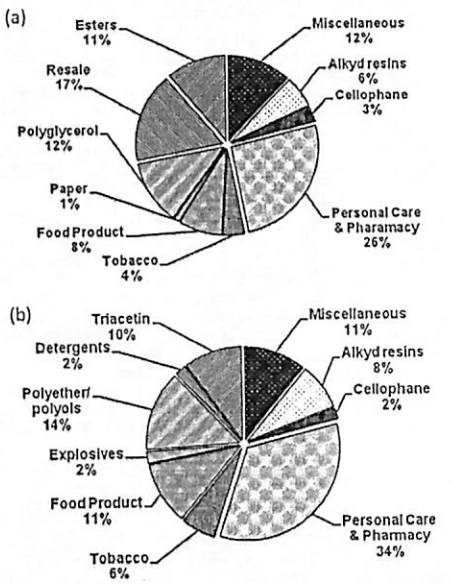

Fig. 10. Comparative end use of glycerol during (a) 1995 [62] and (b) 2006 [63].

a sweetener [65]. It is used as plastic layer in cigarette paper as well as a sweetener in chewing tobacco.

The application of glycerol as a formulation of some alkyd resins is also increasing presently. According to Fig. 10, it can be concluded that glycerol utilization in alkyd resins industry increased from 6% to 8% during these years. These materials are used as productive surface, especially in paints and components of plastics. Glycerol usage as polyether or alcoholic hydroxyl group polyol was also increased in last decade. Basically, it provides one of the basic chemical building blocks for the construction of rigid polyurethane foams. The application of glycerol as ester or triacetin remained round about same (10–11%) during 1995 and 2006. They are artificial compound which are used mostly as food additive and pharmaceutical. Another common use of crude glycerin is to burn the substance with a light temperature of (29–300 °C) for heating of industrial boilers [3]. The application of glycerol is also emerging in explosive industry. It is used for the production of nitroglycerin which is extremely powerful than TNT. Therefore, glycerol is using now as a component during explosive process and its consumption in explosive industry was noted 2% in year 2006 [63].

It can be concluded that glycerol is a non toxic element and an environmental friendly product. Therefore, its allowable quantity can be used in food, tobacco and drug manufacturing industries as a supplement is high. For large scale biodiesel producers, crude glycerol can be refined into a pure form and then it can be used in food, pharmaceutical, or cosmetics industries. For small scale producers, however, purification may too expensive to perform in their manufacturing sites. Hence, new economical applications of glycerol might be a possible solution to overcome this problem. Thus, some new glycerol based products should be added in the present market. Due to this fact, some conventional and uneconomical applications of glycerol may disappear from upcoming market. As a result, glycerol price may rise again that will help to hail its glut resulting from biodiesel production process [62].

7.2. Region-wise application of glycerol

The important applications of glycerol are regionally determined in as shown in Fig. 11 [66]. The regional difference between the percentage of this share in three main regions, i.e. Europe, USA and Japan is shown. For the United States, the largest distinguished single application is personal and oral care products, which is above 40%. In Japan, the largest discerned single application of glycerol (25%) is for pharmaceuticals and the second largest identified application is for personal and oral care (above 15%). For the United States, the second largest application is for food and beverages (22%). Some 10% of the European glycerol market is intended for application in food and beverages with another 8% contribution for pharmaceuticals. Glycerol is used in nearly every industry. With dibasic acids such as phathalic acid, it reacts to make the important class of products known as alkyd resins, which are widely used in coating materials and paints [67]. Alkyd resins market has been increasing in the United States, Europe and Japan where it contributed about 6%, 4% and 2%, respectively. Polyether polyols have their largest share in the European market with about 12% as compared to 8% in the USA and 6% in Japan.

It can be concluded that glycerol application varies in different regions. It may be due to different culture, living style and weather of different regions. Other factors are such as the size of population, occupied area and production policies of these regions.

7.3. Demand-wise applications of glycerol

Fig. 12 illustrates the demand of crude glycerol according to its application in the different fields [37]. This figure also shows a comparative increasing percentage of crude glycerol between its traditional and new alternative uses. According to this figure, the overall increase can be seen in crude glycerol demand (above 127%) for the upcoming year (2010) as compared to that of 2005. In the projected year 2010, it is predicted that usage of glycerol may increase by 94% for new alternative applications compared with conventional application that may increase by just about 33%.

The conventional application of glycerol may increase by 18.8% in organic growth, 9% in China growth and 5.5% in additional substitution applications. For new alternative areas, most of applications are going toward feedstock/disposal and value added biochemical fields with increasing margins of 48.5% and 45.4%, respectively. The feedstock applications belong to be available for crude glycerol for feed production of animals or poultry. Meanwhile, the disposal applications will be contributed by the usage of crude glycerol for biogas production or glycerol soaked wood burn for heat purpose [68].

Presently, some US based companies such as Procter & Gamble, Cargill, Archer Daniels Midland (ADM) and Vantage Oleochemicals are refining the crude glycerol and manufacturing everything from common use toothpaste to polyols as value-added chemicals and then selling them to market [53]. It means that big and famous companies are also helping to utilize glycerol for production of value-added products. With the help of such companies, it might be possible that new alternative uses of glycerol may rise in the future.

It can be analyzed from Fig. 12 that crude glycerol demand for new alternative uses may be three times higher than its conventional applications in future. New alternatives in the future might be involved in its applications as feedstock, disposal or value added bio/chemical products. It can also be predicted that in future crude

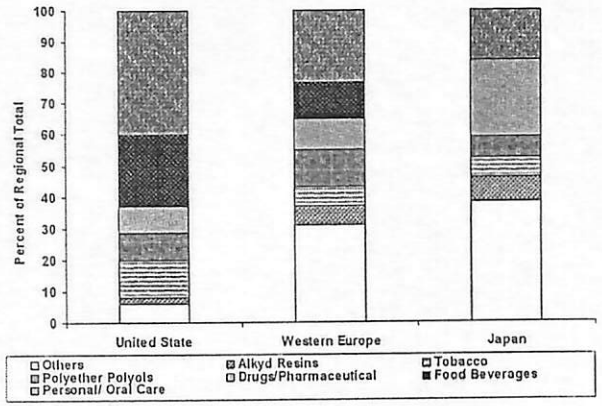

Fig. 11. Region-wise percent application of glycerol [66].

glycerol might be used in higher quantity for application of value-added chemicals' production like glycol and epichlorohyrine.

7.4. Outlook of biodiesel-based glycerol applications

Current market is being flooded with crude glycerol due to exponentially growing production of biodiesel. Therefore, biodiesel producers are seeking some new value-added usage of crude glycerol for up coming future. The reason behind it is prohibitively cost to convert and purify crude glycerol into some conventional materials that can be used for food, cosmetics or drug industries [37,68].

There is a big range of glycerol application that starts from energy bars to cough syrups and goes through till boat coatings. According to SDA report [10], there are more than 1500 uses of glycerol. The crude glycerol derived from biodiesel production through transesterification process can be used for these applications after subjecting it to several purification processes. Actually, the purification process of crude glycerol starts with neutralization with an acid, and then water and alcohol are removed to produce 80–88% pure glycerol that is easy to be sold as crude glycerol in market. For more purification with complex operations, the glycerin is distilled to 99% or higher purity and it is sold to the cosmetic and pharmaceutical markets. Therefore, it is the necessity of present and future

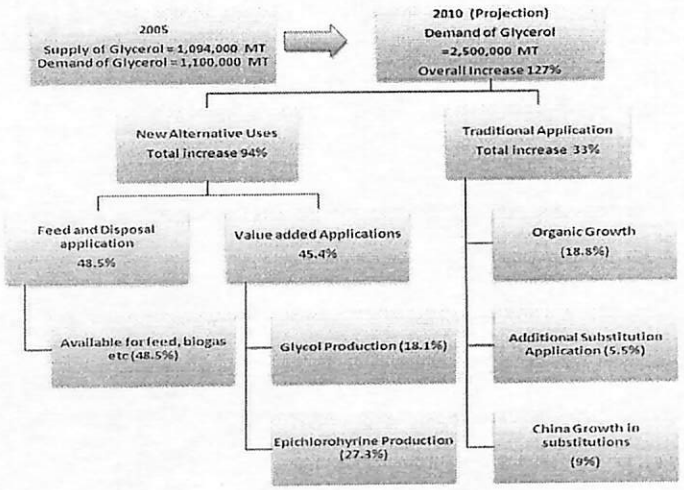

Fig. 12. Estimated demand of glycerol utilization in 2010 [68].

markets to develop some new outlets for crude glycerol resulting from biodiesel production. Equally important is the development of a more sustainable refining processes and more economical plants.

Research and development of new uses for glycerol, it is realistic hope for the industries to increase crude glycerol prices in upcoming market. The new applications may involve a large scale production after their commercial recommendation. The market of glycerol can be expected to be stable enough while at the same time the price of glycerol can rise if these huge utilizations of glycerol become successful on commercial scale. It is anticipated that the new applications of crude glycerol may strengthen the market of glycerol and indirectly support to reduce biodiesel production cost. There is still opportunity to explore more valuable applications of crude glycerol to boost up biodiesel production and to become a vital part of renewable energy.

There are several developments in various stages of the research pipeline which may add values and may provide a new outlet for glycerol industry. These developments include new application of crude glycerol as second generation biofuels, industrial chemical/biological products and livestock feed. If the new outlets for glycerol come to fruition, the price of crude glycerol may be expected to increase in future. The level of glycerol market increase depends on new value-added utilization of crude glycerol. If new outlets for glycerol, especially crude glycerol do not pan out, glycerol prices will continue to lag as experienced in past. Then, excess quantity of crude glycerol might be sold as a waste product or might be used just in incinerators to heat industrial boilers. In fact, glycerol is not a waste product but has been a staple chemical compound in the world economy for many years to come. Therefore new outlooks for glycerol industry should be continuously ventured and these might be helpful for potentially improving the economics of biodiesel production.

8. Conclusions

Glycerol is a nontoxic, biodegradable, biocompatible and versatile substrate that may be converted into numerous chemicals or bio-based products. The crude glycerol production will increase in future due to increasing consumption of biodiesel. The crude glycerol market is a complex and volatile which is mostly dependent on its global demand and supply. The demand and supply of glycerol, especially from the booming biodiesel industry, is directly correlated with its utilization and new outlets. There have been many changes in the crude glycerol market over the last two decades. For that reason, it is difficult to develop a model to predict future spot prices of crude glycerol. New applications of crude glycerol under research and development are promising, which may provide new outlets for large quantities of crude glycerol from biodiesel industry. This will help to relieve the crude glycerol glut and drive greater biodiesel production with improvement in biodiesel overall cost. The crude glycerol resulting from biodiesel production can make a handsome place in global market by using it as a source of feedstock for recovery of useful chemicals. It can be used as an additive in different fuels formulations apart from pharmaceutical and biochemical fields.

Acknowledgments

We gratefully acknowledge the support of USM Fellowship and Research Universities grant for conducting our research work on glycerol production and utilization for value-added products.

References

[1] United States Environmental Protection Agency (USEPA). EPA finalizes regulations for a renewable fuel standard (RFS) program for 2007 and beyond, EPA420-F-07-019. Ann Arbor, MI: Office of Transportation and Air Quality; 2007.
[2] Higgins J. On the road to fueling the future. In: Bioenergy '02, proceedings, paper 2062. Boise, ID, September: published by Pacific Regional Biomass Energy Program; 2002.
[3] The potential impact of rising petrochemical prices on soy use for industrial applications. Omni Tech International Ltd.; 2008. Available at: http://www.omnitechintl.com/pdf/September%202008%20Price%20Trend%20Study.pdf [accessed on 10 January 2012].
[4] Nitayavardhana S, Khanal SK. Biodiesel-derived crude glycerol bioconversion into animal feed: a sustainable option. Bioresour Technol 2011;10:5808–14.
[5] Medeiros MA, Leite CMM, Lago RM. Use of glycerol by-product of biodiesel to produce an efficient dust suppressant. Chem Eng J 2012;39(1):364–9.
[6] Cardona C, Posada J, Montoya M. Use of glycerol from biodiesel production: conversion to added value products. In: Proceedings of European Congress of Chemical Engineering (ECCE-6). 2007. p. 16–20.
[7] U.S. Food and Drug Administration. Glycerin; GRAS status as a direct human food ingredient. Federal Register, 1979; 48(27): 5759–60.
[8] Perry RH, Green DW, Maloney JOH. Perry's chemical engineers' handbook, 7th ed. McGraw-Hill; 1997.
[9] You YD, Shie JL, Chang CY, Huang SH, Pai CY, Yu YH, et al. Economic cost analysis of biodiesel production: case in soybean oil. Energy Fuels 2008;22:182–9.
[10] Glycerine – an overview by Soap and Detergent Association. Available at: www.aciscience.org/docs/Glycerine-an overview.pdf [accessed on 10 January 2012].
[11] Hazimah AH, Ooi TL, Salmiah A. Recovery of glycerol and diglycerol from glycerol pitch. J Oil Palm Res 2003;15:1–5.
[12] Mohtar Y, Tang TS, Salmiah A. Quality of basic oleochemicals produced in Malaysia. Informatics 2001;12:529–36.
[13] Kenkel P, Holcomb R. Feasibility of on-farm or small scale oilseed processing and biodiesel. In: English BC, Menard J, Jensen K, editors. Integration of agricultural and energy systems. Atlanta, Georgia: Global Bioenergy Partnership; 2008.
[14] Pramanik T, Tripathi S. Biodiesel – clean fuel of the future. Hydrocarbon Process 2005;84(2):49–54.
[15] Glycerol. In: Kirk-Othmer, editor. Encyclopedia of chemical technology. New York; John Wiley & Sons, Inc.; 2001.
[16] Wang ZX, Zhuge J, Fang H, Prior BA. Glycerol production by microbial fermentation: a review. Biotechnol Adv 2001;19:201–23.
[17] Zhou CH, Beltramini JN, Fan YX, Lu GQ. Chemoselective catalytic conversion of glycerol as a biorenewable source to valuable commodity chemicals. Chem Soc Rev 2008;37:527–49.
[18] Mootabadi H, Salamatinia B, Bhatia S, Abdullah AZ. Ultrasonic-assisted biodiesel production process from palm oil using alkaline earth metal oxides as the heterogeneous catalysts. Fuel 2010;89(8):1818–25.
[19] Wilson EK. Biodiesel revs up-fuel made from vegetable oil leads the pack of alternatives to petroleum products. Chem Eng News 2002;80:46–9.
[20] Salamatinia B, Mootabadi H, Bhatia S, Abdullah AZ. Optimization of ultrasonic-assisted heterogeneous biodiesel production from palm oil: a response surface methodology approach. Fuel Process Technol 2010;91(5):441–8.
[21] Melero JA, Vicente G, Paniagua M, Morales G, Munoz P. Etherification of biodiesel-derived glycerol with ethanol for fuel formulation over sulfonic modified catalysts. Bioresour Technol 2012;103(1):142–51.
[22] Thompson JC, He BB. Characterization of crude glycerol from biodiesel production from multiple feed stocks. Appl Eng Agric 2006;22(2):261–5.
[23] Singhabhandhu A, Tezuka T. A perspective on incorporation of glycerin purification process in biodiesel plants using waste cooking oil as feedstock. Energy 2010;35:2493–504.
[24] Gonzalez-Pajuelo M, Meynial-Salles I, Mendes F, Andrade JC, Vasconcelos I, Soucaille P. Metabolic engineering of *Clostridium acetobutylicum* for the industrial production of 1,3-propanediol from glycerol. Metab Eng 2005;7:329–36.
[25] Mu Y, Tend H, Zhang D, Wang W, Xiu Z. Microbial production of 1,3-propanediol by *Klebsiella pneumoniae* using crude glycerol from biodiesel preparations. Biotechnol Lett 2006;28:1755–9.
[26] Athalye SK, Garcua RA, Wen Z. Use of biodiesel-derived crude glycerol for producing eicosa pentaenoic acid (EPA) by the fungus *Pythium irregulare*. J Agric Food Chem 2009;57:2739–44.
[27] Abdullah AZ, Razali N, Lee KT. Optimization of mesoporous K/SBA-15 catalyzed transesterification of palm oil using response surface methodology. Fuel Process Technol 2009;90(7–8):958–64.
[28] Xie W, Peng H, Chen L. Transesterification of soybean oil catalyzed by potassium loaded on alumina as a solid-base catalyst. Appl Catal A 2006;300:67–74.
[29] Yazdani SS, Gonzalez R. Anaerobic fermentation of glycerol: a path to economic viability for the biofuels industry. Curr Opin Biotechnol 2007;18:213–9.
[30] US biodiesel demand. Jefferson City, MO: National Biodiesel Board; 2008. Available at: http://www.biodiesel.org/pdf_files/fuelfactsheets/Production_Graph_Slide.pdf [accessed on 10 January 2012].
[31] Smith C. Biodiesel revolution gathering momentum; 2004. Available at: http://www.straight.com/print/3568 [accessed on 10 January 2012].
[32] U.S. glycerine production soars in 2009. Available at: http://www.glycerinereport.com/20091911/us-glycerine-production-soars-2009 [accessed on 10 January 2012].
[33] McCoy M. An unlikely impact: growth of biodiesel has big implications for the oleochemical industry. Chem Eng News 2005;83(8):19–20.

[34] Biodiesel: prospect and challenges. Promar International; 2007. Available at: http://www.asasea.com/download_doc.php [accessed on 10 January 2012].
[35] Glycerin market analysis. ABG Inc. Company; 2007. Available at: http://www.asasea.com/download_doc.php [accessed on 10 January 2012].
[36] Hoh R. Malaysia biofuels annual; 2009. GAIN report number: MY9026, date: 6/12/2009.
[37] Tsobanakis P. Cargill Incorporate, presented at biofuels and feed stocks, Indonesia; 2007. Available at: http://www.cmtevents.com/eventdatas/070112/Pdf/070112.pdf [accessed on 10 January 2012].
[38] Bogaart V. Glycerin Marke Brief, Croda Oleochemicals – new ideas in natural ingredients; 2009. Available at: http://www.npt.nl/vereniging/images/stories/Verslagen/Presentatie_Bogaart_Croda_15042010.pdf [accessed on 10 January 2012].
[39] Biofuel News. The grass farmer. Available at: http://wincustomersusa.com/stockman/index.php?option=com_content&task=view&id=84&Itemid=9 [accessed on 10 January 2012].
[40] Lines S. An exploding market? Utilizing waste glycerol from the biodiesel production process; 2009. Available at: http://snrecmitigation.wordpress.com/2009/04/19/an-exploding-market-utilizing-waste-glycerol-from-the-biodiesel-production-process [accessed on 10 January 2012].
[41] U.S. Census Bureau Foreign Trade Data Dissemination. Available at: http://www.asasea.com/download_doc.php [accessed on 10 January 2012].
[42] Kotrba R. The glycerin spread. Biodiesel Magazine, September 2007. Available at: http://www.biodieselmagazine.com/article.jsp?article_id=1797 [accessed on 10 January 2012].
[43] Johnson DT, Taconi KA. The glycerin glut: options for the value-added conversion of crude glycerol resulting from biodiesel production. Environ Progress 2007;26:338–48.
[44] The promotion of the use of bio-fuels or related other renewable fuels for transport. EU Directive 2003/30/EC of the European parliament and of the council; 8 May 2003.
[45] Biofuels for transport. An international perspective. Paris, France: International Energy Agency; 2004. p. 169.
[46] Tyson KS, Bozell J, Wallace R, Petersen E, Moens L. Biomass oil analysis. research needs and recommendations, vol. 3; 2004. NREL/TP-510-34796, pp. 74–75.
[47] Ju YH, Vali SR. Rice bran oil as a potential source for biodiesel: a review. J Sci Ind Res 2005;64:866–82.
[48] Ahouissoussi NBC, WetzsteiProkop ME. A comparative cost analysis of biodiesel, compressed natural gas, methanol, and diesel for transit bus systems. Available at: http://nationalbiodieselboard.com/resources/reportsdatabase/reports/tra/19940101_tra-030.pdf [accessed on 10 January 2012].
[49] Nelson RG, Hower SA, Weber JA. Potential feedstock supply and costs for biodiesel production. In: Bioenergy 1994, Proceedings of the sixth national bioenergy conference.
[50] Zhang Y, Dub MA, McLean DD, Kates M. Biodiesel production from waste cooking oil: economic assessment and sensitivity analysis. Bioresour Technol 2003;90:229–40.
[51] Miller K. Impact of biodiesel production on the glycerol market; 2006. Available at: http://www.ruralsementes.com.br/produtos/Impact_of_Biodiesel_Production_on_the_Glycerol_Market.pdf [accessed on 10 January 2012].
[52] Gunstone FD, Hemin MPD. Glycerol – an important product of the oleochemical industry. Lip Technol 2004;16(8):177–9.
[53] Groen E. Glycerine US market runs dry – prices in Europe will rise sharply. E-Energy Market; 2010. Available at: http://www.e-energymarket.com/news/link/d8e4c7fb35/browse/4/select_category/359.html [accessed on 10 January 2012].
[54] Chiu CW, Dasari MA, Sutterlin WR, Suppes G. J Ind Eng Chem Res 2006;45:791–5.
[55] Haas MJ. The interplay between feedstock quality and esterification technology in biodiesel production. Lip Technol 2004;16:7–11.
[56] Woo C. Clean fuel trends in Asia: contribution of MTBE. Hydrocarbon Process 2007;86:85–8.
[57] Fan X, Burto R. Recent development of biodiesel feedstocks and the applications of glycerol: a review. Open Fuels Energy Sci J 2009;2:100–9.
[58] Valliyappan T, Bakhshi NN, Dala AK. Pyrolysis of glycerol for the production of hydrogen or syn gas. Bioresour Technol 2008;99:4476–5448.
[59] Tim M. Production and utilization. Liberty Process Technologies; 2006. Available at: http://www.xcelenergy.com/SiteCollectionDocuments/_/UM-Milestone3Report.pdf [accessed on 10 January 2012].
[60] Bozell JJ.Oleochemicals in the biorefinery: glycerol and co-products from biodiesel production 2008 transition to a bioeconomy integration of agricultural and energy systems. 2008.
[61] Duane TJ, Katherine AT. The glycerin glut: options for the value-added conversion of crude glycerol resulting from biodiesel production. Environ Progress 2007;26:338–48.
[62] Bondioli P. From oilseeds to industrial products: present and near future of oleochemistry. Italian J Agron 2003;7:129–35.
[63] Pagliaro M, Rossi M. The future of glycerol. New usages for a versatile raw material. RSC Green Chem Book Ser 2008;5:212–8.
[64] Neumann WHC. Glycerin and its history. In: Jungermann E, Sonntag NOV, editors. Cosmetic science and technology series 11. New York: Marcel Dekker, Inc.; 1991. p. 7–14 (Chapter 2).
[65] Food ingredients. Acme-Hardesty Oleochemicals; 2010. Available at: http://www.acme-hardesty.com/product_categories/flavor%20&%20fragrance [accessed on 10 January 2012].
[66] SRI Consulting. Chemical economics handbook; 2006. Available at: http://www.ingenia.nl [accessed on 10 January 2012].
[67] Moore CG. Oil modification of alkyd resins for protective coatings. JAOCS 1946;23(3):69–70.
[68] Brady S, Tam K, Leung G, Salam Ch. Zero waste biodiesel: using glycerin and biomass to create renewable energy. UCRJ 2007;2:1–11. Available at: http://www.ugrj.ucr.edu/journal/volume2/SeanBrady.pdf [accessed on 10 January 2012].
[69] Gong CS, Du JX, Cao NJ, Tsao GT. Coproduction of ethanol and glycerol. Appl Biochem Biotechnol 2000;84–86(1–9):543–59.
[70] Rosa DS, Bardi MAG, Machado LDB, Dias DB, Silva LGA, Kodama Y. Starch plasticized with glycerol from biodiesel and polypropylene blends: mechanical and thermal properties. J Therm Anal Calorimetry 2010;181–6.
[71] Villamagna F, Hall BD. Explosive compositions containing glycerin, IPCB Class: AC06B3128FI, USPC Class: 149-2; 2008. Available at: http://www.faqs.org/patents/app/20080245450 [accessed on 10 January 2012].
[72] Pagliario M. From glycerol to value added product. Angew Chem Int Ed 2007;46:4434–40.
[73] Cardona C, Posada J, Montoya M. Use of glycerol from biodiesel production: conversion to added value products. In: Proceedings of European Congress of Chemical Engineering (ECCE-6); 2007.
[74] Wang K, Hawley MC, De Athos SJ. Conversion of glycerol to 1,3-propanediol via selective dehydroxylation. Ind Eng Chem Res 2003;42:2913–23.
[75] Jerome F, Pouilloux Y, Barrault J. Rational design of solid catalysts for the selective use of glycerol as a natural organic building block. Chem Sus Chem 2008;1:586–613.
[76] Zheng Y, Chen X, Shen Y. Commodity chemicals derived from glycerol, an important biorefinery feedstock. Chem Rev 2008;108(12):5253–77.
[77] Wibowo TY, Abdullah AZ, Zakaria R. Organo-montmorillonites as catalysts for selective synthesis of glycerol monolaurate. Appl Clay Sci 2010;50:280–1.
[78] Hermida L, Abdullah AZ, Mohammad AR. Post-synthetically functionalized SBA-15 with organosulfonic acid and sulfated zirconia for esterification of glycerol to monoglyceride. J Appl Sci 2010;10(24):3199–206.
[79] Clacens JM, Pouilloux Y, Barrault J. Synthesis and modification of basic mesoporous materials for the selective etherification of glycerol. Stud Surf Sci Catal 2002;143:687–95.
[80] Martin A, Richter M. Oligomerization of glycerol – a critical review. Eur J Lip Sci Technol 2010;56:456–60.
[81] Stella M. Glycerol – the sweetener that doesn't sweeten your life. Available at: http://www.diethealthclub.com/articles/500/diet-and-wellness/glycerol-the-sweetener-that-doesn-t-sweeten-your-life.html [accessed on 10 January 2012].
[82] Bauer R, Katsikis N, Varga S, Hekmat D. Study of the inhibitory effect of the product dihydroxyacetone on *Gluconobacter oxydans* in a semi-continuous two-stage repeated-fed-batch process. Bioproc Biosyst Eng 2005;28:37–43.
[83] Irleb. Vegetable glycerin; 2009. Available at: http://www.vaporden.com/notes/Vegetable_Glycerin [accessed on 10 January 2012].
[84] Lee T, Johnson W, Earl R. May non-nutritive sweetened beverages with glycerine' IPCB Class: AA23L238FI, USPC Class: 426590; 2008. Available at: http://www.faqs.org/patents/app/20080226795 [accessed on 10 January 2012].
[85] Defrain JM, Hippen AR, Kalscheur KF, Jardon PW. Feeding glycerol to transition dairy cows: effects on blood metabolites and lactation performance. J Dairy Sci 2004;87:4195–206.
[86] Lammers PJ, Kerr BJ, Weber TE, Dozier WA, Kidd MT, Bregendahl K, et al. Digestible and metabolizable energy of crude glycerol for growing pigs. J Anim Sci 2008;86(3):602–8.
[87] Cerrate S, Yan F, Wang Z, Coto C, Sacakli P, Waldroup PW. Evaluation of glycerine from biodiesel production as a feed ingredient for broilers. Int J Poult Sci 2006;5(11):1001–7.
[88] Demirbas A. Biodiesel from vegetable oils via transesterification in supercritical methanol. Energy Convers Manage 2002;43:2349–56.
[89] Ito T, Nakashimada Y, Koichiro S, Matsui T, Nishio N. Hydrogen and ethanol production from glycerol-containing wastes discharged after biodiesel manufacturing process. J Biosci Bioeng 2005;100:260–5.
[90] Cortright RD, Davda RR, Dumesic JA. Hydrogen from catalytic reforming of biomass-derived hydrocarbons in liquid water. Nature 2002;418:964–7.
[91] Holm-Nielsen JB, Lomborg CJ, Oleskowicz-Popiel P, Ebensen KH. On-line near infrared monitoring of glycerol-boosted anaerobic digestion processes: evaluation of process analytical technologies. Biotechnol Bioeng 2008;99:302–13.
[92] Hoogendoorn A, Adriaans T, Van-Kasteren JMN, Jayaraj KM. Glycerine purification via biocatalysis and column adsorption for high-quality applications, report no. 0656632-R06; 2007. Available at: http://www.ingenia.nl [accessed on 10 January 2012].
[93] Rahmat N, Abdullah AZ, Mohamed AR. Recent progress on innovative and potential technologies for glycerol transformation into fuel additives: a critical review. Renew Sust Energy Rev 2010;14(3):987–1000.
[94] Papanikolaou S, Aggelis G. Lipid production by *Yarrowia lipolytica* growing on industrial glycerol in a single-stage continuous culture. Bioresour Technol 2002;82:43–9.

[95] Pyle DJ, Garcia RA, Wen Z. Producing docosa hexaenoic acid (DHA)-rich algae from biodiesel-derived crude glycerol: effects of impurities on DHA production and algal biomass composition. J Agric Fooc Chem 2008;56(11):3933–9.
[96] Lee PC, Lee WG, Lee SY, Chang HN. Succinic acid production with reduced by-product formation in the fermentation of *Anaerobiospirillum succiniciproducens* using glycerol as a carbon source. Biotechnol Bioeng 2000;72(1):41–8.
[97] Himmi EH, Bories A, Barbirato F. Nutrient requirements for glycerol conversion to 1,3-propanediol by *Clostridium butyricum*. Bioresour Technol 1999;67(2):123–8.
[98] Xiu ZL, Song BH, Wang ZT, Sun LH, Feng EM, Zeng AP. Optimization of dissimilation of glycerol to 1,3-propanediol by *Klebsiella pneumoniae* in one- and two-stage anaerobic cultures. Biochem Eng J 2004;19(3):189–97.
[99] Tran BL, Hamnik JM, Blubaugh SJ. Hydraulic fluids and fire-resistant fluids comprising glycerin containing by-products. USPTO patent application 20080085846. Class: 508583, ser. no. 11/420,140; 2006.
[100] Bhattacharjee Y. The New York Times, Harnessing biology and avoiding oil for chemical goods; 2008. Available at: http://www.nytimes.com/2008/04/09/technology/techspecial/09chem.html [accessed on 10 January 2012].
[101] Alhanash A, Kozhevnikova EF, Kozhevnikov IV. Hydrogenolysis of glycerol to propanediol over Ru:polyoxometalate bifunctional catalyst. Catal Lett 2008;120:307–11.
[102] Chiu C, Dasari MA, Suppes GJ, Sutterlin WR. Dehydration of glycerol to acetol via catalytic reactive distillation. AIChE J 2006;52(10):3543–8.

Renewable and Sustainable Energy Reviews 16 (2012) 4574–4587

Contents lists available at SciVerse ScienceDirect

Renewable and Sustainable Energy Reviews

journal homepage: www.elsevier.com/locate/rser

Intensification of biodiesel production via ultrasonic-assisted process: A critical review on fundamentals and recent development

Ali Sabri Badday [a], Ahmad Zuhairi Abdullah [a,*], Keat Teong Lee [a], Muataz Sh. Khayoon [a,b]

[a] School of Chemical Engineering, Universiti Sains Malaysia, Engineering Campus, 14300 Nibong Tebal, Penang, Malaysia
[b] Chemical Engineering Department, University of Technology, Baghdad, Iraq

ARTICLE INFO

Article history:
Received 1 February 2011
Received in revised form
3 April 2012
Accepted 6 April 2012

Keywords:
Biodiesel
Reactants immiscibility
Ultrasonic
Emulsification
Process intensification
Continuous process

ABSTRACT

Biodiesel is a good alternative fuel to petroleum diesel. It is produced through transesterification reaction between vegetable oil or animal fats and alcohol. The process faces various problems related to the immiscible nature of the reactants causing poor mass transfer rate. This drawback is responsible for long reaction time and low reaction rate leading to an energy intensive process. Process intensification through the use of active catalyst, pressure reactor, high temperature, high stirring rate or even non-conventional approaches such as supercritical method and Biox process often subjects to drawbacks with respect to energy consumption, product quality and reactants cost. This paper highlights recent development in the production of biodiesel under ultrasonic irradiation conditions. It handles the drawback of poor immiscibility between reactants as ultrasonic energy can emulsify the reactants to reduce the catalyst requirement, reaction time and reaction temperature. Ultrasonic energy also neglects the limitations in the use certain feed stocks. Fundamental aspects of the ultrasonic-assisted process using homogeneous and heterogeneous catalysts are reviewed. Recent achievement and future development in this technology in a batch and continuous process are also highlighted.

Contents

* Corresponding author. Tel.: +604 599 6411; fax: +604 594 1013.
E-mail address: chzuhairi@eng.usm.my (A.Z. Abdullah).

1364-0321/$ - see front matter © 2012 Elsevier Ltd. All rights reserved.
http://dx.doi.org/10.1016/j.rser.2012.04.057

1. Introduction

The depletion of fossil resources and environmental pollution are among the most critical problems that threat humanity. The attention is currently turned towards the use of biomass or biomass-derived materials as replacements to petroleum fuel. In 1893, Rudolf Diesel attempted to make use of peanut oil as fuel for diesel engine [1]. During 1930s and 1940s, vegetable oils replaced diesel fuels in many events, usually in emergency cases. In August 1982, the first international conference was held to discuss the use of vegetable oils as fuels. Many topics were highlighted including the cost of fuel, plausible methods of manufacturing, the characterizations of the fuel and the effects of fuel derived from vegetable oil on the efficiency of diesel engines [2]. These bio oils look promising to replace petroleum fuel but technical hurdles are still lying ahead.

Biodiesel is a mixture of mono alkyl esters with long-chain fatty acids that is derived from vegetable oils or animal fats [3]. It has many good properties compared to diesel fuel. It is an eco friendly fuel and biodegradable. Besides being non toxic, it is mainly free of sulfur components and aromatics [4]. Biodiesel can mix at any percentage with petroleum fuel or it can itself be used as a successful fuel [5].

There are four different methods to produce biodiesel from bioresources. Direct use and blending of raw oils are among the early approaches where vegetable oils are used directly or diluted with petroleum diesel to run the engine [6–9]. Micro-emulsions which is colloidal equilibrium dispersion of optically isotropic fluid usually form spontaneously from two normally immiscible liquids [10]. Thermal cracking that is the conversion of triglycerides to biofuel with or without the presence of catalyst is another approach and it involves the use of high temperature in the absence of air or oxygen [11,12]. As the process in an energy-intensive one, limited success has been achieved in such approach.

Recently, transesterification has been actively investigated as the most popular way to convert vegetable oils or animal fats into fatty acid methyl esters (FAME) [13]. Fig. 1 illustrates the general equation of transesterification reaction [14]. It is the organic reaction that causes the exchange of organic group (R″) of an ester with the organic group (R′) of an alcohol where, R1, R2, R3 are long-chain hydrocarbons, usually called fatty acid chains. The main types of fatty acids in vegetable oils and animal fats are such as palmitic, myristic, stearic, oleic, linoleic and linolenic. Typical compositions of various oils are shown in Table 1. Transesterification mechanism consists of a series of consecutive reversible reactions. Triglyceride molecules react step by step with methanol to form diglyceride, monoglyceride and in the last step, glycerol is formed (Fig. 2).

One mole of FAME is generated in each step of the transesterification process [15]. All of these reactions are reversible and essentially the goal in this reaction is to shift the equilibrium to the products side, forming more fatty acid esters and glycerol. Usually, methanol is used in the biodiesel production process as it is relatively cheap compared to other alcohols and has small chain of carbon. However, as of the reaction is reversible, excess alcohol is needed to shift the reaction to form more products [16]. This reaction is commonly catalyzed by acid or base catalysts while another possibility could be through the use of enzymatic catalyst (biocatalysts) especially lipases.

Biodiesel production process has undergone significant progress in recent years with some innovations introduced to improve efficiency and productivity. Due to recent emergence of ultrasonic-assisted technology for biodiesel production with reported benefits as compared to conventional production process, mature understanding o this topic is deemed necessary. As such, this review aims at improving the understanding of ultrasonic phenomena and their effects on biodiesel production process to meet specific requirements in the process. Reported behaviors in various processes used for biodiesel production are properly analyzed and reviewed.

2. Demands in biodiesel production process

A wide range of studies have been dedicated to the production process of biodiesel using various methods and some of them could achieve good yield and look promising for large scale

$$TG + CH_3OH \underset{k2}{\overset{k1}{\rightleftharpoons}} DG + FAME$$

$$DG + CH_3OH \underset{k4}{\overset{k3}{\rightleftharpoons}} MG + FAME$$

$$MG + CH_3OH \underset{k6}{\overset{k5}{\rightleftharpoons}} GLY + FAME$$

Fig. 2. The sequence of transesterification reaction.

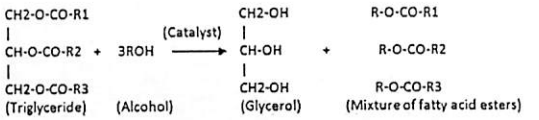

Fig. 1. General-glyceride transesterification to biodiesel.

Table 1
Typical fatty acid composition of various oil sources.

Name	Structure	Formula	Composition (wt.%)					
			Palm	Soybean	Cottonseed	Coconut	Rapeseed	Tallow
Lauric	12:0	$C_{12}H_{24}O_2$	0.1	0.1	0.1	46.5	–	0.1
Myristic	14:0	$C_{14}H_{28}O_2$	1.0	0.1	0.7	19.2	–	0.8
Palmitic	16:0	$C_{16}H_{32}O_2$	42.8	0.2	20.1	9.8	3.5	23.3
Stearic	18:0	$C_{18}H_{36}O_2$	4.5	3.7	2.6	3.0	0.9	19.4
Oleic	18:1	$C_{18}H_{34}O_2$	40.5	22.8	19.2	6.9	64.1	42.4
Linoleic	18:2	$C_{18}H_{32}O_2$	10.1	53.7	55.2	2.2	22.3	10.7
Linolenic	18:3	$C_{18}H_{30}O_2$	0.2	8.6	0.6	–	8.2	0.4

production. Some researchers focus their study on the economic aspects of the process with respect to the types of feed stock, their availability and price that could influence the economy of the process [17]. Fig. 3 that shows the distribution of biodiesel production cost. The main contributor to overall cost of the process is the feed stock (the vegetable oil or animal fats) while the second one is the chemicals that are used in the reaction such as the catalyst and alcohol. In the transesterification process, excess alcohol is commonly used to shift the equilibrium towards the formation of the methyl esters. In this respect, it should be mentioned that catalyst reusability is almost impossible if homogeneous catalyst is used. The development of methods for the production should focus on the reduction of these costs. The investment of cheap recourses of triglyceride and efforts to reduce the amounts of the chemicals used should also be considered. These days, some researchers are actively investigating the enhancements on the process to eliminate or reduce these problems or drawbacks. The aim is always to produce the desired product at an optimum rate while at the same time possesses high quality while at the same time demonstrates good process economy [18].

The enhancements in biodiesel production are generally aimed at generating high quality biodiesel that conforms to international standards such as ASTM or EN standard. One of the approaches is to minimize the quantity of side products or at least to minimize the side reactions [19,20]. High quality biodiesel can be used in diesel engine without any negative effects while at the same time can generates less pollutants to environment [21].

In the other hand, new technology should reduce reaction time needed for the reaction and lower the reaction temperature. These parameters could affect the product quality as the feed stock (vegetable oil or waste cooking oil) can undergo various side reactions at high temperature, especially when long reaction time is needed. Operating a system with high temperature does require huge amount of energy. As such, process improvement towards achieving sharp reduction in reaction temperature is deemed necessary. The reduction in the energy consumption is expected to improve the energy ratio (output energy/input energy) leading to better net energy to be obtained from biodiesel. For example, energy ratio for biodiesel produced from palm oil was found to be 3.53, indicating a net positive energy production [22]. In future, production process with even lower energy input should have a positive influence if sustainable energy supply were to be considered.

Working in a safe environment demands the use of low reaction temperature because of low boiling point of methanol. The risks of exposure to its vapor will be less and the need for a closed system in order to control the evaporation and temperature will be eliminated [23]. Closed systems often require extra control mechanism on the pressure and the need for special equipment design that will have great influence on production costs. Besides, as the products are not continuously removed from the reaction system, equilibrium will be shifted to the reverse reaction especially at high conversion. Thus, the production process should be ideally carried out at atmospheric pressure.

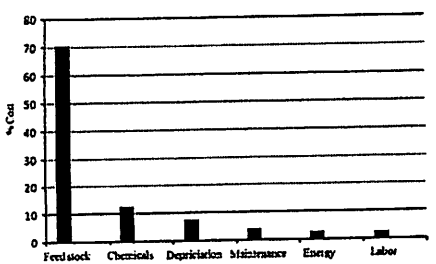

Fig. 3. Costs of biodiesel production [19].

The development of a new technology for biodiesel production should consider the effects on the desired catalyst. It is necessary to find an operating procedure that allows optimum catalytic activity to reduce the catalyst amount to be used. This factor is important as the reduction in the quantity of catalyst will reduce the level of purification step for the product. That will lower the cost of the whole process by reducing the process time to produce the final product [24]. At the same time, better quality of biodiesel will be achieved as some components of the catalyst could leach into the biodiesel [7]. In this study, the main drawbacks and recent development in the production process of biodiesel is critically reviewed. This report also highlights recent topics that receive attention among researchers when attempting the intensification of biodiesel production process.

3. Main drawbacks in biodiesel production process

In biodiesel production through transesterification, serious problems and limitations can be identified. First of all, the immiscible nature of the reactants (alcohol and vegetable oil) coupled with the difference in their densities can lead to poor contact between the reactants. Consequently, reduction in mass transfer rate results loading to low reaction rate and increased reaction time [25]. The reaction between two immiscible fluids is analogous to the heterogeneous transport phenomena (heat, mass and fluid) that are caused by the lag in the film between them. The transport could be accelerated by many ways such as by increasing the driving force including decreasing the thickness of the film or changing some physical properties. The best way that can be applied in this problem is film mixing and it can be achieved by many strategies like vigorous agitation [26,27] or by the application of ultrasonic energy [20].

The biodiesel production process can actually be carried out in two ways i.e. with or without the use of catalyst. The catalyzed production can be divided into homogenous and heterogeneous reactions. For this purpose, strong acid or base catalysts are possible to be used but the latter type is significantly more active. Homogenous reaction systems generally record high yield [28,29]. The drawback of base catalyzed systems is the limitation in the use of several oil feed stocks because of their sensitivity to the presence of free fatty acids (FFA) in the oil. Amounts of FFA larger than 1 wt% will react with the base catalyst to form soap according to the reaction equation as shown in Fig. 4 leading to loss of the catalyst from the system [13]. The soap also complicates the product purification process to leading to a significant increase in overall production cost. Even with low FFA, base homogenous catalysts itself are hard to be removed from the product and requires two or three times of washing with hot water [30].

Homogenous acid catalysts are relatively less active compared to base catalysts but they have no sensitivity towards FFA. Thus, the reaction using these catalysts must be maintained at high temperature but the biodiesel yield in the process could be low. These drawbacks translate into high production costs and low

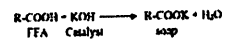

Fig. 4. General equation for soap formation [13].

productivity. Besides that, acidic catalyst is corrosive and destructive to the reactor and other supporting equipment involved in the process [31]. Current focus is therefore shifting towards the use of heterogeneous catalysts which are considered more environmental friendly.

Heterogeneous catalysts can achieve high biodiesel yield [32] and have no tendency to be affected by high content of FFA. For that reason, no foam will be generated and the need for extra purification process is eliminated. Consequently, higher purity of biodiesel and glycerin is obtained. All of these benefits will lead to better economy of the production process [33]. Despite all these advantages, biodiesel yield that is obtained with heterogeneous catalyst is still relatively lower than that of homogenous catalysts. It is therefore a conventional approach to increase the yield by increasing the reaction temperature and pressure. As a result, the production cost is higher even with the use of cheap feed stocks while the net energy obtained from the biofuel is reduced [34].

Despite positive influence in accelerating the biodiesel production process, there are several serious drawbacks that are associated with the use of catalysts. Therefore, mixed arguments are made by various research groups on this matter. Some researchers made several attempts to exclude the use of catalysts in certain non-conventional processes. However, some other researchers are still in favor of catalytic route but with certain modification made to the production process. Recent development on efforts to accelerate biodiesel production process through non-catalytic routes is reviewed in the subsequent sections.

4. Non-catalyzed production of biodiesel

This section reviews two different non-catalytic biodiesel production process that have been reported in literature, i.e. supercritical and Biox processes. Specific process requirements and process behaviors are reviewed while respective drawbacks are highlighted.

4.1. Supercritical method

One of the approaches to overcome problems associated with poor immiscibility between the reactants and technical problems caused by catalysts is to use supercritical method. In this approach, no catalyst is involved. Supercritical alcohol transesterification reaction takes place under extremely high temperature and pressure. When a gas or liquid is exposed to pressure and temperature beyond its critical point, unusual phenomena on its properties are exhibited. Liquid and vapor phase are no longer confined under these conditions and single supercritical fluid phase is generated [13]. In the supercritical method, methanol and oil, which are immiscible liquids at room temperature will form a homogenous fluid. This is due to the sharp drop in the solubility of methanol and reduction in dielectric constant which makes methanol a non-polar substance [35]. Thus, the reaction is accelerated as no limitation with respect to mass transfer is expected under such conditions.

Tan et al. [36] investigated a one step supercritical method to produce biodiesel from palm oil under an optimum reaction temperature of 239 °C and a pressure of 8.1 MPa. Under these conditions, the highest biodiesel yield achieved was 70% in 20 min. On the other hand, Ilham and Saka [37] studied the production of biodiesel using Jatropha curcas oil using a two-step supercritical method. They reported that biodiesel 97% biodiesel yield was obtained in 15 min at 300 °C and 9 MPa.

Supercritical method is also not affected by FFA and no soap generation is involved because of the non-catalytic nature of the reaction. Therefore, the quality of biodiesel and glycerin is expected to be better than that for a catalyzed reaction and the reaction time is significantly low. Besides that, Supercritical method has high reaction rate so that the volume of the reactor can be significantly reduced [38]. Fig. 5 illustrates the typical flow diagram of a supercritical system for biodiesel production. It shows two stages of supercritical process where the separation of glycerol and recovery of the methanol are made in the respective stage.

Despite all the advantages, the main drawback of this method is that it depends on critical conditions of alcohol which demands high pressure (4.9–8.1 MPa) and temperature (239–290 °C) [39]. These requirements translate into high energy input for the process. Also, under such high temperature, the degradation of triglycerides cannot be avoided leading to undesired by-products formation that can affect the biodiesel quality. Besides safety considerations, the extreme reaction conditions also mean that the procedure is hard to be operated and requires specifically designed equipment. All these factors will negatively affect the overall process economy if an industrial scale of operation were to be considered. In closed systems, the reaction will also be shifted towards reversed reaction especially at high conversion due to the presence of more products in the reaction vessel [5]. This phenomenon will defeat the purpose of accelerating the reaction rate via supercritical method. As such, this method is deemed unsatisfactorily to address problems with respect to high net energy supply by biodiesel, mild reaction conditions and high product quality.

4.2. Biox process

Boocock et al. [40] developed a new technique named the Biox process to yield biodiesel non-catalytically with the use of

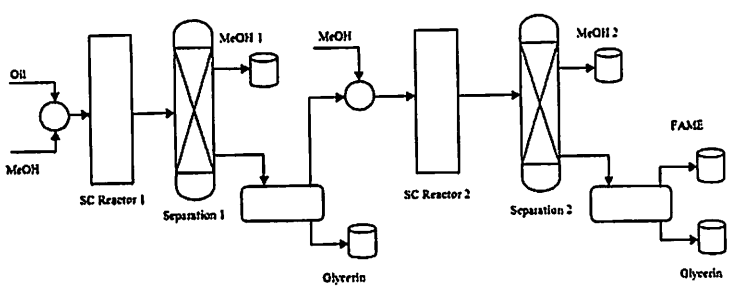

Fig. 5. Flow diagram of supercritical method for biodiesel production [34].

a co-solvent. The co-solvent was primarily used to overcome low solubility of methanol in oil. The process took place at a low temperature of 30 °C and it was able to convert oil with high percentage of FFA (more than 10%) into biodiesel in two steps. In the first step of the process, the conversion of FFA was achieved. The second step involved the conversion of triglyceride. The addition of the co-solvent was done in each step. Short reaction times of 5–10 min were recorded while the process was operated continuously for 90 min. The most common co-solvent to be used is tetrahydrofuran due to its close boiling point to that of methanol [13]. Fig. 6 describes the procedure where the reactor stage refers to individual stage involved while the separation of methanol and co-solvent is achieved in the lower separation process. The co-solvent is recycled and reused through the continuous process. In the separation process, both excess methanol and the co-solvent are recovered from the products.

The basic advantages of this process its ability to handle feeds with high FFA, the reaction time is short and it can be carried out under ambient temperature and pressure. The disadvantage of this process is that even though there is no catalyst present in the product phase, the co-solvent must be completely removed due to its hazardous and toxicity natures [19]. So this factor creates a big economical barrier as the separation of methanol and the co-solvent is difficult due to the very close boiling point of them. This difficulty can translate into added production cost while the residual solvent in the biofuel product can affect the compliance with the international standards [37].

As described above, a number of alternative approaches have been investigated to overcome problems faced in biodiesel production process. Each of the approaches has its own benefits and disadvantages. The following sections highlight another emerging technical approach to solve the problems. It involves the application of ultrasonic field to accelerate the process which is due to be carried out under mild reaction conditions. Fundamentals of its operation, the main advantages and drawbacks of this process will be thoroughly reviewed.

5. Ultrasonic energy and its industrial applications

This section provides some information of ultrasonic energy and its effects on liquid systems leading to its practical use in various industrial applications.

5.1. Introduction to ultrasonic energy

Ultrasound (US) is simply a sound pitch above human hearing ability i.e. usually above 20 kHz. It is a mechanical energy and has plenty of applications in our daily life [41]. The use of ultrasound as a source of energy is common these days and recently it is used to provide assistant to a great number of industries. Fig. 7 shows the general divisions of sound frequencies. The frequencies beyond 20 kHz till 100 kHz are used in industries but the range of industrially useful frequencies can only be extended to 2 MHz due to huge amount of energy needed to generate higher frequencies.

Ultrasound wave generates cavitation bubbles as it passes through the liquid [25]. Ultrasound wave travels like any other sound wave by a successive series of rarefaction and compression cycles vibrating the molecules of the carrier media, in this case the liquid reactants. When the attraction forces between the liquid molecules became less than the negative pressure of the cyclic rarefaction, a gap will be generated and is filled with vapor from the liquid. At the beginning of its lifetime, it begins tiny but within other successive cycles, it grows to form acoustic cavitation bubble.

5.2. Effects of ultrasonic on multiphase liquid systems

The use of ultrasonic energy in biodiesel production process is a new, attractive and effective procedure to solve problems that are faced by conventional methods. Ultrasonic irradiation can enhance mass transfer rate between the reactants which are immiscible liquids. It has been employed in a wide range of

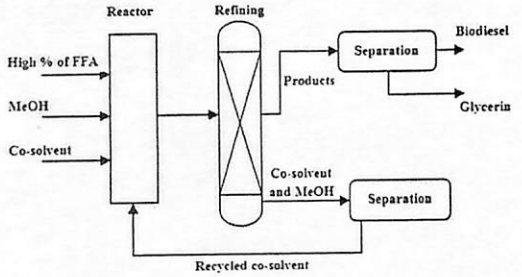

Fig. 6. Flow diagram of the Biox process.

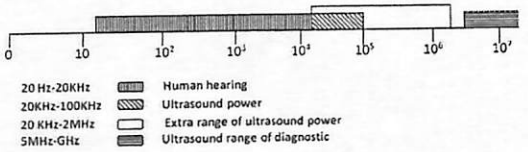

Fig. 7. General divisions of sound frequencies.

chemical processes causing reduction in reaction time and improvement in production yield [25]. Intensified reaction causes shorter reaction time, better product yield and lower catalyst requirement while supporting the use of greener heterogeneous catalysts. Mild reaction conditions translate into better process economy and simpler equipment set up.

Huge number of these bubbles can be generated in the liquid. Some of them are stable and can stand for another cycle while others will undergo vigorous breakdown once reaching certain critical size. The strong collapses generate local pressure in the order of 2000 atm and the temperatures could reach up to 5000 K [42]. It is shown in Fig. 8 that the bubbles are formed at zero time and undergoes breakdown after an approximate period of 400 μs. Small hotspots that are generated from these collapses can offer the energy for some chemical reactions. These phenomena result in severe mixing between the two immiscible liquids close to the phase boundary and force the liquids to inspire micro jets which can reach to a speed up to 200 m/s. The cause for the micro jets generation is the asymmetric breakdown of the cavitation bubbles [25].

One of the advantages of these cavitations is that it causes a local increase in temperature near the boundary layer and this increment will modify the course of the transesterification reaction that consequently offset the requirement for external heating in the production process. On the other hand, the formation of micro jets eliminates the need for intense mechanical agitation to improve mass transfer between the two reactant phases [42]. Ultimately, significant improvement in the reaction rate will result.

5.3. Industrial usages of ultrasonic energy

During 1920s, the earliest use of acoustic waves to generate cavitations to significantly change the reaction rate was attempted. During 1940s, many efforts were done to use ultrasound in polymer manufacturing and chemical processing [43]. No further progress in this topic had been made until 1970, where many successful applications were achieved. In 1960s, the development began after the spread of commercial ultrasonic devices in laboratories of chemistry, biology and metallurgy [44]. In the recent years, ultrasonic irradiation attracted researchers to incorporate it in many new areas such as manufacturing of nanostructured materials [45,46], food industry [47–49], sonodynamic therapy [50–52], processing of biomass [53,54] and sonochemical degradation of pollutant materials and hazardous chemicals [55–57].

A low frequency ultrasonic-assisted system can be used to produce emulsions from immiscible liquids [58–60]. As the feeds for biodiesel production process are immiscible, ultrasonication could be beneficial for transesterification of triglyceride with alcohol and early successes have been reported [61,62]. Besides reduction in reaction time and catalyst requirement, ultrasonic-assisted transesterification also minimizes alcohol to oil molar ratio and limits energy consumption [62]. As such, the objective of achieving better net energy from the biodiesel will be achieved. Mild reaction conditions at short reaction time also mean lower opportunity for the occurrence of undesired side products leading to better quality of the biodiesel product [61].

6. Batch biodiesel production process

This section reviews various biodiesel production processes using batch reactor system. The use of various base and acid catalysts in conventional and ultrasonic-assisted reactor system is compared and properly discussed.

6.1. Introduction

Early attempts on the study of vegetable oils transesterification under ultrasonic field were made using batch process. This process mode is easy to deal with and the control of reaction temperature can be made with the use of appropriate technique (like water bath) [63,64]. In the conventional reactor set up, vigorous agitation process in the reactor is done using a suitable mechanical agitator (magnetic stirring in the case of small scale study or anchor type agitator). Investigation on a batch process to use ultrasonic irradiation instead of mechanical stirring has been made using ultrasonic horn or probe that is immersed in the reaction media [64]. Fig. 9 shows a schematic diagram of ultrasonic-assisted batch reactor system for biodiesel production. It can be seen that the catalyst and the desired alcohol are mixed in pretreatment stage before the reactor. The ultrasonic probe provides the reactor with ultrasonic energy followed by phase separation stage. During the phase separation stage, the product can be collected while the remaining residue can be further separated to extract the catalyst and glycerin. In this study, the review on an ultrasonic-assisted batch reaction system will be divided into homogenous and heterogeneous catalysts. Major highlights to the process behaviors and behaviors are also given in the following sub-sections.

6.2. Biodiesel production process using homogenous catalyst

Production of biodiesel using homogenous catalyst has been investigated by many researchers using conventional batch process. Catalysts such as potassium hydroxide [65], sodium hydroxide (NaOH) [29] and other types of homogenous catalysts [66] have been studied. Compared with other types of catalyst, homogenous catalysts generally attract researchers' attention and widely used in industries. Table 2 summarizes the use of these catalysts under conventional conditions. It could provide high conversion but the reaction time to achieve high yield is large, especially in the case of H_2SO_4. Typically, yields higher than 95% are only possible between 120–180 min. Reaction temperatures also vary but if higher than 65 °C is needed, pressure reaction should be used as methanol will evaporate beyond that temperature which is its boiling point [67].

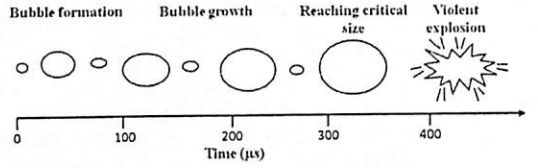

Fig. 8. Formation, growth and collapse of a cavitation bubble.

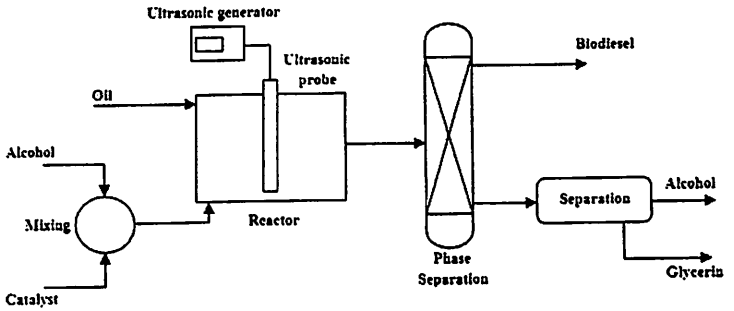

Fig. 9. Basic scheme for ultrasonic batch biodiesel production.

Table 2
Performance of various homogenous catalysts in biodiesel production process using conventional stirring reaction system.

Feed oil	Catalyst	Reaction conditions				Biodiesel yield (%)	Reference
		Alc:oil[a]	W_{cat} (w/w_{oil})	Temperature (°C)	Time (min)		
Rapeseed	KOH	6:1	1	65	120	96.0	[68]
Used frying oil	KOH	7.5:1	1.1	70	30	86.0	[69]
Sunflower	NaOH	6:1	1	60	120	97.1	[70]
Waste cooking	H_2SO_4	20:1	4	95	600	90.0	[31]
Soybean	H_2SO_4	3:1	3	120	60	> 95.0	[5]
Waste cooking	$Fe_2(SO_4)_3$ followed by CaO	7:1	Acid: 0.4 Base: -	60 60	180 180	81.3	[62]

[a] Alcohol to oil molar ratio.

Table 3
Performance of ultrasonic-assisted reaction system for biodiesel production using various homogenous catalysts.

Feed oil	Catalyst	Reaction conditions						
		Alc:oil ratio	Frequency (kHz)	W_{cat} (w/w_{oil})	Temperature (°C)	Time (min)	Biodiesel yield (%)	Ref.
Soybean	KOH	6:1	20	1.5	25, 40, 60	15	99.4	[71]
Triolein		6:1	40	1	30–50	30	Vary	[72]
Coconut		6:1	24	0.75	-	7	98	[80]
Waste cooking oil		6:1	20	1	45	Up to 40	Vary	[64]
Sunflower		7.5:1	40	0.7	32.2	60	88	[74]
Soybean	NaOH	9:1	40	0.2	29	30	100	[75]
Sunflower		7:1	24	2	Meth: 60 Eth: 80	20 40	95 88	[29]
Soybean		6:1	Ultrasound+microwave	1	60	3	97.7	[77]
Palm fatty acid distillate	H_2SO_4	7:1	22	5	40	150	90	[78]
Oreochromis niloticus	H_2SO_4+KOH	9:1	40	2	30	90	98.2	[79]

6.2.1. Homogeneous base-catalyzed process

Recent works on the use of ultrasonic to accelerate biodiesel production process using homogeneous catalysts are summarized in Table 3. It is noted that generally high biodiesel yields (> 95%) were achievable in less than 60 min. In investigating the effect of reaction temperature on production process under ultrasonication, Colucci et al. [71] used soybean oil as the feed to react with methanol and the reaction was catalyzed by KOH. Three levels of temperature, i.e. 40 and 60 °C were carefully studied and high yield of above 90% was achieved at each level in just 15 min. They attributed the high reaction rate to the increase in the interfacial area between the reactants that resulted from cavitation bubbles generated by ultrasonic irradiation. This phenomenon allowed efficient contact between the catalyst and the reactants. Another trial to investigate the optimum reaction temperature was made by Hanh et al. [72] by testing the ultrasonic-assisted transesterification of triolein using KOH as catalyst. The tested temperature was in a range between 30–50 °C. They reported that the concentration of the product increased drastically with increasing temperature.

The use of other feed stock as a source of triglycerides for transesterfication process has been attempted by Teixeira et al. [73]. Beef tallow was used instead of vegetable oil while KOH was used as the catalyst. They concentrated on this type of feed stock due to its low price, highly produced in slaughters and other economic benefits. The results showed that short reaction time was achieved through ultrasonication leading to a reduction in the effects of free fatty acids content in fats even with the use of alkali catalyst. After collecting the results from conventional and

ultrasonic processes, no clear difference was noticed on the yield of biodiesel. Probably, it was due to near equilibrium operation of those systems at high conversion so that difference in the yields at the end of the reaction was not so significant.

Another different type of feed stock was studied by Hingu et al. [64]. They used waste cooking oil and methanol in the production process. A sonochemical reactor was used for studying different parameters affecting the transesterification process. Optimization was subsequently made to identify the optimum conditions and to compare the obtained results with those of conventional mechanically stirred reactor. The same researchers also investigated the ultrasonic rated power dissipation and found that under a power of 200 W, the conversion reached about 89% in less than 40 min. It was mainly attributed to the effect of ultrasound mixing. However, the conversion suffered a decrease when the power was increased to 250 W. That could be associated with the cushioning effect which, in turn, decreased the cavitational activity due to the reduction of the transferred power into the system. Some researchers also studied the effect of ultrasound pulse and found that higher conversion was obtained when ultrasound duration in the pulse was higher. The period between the pulses is important because it reduces the energy consumption and provides a period of cooling for the transducers [43].

Three parameters of reaction variables under ultrasonication were studied by Avramovic et al. [74]. Levels of methanol-to-sunflower oil molar ratio, KOH catalyst loading and the temperature of reaction were subsequently optimized. The most significant factor on the production process was found to be the loading of the catalysts. They explained that the increase in catalyst loading resulted in an increase in the formation of methoxide (the complex formed from the reaction between catalyst and methanol). This yielded an enhancement in the FAME formation and an increment in the positive catalyst affect on the rate constant of the forward reaction. A yield of nearly 90% was achieved in just 60 min.

Another type of homogenous catalyst has been successfully used in conjunction with an ultrasonic system. Santos et al. [75] converted soybean oil to biodiesel by reacting it with methanol catalyzed by NaOH. The methanol to oil ratio was influential in governing the final biodiesel yield. That was because the use of higher concentration of alcohol shifted the reaction equilibrium toward the products. Nearly 100% yield was achieved in just 30 min. Meanwhile, the use of large amount of catalyst under the optimum methanol to oil ratio caused the intensification of side reactions like soap formation. As such, ultrasonication can possibly improve this process on the basis of a reduction in the required amount of the catalyst.

On the other hand, Georgoglanni et al. [76] compared the use of homogenous and heterogeneous catalysts with the presence of ultrasonic waves and under mechanical stirring using rapeseed oil as feed. They found that homogenous catalyst (NaOH) was more active than the other heterogeneous catalysts (Mg-MCM-41, Mg-Al hydrotalcite, and K-impregnated zirconia). They attributed the difference to the diffusion limitations of the bulky oil molecules into the tiny pores of the solid catalysts. The beneficial role of ultrasonic irradiation was demonstrated as a significant reduction in the reaction time for the homogenous catalyst.

Combining both effects of ultrasonic and microwave irradiation was attempted by Hsiao et al. [77] with the intention of achieving optimal ultrasonic mixing and microwave irradiation effects. The conversion of soybean oil with the presence of NaOH was made in two discrete steps. The first step was assisted by ultrasonic mixing while maintaining the temperature near room temperature for one minute. It was followed by the reaction with the assistance of microwave irradiation for 2 min. They recorded that this procedure did not require mechanical stirring and cooling facility. Evaporation of alcohol was also significantly lower and reduced energy consumption resulted due to low reaction temperature requirement. Thus the use of ultrasonic field in combination with microwave looks very promising for biodiesel production.

Recent research findings confirmed that the use of these homogeneous catalysts in combination with ultrasonication is effective, time saving and economical method for producing biodiesel from different types of feed stock [18]. In short, the use of ultrasonic-assisted process could lead to high yields in short reaction time, low reaction temperature and reduce the amount of hydroxide catalysts needed. Beside hydroxides, other type of catalyst to be possibly used is liquid acid catalyst which is especially useful for feed stock with high free fatty acid (FFA) content.

6.2.2. Homogenous acid catalysts

The search for cheap and effective raw material for biodiesel production has been attempted by Deshmane et al. [78]. They used palm fatty acid distillate (PFAD) which is usually a much cheaper raw material compared to vegetable oils in the esterification reaction with methanol. They used concentrated H_2SO_4 catalyst due to its insensitivity to FFA. The researchers investigated the effect of various reaction parameters to reach the optimum conditions. They reported that significant effect of ultrasonic field was achieved at only 40 °C with 90% yield in 2.5 h. The reaction time was much shorter than that reported by Wang et al. [31] using a non-ultrasonic reactor system. They attributed the positive effect to the improved mass transfer rate between the reactants that governed the whole process.

Ultrasonic-assisted process can be also used in two-stage biodiesel production process using feed stock with high FFA content as reported by Santos et al. [79]. They used Oreochromis niloticus (Nile tilapia) oil with methanol using two types of catalysts sequentially. The first catalyst was KOH which reacted with oil in alcoholic saponification process in a single stage followed by an acid hydrolysis step catalyzed by sulfuric acid. After the first stage of the process, acid catalyst was added to the reaction mixture to complete the reaction using ultrasonic irradiation in each step. The researchers also used response surface methodology (RSM) to predict the effects of three of reaction parameters on the biodiesel yield. These parameters were alcohol to oil ratio, sulfuric acid concentration and reaction temperature. It was found in this study that the most important parameter was alcohol to oil ratio because it shifted the equilibrium towards the products side. The results also showed that the application of ultrasonic waves neglected the need of external heating and ultrasonic irradiation had a positive influence on the yield of methyl esters. In their study, a yield of 98% was achieved in just 1.5 h.

6.3. Heterogeneous catalysts

The use of homogenous catalyst has been reported to be successful in the production of biodiesel using ultrasonic technique. However, homogeneous catalysts cannot be reused because they are consumed in the reaction media and the separation process of this type of catalyst is difficult and requires further equipment. These factors can affect the overall process economy and energy consumption [24]. As such, efforts have been recently dedicated to the investigation using heterogeneous catalyst that can achieve the same level of efficiency while providing opportunity for catalyst reuse. For comparison, findings from studies using conventional stirring reaction and ultrasonic-assisted reactor system are reviewed in the next section.

6.3.1. Conventional production using heterogeneous catalysts

Alkaline earth metal oxides, especially CaO and SrO have received much interest due to their relatively high basic strength,

low solubility in reaction media and relatively cheap prices [81–82]. Another type of alkali catalyst that has also been investigated and reported is potassium catalyst supported on SBA-15 [83]. Alkali catalysts could suffer when high concentration of FFA is present in the oil. Therefore, many types of metal oxide catalysts [84] or heterogeneous acid catalysts have been examined such as zirconium oxide (ZrO_2) [85], sulfonic ion-exchange resin [86–87], sulfonic modified silica [26,27] and heteropoly acids (HPAs) [88,89]. Some of the research works utilizing heterogeneous catalyst systems in conjunction with conventional mechanically stirred production process are summarized in Table 4. It is clear that these catalysts could provide high yields but they required long reaction time. Reaction temperatures were moderate except for the sulfonated SBA-15. For all reactions, the molar ratios of alcohol to oil ratio were high compared to the ratios of homogenous catalysts under similar conditions. Whereas high alcohol to oil ratio was needed to shift the equilibrium to the products side, it also resulted in the dilution effect on the oil concentration leading to poor rate of reaction [28].

In fact, there are some other limitations to the successful use of heterogeneous catalyst. One of the limitations is the formation of three phases in the reaction media (oil, methanol and catalysts) which can also cause a reduction in the rate of reaction. One of the solutions to this problem is to use a certain quantity of co-solvent to enhance the miscibility of oil and methanol [94]. However, the other way and the most effective is still the use of ultrasonic-assisted process.

6.3.2. Heterogeneous catalysts under ultrasonic conditions

Reaction parameters and results of some studies that are focused on the use of heterogeneous catalysts in conjunction with ultrasonication are summarized in Table 5. As concluded from this table, the yields of biodiesel achieved were generally high and comparable with those of homogenous catalysts. However, the reaction temperatures were slightly higher while the reaction times were longer. Catalyst loading under ultrasonic field is usually higher than that for homogenous catalysts but this does not significantly affect the economics of the process due to its simple separation process.

Production of biodiesel from palm oil using BaO and SrO as the heterogeneous catalysts has been performed by Salamatinia et al. [95]. They used ultrasonic-assisted process to enhance reaction rate and to study the effects of ultrasonic waves on the reaction parameters. They reported that the basic properties of the catalyst were the main cause for their high activity. The results showed that the low frequency ultrasonic-assisted process had no significant mechanical effects on SrO but there was some effects on BaO. This study confirmed that the ultrasonic significantly improved the process by reducing the reaction time to less than 50 min at a catalyst loading of 2.8 wt.% to achieve biodiesel yields of above 95%. The optimum alcohol to oil ratio was found to be at 9:1.

Another study on alkali earth metals was done by Mootabadi et al. [96]. The researchers investigated the effect of ultrasonic waves at 20 kHz and 200 W on the regenerated catalyst and made comparison between mechanical stirring and ultrasonic irradiation. They used palm oil in the production process and investigated the optimum conditions for the catalysts (CaO, SrO and BaO). Ultrasonic irradiation showed great enhancements on the reaction parameters for the ultrasonic-assisted process, especially for the obtained yield and reaction time. It was concluded that catalyst leaching was the main cause for the drop in activity in the case of regenerated catalyst. BaO catalyst was the least stable to leaching. Under the optimum conditions, 95.2% yield was achieved in just 60 min of reaction for both BaO and SrO catalysts while that of for CaO was only 77.3%. These results were about 30–40% higher than the corresponding results obtained using conventional stirring reactor system.

Table 4
Performance of various heterogenous catalysts in biodiesel production process using conventional stirring reaction system.

Feed oil	Catalyst	Reaction conditions				Biodiesel yield (%)	Ref.
		Alc:oil ratio	W_{cat} (w/w_{oil})	Temperature (°C)	Time (min)		
Soybean	CaO	12:1	8	65	3	95.0	[90]
Soybean	KOH/NaX Zeolite	10:1	3	65	8	85.6	[91]
Waste frying oil	Novozyme 435	25:1	10	50	4	89.1	[16]
Palm	KF/ZnO	11.43:1	5.52	65	9.72	89.2.	[92]
Soybean	KI/Mesoporous silica	-	5	70	8	90.1	[93]
Palm	Sulfonated SBA-15	20:1	6	140	4	95.0	[27]

Table 5
Performance of ultrasonic-assisted reaction system for biodiesel production using various homogenous catalysts.

Feed oil	Catalyst	Reaction conditions						
		Alc:oil ratio	Frequency (kHz)	W_{cat} (w/w_{oil})	Temperature (°C)	Time (min)	Biodiesel yield (%)	Ref.
Palm	BaO SrO	9:1	20	2.8	65	~50	>95.0	[95]
Palm	BaO	9:1	20	3	65	60	95.2	[96]
	SrO						95.2	
	CaO						77.3	
Jatropha curcas	Na/SiO_3	9:1	24	3	Low	15	98.5	[97]
Soybean	Immobilized Novozym 435	6:1	40	6	40	240	96.0	[98]
Frying oils	Mg-MCM-41, Mg-Al hydrotalcite, K/ZrO_2	-	24	-	60	300	>95.0	[99]

To study the performance of an immobilized catalyst, Kumar et al. [97] prepared a supported Na/SiO_2 catalyst to investigate the effects ultrasonication on the process. Under the optimum conditions and with the use of Jatropha curcus oil as feed stock, they managed to achieve 93.5% of biodiesel yield in just 15 min of reaction time. They found that the use of ultrasonic-assisted process reduced the amount of catalyst that must be used in the process. They attributed that finding to the effects of ultrasonic cavitation on increasing the surface area available for the reactants. That, in turn, increased the activity of the catalyst even at minimum catalyst dosage. As a result, the purity of glycerol which is the main by-product of biodiesel production was increased. The researchers also investigated the reusability of the catalyst and found that after five cycles, the reaction conversion showed minimal reduction.

Another attempt to produce biodiesel from soybean oil was made by Yu et al. [98] by combining the use of different types of catalyst known as Novozym 435 (Candida Antarctica lipase B immobilized on polyacrylic resin). The procedure involved the combination between the effects of ultrasonic waves and mechanical vibration instead of mechanical stirring due to its detrimental effects on the catalyst. The researchers studied the effects of reaction parameters on the activity of the catalyst. The catalyst showed good stability with no loss of enzymatic activity after five successive cycles under ultrasonic irradiation. In spite of slightly longer reaction time, high production yield was obtained at low reaction temperature.

Other types of heterogeneous catalysts were used in the work of Georgogianni et al. [99]. They investigated a wide range of catalysts including Mg-MCM-41, Mg–Al hydrotalcite, and K^+-impregnated zirconia. The bases of selection for these catalysts were mesoporosity and surface basicity. The reaction mixture consisting of frying oils, methanol and the desired catalyst was mixed in a batch reactor via mechanical stirrer for 24 h or via ultrasonicaion for 5 h. The results suggested that the basic strength was the cause of the good activity of the catalysts. Mg–Al hydrotalcite achieved the highest reaction conversion of 97% at a reaction temperature of 60 °C. Thus, ultrasonic irradiation significantly enhanced the reaction rate causing a reduction in reaction time.

Comparison between the parameters of reactions listed in Table 5 under ultrasonic field with those in Table 4 for conventional mechanical stirring processes for heterogeneous catalysts clearly shows the enhancements caused by ultrasonic irradiation. Reaction times and catalyst loadings of the ultrasonic-assisted processes were shorter than those for the conventional processes. The molar ratios were less than those of conventional processes and the production yields were higher. As a conclusion, with the use of ultrasonic, high activity of homogenous catalysts can be achieved using the more environmental friendly heterogeneous catalysts.

6.4. Performance of different alcohols under ultrasonic field

Many efforts have been dedicated to investigate the influence of the type of alcohol that is used for biodiesel production under ultrasonic irradiation [80,100,101]. The use of ethanol was attempted by Kumar et al. [80]. They used coconut oil catalyzed by KOH to be reacted with the ethanol to produce biodiesel. It was reported that the justification for the use of ethanol was to reduce the hazard associated with the use of methanol which is highly toxic in the batch process. Ethanol has also more carbon atoms which could provide higher colorific value. However, transesterification using ethanol has been reported to be slightly lower due to its larger molecular size [100]. They compared the results of the production using ultrasonic irradiation with that of conventional stirring to show the differences. Reaction time was found to be reduced by 15–40 times compared to that of mechanical stirring. They also investigated the effects of ultrasonic pulse and amplitude to optimize the yield. It was concluded that the optimum pulse and amplitude were 0.3 s and 60%, respectively. The relatively short reaction time of this process was a good indication of the positive role of ultrasonication in enhancing the process using ethanol.

Other researchers [100] studied the effects of ultrasonication on esterfication process involving short chain alcohols (ethanol, propanol, and butanol) reacted with oleic acid to produce corresponding fatty acid ethyl esters (FAEEs). They used batch esterification process to optimize the reaction parameters using H_2SO_4 as an insensitive catalyst to the presence of FFA. They reported that ultrasonic condition was effective, economic, and time saving in the esterification process, regardless of the type of alcohol used.

The use of different types of alcohol that can be used in conjunction with ultrasonication using common types of alkali catalyst, i.e. KOH and NaOH has also been investigated by Hanh et al. [101]. They discriminated a wide variety of alcohols including methanol, ethanol, propanol, butanol, hexanol, octanol and decanol. The desired alcohol was used to react with triolein oil in the presence of KOH or NaOH. They comparatively investigated the use of both ultrasonic irradiation and mechanical stirring in the reaction. It was found that the type of alcohol had great influence on the yield. It was concretely revealed that the rate of the reaction depended on the type of alcohol. In other words, as the number of carbon in alcohol increases, the rate of the ester formation decreases. That is because alcohol with large number of carbon makes it difficult to separate ester from the unreacted oil. In this respect, it was proven that ultrasonic irradiation could enhance the rate of biodiesel formation using short-chain alcohols as compared to that achieved with conventional mechanically stirred system.

A study on the effects of primary, secondary and tertiary alcohols on the reactant's conversion with the aid of NaOH has been made by Stavarache et al. [62] who examined these types of alcohol for reaction under the effect of ultrasonication. The results showed that normal straight chain alcohols were more reactive. It could achieve 98–99% of conversion under optimum conditions while relatively lower conversion could be achieved using secondary and tertiary alcohols under the same conditions. They attributed that observation to the steric hindrance that hampered or limited the access towards the centre of the reaction and caused lower reaction rate. It was found that low frequency ultrasonication at around 28 kHz could result in a higher conversion but the reaction took longer time than those achieved at high frequencies. However, too high frequencies were not useful at all for the production of biodiesel because the collapses of cavitation bubbles were weaker than impinging of one reactant to the other [101].

Thus, it can be concluded from Table 6 that ultrasonic irradiation can be successfully used to accelerate the reaction with other types of alcohols. Better yield can generally be achieved with primary alcohols and reasonable reaction time and temperature can be used. It is noted that for transesterification process, the reaction temperature and time were less influential than those in esterification process when sulfuric acid was used as the catalyst while the yields of biodiesel of transesterification processes were relatively higher.

7. Continuous process under ultrasonic field

The use of ultrasonic-assisted batch process in the production of biodiesel has been discussed and effects of various reaction parameters have been investigated. Batch process has several

Table 6
Performance of ultrasonic-assisted biodiesel process using various types of alcohol.

Feed oil	Catalyst	Reaction conditions						Ref.
		Alc:oil ratio	Frequency (kHz)	W_{ult} (w/W_{oil})	Temperature (°C)	Time (min)	Biodiesel yield (%)	
Coconut	Ethanol	KOH	6:1	0.75	-	7	98%	[80]
Oleic acid	Ethanol, propanol butanol	H_2SO_4	3:1	5	60	120	> 90%	[100]
Triolein	Wide range	NaOH/KOH	6:1	1	25	60	> 90%	[101]
Commercial edible oil	Primary, secondary and tertiary	NaOH	6:1	0.5	Room	10–20	93–99%	[62]

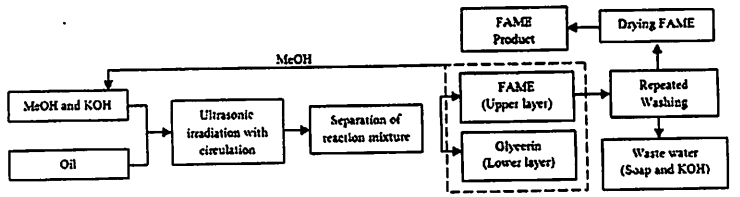

Fig. 10. Flow diagram of ultrasonic-assisted process for biodiesel production [104].

disadvantages, especially when used in large scale. Drawbacks in the batch process such as the requirement of larger reactor, low efficiency due to its start up and shut down requirements and high labor costs will affect the process economics [102]. For these reasons, researchers have tried to study continuous systems provided with ultrasonic irradiation to tackle these problems and to find suitable procedure that can satisfy various needs in biodiesel production. The investigations in the area of continuous systems for biodiesel production should be further developed towards large scale continuous processes [103].

The design of a pilot plant for continuous production of high quality biodiesel has been attempted by Thanh et al. [104]. The pilot scale plant was designated to perform the transesterification in a circulation process in the presence of low-frequency ultrasound. KOH was used as the catalyst to transesterify canola oil and methanol. Using liquid pumps, oil and methanol containing the dissolved catalyst were fed into the ultrasound reactor passing to circulation-separation unit. After that, feeding valves were closed and circulation valves were opened to circulate reaction mixture through the reactor. After this stage, the reaction mixture was left to undergo phase separation in the circulation-separation unit for 4 h. The flow diagram that describes the circulation process is shown in Fig. 10. The aim of the researchers was to produce biodiesel that satisfied several objectives including material saving and low energy consumption. They concluded that one of the advantages of ultrasonic field was the reduction in energy consumption for the whole process. However the use of this method could be just limited to homogenous catalyst.

Design and operation of continuous process assisted by ultrasonic irradiation have been studied by Stavarache et al. [105]. They investigated the effects of various types of vegetable oils and alcohol to oil ratios. The influences of parameters of the continuous process such as reaction volume and residence time of the reactants inside the reactor were particularly investigated. The catalyst used was KOH and the oils were palm oil and commercial edible oil while reaction temperatures were between 38–40 °C. The reactor was initially filled by pumping the reactants of a desired ratio. During the first loading, ultrasound was turned off. After that, the reaction was started in a batch mode for durations equal to the selected residence times. After that, the pumps were started and the reaction was turned to continuous mode for twelve successive volumes. From the results obtained, the researchers proved that ultrasonic irradiation was also suitable for a large-scale continuous transesterification of vegetable oil.

Another study with different type of oil processed using two-step continuous system was made by Thanh et al. [106] and schematically shown in Fig. 11. Waste cooking oil and KOH dissolved in methanol were pumped at a desired ratio to the first reactor where ultrasonic irradiation was provided. The reaction mixture flow rates were kept between 0.5–2.5 L/min. After that, the mixture was fed into a separation unit where phase separation took place. The upper layer that contained FAME, triglyceride and amounts of diglyceride and monoglyceride were fed to the second reactor which was also provided with ultrasonication. As in the first stage, the second one was followed by phase separation unit to collect the final product of FAME. This final product was then sent to a purification unit to extract the remaining catalyst and the excess of methanol. Short residence times of less than one minute were recorded for each reactor but the total time for the whole process was about 15 h due to long time required in the separation units. It was clear from the results of this work that an ultrasonic-assisted continuous system was a plausible and interesting technique for the production of biodiesel from waste cooking oil.

In Table 7, it can be concluded that ultrasonic irradiation can be successfully used in continuous processes as well as for batch processes. The yields of each continuous process were high enough to encourage researchers to further investigate this topic. However, early success in the continuous mode was only achieved using homogenous catalysts. Thus, further investigation should be dedicated to the use of heterogeneous catalysts under continuous operation. Certainly, the involvement of heterogeneous catalysts will require additional technical enhancements.

8. Conclusions

Biodiesel is a renewable, clean and alternative fuel to petroleum diesel. For all the possible methods for biodiesel production, catalytic transesterification of vegetable oil or animal fats with alcohol is the best method with good quality product. However, the production process faces many drawbacks related to the

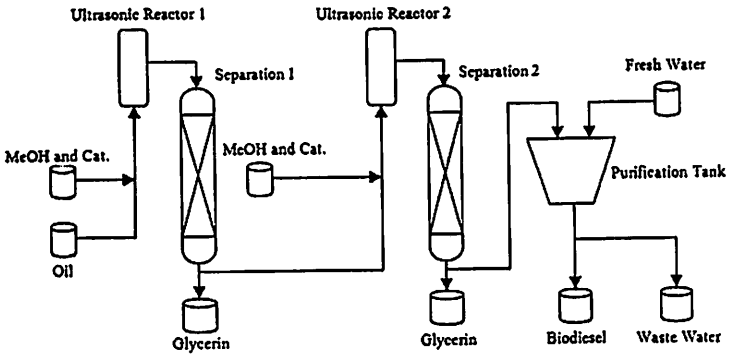

Fig. 11. Flow diagram of two-steps continuous process for biodiesel production [106].

Table 7
Performance of various continuous system of ultrasonic-assisted biodiesel production process.

Process	Feed oil	Catalyst	Reaction conditions						Reference
			Alc:oil ratio	W_{ult} (w/W_{oil})	Temperature (°C)	RT[a] (min)	Rate (L/min)	Yield (%)	
Circulation process	Canola	KOH	5:1	0.7	Room	40	8	99	[104]
Continuous process	Palm	KOH	6:1 and 7.5:1	-	38–40	20	-	~90	[105]
Two stage continuous process	Waste cooking oil	KOH	1st stage 2.5:1 2nd stage 1.5:1	1st stage 0.7 2nd stage 0.3	Room Room	1 1	1st stage 1.5 2nd stage 2	1st stage 81 2nd stage 99	[106]

[a] RT: Residence time.

immiscible nature of the reactants and the presence of free fatty acids in the desired oil. Several approaches have been proposed but only to a limited success. Heterogeneous catalysts which are more environmental friendly usually subject to a drawback of low catalytic activity. Ultrasonic irradiation has been proven to be successfully used in a meaningful way to enhance the emulsification of the reactants to increase the mass transfer rate during the reaction. This enhancement leads to reductions in reaction time, catalyst amount, alcohol-to-oil ratio and reaction temperature causing a significant decrease in the production economics. Ultrasonic irradiation was tested for wide range of homogenous and heterogeneous catalysts and showed promising results on the reaction variables compared with the results of conventional process. Mature understanding on the ultrasound-assisted transesterification process catalyzed by heterogeneous catalysts is yet to be established. However, there have been preliminary few attempts to elucidate the specific behaviors of the process with different types of alcohol, different types of solid catalyst as well as the effects of critical process variables such as temperature, catalyst loading, reactants' ratio etc. Thus, mature understanding on the use of ultrasonic energy to accelerate the transesterification process could be of great future interest for both batch and continuous production systems towards a more sustainable biodiesel production process.

Acknowledgement

Felda Foundation and USM's Research University (RU) grants to support our biodiesel research works at the School of Chemical Engineering, Universiti Sains Malaysia are gratefully acknowledged.

References

[1] Shay EG. Diesel fuel from vegetable oils: status and opportunities. Biomass and Bioenergy 1993;4:227–42.
[2] Hiller EA. Vegetable oil fuels. In: Pratt G, Quick G, Backer L, Kaufman K, Zimmerman D, editors. Proceedings of the International Conference on Plant and Vegetable Oils as Fuels. Herts: American Society of Agricultural Engineers Publication 4-82, American Technical Publishers; 1982.
[3] Manh DV, Chen YH, Chang CC, Chang MC, Chang CY. Biodiesel production from Tung oil and blended oil via ultrasonic transesterification process. Journal of the Taiwan Institute of Chemical Engineers 2011;42(4):640–4.
[4] Lee SB, Lee JD, Hong IK. Ultrasonic energy effect on vegetable oil based biodiesel synthetic process. Journal of Industrial and Engineering Chemistry 2011;17(1):138–43.
[5] Vyas AP, Verma JL, Subrahmanyam N. A review on FAME production processes. Fuel 2010;89:1–9.
[6] Adams C, Peters JF, Rand MC, Schroer BJ, Ziemke MC. Investigation of soybean oil as a diesel fuel extender: endurance tests. Journal of the American Oil Chemists' Society 1983;60:1574–9.
[7] Engler CR, Johnson LA, Lepori WA, Yarbrough CM. Effects of processing and chemical characteristics of plant oils on performance of an indirect-injection diesel engine. Journal of the American Oil Chemists' Society 1983;60:1592–6.
[8] Peterson CL, Auld DL, Korus RA. Winter rape oil fuel for diesel engines: recovery and utilization. Journal of the American Oil Chemists' Society 1983;60:1579–87.
[9] Strayer RC, Blake JA, Craig WK. Canola and high erucic rapeseed oil as substitutes for diesel fuel: preliminary tests. Journal of the American Oil Chemists' Society 1983;60:1587–92.
[10] Ziejewski M, Kaufman KR, Schwab AW, Pryde EH. Diesel engine evaluation of a nonionic sunflower oil-aqueous ethanol microemulsion. Journal of the American Oil Chemists Society 1984;61:1620–6.
[11] Luo Y, Ahmed I, Kubátová A, Stávová J, Aulich T, Sadrameli SM, et al. The thermal cracking of soybean/canola oils and their methyl esters. Fuel Processing Technology 2010;91:613–7.
[12] Seames W, Luo Y, Ahmed I, Aulich T, Kubátová A, Sťávová J, et al. The thermal cracking of canola and soybean methyl esters: Improvement of cold flow properties. Biomass and Bioenergy 2010;34:939–46.

[13] Leung DYC, Wu X, Leung MKH. A review on biodiesel production using catalyzed transesterification. Applied Energy 2010;87:1083–95.
[14] Marchetti JM, Miguel VU, Errazu AF. Possible methods for biodiesel production. Renewable and Sustainable Energy Reviews 2007;11:1300–11.
[15] Veljković VB, Avramović JM, Stamenzović OS. Biodiesel production by ultrasound-assisted transesterification: state of the art and perspectives. Renewable and Sustainable Energy Reviews 2012;16(2):1193–209.
[16] Yin X, Ma H, You Q, Wang Z, Chang J. Comparison of four different enhancing methods for preparing biocicsel through transesterification of sunflower oil. Applied Energy 2012;91(1):320–5.
[17] Abdullah AZ, Salamatinia B, Mootabadi H, Bhatia S. Current status and policies on biodiesel industry in Malaysia as the world's leading producer of palm oil. Energy Policy 2009;37:5440–3.
[18] Salamatinia B, Abdullah AZ, Bhatia S. Quality evaluation of biodiesel produced through untrasound-assisted heterogeneous catalytic system. Fuel Processing Technology 2012;97:1–8.
[19] Math MC, Kumar SP, Chetty SV. Technologies for biodiesel production from used cooking oil—A review. Energy for Sustainable Development 2010;14:339–45.
[20] Abdullah AZ, Razali N, Mootabadi H, Salamatinia B. Critical technical areas for future improvement in biodiesel technologies. Environmental Research Letters 2007;2:1–6.
[21] Deng X, Fang Z, Liu YH, Yu CL. Production of biodiesel from Jatropha oil catalyzed by nanosized solid basic catalyst. Energy 2011;36(2):777–84.
[22] Yee KF, Tan KT, Abdullah AZ, Lee ET. Life cycle assessment of palm biodiesel: revealing facts and benefits for sustainability. Applied Energy 2009;86:S189–96.
[23] Berrios M, Martín MA, Chica AF, Martín A. Study of esterification and transesterification in biodiesel production from used frying oils in a closed system. Chemical Engineering Journal 2010;160:473–9.
[24] Zabeti M, Wan Daud WMA, Aroua MK. Activity of solid catalysts for biodiesel production: a review. Fuel Processing Technology 2009;90:770–7.
[25] Ji J, Wang J, Li Y, Yu Y, Xu Z. Preparation of biodiesel with the help of ultrasonic and hydrodynamic cavitation. Ultrasonics 2006;44:e411–4.
[26] Alba-Rubio AC, Vila F, Alonso DM, Ojeda M, Mariscal R, López Granados M. Deactivation of organosulfonic acid functionalized silica catalysts during biodiesel synthesis. Applied Catalysis E: Environmental 2010;95:279–87.
[27] Melero JA, Bautista LF, Morales G, Iglesias J, Sánchez-Vázquez R. Biodiesel production from crude palm oil using sulfonic acid-modified mesostructured catalysts. Chemical Engineering Journal 2010;161:323–31.
[28] Ferella F, Mazziotti Di Celso G, De Michelis I, Stanisci V, Veglió F. Optimization of the transesterification reaction in biodiesel production. Fuel 2010;89:36–42.
[29] Georgogianni KG, Kontominas MG, Pomonis PJ, Avlonitis D, Gergis V. Conventional and in situ transesterification of sunflower seed oil for the production of biodiesel. Fuel Processing Technology 2008;89:503–9.
[30] Janaun J, Ellis N. Perspectives on biodiesel as a sustainable fuel. Renewable and Sustainable Energy Reviews 2010;14:1312–20.
[31] Wang Y, Ou S, Liu P, Xue F, Tang S. Comparison of two different processes to synthesize biodiesel by waste cooking oil. Journal of Molecular Catalysis A: Chemical 2006;252:107–12.
[32] Xie W, Li H. Alumina-supported potassium iodide as a heterogeneous catalyst for biodiesel production from soybean oil. Journal of Molecular Catalysis A: Chemical 2006;255:1–9.
[33] Nakagaki S, Bail A, VCd Santos, VHRd Souza, Vrubel H, Nunes FS, et al. Use of anhydrous sodium molybdate as an efficient heterogeneous catalyst for soybean oil methanolysis. Applied Catalysis A: General 2008;351:267–74.
[34] Marchetti JM, Errazu AF. Technoeconomic study of supercritical biodiesel production plant. Energy Conversion and Management 2008;49:2160–4.
[35] Demirbas A. Biodiesel from vegetable oils via transesterification in supercritical methanol. Energy Conversion and Management 2002;43:2349–56.
[36] Tan KT, Lee KT, Mohamed AR. Production of FAME by palm oil transesterification via supercritical methanol technology. Biomass and Bioenergy 2009;33:1096–9.
[37] Ilham Z, Saka S. Two-step supercritical dimethyl carbonate method for biodiesel production from Jatropha curcas oil. Bioresource Technology 2010;101:2735–40.
[38] Glisic S, Skala D. The problems in design and detailed analyses of energy consumption for biodiesel synthesis at supercritical conditions. The Journal of Supercritical Fluids 2009;49:293–301.
[39] Demirbas A. Biodiesel production from vegetable oils via catalytic and non-catalytic supercritical methanol transesterification methods. Progress in Energy and Combustion Science 2005;31:466–87.
[40] Boocock DGB, Konar SK, Mao V, Sidi H. Fast one-phase oil-rich processes for the preparation of vegetable oil methyl esters. Biomass and Bioenergy 1996;11:43–50.
[41] Luque de Castro MD, Capote FP. Introduction: fundamentals of ultrasound and basis of its analytical uses. In "echniques and Instrumentation in Analytical Chemistry. Amsterdam: Elsevier; 2007.
[42] Stavarache C, Vinatoru M, Nishimura F, Maeda Y. Fatty acids methyl esters from vegetable oil by means of ultrasonic energy. Ultrasonics Sonochemistry 2005;12:367–72.
[43] Leonelli C, Mason TJ. Microwave and ultrasonic processing: now a realistic option for industry. Chemical Engineering and Processing: Process Intensification 2010;49:885–900.
[44] Lorimer JP, Mason TJ. Sonochemistry. Part 1—The physical aspects. Chemical Society Reviews. 1987;16:239–74.
[45] Jokanovic V, Spasic AM, Uskokovic D. Designing of nanostructured hollow TiO_2 spheres obtained by ultrasonic spray pyrolysis. Journal of Colloid and Interface Science 2004;278:342–52.
[46] Prokhorov VM, Blank VD, Pivovarov GI. Ultrasound characterization of nanostructured Bi_2Te_3-based thermoelectrics. Physics Procedia 2010;3:63–8.
[47] Ashokkumar M, Sunartio D, Kentish S, Mawson R, Simons L, Vilkhu K, et al. Modification of food ingredients by ultrasound to improve functionality: a preliminary study on a model system. Innovative Food Science & Emerging Technologies 2008;9:155–60.
[48] Chemat F, Grondin I, Shum Cheong Sing A, Smadja J. Deterioration of edible oils during food processing by ultrasound. Ultrasonics Sonochemistry 2004;11:13–5.
[49] de la Fuente-Blanco S, Riera-Franco de Sarabia E, Acosta-Aparicio VM, Blanco-Blanco A, Gallego-Juárez JA. Food drying process by power ultrasound. Ultrasonics 2006;44:523–7.
[50] Rosenthal I, Sostaric JZ, Riesz P. Sonodynamic therapy—a review of the synergistic effects of drugs and ultrasound. Ultrasonics Sonochemistry 2004;11:349–63.
[51] Tachibana K, Feril Jr LB, Ikeda-Dantsuji Y. Sonodynamic therapy. Ultrasonics 2008;48:253–9.
[52] Tang W, Liu Q, Wang X, Wang P, Zhang J, Cao B. Potential mechanism in sonodynamic therapy and focused ultrasound induced apoptosis in sarcoma 180 cells in vitro. Ultrasonics 2009;49:786–93.
[53] Nikolic S, Mojovic L, Rakin M, Pejin D, Pejin J. Ultrasound-assisted production of bioethanol by simultaneous saccharification and fermentation of corn meal. Food Chemistry 2010;122:216–22.
[54] Virot M, Tomao V, Le Bourvellec C, Renard CMCG, Chemat F. Towards the industrial production of antioxidants from food processing by-products with ultrasound-assisted extraction. Ultrasonics Sonochemistry 2010;17:1066–74.
[55] Mason TJ. Developments in ultrasound-non-medical. Progress in Biophysics and Molecular Biology 1993;2:166–75.
[56] Sekiguchi K, Sasaki C, Sakamoto K. Synergistic effects of high-frequency ultrasound on photocatalytic degradation of aldehydes and their intermediates using TiO_2 suspension in water. Ultrasonics Sonochemistry 2011;18:158–63.
[57] Thangavadivel K, Megharaj M, Smart RSC, Lesniewski PJ, Naidu R. Application of high frequency ultrasound in the destruction of DDT in contaminated sand and water. Journal of Hazardous Materials 2009;168:1380–6.
[58] Banks CE, Rees NV, Compton RG. Sonoelectrochemistry in acoustically emulsified media. Journal of Electroanalytical Chemistry 2002;535:41–7.
[59] Regueiro J, Llompart M, Garcia-Jares C, Garcia-Monteagudo JC, Cela R. Ultrasound-assisted emulsification-microextraction of emergent contaminants and pesticides in environmental waters. Journal of Chromatography A 2008;1190:27–38.
[60] Towata A, Sivakumar M, Yasui K, Tuziuti T, Kozuka T, Iida Y. Ultrasound induced formation of paraffin emulsion droplets as template for the preparation of porous zirconia. Ultrasonics Sonochemistry 2007;14:705–10.
[61] Sharma YC, Singh B, Upadhyay SN. Advancements in development and characterization of biodiesel: a review. Fuel 2008;87:2355–73.
[62] Lam MK, Lee KT, Mohamed AR. Homogeneous, heterogeneous and enzymatic catalysis for transesterification of high free fatty acid oil (waste cooking oil) to biodiesel: a review. Biotechnology Advances. 28: 500–518.
[63] Zhang J, Chen S, Yang R, Yan Y. Biodiesel production from vegetable oil using heterogenous acid and alkali catalyst. Fuel 2010;89:2939–44.
[64] Hingu SM, Gogate PR, Rathod VK. Synthesis of biodiesel from waste cooking oil using sonochemical reactors. Ultrasonics Sonochemistry 2010;17:827–32.
[65] Kulkarni MG, Dalai AK. Waste cooking oil—An economical source for biodiesel: a review. Industrial and Engineering Chemistry Research 2006;45:2901–13.
[66] Miao X, Li R, Yao H. Effective acid-catalyzed transesterification for biodiesel production. Energy Conversion and Management 2009;50:2680–4.
[67] Lotero E, Liu Y, Lopez DE, Suwannakarn K, Bruce DA, Goodwin Jr JG. Synthesis of biodiesel via acid catalysis. Industrial and Engineering Chemistry Research 2005;44:5353–63.
[68] Rashid U, Anwar F. Production of biodiesel through optimized alkaline-catalyzed transesterification of rapeseed oil. Fuel 2008;87:265–73.
[69] Leung DYC, Guo Y. Transesterification of neat and used frying oil: optimization for biodiesel production. Fuel Processing Technology 2006;87:883–90.
[70] Rashid U, Anwar F, Moser BR, Ashraf S. Production of sunflower oil methyl esters by optimized alkali-catalyzed methanolysis. Biomass and Bioenergy 2008;32:1202–5.
[71] Colucci JA, Borrero EE, Alape F. Biodiesel from an alkaline transesterification reaction of soybean oil using ultrasonic mixing. Journal of the American Oil Chemists' Society 2005;82:525–30.
[72] Hanh HD, Dong NT, Okitsu K, Maeda Y, Nishimura R. Test temperature dependence of transesterification of triolein under low-frequency ultrasonic irradiation condition. Japanese Journal of Applied Physics. Regular Papers and Short Notes and Review Papers 2007;46:4771–4.
[73] Teixeira LSG, Assis JCR, Mendonça DR, Santos ITV, Guimarães PRB, Pontes LAM, et al. Comparison between conventional and ultrasonic preparation of beef tallow biodiesel. Fuel Processing Technology 2009;90:1164–6.
[74] Avramovic JM, Stamenkovic OS, Todorovic ZB, Lazic ML, Veljkovic VB. The optimization of the ultrasound-assisted base-catalyzed sunflower oil methanolysis by a full factorial design. Fuel Processing Technology 2010;91:1551–7.

[75] Santos FFP, Rodrigues S, Fernandes FAN. Optimization of the production of biodiesel from soybean oil by ultrasound assisted methanolysis. Fuel Processing Technology 2009;90:312–6.
[76] Georgogianni KG, Katsoulidis AK, Pomonis PJ, Manos G, Kontominas MG. Transesterification of rapeseed oil for the production of biodiesel using homogeneous and heterogeneous catalysis. Fuel Processing Technology. 90: 1016–1022.
[77] Hsiao M-C, Lin C-C, Chang Y-H, Chen L-C. Ultrasonic mixing and closed microwave irradiation-assisted transesterification of soybean oil. Fuel 2010;89:3618–22.
[78] Deshmane VG, Gogate PR, Pandit AB. Ultrasound-assisted synthesis of biodiesel from palm fatty acid distillate. Industrial and Engineering Chemistry Research 2009;48:7923–7.
[79] Santos FFP, Malveira JQ, Cruz MCA, Fernandes FAN. Production of biodiesel by ultrasound assisted esterification of Oreochromis niloticus oil. Fuel 2010;89:275–9.
[80] Kumar D, Kumar G, Poonam Singh CP. Fast, easy ethanolysis of coconut oil for biodiesel production assisted by ultrasonication. Ultrasonics Sonochemistry 2010;17:555–9.
[81] Liu X, He H, Wang Y, Zhu S. Transesterification of soybean oil to biodiesel using SrO as a solid base catalyst. Catalysis Communications 2007;8:1107–11.
[82] Vicente G, Martínez M, Aracil J. Optimisation of integrated biodiesel production. Part I. A study of the biodiesel purity and yield. Bioresource Technology 2007;98:1724–33.
[83] Abdullah AZ, Razali N, Lee KT. Optimization of mesoporous K/SBA-15 catalyzed transesterification of palm oil using response surface methodology. Fuel Processing Technology 2009;90:958–64.
[84] Yoo SJ, Lee H-s, Veriansyah B, Kim J, Kim J-D, Lee Y-W. Synthesis of biodiesel from rapeseed oil using supercritical methanol with metal oxide catalysts. Bioresource Technology 2010;101:8686–9.
[85] Sunita G, Devassy BM, Vinu A, Sawant DP, Balasubramanian VV, Halligudi SB. Synthesis of biodiesel over zirconia-supported isopoly and heteropoly tungstate catalysts. Catalysis Communications 2008;9:696–702.
[86] Talpur FN, Bhanger MI, Rahman AU, Memon GZ. Application of factorial design in optimization of anion exchange resin based methylation of vegetable oil and fats. Innovative Food Science & Emerging Technologies 2008;9:608–13.
[87] Zanette AF, Barella RA, Pergher SBC, Treichel H, Oliveira D, Mazutti MA, et al. Screening, optimization and kinetics of Jatropha curcas oil transesterification with heterogeneous catalysts. Renewable Energy 2011;36:726–31.
[88] Katada N, Hatanaka T, Ota M, Yamada K, Okumura K, Niwa M. Biodiesel production using heteropoly acid-derived solid acid catalyst $H_4PNbW_{11}O_{40}/WO_3$–Nb_2O_5. Applied Catalysis A: General 2009;363:164–8.
[89] Morin P, Hamad B, Sapaly G, Carneiro Rocha MG, Pries de Oliveira PG, Gonzalez WA, et al. Transesterification of rapeseed oil with ethanol: I. Catalysis with homogeneous Keggin heteropolyacids. Applied Catalysis A: General 2007;330:69–76.
[90] Liu X, He H, Wang Y, Zhu S, Piao X. Transesterification of soybean oil to biodiesel using CaO as a solid base catalyst. Fuel 2008;87:216–21.
[91] Xie W, Huang X, Li H. Soybean oil methyl esters preparation using NaX zeolites loaded with KOH as a heterogeneous catalyst. Bioresource Technology 2007;98:936–9.
[92] Hameed BH, Lai LF, Chin LH. Production of biodiesel from palm oil (Elaeis guineensis) using heterogeneous catalyst: an optimized process. Fuel Processing Technology 2009;90:606–10.
[93] Samart C, Sreetongkittikul P, Sookman C. Heterogeneous catalysis of transesterification of soybean oil using KI/mesoporous silica. Fuel Processing Technology 2009;90:922–5.
[94] Gryglewicz S. Rapeseed oil methyl esters preparation using heterogeneous catalysts. Bioresource Technology 1999;70:249–53.
[95] Salamatinia B, Mootabadi H, Bhatia S, Abdullah AZ. Optimization of ultrasonic-assisted heterogeneous biodiesel production from palm oil: a response surface methodology approach. Fuel Processing Technology 2010;91:441–8.
[96] Mootabadi H, Salamatinia B, Bhatia S, Abdullah AZ. Ultrasonic-assisted biodiesel production process from palm oil using alkaline earth metal oxides as the heterogeneous catalysts. Fuel 2010;89:1818–25.
[97] Kumar D, Kumar G, Poonam Singh CP. Ultrasonic-assisted transesterification of Jatropha curcus oil using solid catalyst, Na/SiO_2. Ultrasonics Sonochemistry 2010;17:839–44.
[98] Yu D, Tian L, Wu H, Wang S, Wang Y, Ma D, et al. Ultrasonic irradiation with vibration for biodiesel production from soybean oil by Novozym 435. Process Biochemistry 2010;45:519–25.
[99] Georgogianni KG, Katsoulidis AP, Pomonis PJ, Kontominas MG. Transesterification of soybean frying oil to biodiesel using heterogeneous catalysts. Fuel Processing Technology 2009;90:671–6.
[100] Hanh HD, Dong NT, Okitsu K, Nishimura R, Maeda Y. Biodiesel production by esterification of oleic acid with short-chain alcohols under ultrasonic irradiation condition. Renewable Energy 2009;34:780–3.
[101] Hanh HD, Dong NT, Okitsu K, Nishimura R, Maeda Y. Biodiesel production through transesterification of triolein with various alcohols in an ultrasonic field. Renewable Energy 2009;34:766–8.
[102] Darnoko D, Cheryan M. Continuous production of palm methyl esters. Journal of the American Oil Chemists' Society 2000;77:1269–72.
[103] Fonseca FAS, Vidal-Vieira JA, Ravagnani SP. Transesterification of vegetable oils: Simulating the replacement of batch reactors with continuous reactors. Bioresource Technology 2010;101:8151–7.
[104] Thanh LT, Okitsu K, Sadanaga Y, Takenaka N, Maeda Y, Bandow H. Ultrasound-assisted production of biodiesel fuel from vegetable oils in a small scale circulation process. Bioresource Technology 2010;101:639–45.
[105] Stavarache C, Vinatoru M, Maeda Y, Bandow H. Ultrasonically driven continuous process for vegetable oil transesterification. Ultrasonics Sonochemistry 2007;14:413–7.
[106] Thanh LT, Okitsu K, Sadanaga Y, Takenaka N, Maeda Y, Bandow H. A two-step continuous ultrasound assisted production of biodiesel fuel from waste cooking oils: A practical and economical approach to produce high quality biodiesel fuel. Bioresource Technology 2010;101:5394–401.

Renewable Energy 62 (2014) 10–17

Contents lists available at SciVerse ScienceDirect

Renewable Energy

journal homepage: www.elsevier.com/locate/renene

Transesterification of crude Jatropha oil by activated carbon-supported heteropolyacid catalyst in an ultrasound-assisted reactor system

Ali Sabri Badday [1], Ahmad Zuhairi Abdullah*, Keat-Teong Lee [1]

School of Chemical Engineering, Universiti Sains Malaysia, 14300 Nibong Tebal, Penang, Malaysia

ARTICLE INFO

Article history:
Received 12 September 2012
Accepted 25 June 2013
Available online

Keywords:
Biodiesel
Tungstophosphoric acid
Activated carbon
Ultrasound-assisted process
Jatropha oil
Water content

ABSTRACT

Transesterification of crude Jatropha oil in presence of tungstophosphoric acid (TPA) supported on activated carbon (AC) using ultrasound-assisted process was investigated. The generated catalysts were characterized for physical and chemical properties to examine the effects of different TPA loadings (15%, 20%, 25% w/w). The catalysts were then used in the transesterification of Jatropha oil with high free fatty acid content. The catalyst with 20% TPA loading achieved the best methyl ester yield, achieving 87.33% in just 40 min. The quality of the feed stock was varied by increasing the water content and FFA content to test the tolerance of the catalysts towards these parameters separately. The catalyst showed good water tolerance to a limit of 1% w/w and proven to be insensitive to the increment of FFA in the feed stock. The catalyst was also investigated for possible reusability and TPA leaching under ultrasonic conditions.

1. Introduction

Biodiesel is considered as an interesting green energy resource as it is a renewable, biodegradable and non-toxic material. The most successful method for producing the mixture of alkyl esters which form the biodiesel is by transesterifying vegetable oils or animal fats with suitable alcohol [1]. This process involves consecutive reaction steps in that lead to the conversion of a triglyceride to fatty acid alkyl esters and glycerin as the main co-product. Generally, excess alcohol is used to favor the forward reaction and the reaction is carried out in the presence of a suitable catalyst [2]. However edible vegetable oils such as palm oil, sunflower oil, rapeseed oil and soybean oil are considered as the most suitable feed stock for biodiesel production [3]. Recently, non-edible oils such as Polanga oil, Karanja oil, and Jatropha oil attracted great attention as feed stocks in biodiesel production [4,5].

Jatropha oil is a source of triglyceride which possesses good potential for biodiesel production as it is a non-edible oil and has no conflicting interest when used for edible purposes [4]. However, this type of oil has high FFA and water content that present some drawbacks when base catalysts are considered for biodiesel production process. Therefore, possibility for the application of highly active solid acid catalysts should be explored to convert this oil to biodiesel. In this respect, Acid catalyzed systems seem to be an interesting research field to be investigated to improve the biodiesel production from non-edible triglycerides resources.

Base catalysts have a great limitation to be used with wide range of feed stock. As the percentage of free fatty acids in vegetable oil exceeds 1%, a side reaction will occur consuming the catalyst and forming metal soap [6,7]. So homogenous acid catalysts are suggested to catalyze the reaction due to its insensitivity towards high FFA content coupled with its ability to catalyze esterification and transesterification simultaneously [8,9]. However, they generally require high reaction temperature and high oil to alcohol molar ratio as the reaction rate is relatively lower, especially in the case of solid acid catalysts. These days, solid acid catalysts attract researchers' attention due to their better tolerance towards high FFA and water content. At the same time, they can be easily separated from the reaction mixture after the reaction [10,11]. Both esterification and transesterification reaction can occur simultaneously neglecting the needs for two-step biodiesel production [12]. This will positively affect the production cost as no further requirement for unnecessary extra equipment is expected. Solid acid catalysts such as zirconia [13], sulfonic acid-functionalized silica [14], carbon-based solid acid catalyst [15] and heteropolyacids (HPAs) [16] have been reported for biodiesel production from various triglyceride sources.

* Corresponding author. Tel.: +60 4 5996411; fax: +60 4 5941013.
E-mail addresses: chzuhairi@eng.usm.my, azuhairi@yahoo.com (A.Z. Abdullah).
[1] Tel.: +60 4 5996411; fax: +60 4 5941013.

0960-1481/$ – see front matter © 2013 Elsevier Ltd. All rights reserved.
http://dx.doi.org/10.1016/j.renene.2013.06.037

Author's personal copy

Besides its great water tolerance and insensitivity towards FFA, HPAs possess strong Brönsted acidity and high proton mobility [17]. HPAs such as $H_3PW_{12}O_{40}$, $H_4SiW_{12}O_{40}$, $H_3PMo_{12}O_{40}$ and $H_4SiMo_{12}O_{40}$ have been used to catalyze a wide range of acid-catalyzed reactions including vegetable oil transesterification for biodiesel production. This is because the acid sites are more identical and easier to manage compared to those in other acid catalysts [18]. Thus, this group of materials provides interesting option for use in biodiesel production process.

Biodiesel production using HPAs as homogenous catalysts has been investigated by Morin et al. [16]. The activity of the studied HPAs was found to be comparable to those of H_2SO_4 and H_3PO_4. Due to the solubility of HPAs in methanol and ethanol, Zhang et al. [18] used a derived Cs salt of HPAs with the objectives of reducing their the solubility while at the same time increasing the surface area of the parent HPA. Various types of supports have also been used to immobilize HPAs such as silica [19], zeolites [20] and activated carbon [21] to increase the low surface area and to create heterogeneity for HPAs. For example, Katada et al. [22] successfully improved the activity of $H_4PNbW_{11}O_{40}/WO_3–Nb_2O_5$ catalyst used in the transesterification process of triolein and ethanol. Other acid derived solid catalyst has been investigated by Sunita et al. [23]. They conducted a study to demonstrate the activity of zirconia-supported isopoly and heteropoly tungstate catalysts for biodiesel synthesis. Generally, good catalytic activity was demonstrated by the catalysts. However, suitable modification on the process set up is deemed necessary to significantly increase the low reaction rate resulted by the immiscible nature of the reactants.

Ultrasonic technology is an attractive and effective procedure to solve the problems related low reaction rate in biodiesel production. This problem stems from the poor contact between the reactants due to their mutual immiscibility. The use of ultrasonic irradiation in the process can enhance the mass transfer rate between the reactants leading to significant improvement in the reaction rate [24]. Application of ultrasound in biodiesel production process has been demonstrated to accelerate the reaction leading to significant reduction in reaction time with some improvement in the production yield [25,26]. The use of ultrasonic energy in base-catalyzed biodiesel production or in two stage process has been investigated and reported in literature [27,28]. However, the use of heterogeneous acid catalyst under ultrasonic conditions stills an immature research area that requires further investigation. As solid acid catalysts are relatively less active than base catalysts, accelerating the reaction by means of an ultrasonic irradiation will provide interesting opportunity towards a more productive and economical biodiesel production process.

In this study, the ultrasonic-assisted transesterification of crude Jatropha oil with methanol over tungstophosphoric acid (TPA) ($H_3PW_{12}O_{40}$) immobilized on activated carbon has been investigated. Particular focus has been given to the effects of TPA loading on the characteristics of the catalyst and the subsequent influences on the transesterification reaction. Influence of FFA and water content in oil feed stock has been elucidated to highlight the rule of the prepared catalyst on conducting significant transesterification for high FFA systems. Finally, the stability of the catalyst towards leaching and potential for the reusability of the catalyst under the ultrasonic irradiation conditions has been demonstrated.

2. Experimental

2.1. Reagents and materials

Tungstophosphoric acid ($H_3PW_{12}O_{40}$) active component, abbreviated as TPA in this work was purchased from Merck (Malaysia) while activated carbon (AC) support was purchased from Galcon Carbon Corporation (USA). The AC was first ground to mean particle sizes between 250 and 500 μm. Crude Jatropha oil as the source of triglyceride in this study was supplied by Telaga Madu Resources (Malaysia). The properties of the crude Jatropha oil, FFA content and water content are given in Table 1. Methanol that was used in the transesterification reaction was supplied by Thermo Fisher Scientific Inc. (USA). Ethanol (for catalyst preparation) and n-hexane (for product analysis) were purchased from Merck (Malaysia). Meanwhile, reference fatty acid methyl ester (FAME) standards were supplied by NuChek Prep. Inc. (Australia).

2.2. Catalyst preparation

In order to prepare the supported catalyst, a pretreatment was first conducted by washing the support with 0.1 M NaOH solution, followed by the second treatment with 0.1 M HCl. They were performed to remove any soluble alkaline and acidic impurities from the AC [29]. The supported catalysts were prepared by dissolving the desired amounts of TPA in a mixture of deionized water and ethanol solution (50:50 v/v). Wet impregnation method was then adopted by contacting the support with the solution (4 ml/g support) for 72 h under constant shaking. Then, excess solution was removed by means of a rotary evaporator and the catalyst was subsequently washed excessively with deionized water followed by drying over night. The dry catalyst was then calcined at 453 K in air for 4 h [30].

2.3. Catalyst characterization

The surface properties of AC and other catalysts were examined by means of a Micrometrics ASAP 2020 surface analyzer. FT-IR spectra of the supported TPA-AC catalysts were obtained using a Perkin–Elmer FTIR spectrophotometer. The surface morphology and TPA distribution over the carbon support was observed using an SEM unit (Oxford INCA/ENERGY-350) equipped with an energy dispersive X-ray analysis (EDAX) system. Surface acidity of the AC and the immobilized catalysts was determined using an acid-base titration [31].

2.4. Ultrasound-assisted transesterification process

The ultrasound-assisted transesterification process was conducted in a three-neck glass batch reactor placed in a water bath to maintain the reaction temperature. A condenser was attached to the reactor to contain the evaporated methanol and condense it back to the reaction vessel. Ultrasonication was achieved by means of an ultrasonic processor with a probe type transducer. The ultrasonic energy was supplied using a Branson (USA) ultrasonic processor capable of generating a frequency of 20 kHz with a highest power of 400 W.

Blank experimental runs were first carried out in the absence of catalyst or ultrasonic irradiation. The absence of catalyst was tested by providing ultrasonic irradiation at 75% of the maximum power with a methanol/oil ratio of 20 for 60 min. The same conditions were used in the presence of activated carbon at a loading of 4%. An

Table 1
Properties of Jatropha oil used in this study.

Property	Value
Density (kg/m^3)	921
Viscosity (cSt)	38.12
Molecular weight	870
Water content (w %)	0.161
FFA content (w %)	10.5

experimental run under mechanical stirring was also performed under the same reaction conditions in the presence of catalyst.

In a typical experimental run, the desired amount of oil was transferred to the reactor and placed in the water bath until it reached the desired reaction temperature. Then, a required pre-heated amount of methanol was added to the oil at a molar ratio 20:1 followed by the desired amount of catalyst (4% wt/wt oil). At this point, ultrasonification was started and the condenser attached to recover the evaporated methanol. Ultrasonic energy was supplied in a discrete pattern with 10 s on and 3 s off with the ultrasonic amplitude set at 75% of the maximum power. After the desired reaction time (60 min), the reaction mixture was quenched and the excess methanol was distilled out. The reaction mixture was then separated into two layers by centrifugation at 3000 rpm for 20 min. The upper FAME layer was then collected for GC analysis.

For studying the effect of reaction time, the same previous procedure was conducted at different time intervals between 30 min and 120 min. The effects of water content in Jatropha oil was studied by adding the desired amount of water to the oil at various weight ratios (1%, 2%, 3%, 4% w H_2O/w oil). Meanwhile, testing of FFA effects was conducted by adding the desired amounts of FFA to the Jatropha oil under heating and continuous stirring. For all experimental runs, the water bath temperature was fixed at about 56 °C. Due to heat energy that was also generated by the ultrasonic wave, the reaction temperature was steadily maintained at 65 ± 1 °C.

In order to study the leaching of $PW_{12}O_{40}^{3-}$ heteropoly anion into the polar reaction mixture and to examine the effect of ultrasonic irradiation on the catalyst stability, an experiment similar to the "hot-filtration experiment" was conducted [19,21]. The catalyst was first mixed with methanol and ultrasonically treated under the reaction conditions. After the desired reaction time, the solid catalyst was filtered out and a desired amount of oil was added to the methanol. The reaction was then performed without the use of any catalyst for the optimum reaction time and the product was collected for analysis. All the experiments were carried out in the presence of air under atmospheric pressure.

2.5. Product analysis

A gas chromatograph (Agilent tech 7890 A GC systems) equipped with a capillary column (Agilent Technologies, Inc. 19091 J-413 hp-5) were used for product analysis. The system was equipped with a flame ionization detector (FID) and helium was used as the carrier gas. The analysis of FAME for each reaction mixture was carried out by dissolving the sample in n-hexane according to the desired dilution factor and 1 μl of the mixture was then injected into the GC.

3. Results and discussion

3.1. Catalyst characterization

Surface characteristics of AC and the TPA-AC catalysts combined with the surface acidity data are summarized in Table 2.

Table 2
Physical properties of AC and TPA catalysts.

Sample	Surface area (m^2/g)		Pore volume (cm^3/g)		Surface acidity (μmol/g_{cat})
	BET	Micropore	Total	Micropore	
AC	750	547	0.47	0.29	520
TPA15-AC	651	491	0.41	0.26	1530
TPA20-AC	621	467	0.39	0.25	1570
TPA25-AC	612	462	0.38	0.24	1690

Tungstophosphoric acid itself is a non-porous material and the surface area is reported to be only about 1–2 m^2/g [30]. The BET surface area of the AC support used in this research was 750 m^2/g and the area contributed by micropores was about 73% of the total surface area. It is noted from the table that immobilization of TPA on AC resulted in slight reductions in surface area, microporous volume and total porous volume. The magnitude of reduction was found to increase with increasing amount of TPA in the catalyst. This could be attributed to the partial blockage of pores by the active species. As a highly porous material, AC could accommodate high loading of TPA without experiencing significant drop in its porosity. A reduction in surface area after tungstophosphoric acid incorporation into an activated carbon was also observed Oball et al. [30].

The calculated values of surface acidity as shown in Table 2 reveal that AC was a material with low surface acidity and the catalysts showed significantly higher acidity with the increasing loading of TPA. As significant drop in the surface area was not observed, the acid sites were deemed accessible for reactants during the reaction which could bring about the desirable effect on the reaction rate. These results concluded that loading of TPA into the catalyst successfully introduced significant number of strong acid sites on the surface of the support material to act as good solid acid catalysts.

The FT-IR spectra for supported TPA-AC catalysts are shown in Fig. 1. The spectra of pure TPA showed four major bands. These bands are attributed to the stretching modes of oxygen to phosphorous and tungsten in the adsorption mode of the Keggin ion $(PW_{12}O_{40})^{-3}$. Bands at 800 cm^{-1} (W–O–W at the edge), 890 cm^{-1} (W–O–W at the corner), 980 cm^{-1} (W=O) and at 1080 cm^{-1} (P–O) can be detected for the Keggin ion which were in agreement with the results of Ferreira et al. [21]. Based on Fig. 1, no characteristic band could be detected for AC while for the immobilized catalysts, three major bands could be detected with increasing intensity with the amount of TPA loaded. For these bands, some shifts in their positions were noticed due to the new interactions that occurred between AC and TPA. The achieved results showed good agreements with those reported by Oball et al. [30] and Ferreira et al. [21]. These results suggested the successful synthesis of TPA-AC catalysts without excessive loading of active component that could subsequently affect the activity.

The SEM images of AC and the supported catalysts are shown in Fig. 2. The micro images of the catalysts were obtained using the fresh catalysts before being used in the transesterification reaction.

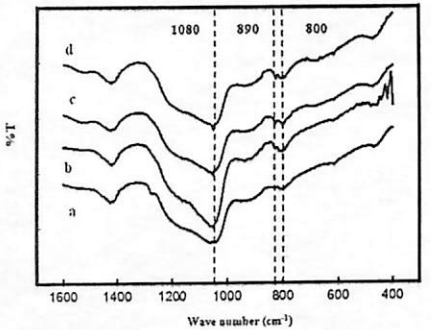

Fig. 1. FT-IR spectra for (a) AC (b) TPA15-AC (c) TPA20-AC (d) TPA25-AC.

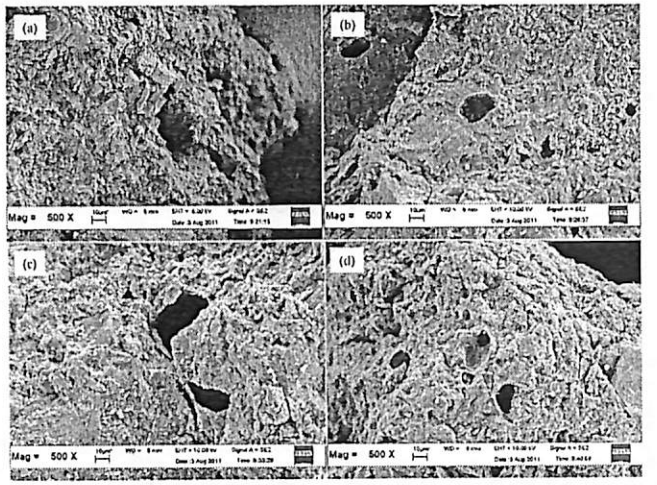

Fig. 2. Scanning electron micrographs (SEM) images of (a) AC (b) TPA15-AC (c) TPA20-AC (d) TPA25-AC.

The acid functionalized catalysts showed irregular distributions of the TPA on the AC surface. The deposition of TPA on the surface of AC not only responsible for the partial reduction on the surface area as the amount of the TPA increased but also resulted in the activity increase for the catalysts.

The EDAX results for the support and the immobilized catalysts can be seen in Fig. 3. These results prove that the existence of metallic materials attached to AC surface. EDAX result for AC correctly gave only carbon element while for the other catalysts, the presence of the Keggin anion $(PW_{12}O_{40})^{-3}$ can be detected. It can be concluded from these results that the amount of tungsten, oxygen and phosphorous increased with the increasing loading of TPA on AC. This, in turn, increased the catalyst activity in the transesterification of Jatropha oil.

3.2. Catalytic activity

3.2.1. Blank experiments

The results of blank experimental runs revealed that transesterification reaction did not significantly occur within a short reaction time of 60 min with the presence of AC only or without the use of any catalyst (Fig. 4). This was mainly due to the absence of acid active sites to catalyze the reaction. It also led to the conclusion that a suitable catalyst was indeed essential to achieve significant reaction. However, it is inaccurate to conclude that ultrasonic irradiation could activate the catalyst. Actually, this external energy could accelerate the reaction by improving mass transfer between the two immiscible reactants. Conducting the reaction without the use of ultrasound (mechanically stirred) also resulted in negligible reaction due to the short reaction time coupled with the poor catalytic activity of the solid acid catalysts. It has been reported that conventional acid catalyzed reactions requires long reaction time (5–6 h) due to the slow reaction rate [5]. Meanwhile, base-catalyzed process could be carried out with relatively shorter reaction times (2–3 h) [4,32].

It has been generally reported that higher molar ratio of methanol to oil can be used in order to prevent backward reaction to achieve higher biodiesel yield [3,5,15]. However, the methanol to oil ratio used in this study was already high i.e. at 20:1. High ratio also means that the concentration of Jatropha oil as the limiting reactant in the system is low to bring about undesired effect as far as the reaction rate is concerned. As such, certain suitable level of this ratio should be used. In this study, effect of reactants' ratio was beyond the main scopes to be investigated. However, it is agreeable that this variable could also affect certain behaviors of the reaction but discussion on this matter will be reported separately.

The activity of the AC-based TPA catalysts was found to be slightly better than that reported previously using alumina-based TPA catalysts [33]. For comparison, 20 wt. % TPA loading in alumina led to a FAME yield of about 50% in 60 min while the yield simply exceeded 70% in this study. Differences in the activity could be associated with the significantly higher surface area of the AC-based catalyst used in the present study (93 m^2/g versus 621 m^2/g). Thus, surface area could play a major role in the activity of the catalyst in this ultrasound-assisted reaction.

3.2.2. The effect of HPA loading

The results of catalytic experiments for FAME production yield from Jatropha oil under ultrasonic irradiation for different catalyst loadings are presented in Fig. 4. The reaction yield increased as the TPA content in the catalyst was increased and reached its highest level with TPA20-AC. Meanwhile, the catalyst with higher TPA amount did not show better yield as expected. At low TPA content, the presence of active sites on the surface of the support promoted the conversion of the reactants and drove the system towards forward reaction. Excessive amount of TPA in TPA25-AC led to a slight decrease in the reaction yield mainly due to a reduction in the catalyst surface area accessible by the reactants. This behavior was caused by partial blockage of the pores by the active sites leading to internal diffusion limitation for the reactants. Deposition of TPA particles on the pore mouths could cause the surface area within

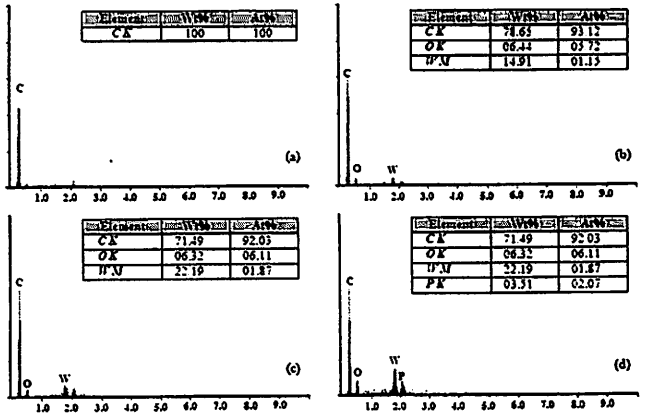

Fig. 3. EDAX for the surface of (a) AC (b) TPA15-AC (c) TPA20-AC (d) TPA25-AC.

the pores to be unavailable for the reaction. Low accessibility of the reactants to the active sites in the internal pores resulted in negative effect on the reaction yield. Based on these results, TPA amounts above 20% w/w loading were not recommended due to the decrease in pore volume and surface area due to pore plugging.

In any supported catalyst system, the impregnation of excessive amount of active component will usually lead to loss of surface area and pore volume as observed in this study. As impregnation method was used to prepare the catalyst, the deposition of TPA on the external surface could not be totally avoided. The support material used was also known to contain irregular pore shapes and sizes [15]. As such, it is understandable that if the deposition of the active component occurs at pore mouths, internal diffusion resistance could result. Thus, decreases in these surface properties could affect the catalytic activity in this heterogeneous reaction system. In this respect, SEM images could not clearly show pore mouth blockage as it could also occur at internal narrow areas of the pores.

3.2.3. Effect of reaction time

Effect of reaction time on the methyl ester yield under ultrasonic condition can be seen in Fig. 5 for both TPA20-AC and TPA25-AC catalysts. For a low reaction time of 20 min, insufficient contact time between the reactants led to low reaction yield. The yield increased with increasing reaction time, reaching its maximum levels in 40 min for both catalysts. The highest reaction yields were 87.33% and 71.19% for TPA20-AC and TPA25-AC, respectively. The behavior of the reaction between 30 and 50 min in the presence of heterogeneous catalyst can be explained based on the role of ultrasonic mixing in achieving emulsifying effects between the reactants. The ultrafine mixing provided a dispersion effect to the catalyst particles through the reaction media that facilitated the reactants molecules to spread and reach the active sites on the surface of the catalyst. The role of ultrasonic irradiation in enhancing the reaction rate for heterogeneous biodiesel production system has been highlighted by Salamatinia et al. [34] and Mootabadi et al. [35]. In these studies, the reaction times to reach yields exceeding 90% in a base-catalyzed transesterification of palm oil

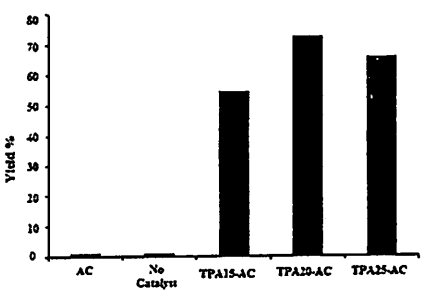

Fig. 4. Transesterification of Jatropha oil by ultrasonic-assisted process over TPA immobilized on AC (reaction time 60 min, methanol/oil molar ratio 20:1, catalyst amount 4% (w/w), and ultrasonic power 75%).

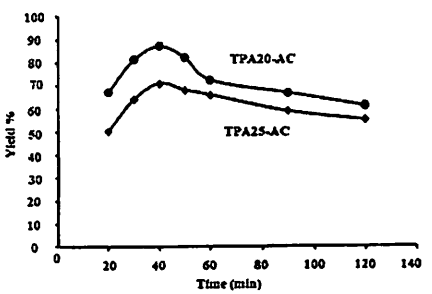

Fig. 5. Effect of reaction time on biodiesel yield (methanol/oil molar ratio 20:1, catalyst amount 4% (w/w), and ultrasonic power 75%).

were about ~50 min and 60 min, respectively. The results were significantly lower than those generally reported for non-ultrasonic reaction systems.

Although the use of ultrasonic irradiation managed to shorten the reaction time, decreases in FAME yields for both catalysts were observed after 60 min. It has been reported for ultrasound-assisted transesterification system that monoglycerides content was high at times beyond 60 min due to the slow reaction rate to convert it to glycerol and FAME [36]. Thus, in the current investigated system, the reaction mixture could contain sufficient amounts of monoglycerides at high reaction time that could enhance the solubility of FAME in the glycerol to result in FAME glycerolysis. Besides that, side (esterification) reactions between FFA and glycerol led to the formation of monoglycerides, diglycerides and finally triglycerides that would negatively affect the reaction yield [15]. Esterification reaction is known to be an acid-catalyzed reaction.

Transesterification process of vegetable oil and methanol is widely reported to be catalyzed by either acid or base catalyst. The reaction rate is influenced by many factors such as the reaction temperature, type of catalyst, ratio of reactants, concentration of the limiting reactant etc. [13,14]. In this study, high concentration of FAME was expected after a certain duration of time, especially when the FAME yield exceeded about 70%. At this stage, FAME glycerolysis could occur at a significantly high rate leading to lower FAME yield. At the same time, the formation of FAME through transesterification between the oil and methanol occurred simultaneously but at low rate due to the low concentration oil as the limiting reactant. As such, with progressing reaction time, more FAME could have been used in the glycerolysis compared to that formed through the transesterification reaction.

Cao et al. [37] reported that by using $H_3PW_{12}O_{40}$–$6H_2O$ as the catalyst, the highest transesterification yield of 87% could be achieved with high reactants' molar ratio of 70:1 and long reaction time of 14 h under mechanical stirring. On the other hand, with the use of immobilized form of HPA (zirconia-supported HPA catalyst), Sunita et al. [23] recorded that the optimum reaction time under conventional process to achieve 97% of biodiesel yield at 200 °C was 5 h. Thus, the ultrasonic-assisted reactor system significantly reduced the requirement for a very high methanol to oil ratio for the acid catalyzed process. In addition, significant reductions in reaction time and reaction temperature were achieved. Thus, the reaction could be carried out in a more cost efficient manner.

3.2.4. Effect of water and FFA content

The effect of feed stock water content on FAME yield for both catalysts can be seen in Fig. 6. It is noted that by increasing the content of water in Jatropha oil to 1% (w H_2O/w oil), only a slight decrease in the yields for both catalysts resulted. The results revealed the tolerance of the catalysts towards water. For TPA20-AC, the amount of water beyond 1% led to a sharp decrease in the biodiesel yield while lower yield was recorded for the higher water content (4%). In the case of TPA-25AC catalyst, increasing water content gradually decreased the methyl ester yield. However, water contents beyond 2% did not result in significant decrease in the yield. It could be due to the excess amount of TPA loaded onto the AC.

As a conclusion, a decrease in reaction yield with increasing of water content could be attributed to the hydrolysis of the esters at high water content. The presence of large amount of water could negatively affect the strength of Brönsted acid sites presented in the catalyst. The hydration of these acid sites could reduce the catalyst activity that in turn, resulted in negative effects on the reaction yield. Nakajima et al. [38] reported the same behavior for carbon based acid catalyst used in the presence of high water content. Good tolerance to high water content as demonstrated by TPA25-AC catalyst could be related to the higher number of active sites that reduced the effects of acid sites hydration.

The effect of FFA % content in the crude vegetable oil on the reaction yield is presented in Fig. 7 for TPA20-AC and TPA25-AC catalysts. It can be concluded that both catalysts were insensitive to the presence of FFA. Beyond 17.5 FFA %, slight reductions in the reaction yields for both of catalysts were noticed. This could be attributed to the effect of high amount of water generated during the esterification reaction due to the high FFA content. The presence of water can affect negatively on the production yield as it can hydrolyze the esters. Meanwhile, the studied catalysts showed good water and FFA tolerance which would enable the use of low grade, cheap price and non-edible vegetable oils for biodiesel production.

3.2.5. Catalyst reusability and stability

In order to study the catalyst reusability under the ultrasonic conditions, consecutive reaction runs were carried out using the same catalyst. After the first experimental run, the TPA20-AC catalyst was filtered and washed several times with ethanol to remove any polar impurities followed by washing with n-hexane to eliminate any non-polar components. The washed catalyst was dried at 100 °C for 2 h and reused again for the transesterification reaction. Fig. 8 shows the catalyst activity for up to three times of use at 75% of ultrasonic amplitude, 40 min of reaction time and reactants' molar ratio of 20. The results revealed that a drop in the catalytic activity as indicated by a decrement in the reaction yield

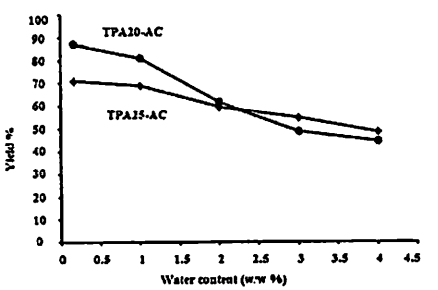

Fig. 6. Effect of water content on biodiesel yield (reaction time 40 min, methanol/oil molar ratio 20:1, catalyst amount 4% (w/w), and ultrasonic power 75%).

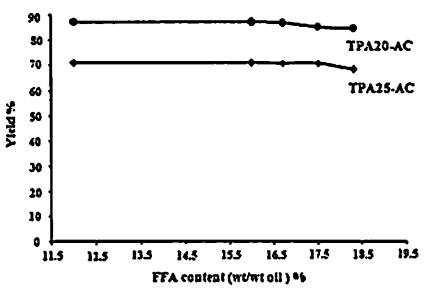

Fig. 7. Effect of FFA content on FAME yield (reaction time 40 min, methanol/oil molar ratio 20:1, catalyst amount 4% (w/w), and ultrasonic power 75%).

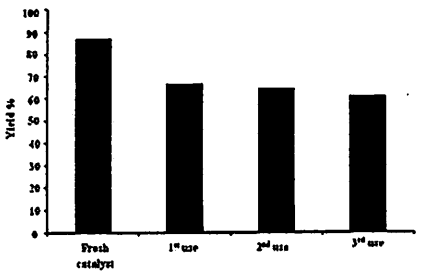

Fig. 8. Catalytic activity for successive reaction runs (reaction time 40 min, methanol/oil molar ratio 20:1, catalyst amount 4% (w/w), and ultrasonic power 75%).

was noticed. For the first run, 77% of the original activity was achieved. The reduction in activity could be attributed to the catalyst deactivation, leaching and the loss during washing process between the reuse cycles. A small portion of the solid catalyst was collected as soot in the filtration step during the study. These small carbon particles were formed as a result of the impact of ultrasonic irradiation on the porous solid particles. If the small loss of unrecovered catalyst were to be considered, small drop in the activity from the first run to the third reuse cycle could indicate the stability of the catalyst for repeated use in the process.

The stability of the AC-based TPA catalysts was found to be slightly lower than that reported previously using alumina-based TPA catalysts [33]. For comparison, 20 wt. % TPA loading in AC showed about 27% drop FAME yield after the 3rd cycle of reuse while it was only about 12% in the case of the alumina-based TPA catalyst. Differences in the activity could be associated with the higher structural stability of the alumina-based catalyst. Thus, structural stability could play a major role in the activity of the catalyst in this ultrasound-assisted reaction. Due to higher porosity of AC-based catalyst, its structural stability was expected to be significantly lower compared to that of alumina-based catalyst.

3.2.6. Catalyst leaching

Investigation on the catalyst stability under the ultrasonic reaction conditions revealed that 12% of the reaction yield was achieved due to the $PW_{12}O_{40}^{3-}$ anion which leached out from the heterogeneous catalyst. The result showed that major part of the reaction yield was achieved through heterogeneous catalysis. Leaching of active sites from the catalyst occurred due to the good solubility of TPA in the polar reaction mixture and the exposure of the solid catalyst to direct ultrasonic irradiation. However, significant solubilization of TPA did not occur as it was strongly fixed on the surface through calcination and the small pore sizes of the AC support.

Compared with other immobilized forms of HPA on different supports such as zirconia and silica [39], HPA supported on AC used in the current study showed minimal leaching due to the strong fixation of HPA over the surface of activated carbon. Some TPA particles were trapped inside the small pores of the support due to textural porous properties of the support material. Strong electrostatic attraction between TPA species and AC could also happen due to the existence of specific functional groups on the surface of AC [39]. The same behavior of HPA immobilized on AC catalyst was reported for other polar reaction mixtures such as acetylation of glycerol with acetic acid [21] and liquid phase esterification of acetic acid with butanol [40].

4. Conclusions

Ultrasonic-assisted transesterification of crude Jatropha oil with the presence of activated carbon-supported tungstophosphoric acid (TPA) catalysts was studied. The catalysts were tested to show their activity in FAME production from Jatropha oil with high FFA content using an ultrasound-assisted reactor system. Amount of TPA deposited on the support had significant effects on the catalyst characteristics and subsequently on methyl ester yield in the ultrasound-assisted reaction. TPA20-AC and TPA25-AC catalysts achieved methyl ester yields of up to 87.33% and 71.19%, respectively in just 40 min. Further increase in reaction time beyond 60 min resulted in a reduction in the yield due to the effects of some side reactions. Effect of water and FFA contents in the Jatropha oil on the reaction yield was successfully elucidated. The catalysts showed moderate water tolerance to a limit of 1% w/w water content. The catalysts were also used with high FFA content feed stocks and the results revealed that the catalysts were rather insensitive toward FFA increment in the crude oil. The catalyst reusability and leaching study performed on TPA20-AC catalyst revealed that the reaction was mainly heterogeneous in nature with an appreciable contribution of homogeneous reaction.

Acknowledgment

A Short Term research grant (60312010) and a Research University grant (814144) from Universiti Sains Malaysia to support this research work are gratefully acknowledged.

References

[1] Santacesaria E, Di Serio M, Tesser R, Tortorelli M, Turco R, Russo V. A simple device to test biodiesel process intensification. Chem Eng Proc 2011;50:1085–94.
[2] Qiu Z, Zhao L, Weatherley L. Process intensification technologies in continuous biodiesel production. Chem Eng Proc 2010;49:323–30.
[3] Ma F, Hanna MA. Biodiesel production: a review. Bioresour Technol 1999;70:1–15.
[4] Koh MY, Ghazi TIM. A review of biodiesel production from Jatropha curcas L. oil. Renew Sust Energ Rev 2011;15:2240–51.
[5] Leung DYC, Wu X, Leung MKH. A review on biodiesel production using catalyzed transesterification. Appl Energ 2010;87:1083–95.
[6] Boey PL, Ganesan S, Maniam GP, Khairuddean M, Lim SL. A new catalyst system in transesterification of palm olein: tolerance of water and free fatty acids. Energ Convers Manag 2012;56:46–52.
[7] Elsheikh YA, Man Z, Bustam MA, Yusup S, Wilfred CD. Brønsted imidazolium ionic liquids: synthesis and comparison of their catalytic activities as pre-catalyst for biodiesel production through two stage process. Energ Convers Manag 2011;52:804–9.
[8] Math MC, Kumar SP, Chetty SV. Technologies for biodiesel production from used cooking oil – a review. Energ Sust Dev 2010;14:339–45.
[9] Jacobson K, Gopinath R, Meher LC, Dalai AK. Solid acid catalyzed biodiesel production from waste cooking oil. Appl Catal B 2008;85:86–91.
[10] Semwal S, Arora AK, Badoni RP, Tuli DK. Biodiesel production using heterogeneous catalysts. Bioresour Technol 2011;102:2151–61.
[11] Vyas AP, Verma JL, Subrahmanyam N. A review on FAME production processes. Fuel 2010;89:1–9.
[12] Kulkarni MG, Dalai AK. Waste cooking oil – an economical source for biodiesel: a review. Ind Eng Chem Res 2006;45:2901–13.
[13] Jitputti J, Kitiyanan B, Rangsunvigit P, Bunyakiat K, Attanatho L, Jenvanitpanjakul P. Transesterification of crude palm kernel oil and crude coconut oil by different solid catalysts. Chem Eng J 2006;116:61–6.
[14] Melero JA, Bautista LF, Morales G, Iglesias J, Sánchez-Vázquez R. Biodiesel production from crude palm oil using sulfonic acid-modified mesostructured catalysts. Chem Eng J 2010;161:323–31.
[15] Shu Q, Nawaz Z, Gao J, Liao Y, Zhang Q, Wang D, et al. Synthesis of biodiesel from a model waste oil feedstock using a carbon-based solid acid catalyst: reaction and separation. Bioresour Technol 2010;101:5374–84.
[16] Morin P, Hamad B, Sapaly G, Carneiro-Rocha MG, de Oliveira PGP, Gonzalez WA, et al. Transesterification of rapeseed oil with ethanol: I. Catalysts with homogeneous Keggin heteropolyacids. Appl Catal A 2007;330:69–76.
[17] Chai F, Cao F, Zhai F, Chen Y, Wang X, Su Z. Transesterification of vegetable oil to biodiesel using a heteropolyacid solid catalyst. Adv Synth Catal 2007;349:1057–65.

[18] Zhang S, Zu YG, Fu YJ, Luo M, Zhang DY, Efferth T. Rapid microwave-assisted transesterification of yellow horn oil to biodiesel using a heteropolyacid solid catalyst. Bioresour Technol 2010;101:931–6.
[19] Tropecêlo AI, Casimiro MH, Fonseca IM, Ramos AM, Vital J, Castanheiro JE. Esterification of free fatty acids to biodiesel over heteropolyacids immobilized on mesoporous silica. Appl Catal A 2010;390:183–9.
[20] Mukai SR, Lin L, Masuda T, Hashimoto K. Key factors for the encapsulation of Keggin-type heteropoly acids in the supercages of Y-type zeolite. Chem Eng Sci 2001;56:799–804.
[21] Ferreira P, Fonseca IM, Ramos AM, Vital J, Castanheiro JE. Acetylation of glycerol over heteropolyacids supported on activated carbon. Catal Commun 2011;12:573–6.
[22] Katada N, Hatanaka T, Ota M, Yamada K, Okumura K, Niwa M. Biodiesel production using heteropoly acid-derived solid acid catalyst $H_4PNbW_{11}O_{40}$/WO_3-Nb_2O_5. Appl Catal A 2009;363:164–8.
[23] Sunita G, Devassy BM, Vinu A, Sawant DP, Balasubramanian VV, Halligudi SB. Synthesis of biodiesel over zirconia-supported isopoly and heteropoly tungstate catalysts. Catal Commun 2008;9:696–702.
[24] Badday AS, Abdullah AZ, Lee KT, Khayoon MS. Intensification of biodiesel production via ultrasonic-assisted process: a critical review on fundamentals and recent development. Renew Sust Energ Rev 2012;16:4574–87.
[25] Gogate PR. Cavitational reactors for process intensification of chemical processing applications: a critical review. Chem Eng Proc 2008;47:515–27.
[26] Ji J, Wang J, Li Y, Yu Y, Xu Z. Preparation of biodiesel with the help of ultrasonic and hydrodynamic cavitation. Ultrasonics 2006;44:e411–4.
[27] Deng X, Fang Z, Liu YH. Ultrasonic transesterification of Jatropha curcas L. oil to biodiesel by a two-step process. Energ Convers Manag 2010;51:2802–7.
[28] Hanh HD, Dong NT, Starvarache C, Okitsu K, Maeda Y, Nishimura R. Methanolysis of triolein by low frequency ultrasonic irradiation. Energ Convers Manag 2008;49:276–80.
[29] Chimienti ME, Pizzio LR, Cáceres CV, Blanco MN. Tungstophosphoric and tungstosilicic acids on carbon as acidic catalysts. Appl Catal A 2001;208:7–19.
[30] Oball Z, Doğu T. Activated carbon–tungstophosphoric acid catalysts for the synthesis of tert-amyl ethyl ether (TAEE). Chem Eng J 2008;138:548–55.
[31] Alemdaroglu T. Determination methods for the acidity of solid surfaces. Commun Fac Sci Univ Ank Ser B 2001;47:27–35.
[32] Taufiq-Yap YH, Lee HV, Yunus R, Juan JC. Transesterification of non-edible Jatropha curcas oil to biodiesel using binary Ca–Mg mixed oxide catalyst: effect of stoichiometric composition. Chem Eng J 2011;178:342–7.
[33] Badday AS, Abdullah AZ, Lee KT. Ultrasound-assisted transesterification of crude Jatropha oil using alumina-supported heteropolyacid catalyst. Appl Energ 2013;105:380–8.
[34] Salamatinia B, Mootabadi H, Bhatia S, Abdullah AZ. Optimization of ultrasonic-assisted heterogeneous biodiesel production from palm oil: a response surface methodology approach. Fuel Proc Technol 2011;91:441–8.
[35] Mootabadi H, Salamatinia B, Bhatia S, Abdullah AZ. Ultrasonic-assisted biodiesel production process from palm oil using alkaline earth metal oxides as the heterogeneous catalysts. Fuel 2010;89:1818–25.
[36] Stavarache C, Vinatoru M, Maeda Y. Aspects of ultrasonically assisted transesterification of various vegetable oils with methanol. Ultrason Sonochem 2007;14:380–6.
[37] Cao F, Chen Y, Zhai F, Li J, Wang J, Wang X, et al. Biodiesel production from high acid value waste frying oil catalyzed by superacid heteropolyacid. Biotechnol Bioeng 2008;101:93–100.
[38] Nakajima K, Hara M, Hayashi S. Environmentally benign production of chemicals and energy using a carbon-based strong solid acid. J Am Ceram Soc 2007;90:3725–34.
[39] Sepúlveda JH, Yori JC, Vera CR. Repeated use of supported $H_3PW_{12}O_{40}$ catalysts in the liquid phase esterification of acetic acid with butanol. Appl Catal A 2005;288:18–24.
[40] Alsalme A, Kozhevnikova EF, Kozhevnikov IV. Heteropoly acids as catalysts for liquid-phase esterification and transesterification. Appl Catal A 2008;349:170–6.

Renewable Energy 50 (2013) 427–432

Contents lists available at SciVerse ScienceDirect

Renewable Energy

Journal homepage: www.elsevier.com/locate/renene

Optimization of biodiesel production process from Jatropha oil using supported heteropolyacid catalyst and assisted by ultrasonic energy

Ali Sabri Badday [1], Ahmad Zuhairi Abdullah*, Keat-Teong Lee [1]

School of Chemical Engineering, Universiti Sains Malaysia, 14300 Nibong Tebal, Penang, Malaysia

ARTICLE INFO

Article history:
Received 29 July 2011
Accepted 15 July 2012
Available online xxx

Keywords:
Biodiesel
Jatropha oil
Ultrasonic irradiation
Tungstophosphoric acid catalyst
Optimization
Interaction

ABSTRACT

Application of ultrasound-assisted biodiesel production process from Jatropha oil catalyzed by activated carbon-supported tungstophosphoric acid catalyst was studied. Influences of ultrasonic energy on different process variables were elucidated. Reaction variables i.e. reaction time (10–50 min), reactants' molar ratio (5:1–25:1), ultrasonic amplitude (30–90% of the maximum sonifier power) and catalyst amount (2.5–4.5 w/w oil) were studied. A mathematical representation for biodiesel yield was successfully generated. A yield of 91% was achieved in just 40 min at a moderate ultrasonic amplitude (~60%), high molar ratio (25:1) and low reaction temperature (65 °C). Interactions between the variables were also validated statistically. Leaching study revealed that the reaction was predominately heterogeneous in nature.

1. Introduction

Transesterification reaction to produce biodiesel consists of a series of consecutive reversible reactions (Fig. 1) to produce 3 mol of ester and glycerol as a co-product [1–3]. Edible vegetable oils such as palm oil, sunflower oil, rapeseed oil and soybean oil are generally suitable feedstocks for biodiesel production [4,5]. However, non-edible oils such as Karanja oil, Polanga oil and Jatropha oil have attracted great attention as they do not face the 'food vs fuel' dilemma when used as feedstocks in fuel industry [6,7].

Unfortunately, non-edible oils such as crude Jatropha oil usually have high free fatty acid contents (around 15%) that are beyond the practical limit of a wide range of base catalysts [8–11]. As such, acid catalysts should be used. Heteropolacids (HPA) can be used in acid catalyzed transesterification reaction for biodiesel production as it possesses strong Brönsted acidity and high water tolerance [12]. As they are non-porous materials and soluble in polar media, efforts to distribute HPA on suitable porous materials to improve the catalytic activity are deemed worthwhile.

The immiscible nature, coupled with variation in the density of reactants (alcohol and vegetable oil) in the transesterification reaction are responsible for poor interaction between them leading to poor mass transfer. This leads to low reaction rates which in turn, increases the reaction time to achieve high biodiesel yield [13,14]. For acid catalyzed systems, it is reported that the reaction under conventional process usually requires high reaction temperature due to slow reaction rate [15].

Application of ultrasonic energy in biodiesel production is an attractive and effective technique to solve the problems related with the immiscible nature of the reactants [16,17]. Subjecting ultrasonic waves to the reaction mixture force the fluids to generate huge number of cavitation bubbles which grow rapidly and subsequently undergo violent collapse. The vigorous collapses of these bubbles will lead to the formation of micro jets generating fine emulsion between the reactants. Besides that, these collapses also generate local temperature increment within the reaction mixture [18]. The use of ultrasonic energy in homogenous [19,20] or heterogeneous [17–21] biodiesel production has been investigated and encouraging results have been demonstrated. However, the use of heterogeneous acid catalyst for ultrasonic-assisted biodiesel production process is still hardly reported.

The main objective of this study is to elucidate the role of ultrasonic energy and its effects on the reaction. Transesterification of crude Jatropha oil with methanol has been conducted in the presence of an activated carbon-supported heteropolyacid catalyst. The objective is to validate the effectiveness of the combination of ultrasonic wave with an acid catalyst for biodiesel production. The obtained experimental data have been used to generate a historical design and to identify the optimum conditions by means of a response surface methodology (RSM) approach.

* Corresponding author. Tel.: +604 5996411; fax: +604 5941013.
E-mail addresses: chzuhairi@eng.usm.my, azuhairi@yahoo.com (A.Z. Abdullah).
[1] Tel.: +604 5996411; fax: +604 5941013.

0960-1481/$ – see front matter © 2012 Elsevier Ltd. All rights reserved.
http://dx.doi.org/10.1016/j.renene.2012.07.013

$$\text{Triglyceride (TG)} + \text{R}'\text{OH} \longleftrightarrow \text{Diglyceride (DG)} + \text{R}'\text{COOR}_1$$
$$\text{Diglyceride (DG)} + \text{R}'\text{OH} \longleftrightarrow \text{Monoglyceride (MG)} + \text{R}'\text{COOR}_2$$
$$\text{Monoglyceride (MG)} + \text{R}'\text{OH} \longleftrightarrow \text{Glycerol (GL)} + \text{R}'\text{COOR}_3$$

Fig. 1. Consecutive reversible reactions involved in the transesterification process.

2. Experimental

2.1. Reagents and materials

Tungstophosphoric acid ($H_3PW_{12}O_{40}.nH_2O$) was purchased from Merck (Malaysia) while activated carbon (AC) was purchased from Galcon Carbon Corporation (USA). The support was first ground to particle sizes between 250 and 500 μm. Crude Jatropha oil was supplied by Telaga Madu Resources (Malaysia) while methanol was supplied by Thermo Fisher Scientific Inc. (USA). The properties of the crude Jatropha oil are given in Table 1. Ethanol and n-hexane were purchased from Merck (Malaysia). Meanwhile, fatty acid methyl ester (FAME) GC standards were supplied by NuChek Prep. Inc. (Australia).

2.2. Catalyst preparation

A pretreatment of AC support to remove its impurities was done by washing with 0.1 M NaOH and subsequently with 0.1 M HCl [22]. Then, it was treated with 30 wt. % solution of HNO_3 in a reflux system for 2 h. The supported catalyst was produced by dissolving the desired amount of HPA in (50:50 v/v) solution of deionized water and ethanol. Wet impregnation method was used by contacting the support with the solution (4 ml/g of support) for 72 h. The obtained catalyst was calcined at 453 K for 4 h. The catalyst was characterized using a Micrometrics ASAP 2020 system.

2.3. Experimental setup

The setup for the transesterification process consisted of a three-neck glass batch reactor partially submerged in a water bath. A condenser was fitted to the reaction vessel to return the evaporated methanol back to the reaction vessel. Ultrasonic energy was supplied using a Branson (USA) ultrasonic processor capable of generating a frequency of 20 kHz with a highest power of 400 W (at 100% level).

Blank experiments were carried out in the absence of catalyst or under ultrasonic irradiation alone. They were performed by providing ultrasonic irradiation at 75% of the maximum power for 60 min at a methanol/oil ratio of 20. The same conditions were tested in the presence of AC alone at 4% w/w loading. An experiment under mechanical stirring was also performed under the same reaction conditions.

In a typical run, water bath temperature was fixed at 56 °C and the desired amount of oil was transferred into the reactor. Then, the required pre-heated amount of methanol was added to the oil followed by the catalyst. Ultrasonic irradiation was then provided in a discrete pattern with 9 s on and 3 s off. In this system, the heat generated by the ultrasonic probe combined with the heat gained from the water bath successfully kept the reaction vessel at 65 ± 1 °C. After the reaction, the products were quenched in water and excess methanol was distilled out. After centrifugation at 3000 rpm for 20 min, the biodiesel layer was collected for analysis.

In order to study the leaching of $PW_{12}O_{40}^{3-}$ heteropoly anion in the reaction mixture and to examine the effect of ultrasonic irradiation on the catalyst stability, an experiment as reported in [23,24] was conducted. The catalyst was first allowed to have contact with methanol and mixed ultrasonically under the optimum reaction conditions. After the reaction, the catalyst was filtered and the desired amount of oil was added to fresh methanol. The reaction was then carried out under the same conditions without the use of catalyst.

2.4. Product analysis

The products were analyzed using an Agilent 7890 a gas chromatograph unit equipped a capillary column (Agilent Technologies, Inc. 19091 J-413 HP-5). The analyses of the biodiesel standards and the reaction product were then carried out by dissolving the samples in n-hexane. 1 μl of the mixture was then injected into the GC.

2.5. Experimental design

A central composite design (CCD) was applied with four design factors i.e. reaction time (X_1), methanol to oil molar ratio (X_2), ultrasonic amplitude (X_3) and catalyst amount (X_4). Four zero levels (central values) selected for the experimental design were the reaction time (30 min), molar ratio (15:1), ultrasonic amplitude (60%) and catalyst amount (3.5% w/w oil) (Table 2). The central values were chosen based on the most suitable levels reported for acid catalyzed transesterification [2]. 60% amplitude was selected as the central level based on the observation that levels lower than 30% were too low to create any positive effect. The selection of the central values of the reaction time was critical in examining the performance of the ultrasonic-assisted process in enhancing the reaction. With that, long reaction time that is generally required for conventional acid transesterification processes can be significantly shortened [15].

A 2^4 full-factorial CCD for three levels of the four independent variables was used in this work giving a total of 30 experiments according to $2^k + 2k + 6$, where k is the number of independent variables [25]. The twenty four experiments were improved with six replications at the center points to evaluate the pure error. For regression and graphical analyses of the data, Design Expert 6.0.6 software was employed by taking the maximum production yield values as the design experiment responses. A general second degree form of the polynomial equation [26] is as shown in Equation (1).

$$Y = \lambda_0 + \sum_{i=1}^{k} \lambda_i x_i + \sum_{i=1}^{k} \lambda_{ii} x_i^2 + \sum_{i=1}^{k} \sum_{j=i+1}^{k} \lambda_{ij} x_i x_j + e \quad (1)$$

Where, Y is the response, i and j are the linear and quadratic coefficients, respectively, k is the number of studied and optimized

Table 1
Properties of Jatropha oil used in this study.

Property	Value
Density (kg/m³)	921
Viscosity (cSt)	38.1
Molecular weight	870
Water content (wt. %)	0.16
FFA[a] content (wt. %)	10.5

[a] FFA = free fatty acid.

Table 2
Coded and actual reaction variables used in the experimental design.

Real variable	Coded variable	Level		
		−1	0	+1
Reaction time (min)	X_1	10	30	50
Molar ratio	X_2	5:1	15:1	25:1
Ultrasonic amplitude (%)	X_3	30	60	90
Catalyst amount (w/w %)	X_4	2.5	3.5	4.5

factors in the experiments, λ is the regression coefficient, and ε is the arbitrary error. For the sake of accuracy, of two replications were taken instead of individual data points.

3. Results and discussion

3.1. Product and catalyst properties

Tungstophosphoric acid itself was not a sufficiently porous material to be used as a catalyst with a reported surface area of about 1–2 m^2/g [27]. The surface area of AC support used was 751 m^2/g and the area contributed by micropores was about 73% (Table 3). Immobilization of HPA on the carbon resulted in minimal reductions in surface area, microporous volume and total pore volume. This was attributed to partial blockage of pores by the active species. Low loading of HPA was responsible for the minimal changes in the pore characteristics. Similar observation for HPA immobilized on carbon was also reported [27].

Table 4 provides the chemical composition of the produced FAME mixture after the reaction. It can be seen that the FAMEs consisted of five main compounds. Saturated and unsaturated C_{19} components were the dominant substances in the produced FAMEs. Further compositional analysis was not done as it was beyond the scope of this research work. The intensified production of FAMEs from high FFA and high moisture content oil was proven using the investigated system. Further research work to enhance the quality of the produced product to fit the international fuel standards and to examine the reusability and regeneration of the catalyst is in progress and will be reported separately.

3.2. Blank experiments

Results of blank experimental runs revealed that significant transesterification reaction did not occur with the presence of only AC or in the case of the run without the use of any catalyst. This was mainly due to the absence of acid active sites to catalyze the reaction. Conducting the reaction without ultrasonic irradiation (using only mechanical stirring) also resulted in no significant reaction due to the insufficient reaction time to achieve significant conversion in 50 min. It has been reported that conventional acid catalyzed reactions usually require long reaction time (5–6 h) due to the slow reaction rate [7]. Meanwhile, base-catalyzed process could be carried out with relatively shorter reaction times (2–3 h) [6].

Table 3
Physical properties of AC and HPA/AC catalyst.

Sample	Surface area (m^2/g)		Pore volume (cm^3/g)	
	BET[a]	Micropore	Total	Micropore
AC	751	548	0.47	0.29
HPA/AC	621	468	0.39	0.25

[a] Brunauer-Emmett-Teller surface area.

Table 4
Typical FAME composition produced under the optimum reaction conditions.

Component	Formula	Name	Content (wt. %)
9-Hexadecenoic acid, methyl ester	$C_{17}H_{32}O_2$	–	7.40
Hexadecanoic acid, methyl ester	$C_{17}H_{34}O_2$	Methyl palmitate	19.00
9,12-Octadecadienoic acid (Z,Z)-, methyl ester	$C_{19}H_{34}O_2$	Methyl linoleate	28.47
9-Octadecenoic acid, methyl ester, (E)-	$C_{19}H_{36}O_2$	Methyl oleate	30.81
Octadecanoic acid, methyl ester	$C_{19}H_{38}O_2$	Methyl stearate	11.38
Other components	–	–	2.95

3.3. Regression surface analysis and the analysis of variance (ANOVA)

The point type, non coded values of the reaction parameters and the responses for the experiments are shown in Table 5. The second order polynomial equation based on the coded values that was obtained using multiple regression analysis of the experimental data is presented as;

$$Y = -69.81 + 2.66X_1 + 4.06X_2 + 0.88X_3 + 3.06X_4 - 0.04X_1^2 - 0.12X_2^2 - 6.13\times10^{-3}X_3^2 + 0.058X_1X_2 - 6.04\times10^{-3}X_1X_3 + 8.90\times10^{-3}X_2X_3 \quad (2)$$

Here, Y is the response (yield of FAME), and X_1, X_2, X_3 and X_4 are the values in the coded form of the studied variables.

Table 6 shows ANOVA results from the fitting of the experimental data to a second-order response surface model. High significance of the regression model can be seen in the Fisher F-test for the model (F = 50.61) with a very small probability value (Prop.>F < 0.0001). According to the value of the determination

Table 5
Central composite design matrix for four variables and the response.

Run	Point type	Real variables				Yield (%)
		Time (min)	M/O	Amplitude (%)	Catalyst amount (w/w %)	
1	Fact	10	5	30	2.5	12.1
2	Fact	50	5	30	2.5	12.3
3	Fact	10	25	30	2.5	20.4
4	Fact	50	25	30	2.5	82.3
5	Fact	10	5	90	4.5	9.5
6	Fact	50	5	90	4.5	12.1
7	Fact	10	25	90	4.5	42.3
8	Fact	50	25	90	4.5	78.2
9	Fact	10	5	30	4.5	10.7
10	Fact	50	5	30	4.5	14.7
11	Fact	10	25	30	4.5	27.4
12	Fact	50	25	30	4.5	93.9
13	Fact	10	5	90	4.5	8.4
14	Fact	50	5	90	4.5	12.5
15	Fact	10	25	90	4.5	53.5
16	Fact	50	25	90	4.5	85.6
17	Axial	4	15	60	3.5	17.6
18	Axial	56	15	60	3.5	70.8
19	Axial	30	2	60	3.5	7.3
20	Axial	30	28	60	3.5	94.3
21	Axial	30	15	21	3.5	52.3
22	Axial	30	15	99	3.5	72.6
23	Axial	30	15	60	2.2	63.9
24	Axial	30	15	60	4.8	80.6
25	Center	30	15	60	3.5	62.2
26	Center	30	15	60	3.5	75.1
27	Center	30	15	60	3.5	71.9
28	Center	30	15	60	3.5	67.1
29	Center	30	15	60	3.5	69.7
30	Center	30	15	60	3.5	70.4

Author's personal copy

Table 6
Analysis of variance (ANOVA) for the quadratic model.

Sources of variations	Sum of squares	Degrees of freedom	Mean square	F-value	Prob.>F
Model	26,531.08	10	2654.72	50.61	<0.0001
Residual	996.62	19	52.45	–	–
Lack of fit	899.41	14	64.24	3.30	0.0968
Pure error	97.21	5	19.44	–	–
Total	27,543.77	29	–	–	–

R^2 = 0.9638, Adj. R^2 = 0.9448, C.V. = 14.97, Std. Div = 7.24.

coefficient (R^2 = 0.9638), it could be inferred that 96.38% of the effect on the FAME yield could be attributed to the variation in the independent variables and the remaining response (3.62%) could be explained as residues.

Effects of different reaction variables on the response can be studied based on data in Table 7. The table provides the F-values and Prop > F values that indicate the significance of each coefficient. In general, larger F-value and smaller Prob. > F value indicate higher significance of the corresponding coefficient [28]. It can be seen in Table 7 that the most influencing variables on the model response were the reaction time and the reaction molar ratio. Beside their single effects, the influences of their squared values and the two–level interaction between these two parameters were also found to significantly affect the process yield.

For slow reactions such as the transesterification reaction, the response is understandably influenced by the reaction time. However, the reaction time tested in this study was only up to 50 min. This range was deemed suitable for the ultrasonic-assisted process as compared to that of non-ultrasonic reactors that could extend to few hours [9,11]. This observation clearly suggested the positive influence of ultrasonic irradiation in accelerating the rate of reaction.

3.4. The interaction between the parameters

Fig. 2(a) shows the interaction between reaction time and reactants' molar ratio while maintaining the other parameters at their center values (ultrasonic amplitude of 60%, catalyst amount of 3.5% w/w). At short reaction time, increasing molar ratio apparently increased the yield but the values were still low for all the ratios. This could be attributed to the insufficient reaction time so that the reactants could not reach the equilibrium. For high reaction time, increasing molar ratio sharply increased the reaction yield from the minimum value (13%) to the maximum value (94%). Low reaction rate at low molar ratio of 5:1 was due to insufficient methanol concentration to drive the forward reaction to the product side.

Under ultrasonic conditions, ultra fine mixing created by ultrasonication led to severe dispersion of the produced FAMEs into the glycerol layer. The severe mixing effects made it hard to extract the desired product (the FAMEs) from the undesired one (glycerol) resulting in a sharp reduction in the reaction yield. Based on the same figure, increasing time at the maximum molar ratio increased the yield until it reached a plateau at about 40 min. Another phenomenon that can be observed at reaction times beyond the optimum value could be explained on the basis of the solubility of FAME in glycerol. As the transesterification reaction is a consecutive reaction, the reaction vessel contained sufficient amount of monoglycerides at the final stages of the process that could promote the glycerolysis of FAME. The same behavior was noticed with the transesterification process of high FFA oil for long reaction time as reported by Shu et al. [29].

Table 7
Results of regression analysis for the full second-order polynomial model.

Model parameters	Estimated coefficient	F-value	Prob.>F
Intercept	70.52941	50.61092	< 0.0001
X_1	14.26098	75.14131	< 0.0001
X_2	26.02951	250.3295	< 0.0001
X_3	2.818206	2.934442	0.1030
X_4	3.058085	3.455246	0.0785
X_1^2	−16.331	37.02062	< 0.0001
X_2^2	−12.4283	21.4408	0.0002
X_3^2	−5.51419	4.22064	0.0540
X_1X_2	11.58482	40.93781	< 0.0001
X_1X_3	−3.62693	4.01259	0.0596
X_2X_3	2.671331	2.176715	0.1565

The interactive effect between reaction time and ultrasonic amplitude while the other parameters kept at their center values is shown in Fig. 2(b). It can be concluded that at low reaction time, increasing ultrasonic amplitude led to a slight increase in the yield. This was because any increment in the ultrasonic amplitude at the initial stage of the reaction could lead to a noticeable increase in the reaction rate. Meanwhile, increasing amplitude under maximum reaction time level led to a decrease in the yield after a certain level of amplitude (~60%).

Subjecting the reacting mixture to high ultrasonic energy led to the generation of large number of cavitation bubbles in the liquid mixture. Many of these cavitation bubbles would combine to form larger, more stable and stable bubbles which could act as barriers to the transfer of acoustic energy through the reaction mixture. Besides that, large cavitation bubbles also led to poor mixing effects between the two immiscible layers (alcohol and oil). This resulted in low emulsification effects so that transesterification reaction would take place at the boundary between the two layers. Similar behavior of ultrasonic-assisted biodiesel production systems could be observed at high ultrasonic energy as reported by Kumar et al. [14] and Stavarache et al. [30].

The interaction between molar ratio and the ultrasonic amplitude while keeping the other parameters at their center values can be seen in Fig. 2(c). It can be observed that an increase in molar ratio improved the reaction yield for both the minimum and maximum ultrasonic amplitude values. This could be related to the fact that increasing methanol amount would increase the number of cavitation bubbles that would collapse to form an emulsion between the two layers. The rise in the ultrasonic amplitude did not have significant effect on the reaction yield at low molar ratio. In contrast, under high molar ratio, increasing ultrasonic amplitude had a positive effect on the reaction yield. This was due to the increment in the droplets size and the number of the bubbles that in turn, increased the interface area between methanol and oil. After a certain plateau (at about 60% of amplitude), the cavitation bubbles did not significantly enhance the mixing between the two layers. The same behavior could be seen in other reported ultrasonic-assisted systems under high ultrasonic amplitude with high molar ratios [31,32].

The interactive effect between the ultrasonic amplitude and the catalyst amount can be examined in Fig. 2(d). This figure suggests that increasing the catalyst amount under minimum and maximum ultrasonic values enhanced the reaction yield. This could be attributed to the increase in the number of catalytic active sites which accelerated the forward reaction. For increasing ultrasonic amplitude under low and high catalyst amounts, the reaction yields showed increases until they reached the maximum levels at amplitudes of about 60–70% and decreased beyond those levels. The role of optimum ultrasonic amplitude in enhancing the reactivity of the heterogeneous catalyst could be attributed to the ultrasonic dispersion of the reactants on the surface of the catalyst.

For heterogeneous catalytic systems, the main deciding factor in the process is the contact between the reactants and the catalyst. In this system, cavitational shear that was created by the ultrasonic irradiation generated much smaller reactant droplets resulting in improving the utilization between the reactants and the catalyst.

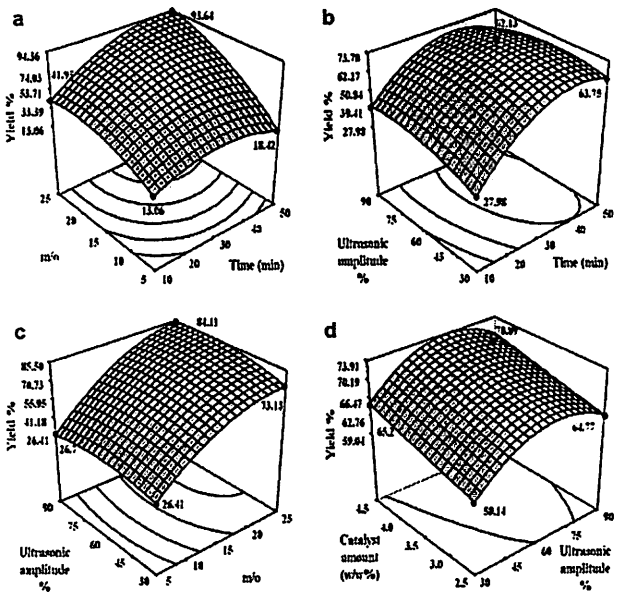

Fig. 2. Interactions between, (a) reaction time and methanol/oil ratio, (b) reaction time and ultrasonic amplitude, (c) methanol/oil ratio and ultrasonic amplitude, and (d) ultrasonic amplitude and catalyst amount.

That in turn, increased the surface area available for this chemical reaction. The role of moderate level of ultrasonic energy in achieving the optimum reaction yield was highlighted by previous researchers [14,20,30].

3.5. Discussion

Under conventional mixing process, HPA as an unsupported catalyst [33] or zirconia-supported HPA catalyst [34] have been reported to achieve 97% of biodiesel yield in about 5 h. It can be seen in Table 8 that the reaction under ultrasonic condition needed noticeably shorter reaction time (~40 min) to achieve ~90% of FAME yield. Therefore, ultra fine mixing effects between the reactants that were created by the ultrasonication allowed better accessibility of the reactants to the surface of the heterogeneous catalyst leading to intensified reaction rate.

Cao et al. [33] reported that the optimum molar ratio value using $H_3PW_{12}O_{40}{-}6H_2O$ as a catalyst when a conventional stirring reactor system was used was 70:1. In this study, the maximum yield was achieved with a molar ratio of only about 25:1. Thus, the ultrasonic-assisted reactor system significantly reduced the requirement for such a very high methanol to oil ratio for the acid-catalyzed process. Usually, for heterogeneous catalyst systems, the processes possess low reaction rate [35,36]. Besides that, excessive amounts of methanol are required to promote the reaction and to enhance the yield [15,36]. As the use of an ultrasonic-assisted process catalyzed by HPA supported on AC catalyst in this work significantly enhanced the reaction rate, too high methanol ratio was not needed. Mootabadi et al. [37] reported the same behavior for the role of ultrasonic irradiation in reducing the methanol to oil molar ratio in a heterogeneous base-catalyzed biodiesel production process from palm oil.

Kumar et al. [14] reported that high biodiesel yield was achieved using an ultrasonic-assisted process in the presence of Na/SiO_2 catalyst. The transesterification of crude Jatropha oil was conducted for a short reaction time and 9:1 methanol to oil molar ratio. In this study, heterogeneous acid catalyst was used for the transesterification of crude Jatropha oil with high FFA and water contents without prior pretreatment of the feedstock. Thus, the conversion to FAMEs could be done in a single step process and this is economically very interesting as far as the production costs are concerned.

High temperature is needed in the transesterification process to reduce the viscosity of the reactants to achieve an acceptable level of mixing. In the current study, the reaction temperature was maintained at 65 °C. It should be highlighted that to achieve this constant temperature, the water bath temperature was maintained at about 56 °C. This indicated the significant role of ultrasonic-

Table 8
Predicted and experimental results at the optimum conditions for model validation.

Run	Reaction conditions				Predicted yield (%)	Experimental yield (%)	Error (%)
	Time (min)	Molar ratio	Amplitude (%)	Catalyst amount (w/w)			
1	40.38	24.90	80	3.8	94.61	90.67	4.21
2	41.27	24.36	49	4.42	95.76	91.97	3.86
3	37.51	25.00	73	4.23	96.26	91.34	5.11

assisted process in decreasing the energy input requirement due to the heat generation during collapse of the cavitation bubbles [38]. This neglected the needs for extra heating to support the process. Besides that, the economy of the whole process would be improved due to the reduction in the intensity of the process variables while the needs for complex instrumentation in a closed reaction system can be avoided.

3.6. Catalyst leaching

An investigation on the stability of the catalyst under the optimum reaction conditions was carried on using a 'hot filtration experiment' as reported by Ferreira et al. [23]. The results revealed that only 11% of the reaction yield was achieved during the test and it was attributed to the $PW_{12}O_{40}^{3-}$ anion that underwent leaching from the heterogeneous catalyst. This problem stemmed from the solubility of HPA in the polar reaction mixture and the exposure of the solid catalyst to the ultrasonic irradiation. However, this result proved that heterogeneous reaction was predominant during the transesterification process.

Compared with other immobilized forms of HPA on different supports such as zirconia and silica [39], HPA supported on AC used in the current study showec only minimal leaching effects. This was attributed to the strong interaction between HPA and the surface of activated carbon. Similar behavior of HPA/AC catalysts was reported for other polar reaction mixtures such as acetylation of glycerol with acetic acid [23] and liquid phase esterification of acetic acid with butanol [39]. Thus, supporting HPA on activated carbon could result in catalysts with higher stability towards leaching of active component during many o.eochemical reactions.

4. Conclusions

The advantage of an ultrasonic-assisted transesterification of Jatropha oil catalyzed by HPA/AC catalyst was demonstrated. The maximum yield of 91% was achieved in just about 40 min at a molar ratio of 25:1. The more dominant variables that affected the reaction response were the reaction time and the reactants' molar ratio. Ultrasonic irradiation significantly decreased the reaction time as compared to conventional mixing process under the same conditions. Low reaction temperature was recorded as compared to other acid catalyzed processes. Short reaction time and low reaction temperature would help in improving the overall economy of the biodiesel production process. The catalyst leaching study revealed that the catalytic activity was mainly contributed by heterogeneous reaction.

References

[1] Abdullah AZ, Salamatinia B, Mootabadi H, Bhatia S. Current status and policies on biodiesel industry in Malaysia as the world's leading producer of palm oil. Energ Policy 2009;37:5440–8.
[2] Marchetti JM, Miguel VU, Errazu AF. Possible methods for biodiesel production. Renew Sust Energ Rev 2007;11:1300–11.
[3] Singh SP, Singh D. Biodiesel production through the use of different sources and characterization of oils and their esters as the substitute of diesel: a review. Renew Sust Energ Rev 2010;14:200–16.
[4] Ma F, Hanna MA. Biodiesel production: a review. Bioresour Technol 1999;70:1–15.
[5] Sharma YC, Singh B, Upadhyay SN. Advancements in development and characterization of biodiesel: a review. Fuel 2008;87:2355–73.
[6] Koh MY, Mohd TI. Ghazi, A review of biodiesel production from Jatropha curcas L. oil. Renew Sust Energ Rev 2011;15:2240–51.
[7] Leung DYC, Wu X, Leung MKH. A review on biodiesel production using catalyzed transesterification. Appl Energ 2010;87:1083–95.
[8] Jacobson K, Gopinath R, Meher LC, Dalai AK. Solid acid catalyzed biodiesel production from waste cooking oil. Appl Catal B-Environ 2008;85:86–91.
[9] Juan JC, Kartika DA, Wu TY, Hin T-YY. Biodiesel production from jatropha oil by catalytic and non-catalytic approaches: an overview. Bioresour Technol 2011;102:452–60.
[10] Keera ST, El Sabagh SM, Taman AR. Transesterification of vegetable oil to biodiesel fuel using alkaline catalyst. Fuel 2011;90:42–7.
[11] Lu H, Liu Y, Zhou H, Yang Y, Chen M, Liang B. Production of biodiesel from Jatropha curcas L. oil. Comput Chem Eng 2009;33:1091–6.
[12] Morin P, Hamad B, Sapaly G, Carneiro Rocha MG, Pries de Oliveira PG, Gonzalez WA, et al. Transesterification of rapeseed oil with ethanol: I. Catalysis with homogeneous Keggin heteropolyacids. Appl Catal A-Gen 2007;330:69–76.
[13] Ji J, Wang J, Li Y, Yu Y, Xu Z. Preparation of biodiesel with the help of ultrasonic and hydrodynamic cavitation. Ultrasonics 2006;44:e411–4.
[14] Kumar D, Kumar G, Poonam, Singh CP. Ultrasonic-assisted transesterification of Jatropha curcus oil using solid catalyst, Na/SiO_2. Ultrason Sonochem 2010;17:839–44.
[15] Lam MK, Lee KT, Mohamed AR. Homogeneous, heterogeneous and enzymatic catalysis for transesterification of high free fatty acid oil (waste cooking oil) to biodiesel: a review. Biotechnol Adv 2010;28:500–18.
[16] Singh AK, Fernando SD, Hernandez R. Base-catalyzed fast transesterification of soybean oil using ultrasonication. Energ Fuel 2007;21:1161–4.
[17] Vyas AP, Verma JL, Subrahmanyam N. A review on FAME production processes. Fuel 2010;89:1–9.
[18] Leonelli C, Mason TJ. Microwave and ultrasonic processing: now a realistic option for industry. Chem Eng Process 2010;49:885–900.
[19] Hingu SM, Gogate PR, Rathod VK. Synthesis of biodiesel from waste cooking oil using sonochemical reactors. Ultrason Sonochem 2010;17:827–32.
[20] Kumar D, Kumar G, Poonam, Singh CP. Fast, easy ethanolysis of coconut oil for biodiesel production assisted by ultrasonication. Ultrason Sonochem 2010;17:555–9.
[21] Salamatinia B, Mootabadi H, Bhatia S, Abdullah AZ. Optimization of ultrasonic-assisted heterogeneous biodiesel production from palm oil: a response surface methodology approach. Fuel Process Technol 2010;91:441–8.
[22] Chimienti ME, Pizzio LR, Cáceres CV, Blanco MN. Tungstophosphoric and tungstosilicic acids on carbon as acidic catalysts. Appl Catal A-Gen 2001;208:7–19.
[23] Ferreira P, Fonseca IM, Ramos AM, Vital J, Castanheiro JE. Acetylation of glycerol over heteropolyacids supported on activated carbon. Catal Commun 2011;12:573–6.
[24] Tropecêlo AI, Casimiro MH, Fonseca IM, Ramos AM, Vital J, Castanheiro JE. Esterification of free fatty acids to biodiesel over heteropolyacids immobilized on mesoporous silica. Appl Catal A-Gen 2010;390:183–9.
[25] Sen R. Response surface optimization of the critical media components for the production of surfactin. J Chem Technol Biot 1997;68:263–70.
[26] Balussu R, Paduru RR, Kuravi SK, Seenayya G, Reddy G. Optimization of critical medium components using response surface methodology for ethanol production from cellulosic biomass by Clostridium thermocellum SS19. Process Biochem 2005;40:3025–30.
[27] Obali Z, Doğu T. Activated carbon—tungstophosphoric acid catalysts for the synthesis of tert-amyl ethyl ether (TAEE). Chem Eng J 2008;138:548–55.
[28] Avramović JM, Stamenković OS, Todorović ZB, Lazić ML, Veljković VB. The optimization of the ultrasound-assisted base-catalyzed sunflower oil methanolysis by a full factorial design. Fuel Process Technol 2010;91:1551–7.
[29] Shu Q, Nawaz Z, Gao J, Liao Y, Zhang Q, Wang D, et al. Synthesis of biodiesel from a model waste oil feedstock using a carbon-based solid acid catalyst: reaction and separation. Bioresour Technol 2010;101:5374–84.
[30] Stavarache C, Vinatoru M, Nishimura R, Maeda Y. Fatty acids methyl esters from vegetable oil by means of ultrasonic energy. Ultrason Sonochem 2005;12:367–72.
[31] Thanh LT, Okitsu K, Sadanaga Y, Takenaka N, Maeda Y, Bandow H. Ultrasound-assisted production of biodiesel fuel from vegetable oils in a small scale circulation process. Bioresour Technol 2010;101:639–45.
[32] Thanh LT, Okitsu K, Sadanaga Y, Takenaka N, Maeda Y, Bandow H. A two-step continuous ultrasound assisted production of biodiesel fuel from waste cooking oils: a practical and economical approach to produce high quality biodiesel fuel. Bioresour Technol 2010;101:5394–401.
[33] Cao F, Chen Y, Zhai F, Li J, Wang J, Wang X, et al. Biodiesel production from high acid value waste frying oil catalyzed by superacid heteropolyacid. Biotechnol Bioeng 2008;101:93–100.
[34] Sunita G, Devassy BM, Vinu A, Sawant DP, Balasubramanian VV, Halligudi SB. Synthesis of biodiesel over zirconia-supported isopoly and heteropoly tungstate catalysts. Catal Commun 2008;9:696–702.
[35] Liu X, He H, Wang Y, Zhu S. Transesterification of soybean oil to biodiesel using SrO as a solid base catalyst. Catal Commun 2007;8:1107–11.
[36] Xie W, Peng H, Chen L. Transesterification of soybean oil catalyzed by potassium loaded on alumina as a solid-base catalyst. Appl Catal A-Gen 2006;300:67–74.
[37] Mootabadi H, Salamatinia B, Bhatia S, Abdullah AZ. Ultrasonic-assisted biodiesel production process from palm oil using alkaline earth metal oxides as the heterogeneous catalysts. Fuel 2010;89:1818–25.
[38] Abdullah AZ, Razali N, Mootabadi H, Salamatinia B. Critical technical areas for future improvement in biodiesel technologies. Environ Res Lett 2007;2.
[39] Sepúlveda JH, Yori JC, Vera CR. Repeated use of supported $H_3PW_{12}O_{40}$ catalysts in the liquid phase esterification of acetic acid with butanol. Appl Catal A-Gen 2005;288:18–24.

Engineering Applications of Nanoscience and Nanomaterials

Edited by
Ajay Bansal and Rajesh J. Tayade

TTP TRANS TECH PUBLICATIONS

Materials Science Forum

ISSN 0255-5476

Founding Editor:
Fred H. Wöhlbier

Editors:
Yu Wing Mai
Graeme E. March

Editorial Advisory Board: *see back inside cover*

Aims and Scope:
Materials Science Forum publishes only complete volumes on given topics, proceedings and complete special topic volumes. Thus, we are not able to publish stand-alone papers.

Materials Science Forum specializes in the rapid publication of international conference proceedings and stand-alone volumes on topics of current interest. It covers all areas of Materials Science, Solid State Physics and Solid State Chemistry. The periodical is covered by SCOPUS and documented by all major abstract sources. It is one of the largest periodicals in its field.

Indexed by Elsevier: SCOPUS www.scopus.com and El Compendex (CPX) www.ei.org/, Cambridge Scientific Abstracts (CSA) www.csa.com, Chemical Abstracts (CA) www.cas.org, Google and Google Scholar google.com, ISI (ISTP, CPCI, Web of Science) www.isinet.com, Institution of Electrical Engineers (IEE) www.iee.org, etc.

Internet:
The periodical is available in full text via www.scientific.net

Subscription Information:
32 volumes per year. In 2013, volumes 729-760 are scheduled to be published.

The subscription rate web access only is EUR 2112.00 per year, for web plus print EUR 2720.00 including postage/handling charges.

ISSN print 0255-5476 ISSN cd 1662-9760 ISSN web 1662-9752

Trans Tech Publications Ltd
Kreuzstr. 10 • 8635 Zurich-Durnten • Switzerland
Fax +41 (44) 922 10 33 • e-mail: ttp@ttp.net
http://www.ttp.net
http://www.scientific.net

Engineering Applications of Nanoscience and Nanomaterials

Edited by
Ajay Bansal
Rajesh J. Tayade

Engineering Applications of Nanoscience and Nanomaterials

Special topic volume with invited peer reviewed papers only

Edited by

Ajay Bansal and Rajesh J. Tayade

Trans Tech Publications Ltd
Kreuzstrasse 10
CH-8635 Durnten-Zurich
Switzerland
http://www.ttp.net

Volume 757 of
Materials Science Forum
ISSN print 0255-5476
ISSN cd 1662-9760
ISSN web 1662-9752

Full text available online at *http://www.scientific.net*

***Distributed** worldwide by*

Trans Tech Publications Ltd
Kreuzstrasse 10
CH-8635 Durnten-Zurich
Switzerland

Fax: +41 (44) 922 10 33
e-mail: sales@ttp.net

and in the Americas by

Trans Tech Publications Inc.
PO Box 699, May Street
Enfield, NH 03748
USA

Phone: +1 (603) 632-7377
Fax: +1 (603) 632-5611
e-mail: sales-usa@ttp.net

printed in Germany

Preface

Nanoscience and nanotechnology are the study and application of extremely small things or materials with typical dimension spans from subnanometer to several hundred nanometer and can be used across all the other science fields, such as chemistry, biology, physics, materials science, and engineering. Nanotechnology is not just a new field of science and engineering, but a new way of understanding the behaviour materials at nanoscale. Nanoscience and nanotechnology involve the ability to see and to control individual atoms and molecules. Everything on Earth is made up of atoms—the food we eat, the clothes we wear, the buildings and houses we live in, and our own bodies. Nanotechnology is serving to improve for the revolution in many technologies and industry sectors such as information technology, energy, environmental science, medicine, food safety, and transportation, among many others. Most benefits of nanotechnology depend on the fact that it is possible to tailor the essential structures of materials at the nanoscale to achieve specific properties, thus greatly extending the well-used toolkits of materials science. Using nanotechnology, materials can effectively be made to be stronger, lighter, more durable, more reactive, more sieve-like, or better electrical conductors, among many other traits. There already exist over 800 everyday commercial products that rely on nanoscale materials and processes.

Till today, the nanoscience and nanotechnology was primarily concerned with electronics, manufacturing, supercomputers, and data storage devices. Recently scientist have broadened the applications of nanotechnology in a number of prominent fields including optoelectronics, biomedical, pharmaceutical, cosmetic agent, sensors, environmental cleanup, energy assisted and catalytic materials. This has increased the interaction between various scientific fields such as electronics, chemistry, physics, biology, material science, medical sciences, and information & communication sciences. All the development in this field is scattered and difficult to get below one umbrella. This has prompted to us to bring all development related to engineering applications of nanoscience and nanotechnology in various specialized fields together in the form of compact data base. This Volume of Materials Science Forum titled "Engineering Applications of Nanoscience and Nanomaterials" reports the latest developments and original applications, and theoretical researches in the area of nanoscience and nanomaterials.

This Special Topic Volume is a result from the contribution of thirty seven experts from the international scientific community in the respective field of research. It thoroughly covers various engineering applications of nanomaterials in various fields such as catalysis, sun protective materials, organic synthesis, sensor, coatings, energy efficient hear transfer, thermoplastics, waste water treatment, electronic component, solid oxide fuel cell, photocatalysis, It gives a

Materials Science Forum Vol. 757 (2013) pp 1-24
© (2013) Trans Tech Publications, Switzerland
doi:10.4028/www.scientific.net/MSF.757.1

Application of Heteropolyacid-Based Heterogeneous Catalysts for Conversion of Oleochemicals into Renewable Fuels and Other Value-Added Products

Ali Sabri Badday, Ahmad Zuhairi Abdullah*, Keat-Teong Lee

School of Chemical Engineering, Universiti Sains Malaysia,

Engineering Campus, 14300 Nibong Tebal, Penang, Malaysia

Tel: +604-599 6411 Fax: +604-594 1013

Email: chzuhairi@eng.usm.my

Keywords: Heteropoly acid; solid catalyst; mesoporous; oleochemical conversion; shape-selective; catalyst stability.

Abstract

Oleochemicals offer viable choices to replace petrochemicals in a wide range of applications such as fuels, lubricants and surfactants. Many of the conversions require the use of suitable solid acids as the catalysts. The chemical and physical properties of the feedstock in oleochemical processes often result in difficulties and challenges that limit the success. Large amount of free fatty acids and high water content create barriers towards the successful use of broad range of oleochemicals as raw materials. To overcome this problem, efforts have been dedicated to the development of new technologies involving new types of catalyst. Solid acid catalysts based on heteropolyacids (HPAs) for various oleochemical conversions especially esterification reaction of fatty acids and transesterification of vegetable oils have been successfully developed. This type of catalyst already secured a tangible success in solving some problems associated with the earlier types of catalyst leading to higher productivity in the process while satisfying the needs of sustainable and environmental friendly industrial processes. Incorporation of HPAs active component into mesoporous supports can produce heterogeneous catalysts with high acid sites dispersion, stability to high temperature, recyclable and they usually demonstrate low leaching of active components in the reaction medium. This article reviews common oleochemical processes where various HPA catalysts already found successful application with some insight into the specific characteristics of the catalysts. Their advantages and drawbacks as well as specific process behaviors in few important oleochemical conversions of industrial importance will be discussed.

1. Introduction

Among various acid catalysts, heteropolyacid-based catalysts received great interest recently for application as either heterogeneous or homogeneous catalysts depending on their composition and the nature of reaction medium [1]. Besides having high water tolerance, heteropolyacids have their inherent advantages like ease of handling and removal, potential for reusability, fewer side reactions, strong Brönsted acidity (approaching the superacid region) as well as high proton mobility and stability [2]. HPAs such as $H_3PW_{12}O_{40}$, $H_4SiW_{12}O_{40}$, $H_3PMo_{12}O_{40}$ and H_4Si- $Mo_{12}O_{40}$ have been successfully used to catalyze a wide range of acid-catalyzed reactions. These include vegetable oil transesterification for biodiesel production and esterification of free fatty acid as the acid sites are more identical and easier to be managed than those in other acid catalysts [3]. Though HPAs can be presented in many structural types, the Keggin type represents the most common form of acid structure for catalytic application in wide range of industrial applications [4].

Chemical industries often rely on renewable resources such as carbohydrate, starch, cellulose, sucrose, proteins, natural oils and fats as the key feed stocks [5]. Oleochemical industry is a field of bioresource industry that involves the use of vegetable oil or fats as the feed stocks for the chemical reaction. Unlike petrochemicals that are derived from a non-renewable source, oleochemicals represent the chemicals that are derived from bio-based and renewable resources. Oleochemical reactions provide great enhancement to the industrial sector on both economical and environmental aspects [6]. Environmentally, the emission of CO_x and NO_x associated with the petroleum based industries creating severe air pollution and green house effects can be avoided. Recently, the world wide concerns have been dedicated to search for the appropriate solutions to these serious issues and oleochemicals provide promising alternatives [7].

Switching from petrochemicals to oleochemicals has been ultimate goal during the earlier decades due to the steady increase in the price of the crude oil and its downstream products [8]. Meanwhile, the world's energy demands still depend extensively on finite fossil resources such as petroleum, coal and natural gases. The accelerated rate of exhaustion of these resources is one of the serious problems facing the mankind [9-10]. As oleochemicals are identified as plausible alternatives to fossil fuels, rapid development in this area has been seen in the last few decades. For the conversions to value-added products, the development of innovative and effective catalysts is deemed indispensable.

2. Oleochemical Reactions of Industrial Importance

One of the common feedstock for oleochemical industry is vegetable oil. The nature of the vegetable oil differs from one source to another. However, they share the same general individual components of free fatty acids and generally contain water in various proportions, depending on the oil source [11]. Oils and fats can be converted to other oleochemicals such as fatty acids and glycerol that, in turn, can be further converted to value-added substances through suitable reactions with other biomaterials. Figure 1 shows some of the established reactions between different oleochemicals and their respective derivatives. The applications that use vegetable oil can be further divided into three branches i.e. vegetable oil transesterification, esterification of free fatty acids and free fatty acids hydrogenation [12].

Fatty acids that exist in the vegetable oil can be classified into two types, saturated and unsaturated fatty acids as shown in Figure 2. Saturated free fatty acids consist of straight organic chains that do not contain any double bonds or other functional groups in the chain. Usually, these fatty acids have higher melting and boiling points and predominantly found in animal fats rather than vegetable oils.

Meanwhile, unsaturated fatty acids possess one or more C=C double bonds that exist in the hydrocarbon chain [13]. Unsaturated fatty acids are not preferred in oleochemical industrial applications as the presence of the double bond will decrease their melting point. Besides that, the unsaturated bonds can reduce the shelf-life and heat stability due to higher susceptibility toward ambient oxidation [12]. Increasing the melting point and improving the quality of the fatty acids can generally be achieved by converting the unsaturated fatty acid to a saturated one using simple hydrogenation process as shown in Figure 3.

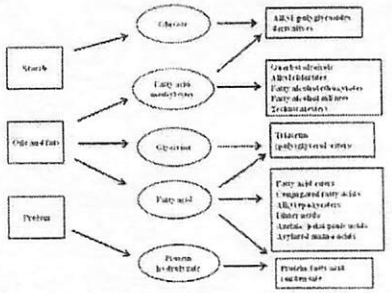

Fig. 1. Important industrial oleochemical processes and their respective derivatives [5].

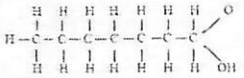

Saturated fatty acid

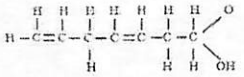

Unsaturated fatty acid

Fig. 2. Typical examples of saturated and unsaturated fatty acids.

$$R1-CH=CH-R2-COOH+H_2 \longrightarrow R1-CH_2-CH_2-R2-COOH$$

Fig. 3. The Hydrogenation of unsaturated fatty acid.

Another application using fatty acids that are derived from vegetable oils is fatty acid esters formation through esterification process with alcohol in the presence of a suitable catalyst. Esterification is slow and reversible reaction at room temperature in which the reactants, alcohol and the fatty acid, will react in the presence of suitable acid catalyst to produce ester and water as the products [14]. Usually, esterification process is carried out in batch mode using homogenous acid catalysts and excess amount of alcohol is needed to shift the equilibrium towards forward reaction forming the desired product. Traditionally, strong Brönsted acids in liquid phase such as sulfuric acid and hydrochloric acid are used to catalyze the reaction [15]. The general representation of an esterification reaction is shown in Figure 4. In this reaction, stronger acid catalysts will lead to higher reaction rate and no issue with respect to product selectivity is generally encountered as a single product is produced. Converting fatty acids to a mixture of fatty acid alkyl esters is one of the basic reactions involved in biodiesel production [14]. Developing alternative energy resources based on vegetable oils through esterification is an important research field to overcome the problem of fossil fuel depletion and for better protection of environment towards polluting emissions associated with fossil fuels [16-17].

$$R-COOH+R^1-OH \longrightarrow R-COO-R^1+H_2O$$

Fig. 4. Esterification of fatty acid with alcohol.

Oleochemical reaction towards renewable biodiesel production through transesterification of vegetable oils is considered as one of the important roles of oleochemistry in the area of alternative energy [16]. Transesterification is the organic reaction involving the exchange of the organic group R^1 of an ester with the organic alkoxy group R^2 of an alcohol. Figure 5 illustrates the general representation of a transesterification reaction [18].

$$R-COO-R^1+R^2-OH \longrightarrow R-COO-R^2+R^1-OH$$

Fig. 5. Transesterification of triglyceride with alcohol.

This reaction can be catalyzed by basic or acidic catalysts. However, basic catalysts can result in higher rate of reaction while acid catalysts are more preferred in the case of significant impurities present in the reactants. Usually, methanol is the most commonly used alcohol for producing biodiesel as it is relatively cheap and has smaller carbon chain. The predominant fatty acids in vegetable oils and animal fats are: palmitic, myristic, stearic, oleic, linoleic, and linolenic as shown in Table 1. However, the specific composition could vary with the variability in the source of the oil or fat.

Mechanism of the transesterification process consists of series consecutive reversible reactions. In this process, the triglyceride (TG) reacts step by step with methanol to form diglyceride (DG), monoglyceride (MG) and finally glycerol while one mole of fatty acid methyl ester (FAME) is generated in each step [19]. Figure 6 shows the representation of this reactions sequence.

Table 1. Typical fatty acid composition of common vegetable oils or animal fat [1].

Name	Structure	Formula	Oil source					
			Palm	Soya bean	Cotton seed	Coconut	Rapeseed	Tallow
Lauric	12:0	$C_{12}H_{24}O_2$	0.1	0.1	0.1	46.5	-	0.1
Myristic	14:0	$C_{14}H_{28}O_2$	1.0	0.1	0.7	19.2	-	0.8
Palmitic	16:0	$C_{16}H_{32}O_2$	42.8	0.2	20.1	9.8	3.5	23.3
Stearic	18:0	$C_{18}H_{36}O_2$	4.5	3.7	2.6	3.0	0.9	19.4
Linoleic	18:1	$C_{18}H_{32}O_2$	40.5	22.8	19.2	6.9	64.1	42.4
Linolenic	18:2	$C_{18}H_{30}O_2$	10.1	53.7	55.2	2.2	22.3	10.7

The reaction is commonly catalyzed by acid catalyst, base catalyst or by enzymatic catalyst (biocatalysts) particularly lipases [20].

$$TG + CH_3OH \underset{k2}{\overset{k1}{\rightleftharpoons}} DG + FAME$$

$$DG + CH_3OH \underset{k4}{\overset{k3}{\rightleftharpoons}} MG + FAME$$

$$MG + CH_3OH \underset{k6}{\overset{k5}{\rightleftharpoons}} GLY + FAME$$

Fig. 6. The sequence of transesterification reaction.

Conventionally, liquid catalysts are used but current researches have been focused towards the use of heterogeneous catalysts due to the potential for catalyst reuse and ease of product separation. Various novel solid acid catalysts have been reported for this application. However, limited success has been achieved due to low porosity of the catalyst while slow diffusion of reactant and/or reaction products within the small internal pores could be the limiting mechanism in the reaction [19]. The overall reaction rate can be improved if the rate of this limiting step can be accelerated with the use of a suitable solid catalyst.

3. Keggin Type of Heteropolyacids

There are about 100 different compositions and structures of heteropolyacids that are recognized so far. The specific structure of the Keggin type of heteropolyacids is usually the main reason that attracts great researchers' interest for use as acid catalysts. This is due to the variation in their oxidizing potential and acidity while showing similarity in catalytic effects either in solution or in solid state [21]. Usually, the Keggin types of heteropolyacids have the general form of $H_{8-x}X_xM_{12}O_{40}$ where X is either Si^{IV}, Ge^{IV}, P^{V}, or As^{V}, while M is either Mo^{VI} or W^{VI}. The Keggin HPAs consist of heteropoly anions of the formula $[XM_{12}O_{40}]^{n-}$ (α-isomer). The structures of the Keggin anions generally comprise of a central tetrahedron XO_4 surrounded by 12 edge- and corner-sharing metal-oxygen octahedrals MO_6 [22] as shown in Figure 7. The relative acid strength of heteropolyacids depends on anionic charge. Generally, as the charge of a conjugate base (here, the heteropolyanion) decreases, its stability increases, which increases the strength of the "conjugate" acid. Thus, in the Keggin family of heteropolyacids, $H_3PW_{12}O_{40}$ forms the strongest acid as the $PW_{12}O_{40}$ anion has the lowest negative charge [23]

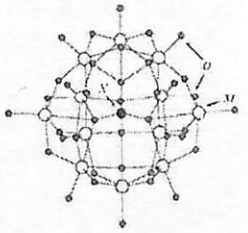

Fig. 7. The General Structure of Keggin Heteropolyacid [22].

Due to their unique physicochemical properties, heteropolyacids have been widely used as acid catalysts in various chemical reactions and oxidation processes [21]. Several successful applications of heteropolyacid catalysts in liquid phase acid reactions such as esterification and alkylation of organic substances are summarized in Table 2. The catalysts could either be unsupported or supported ones. However, due to the non-porous characteristic of heteropolyacids, supported catalysts generally perform better in the reaction. It should be noted that generally support materials with larger pore sizes such as SiO_2, MCM-41 are preferred to facilitate the reactant and/or product diffusion within the internal pores of the catalysts. Accelerated diffusion will result in significant improvement in the reaction rate [10].

Table 2. Different reactions that can be catalyzed by heteropolyacid catalysts.

Reaction	Catalyst	Reference
Esterification of acetic acid with n-octanol	TPA/MCM41	[24]
Esterification of butanol with methanol	$H_6P_2W_{21}O_{71}$, $H_8P_2W_{18}O_{62}$, $H_6As_2W_{21}O_{69}$, $H_3PW_{12}O_{40}$	[21]
Esterification of acetic acid with butanol	$H_3PW_{12}O_{40}$/AT-GMB $H_4SiW_{12}O_{40}$/AT-GMB $H_3PMo_{12}O_{40}$/AT-GMB	[25]
Alkylation o-toluene with 1-octene	$H_3PW_{12}O_{40}$/MCM41 $H_4SiW_{12}O_{40}$/MCM41 $H_3PMo_{12}O_{40}$/MCM41	[26]
Alkylation o-phenol with 1-octene	$H_{14}[NaP_5W_{30}O_{110}]$	[27]
Acetoxylation of camphene with acetic acid	$H_3PW_{12}O_{40}/SiO_2$	[28]

The catalytic activity of TPA/MCM41 in Pechmann, esterification and Friedel–Crafts acylation reactions was significantly high thus the catalyst is potentially promising for acid-catalyzed organic transformations in environmentally friendly processes [24]. Meanwhile HPA supported by AT-GMB acted as efficient stable solid acid catalyst for esterification of acetic acid with butanol producing their corresponding esters [25]. 100% conversion of 1-octene was nearly achieved in the reaction conditions explored by using HPA/MCM41. Supported catalysts presented better performance as compared to bulk HPA. This can be attributed to the difference of surface area of bulk HPA and supported catalysts [26]. On the other hand, Long-term activity and high reusability potential was noticed by testing $H_{14}[NaP_5W_{30}O_{110}]$ in alkylation of phenol with 1-octene [27]. HPAs based catalysts seems to be promising and effective materials for wide range of acid catalyzed reactions showing good reaction activity and adorable reusability potential.

4. Heteropolyacid for Esterification Reaction

It is known that esterification reactions of industrial importance are commonly catalyzed by homogenous acid catalysts. The drawback of such homogeneous process is the mineral acids used in liquid form are highly corrosive and excess acid should be neutralized after the reaction. The naturalization using basic materials creates large amount of salts to be disposed off into the environment [29]. For that reason, research focuses are currently on shifting towards heterogeneous acid catalysts to replace the conventional homogenous ones. The use of solid acid catalysts such as ion-exchange resins [30], zeolites [31], carbon-based materials [32] and heteropolyacids [14] have been reported to catalyze the reaction. Unlike homogenous catalysts which usually not environmentally friendly and corrosive, these types of acid catalysts keep the conversion efficiency at ratios as closer as possible to the ones observed in homogeneous catalysts [14]. Heterogeneity of these catalysts enables easy separation from the products by filtration process and therefore, the undesirable catalyst naturalization step from the product mixture is eliminated [33].

The use of Keggin types of heteropolyacids as acid catalysts for esterification reaction has some drawbacks due to their high solubility in polar media and low surface area [34]. To overcome these disadvantages, supported catalysts based on HPAs can be synthesized. Mainly due to its high acidity, earlier works on supported heteropolyacid catalysts have been demonstrated using 12-

tungstophosphoric acid (TPA) for the preparation of the heterogeneous catalysts to be used in esterification reaction. Zirconia was chosen as the catalyst support to TPA and the supported catalyst successfully kept its catalytic activity in the esterification [14]. The reaction studied was oleic acid esterification with ethanol as a model reaction to produce long chain esters. Different levels (5, 10, 15, 20, 25, 40 and 60 wt %) of TPA loaded on zirconia were investigated for possible effect on the esterification. The thermal test on the supported catalyst revealed that no Keggin structure loss occurred upon heating up to 500 °C. The reusability tests for the spent catalyst showed that after the treatment, the catalyst still recorded conversion values as high as 70 %. These results provided some evidences on the high activity and stability of supported heteropolyacid in the reaction.

Other innovative support materials was used to synthesize TPA-based mesoporous catalyst by Brahmkhatri and Patel [35]. They used mesoporous silica (SBA-15) to anchor the heteropolyacid used for esterification of oleic acid with methanol. They detected the interaction between surface silanol (Si-OH) in the SBA-15 with the heteropolyacid that led to better immobilization of the active component. The interaction between HPA and SBA-15 support is schematically shown in Figure 8. They also demonstrated the effects of various reaction parameters on the fatty acid methyl ester yield in the transesterification of waste cooking oil. Generally, sufficiently high catalytic activity was demonstrated by the catalyst. Their study also included the reusability test for the catalyst and reaction kinetics. Kinetic analysis revealed that esterification reaction of oleic acid with methanol followed a first order dependence on oleic acid concentration.

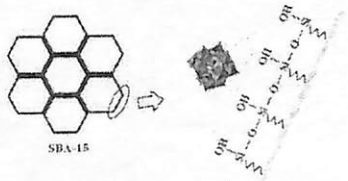

Fig. 8. Interaction between TPA and SBA-15 support [35].

SBA-15 was also chosen as a support material for other types of HPAs in a study performed Tropecelo et al. [36]. In that study, esterification reactions of palmitic acid with methanol catalyzed by tungstophosphoric acid (TPA), molybdophosphoric acid (PMo) and tungstosilicic acid (SiW) catalysts immobilized on SBA-15 were investigated. The results revealed that the activities of the catalysts were in the sequence of TPA-SBA-15 > SiW-SBA-15 > PMo-SBA-15. Optimization of the reaction conditions by the TPA-SBA-15 catalyst was then carried out and leaching of the active component from the support was also investigated. Minimal leaching of acidic active components was detected after the reaction due to good stability of the catalyst towards polar media. The use of ethanol for esterification of palmitic acid at 60 °C led to lower conversion compared to that achieved with methanol. They attributed the result to the slower reaction rate of ethanol at this temperature since the ethyl nucleophile is less reactive than methyl nucleophile. Higher palmitic acid conversion was achieved when the reaction temperature was increased to 80 °C. Thus, forward

reaction was accelerated at higher temperature. In this case, higher temperature caused a decrease in the viscosity of fatty acids to allow faster diffusion within the internal pores of the catalyst. Internal diffusion has been suggested as the rate limiting step in the reaction [14-15].

Sol-gel technique for immobilizing tungstophosphoric acid, molibdophosphoric acid and tungstosilicic acid on silica was used by Caetano et al. [15]. The synthesized catalysts used for esterification of palmitic acid with methanol and the same activity sequence i.e. TPA-silica > SiW-silica > PMo-silica was obtained. This result clearly suggested that tungstophosphoric acid was the relatively stronger acid catalyst. The most active catalyst was then used for stability test by performing consecutive batch runs with the same catalyst sample and minimum drop in the activity was observed in the second run. The heteropolyacid lixiviation was also investigated and the results showed that the reaction only occurred in the heterogeneous phase and only 4 % of the catalyst active component was lixiviated after the fourth run. This result suggested the stability of the supported heteropolyacid catalyst in this oleochemical reaction. They also used the catalyst for esterification of other types of fatty acids such as oleic and stearic acid and it showed sufficiently good catalytic activity.

A viable option for preparing partially and fully proton-exchanged catalysts for esterification of palmitic acid has been attempted by Giri et al. [29]. Tungstophosphoric acid, which is soluble in water and polar solvents, was converted to its salt by exchanging the protons with ammonium ions having the general formula of $[(NH_4)_xH_{3-x}PW_{12}O_{40}]$. The comparison between the activities of the partially and fully proton-exchanged catalysts showed that partially proton-exchanged catalyst had higher acidic strength than fully exchanged ammonium salt leading to a better catalytic activity.

A sol-gel hydrothermal method was used by Xu et al. [37] to synthesize mesoporous polyoxometalate tantalum pentoxide composite solid acid catalyst ($H_3PW_{12}O_{40}/Ta_2O_5$). The prepared catalyst was then used for esterification reaction of lauric acid. The catalyst reusability and leaching test proved that only heterogeneous reaction occurred and virtually no catalyst leaching was detected. Upon regeneration of the catalyst by boiling in ethanol and washing with hexane overnight, 95.6–94.8 % ester yields were still achievable. Therefore, the catalyst reusability potential was confirmed.

The optimum reaction conditions and the performance achieved in the presence of specific HPA-based catalysts for several oleochemical esterification reactions are tabulated in Table 3. Among the HPAs studied, tungstophosphoric acid showed the higher esterification activity for wide range of fatty acids. Either immobilized over different supports or converted to its salt, this Keggin type of HPAs demonstrated the highest catalytic activity because it is the strongest acid among the Keggin series of heteropolyacids. For all the reactions, moderate to high reaction temperatures were recorded to achieve high reaction rate. It can be seen that esterification of palmitic acid requires relatively higher reactant molar ratio and reaction time compared to other fatty acids. This was associated with the saturation of the molecule leading to relatively higher melting point and viscosity under similar conditions than other fatty acids. These two properties are directly involved in influencing on the diffusion rate within the internal pores of the catalysts.

5. HPA Catalysts for Transesterification of Vegetable Oil

Transesterification of vegetable oils or animal fats is one of the most successful methods for biofuel production [16]. The main product is a mixture of fatty acid methyl esters (FAME) better known as biodiesel. The composition of FAME is influenced by the type of oil/fat used as the feedstock. Conventionally, homogenous base catalysts such as KOH and NaOH are used to catalyze the reaction due to high reaction rate and low reaction temperature requirement [38-39]. However, this type of catalyst has a great limitation to be successfully used with wide range of feedstock. As the content of free fatty acids (FFA) in the vegetable oil or animal fat usually exceeds 1 %, a side reaction will consume the catalyst forming metal soap as shown in Figure 9.

Table 3 Reaction Conditions of Different Esterification Reactions.

Reactants	Catalyst	Optimum conditions				Conversion %	Ref.
		Acid: alcohol ratio	Temp. [°C]	Catalyst wt. %	Time [h]		
Oleic acid with ethanol	$H_3PW_{12}O_{40}$/ ZrO_2	1:6	100	20	4	88	[14]
Oleic acid with methanol	$H_3PW_{12}O_{40}$/ SBA-15	1:40	40	23	4	90	[35]
Palmitic acid with methanol	$H_3PW_{12}O_{40}$/ SBA-15	1:98	60	7.3	4	96	[36]
Palmitic acid with methanol	$H_3PW_{12}O_{40}$/ SiO_2	-	60	4.2	30	100	[15]
Palmitic acid with methanol	Ammonium salt of $H_3PW_{12}O_{40}$	-	-	-	8	> 90	[29]
Lauric acid with ethanol	$H_3PW_{12}O_{40}$/ Ta_2O_5	1:7	~ 78	-	3	99.9	[37]

Besides that, the side reaction will negatively affect the production yield and creates difficulties during the separation of the product from the glycerin layer [16].

$$\underset{\text{FFA}}{\text{R-COOH}} + \underset{\text{Catalyst}}{\text{KOH}} \longrightarrow \underset{\text{Soap}}{\text{R-COOK}} + H_2O$$

Fig. 9. Soap formation by the reaction between basic catalyst and free fatty acid.

Edible oils such as palm oil, rapeseed oil, sunflower oil, and soybean oil have all become major feedstocks for biodiesel production. However, there are serious concerns regarding the use of edible oil in biodiesel. While priority is on edible purposes, the higher prices of these oils can negatively affect the biofuel industry. The cost of the feedstock can contribute about 60–80 % of the whole production costs [40]. Thus, the stability of the catalyst against a wide range of low grade oils including crude oils, used cooking oils and waste oils promises a great advantage to the overall process economy. If that objective can be achieved, future feedstock for biodiesel would mainly be the low grade vegetable oils rather than virgin oils which are competing with edible purposes.

In recent years, researchers' efforts have been shifted towards developing sustainable solid acid catalysts for transesterification reaction that have no sensitivity towards FFA in the feedstock and subsequently easy to be separated from the reaction products. Solid acid catalysts such as ZrO_2 [41], sulfonic acid-functionalized silica [42], carbon-based solid acid catalyst [43] and HPAs [44] have been successfully used in transesterification reaction of different triglyceride sources. Besides its great water tolerance and insensitivity towards FFA, HPAs possess strong Brönsted acidity and high proton mobility [2]. Transesterification of rapeseed oil with methanol and ethanol using Keggin type of HPA as the acid catalyst has been studied by Morin et al. [44]. Comparison between activities of HPAs with other mineral acids such as sulfuric acid and phosphoric acid showed higher activities for HPAs attributed to their higher acid strength. By comparing the activities of different Keggin type HPAs, the strength of the acids arranged as TPA > SiW > PMo > SiMo had been concluded.

An investigation to show the activity of tungstophosphoric acid in transesterification involving high free fatty acids and high water content has been carried out by Coa et al. [45]. The catalyst was used in two separated reactions, esterification of long-chain palmitic acid and transesterification of waste cooking oil with methanol. The results showed high activity in both reactions with great water tolerance and insensitivity towards the FFA. HPA-based catalysts for transesterification reactions can be classified into two groups, supported HPAs catalysts and HPAs salts catalysts as discussed in the following sections.

5.1. Supported HPA Catalysts

The solubility problem and low surface area of the HPAs (1-5 m^2/g) [34] are the main reasons for the immobilization of the active acidic component on appropriate porous support material. The supported catalyst should offer the stability of a heterogeneous catalyst while providing the suitable surface area for the active components. The catalyst should also promote the reaction with the same activity of homogenous catalysts [46]. The surface areas of various supported HPAs on different supports are shown in Table 4. It is noted that the surface areas for all the supported catalysts were dramatically increased providing a sufficient area for the reactants during the reaction. Besides that, immobilizing HPAs on materials that resist solubility in polar reaction media provides a great enhancement on the catalyst stability.

Transesterification of sunflower oil with methanol catalyzed by zirconia-supported isopoly and heteropoly tungstate to produce fatty acid methyl esters has been investigated by Sunita et al. [47]. The supported isopoly tungstate was synthesized by impregnating ammonium metatungstate on zirconium oxyhydroxide. Meanwhile zirconia-supported heteropolyacid was prepared through impregnation of tungstophosphoric acid (TPA) and tungstosilicic acid (SiW) on zirconium oxyhydroxide. The results showed that zirconia-supported isopoly tungstate was more active than zirconia-supported HPA in the transesterification. The characterization tests for both types of catalysts showed that zirconia-supported tungstophosphoric acid had the highest total acidity while zirconia-supported isopoly tungstate had the highest Brönsted acidity causing higher reaction conversion. They reported that the catalyst was also effective in producing biodiesel from various types of feedstock such as mustard oil and sesame oil and it could be regenerated without significant loss of its activity.

Table 4. Surface Areas for Different Supported Catalysts Based on HPA.

Reaction	HPA % (w/w support)	Supported catalyst	Surface area [m^2/g]	Ref
Esterification	20	$H_3PW_{12}O_{40}/ZrO_2$	9	[14]
Esterification	2.5[a]	$H_3PW_{12}O_{40}/SiO_2$	489	[15]
	5.7[a]	$H_4SiW_{12}O_{40}/SiO_2$	332	
	3.7[a]	$H_3PMo_{12}O_{40}/SiO_2$	478	
Esterification	30	$H_3PW_{12}O_{40}$/SBA-15	714	[35]
Esterification	7.3[a]	$H_3PW_{12}O_{40}$/SBA-15	754	[36]
Transesterification	15	$H_4SiW_{12}O_{40}/ZrO_2$	55	[47]
	15	$H_3PW_{12}O_{40}/ZrO_2$	53	
Transesterification	10	$H_3PW_{12}O_{40}$/K10	195	[48]

[a]HPA loading determined by ICP analysis.

Identifying the most suitable catalyst support for HPAs used in biodiesel production among clay (K-10), activated carbon, ZSM-5, H-beta and TS-1 has been attempted by Bokade and Yadav [48]. They reported that despite having lower porosity, clay (K-10) was the best support for transesterification of sunflower oil with methanol and subsequently, they modified the layered material by loading it with different types of HPAs. The most successful clay catalyst (10%TPA/Clay) was then used for transesterification of refined, crude and used vegetable oils (edible and non-edible) containing higher than 5–6 % free fatty acids. They reported that the catalyst was stable and tolerant to free fatty acid in the transesterification process.

Transesterification between triolein and ethanol to produce ethyloleate using $H_4PNbW_{11}O_{40}/WO_3$–Nb_2O_5 as the heterogeneous catalyst was carried out by Katada et al. [49]. The comparison was conducted between this type and other HPAs such as $H_3PW_{12}O_{40}$, $H_4SiW_{12}O_{40}$, $H_4SiMo_{12}O_{40}$ and a cesium salt ($Cs_{2.5}H_{0.5}PW_{12}O_{40}$) showed insolubility of the catalysts in the reaction media and good reaction yield. The optimum reaction conditions of transesterification reactions using few reported supported catalysts are summarized in Table 5. It can be concluded that low catalysts activities generally lead to higher reaction time, high catalyst loading and high reaction temperature to reach high conversion. High reaction temperatures were required to reduce the fatty acids viscosities improving the internal diffusion into the internal pores of the solid catalysts. High oil to alcohol ratio could also be needed to shift the equilibrium towards forward reaction.

5.2. HPAs Salt Catalysts

Partial substitution of H^+ in HPA with alkaline cations is considered as an appropriate technique to create major effects on the surface area, pore structure, solubility and hydrophobicity, and other properties of the parent HPA [50]. Reducing the solubility of a catalyst in water and other polar solvents will improve its resistant towards deactivation.

Table 5. Typical Reaction Conditions of Several Transesterification Processes.

Reactants	Catalyst	HPA loading (% w/w support)	Reaction conditions				Conversion (%)	Ref
			Oil:alcohol ratio	Temp. (°C)	Catalyst % (w/woil)	Time (h)		
Sunflower oil with methanol	$H_3PW_{12}O_{40}/ZrO_2$	15	1:15	260	3	5	97	[47]
Sunflower oil with methanol	$H_3PW_{12}O_{40}$/K10	10	1:15	170	5	8	86	[48]
Triolein with ethanol	$H_4PNbW_{11}O_{40}/WO_3$–Nb_2O_5	40	1:15	100	11	8	81	[49]

This will lead to an improvement in its recycle potential and significantly contribute to achieve the objective of an eco-friendly process [51]. HPAs salts with large monovalent ions such as Cs^+, NH_4^+ and Ag^+ have attracted the interest due to dramatic increases in surface area and changes in solubility over the original HPAs [3]. Partial substitution of protons by these cations can also result in the increase in the number of available surface acidic sites [50].

A cesium salt $Cs_{2.5}H_{0.5}PW_{12}O_{40}$ was used for biodiesel production through transesterification of Eruca sativa gars (ESG) oil with methanol by Chai et al. [2]. A study on the optimum reaction conditions and an investigation on the effects of increasing FFA and water content in the feed stock were also conducted. The results showed that the catalyst was insensitive to FFA for up to 10 % w/w oil achieving a maximum biodiesel yield of 99 % from the low grade and cheap non-edible oil. Cs-exchanged silicotungstic acid catalysts with a general formula of $Cs_xH_{4-x}SiW_{12}O_{40}$ were synthesized and tested by Pesaresi et al. [52] for palmitic acid esterification with methanol as well as C_4 and C_8 triglyceride transesterification to produce biodiesel. A series of Cs doped $H_4SiW_{12}O_{40}$ catalysts had been synthesized and the results revealed that Cs substitution promoted recrystallisation of the original $H_4SiW_{12}O_{40}$ polyoxometallate. The maximum mesopore volume was obtained with the material containing 2.8 Cs atoms per Keggin unit. They also reported that the catalyst was active towards both triglyceride transesterification and FFA esterification. The reactivity was found to be directly related to the number of accessible H^+ sites that presented within the mesopores [26].

Narasimharao et al. [53] synthesized a family of insoluble tungstophosphoric acid ($H_3PW_{12}O_{40}$) salts $Cs_xH_{3-x}PW_{12}O_{40}$ (x=0.9–3) for tributyrin transesterification and palmitic acid esterification. The highest catalytic activity was achieved with x values between 2.0–2.3 and it was correlated with the accessibility of surface acid sites by the reactants. The proposed structural model for $Cs_2PW_{12}O_{40}$ is shown in Figure 10. The catalysts were also found to be suitable for esterification and transesterification reactions simultaneously with up to 100 % conversion of palmitic acid and up to 52 % conversion of tributyrin. A study on reusability of the catalyst revealed their high resistant to leaching and they could also be recycled without significant loss in activity.

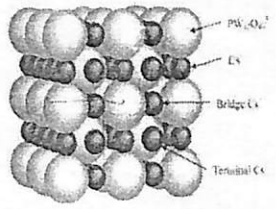

Fig. 10. Structural Model of Cs Heteropolyacid Salt [53]

Silver salts of tungstophosphoric acid were prepared and tested for the conversion of triglycerides with methanol under mild conditions by Zieba et al. [54]. Methanolysis of natural oils, such as triacetin and castor oil catalyzed by $H_3PW_{12}O_{40}$ and its silver salts $Ag_xH_{3-x}PW_{12}O_{40}$ with various Ag contents (x=0.5 up to 3) has been investigated. It was concluded that for Ag contents with x values lower than 1, the catalysts were partially soluble in the reaction media. Thus, it resulted in homogeneous rather than heterogeneous mode of reaction due to HPA leaching and dissolved into the methanol phase. For x values higher than 1, the presence of homogenous catalysts in the reaction media was not detected. After the reaction, the catalysts were also found to be in colloidal dispersion that made it hard to be separated from the reaction mixture. Therefore, they recommended the dispersion of the salts on appropriate support materials.

The optimum reaction conditions identified in different transesterification catalyzed by HPA salts are shown in Table 6. It can be concluded that HPA salts generally act as active catalysts for both the transesterification and esterification of vegetable oils to produce biodiesel. Low reaction temperature and short reaction time as compared to those with immobilized form of HPA revealed the enhancement of the process conditions. The catalysts also showed great water and FFA tolerance that will enable the biodiesel industry to use cheap and readily available feed stocks. This will improve the overall economy of the production process. Besides that, the elimination of vegetable oil treatment and ease of catalyst separation after the process will significantly reduce the cost and energy requirement supporting the whole production process.

6. Heteropolyacids Leaching and Reusability

As discussed earlier, solid acid (heterogeneous) catalysts have a unique advantage in esterification and transesterification reactions which enhances the use of high acid value oil as feedstock for oleochemical reactions. Deactivation with time is the main factor that governs the reuse of the solid catalyst which is attributed to many possible phenomena, such as leaching, sintering, and poisoning [1]. Poisoning of the catalyst is usually evident when the process involves used oils that contain impurities. Catalyst leaching is the most general and dramatic problem which not only can increase the operational cost as a result of replacing the catalyst but also leads to product contamination.

Table 6. Reaction Conditions of Several Transesterification Processes Using HPA Salts as Catalysts.

Reactant	Catalyst	Reaction conditions				Conversion (%)	Ref.
		Oil:alcohol ratio	Temp. (°C)	Catalyst (wt. %)	Time (h)		
ESG oil with methanol	$Cs_{2.5}H_{0.5}PW_{12}O_{40}$	1:5.3	55	0.185	0.75	99	[2]
Tributyrin with methanol	$Cs_{2.5}H_{0.5}PW_{12}O_{40}$	-	60	-	6	50.2	[53]
Castor oil or triacetin with methanol	Ag salt of $H_3PW_{12}O_{40}$	1:29	60	8.3	3	~80	[54]

In particular, the use of robust materials able to resist attrition is essential. Furthermore, enhancing the interaction between the active phase and the support is an important consideration. This enhancement can be obtained by tuning the parameters of catalyst preparation [55]. However, the catalyst can undergo deactivation in most of oleochemical reactions and has to be reactivated by calcination or dosing with compounds. Even after reactivation, there is a limited runs for which a catalyst can work after which it has to be discarded [56]. Testing of the heteropolyacids leaching in esterification of palmatic oil has been conducted by Caetano et al. [15]. Sol–gel technique was used to immobilize Tungstophosphoric acid (TPA), molibdophosphoric acid (PMo), and tungstosilicic acid (SiW) on silica. The leaching of the catalysts was examined by centrifuging the catalyst that was dissolved previously in methanol for 72 h and then adding the methanol to palmitic acid. They reported that negligible conversion of the reaction confirmed the heterogeneous nature of the catalyst. Only 3% loss of the TPA from the silica support was measured by ICP after the methanol contact proved that homogenous nature have no potential to carry on the reaction.

Catalyst stability and reusability have been studied for tungstophosphoric acid immobilized by SBA-15 used in esterification of palmitic acid with methanol by Tropecêlo et. al. [36]. The catalyst was filtered after the reaction and soaked in hexane overnight to remove esters that presented on the surface followed by drying over night prior to reuse. They attributed the decrement in activity to the leaching and the loss of the fine particles of the catalyst during filtration. This loss of activity was also noticed due to the presence of water produced by esterification on the catalyst. Hot-filtration experiment was carried out to test the catalyst leaching by contacting the catalyst with methanol under stirring for 48 h. The catalyst was centrifuged and the palmatic acid was added to the spent methanol. The comparsion of the activites of the catalyzed reactions and leaching reaction suggested that heteropolyacid leaching from SBA-15 to the reaction mixture seemed to be small.

The leaching of $PW_{12}O_{40}^{3-}$ heteropoly anion from CsPW and supported TPA catalysts into methanol and water upon reflux was determined using UV-vis spectroscopy in the work of Alsalme et. al [57]. Cs salt form and supported forms of HPAs were used for esterification of hexanoic acid and transesterification of ethyl propanoate and ethyl hexanoate with methanol. For immobilized TPA forms, it was found that leaching in water was larger than leaching in methanol due to the higher reflux temperature and greater solubilisation power of water. While CsPW was found to be the most stable catalyst towards leaching upon reflux in methanol or water. They recorded that for the

supported TPA catalysts, aging and calcinations temperature as well as support surface area caused a profound effect on the TPA leaching. For silver doped heteropolyacid ($Ag_xH_{3-x}PW_{12}O_{40}$), Ziebacl al. [54] noticed that a catalyst loading up to x=1 showed leaching of the catalyst causing homogeneous pathway reaction. Meanwhile x > 1 resulted in lowering the homogeneous nature and occurrence of heterogeneous pathway in the transesterification of triglycerides with methanol.

It can be concluded that partially exchanging Cs^+,Ag^+cations for protons in 12-tungstophosphoric acid converts a polar-soluble low-surface area (<5m^2/g) HPA into a polar-insoluble acid salt consist of microprticles with a surface area (>100 m^2 /g) [53]. The small particles that formed were the reason for large surface area that was observed. In the other hand, dispersion of HPA on the surface of support material created a stable catalyst toward losing the activity by leaching of the active phase in the polar media and increased the available surface area of the reactants.

7. Experimental Section

7.1 Reagents and Materials

Tungstophosphoric acid ($H_3PW_{12}O_{40}.nH_2O$), abbreviated as TPA in this main script, used as active component was purchased from Merck (Malysia). Activated carbon (AC) support was purchased from Galcon Carbon Corporation (USA) while gamma alumina support was purchased from Merck (Malaysia). AC was first grounded to a mean particle size of 250-500 µm. Crude Jatropha oil, the source of triglyceride, was supplied by Telaga Madu Resources (Malaysia). The properties of the crude Jatropha oil, FFA content and water content are tabulated in Table. 7. Methanol used in the transesterification reaction was supplied by Thermo Fisher Scientific Inc. (USA). Ethanol (for catalyst preparation) and n-hexane (for product analysis) were purchased from Merck (Malaysia). Meanwhile, reference FAME standards were supplied by NuChek Prep. Inc. (Australia).

Table. 7 Jatropha oil properties.

Property	Value
Density (kg/m^3)	921
Viscosity (cSt)	38.12
Molecular weight	870
Water content (w %)	0.161
FFA content (w %)	10.5

7.1.1. Catalysts synthesis

In order to prepare the activated carbon supported catalyst, support pretreatment was conducted by washing with a solution of 0.1 M NaOH, followed by washing with 0.1M HCl solution to remove soluble alkaline and acidic impurities from AC [58]. The supported catalysts were synthesized by dissolving the desired amounts of TPA in (50:50 v/v) deionized water and ethanol solution. Wet impregnation method was adopted by contacting the support with the solution (4 ml/g support) for 72 h under constant shacking. After the contact time, the excess solution was removed by rotary evaporation and the catalyst was washed excessively with deionized water followed by drying over night. The dry catalyst was calcined at 453 K [59] in a flow of air for 4 h.

The alumina supported catalysts were synthesized by wet impregnation method by contacting the support with TPA solution for 20 h under constant stirring. After the contact time, excess solution was removed by rotary evaporation and the catalyst was washed excessively with deionized water followed by drying for 2 h. The dry catalysts were then calcined at 400 ^{0}C in a flow of air for 4 h.

7.1.2. Experimental Setup

Experimental runs were conducted in a three-neck glass batch reactor placed in a water bath to adjust the temperature. The reaction temperature was controlled and monitored through thermocouple thermometer while a condenser was attached to the reactor to regulate the evaporated methanol and condense it back to the reaction vessel. Ultrasonic energy was used to accelerate the reaction and it was supplied by means of an ultrasonic processor with a probe type transducer. The ultrasonic energy was supplied using a Bransen (USA) ultrasonic processor capable to generate a frequency of 20 kHz with a highest power of 400 W.

In a typical experimental run, the desired amount of oil was transferred to the reactor and placed in the water path until it reached to the reaction temperature. Then, the required pre-heated amount of methanol was added to the oil according to molar ratio 20:1 followed by the desired amount of the catalyst (4% wt/ wt oil). At this point, ultrasonification was started and the condenser turned on to recover the evaporated methanol. The ultrasonic energy was supplied in a discrete pattern of 10 s on and 3 s off with ultrasonic amplitude of 75 % of the maximum power. After the desired reaction time (60 min), the reaction mixture was quenched and the excess methanol was distilled out. The reaction mixture was then separated into two layers by centrifugation in an Eppendorf centrifuge at 3,000 rpm for 20 min. The upper layer, FAME layer, was collected for the chromatographic analysis.

Blank experiments were carried out in the absence of catalyst or ultrasonic irradiation. The absence of catalyst was tested by conducting the same reaction conditions in the absence of the catalyst. The same conditions were tested in the presence of activated carbon and alumina with 0 % TPA loading. The experiment with zero ultrasonic amplitude (mechanical stirring) was also tested under the same reaction conditions in the presence of the catalysts. Testing the effects of water content in Jatropha oil was carried out by adding the desired amount of water to the oil according to the weight ratio (1 %, 2 %, 3 %, 4 % w H_2O/w oil). While the testing of FFA effects was conducting by adding solid Jatropha oil FFA to the desired amount of oil under heating and continuous stirring. For all experiments, the water bath temperature was fixed at 55 °C yet the heat generated by the ultrasonic probe combined with the heat gained from the water bath successfully kept the reaction temperature at 65 ± 1 °C.

7.1.3. Product Analysis

A gas chromatograph (Agilent tech 7890 A GC systems) equipped with a capillary column (Agilent Technologies, Inc. 19091 J-413 hp-5) with dimensions 30 m × 0.32 mm × 0.25 µm. The system was equipped with a flame ionization detector (FID) and helium was used as carrier gas. The GC was run by auto injection mode and controlled by PC. The analysis of biodiesel for each reaction mixture was carried out by dissolving the product sample in n-hexane hexane according to the desired dilution factor and sample of 1 µl of the mixture was injected to the GC in each analysis.

7.1.4. Catalysts Characterization

The external properties of activated carbon, gamma alumina and the prepared catalysts were examined by nitrogen adsorption isotherm at -197 °C using micrometrics ASAP 2020 surface area instrument. The surface acidity of the supports and the immobilized catalysts was conducted by manual gravimetric determination of acid-base titration [60]. It can be concluded from the results tabulated in Table. 8 that the surface area for both supports decreased with the increasing of TPA content in the catalyst while the surface acidity increased as the presence of TPA increased. This can be resulted by the increment of the strong acid sites attached to support surface leading to increasing in the catalytic activity of the catalysts. The reduction in BET surface area, total pore volume and pore diameter for the catalysts can be resulted by the blockage of pores by active species. The behavior of the reduction of surface area and the pores was also noticed in the work of Oball et. al [59] for TPA supported by activated carbon catalyst and Hernández-Cortez et al. [61] for TPA supported by alumina catalyst.

Table 8. Physical properties of Al and the TPA catalysts.

Sample	BET Surface area (m^2/g)	Total pore volume (cm^3/g)	Average pore diameter (Å)	Surface Acidity (μmol/g catalyst)
AC	750	0.47	25.23	520
TPA15-AC	651	0.41	25	1530
TPA20-AC	621	0.39	25	1570
TPA25-AC	612	0.38	24.9	1690
Al	109.4	0.23	82.6	900
TPA25-Al	93.3	0.13	54.9	1300
TPA30-Al	83.4	0.10	52.0	1490
TPA35-Al	71.9	0.09	49.8	1570

8. Results and discussion

8.1 Results of blank experiment

The results of blank experimental runs revealed that the significant transesterification reaction did not occur with the presence of AC, Al only or without the catalyst (the reactants alone) as it can be seen in Fig. 11 and 12. This was mainly due to the absence of acid active sites to catalyze the reaction. Conducting the reaction with zero ultrasonic amplitude (mechanical stirring) also resulted in no significant reaction due to the insufficient reaction time.

8.2 Effects of Catalyst Loading

The results of catalytic experiments for FAME production yield with the presence of different catalyst loading are presenting in Fig. 11 for activated carbon and Fig. 12 for alumina. It can be concluded from Fig. 11 that the reaction yield increased as the TPA content in the catalyst increased reaching maximum value with TPA20-AC while the catalyst with higher TPA amount slightly decreased the yield. The same behavior can be noticed for TPA loading on alumina represented by the maximum reaction yield achieved for TPA25-Al catalyst. The behavior of the catalysts with the

presence of low TPA loading on the support can be explained by the insufficient active sites presented on the catalyst surface to promote the reactants and derive the forward reaction to took place. For both catalysts, high amount of TPA led to slightly decrease in the reaction yields due to the reduction in the catalysts surface areas. This behavior caused by the blockage of the catalyst pores by the active sites led to internal diffusion limitation towards the reactants. Low accessibility of the reactants to the active sites resulted on negative effects on the reaction yield.

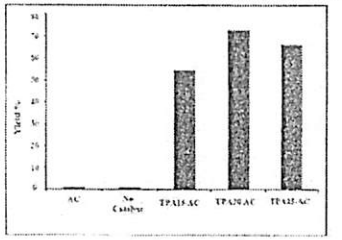

Figure 11. Transesterification of Jatropha oil by Ultrasonic-assisted Process over TPA Immobilized on AC (Reaction Time 60 min, Methanol/oil Molar Ratio 20:1, Catalyst Amount 4% (w/w), and Ultrasonic Power 75%).

Comparing the activity of the optimum catalyst loadings revealed that immobilization of TPA on activated carbon resulted in higher production yield of 73 % than 64.3% reaction yield achieved by TPA supported by alumina. Besides that, the percentage of TPA % in the carbon based catalysts was less than that for alumina catalyst leading to better catalytic activity. This can be attributed to high surface area available for the reactants provided by the high porous activated carbon and the high surface acidity of TPA20-AC compared with TPA25-Al acidity.

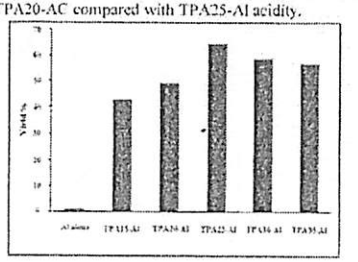

Figure 12. Transesterification of Jatropha oil through an ultrasonic-assisted process over TPA immobilized on alumina (reaction time 60 min, methanol/oil molar ratio 20:1, catalyst amount 4% (w/w), and ultrasonic power 75%).

8.3 Effect of Water and FFA Content in the Feed Stock

The effect of water content in the feedstock on the reaction yield for TPA20-AC and TPA25-Al can be seen in Fig. 13. It can be concluded that the alumina based catalyst showed less sensitivity to the presence of water in the oil while the reaction yield decreased sharply beyond 1% water content for

TPA20-AC. This reduction in the reaction yield can be attributed to the hydration effects of water on the active sites of the catalyst. The presence of large amount of water affected negatively the strength of Brönsted acid sites presented in the catalyst and led to a reduction in the catalytic activity. Nakajima et al. [62] reported the same behavior of carbon based acid catalyst in the presence of high water content. Alumina catalyst showed more tolerance in high water content system than that for carbon catalyst due to the higher number of active sites presented in the catalyst that reduced the effects of sites hydration.

The effect of FFA % content in the crude vegetable oil on the reaction yield is presented in Fig. 14 for TPA20-AC and TPA25-Al catalysts. It can be concluded that both catalysts were insensitive to the presence of FFA. Beyond 17.5 FFA %, slight reductions in the reaction yields for both of catalysts were noticed. This can be attributed to the effect of high amount of water generated during the esterification reaction due to the high FFA content. The presence of water can affect negatively on the production yield since it can hydrolyze the esters. Meanwhile, the studied catalysts showed good water and FFA content tolerance which contributed the investment of low grade, cheap price and non-edible vegetable oils in biodiesel production.

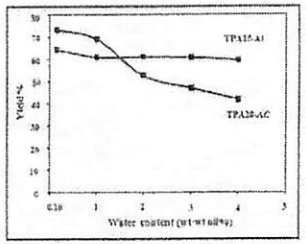

Figure 13. Effect of Water Content on Biodiesel Yield. (Reaction Time 40 min, Methanol/oil Molar Ratio 20:1, Catalyst Amount 4% (w/w), and Ultrasonic Power 75%).

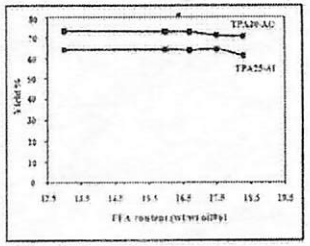

Figure 14. Effect of FFA Content on Biodiesel Yield. (Reaction Time 40 min, Methanol/oil Molar Ratio 20:1, Catalyst Amount 4% (w/w), and Ultrasonic Power 75%).

9. Conclusions

It can be concluded that HPA-based catalysts are successful and promising solid acid catalysts for various oleochemical reactions. Due to its unique physicochemical properties, FFA insensitivity and water tolerance, they represent viable catalysts for converting fatty acids and vegetable oils to biodiesel and other value-added products. For esterification of a wide range of fatty acids, HPAs in both immobilized form and HPAs salts generally demonstrate good activity particularly with the catalysts based on $H_3PW_{12}O_{40}$. The activity can be further improved by the use of suitable porous supports with relatively large pore sizes. It is due to the known fact that generally internal diffusion of reactant and/or product is the rate-limiting step in many oleochemical reactions. Tungstophosphoric acid is a member of Keggin HPAs that possesses strong Bronsted acidity that results in high catalytic performance. The high performance has been demonstrated with $H_3PW_{12}O_{40}$ in transesterification reaction of different vegetable oils for biodiesel production. Immobilizing HPAs on appropriate supports will improve their catalytic performance due to the significant increase in surface area and the positive change in its polar solubility. Experiments for ultrasound-assisted crude Jatropha oil transesterification in the presence of $H_3PW_{12}O_{40}$ immobilized on activated carbon and gamma alumina were conducted. The experimental results revealed that activated carbon based catalyst had higher catalytic activity than alumina based catalyst due to the higher porosity and surface acidity. The catalysts were also investigated for high FFA and water content feedstock and the results revealed that the catalysts were insensitive toward FFA and water contents. Meanwhile salt form of $H_3PW_{12}O_{40}$ with either Cs^+ or Ag^+ ions can lead to reasonable improvements in its stability towards solubilization the solubility nature in the reaction media to achieve good activity in oleochemical reactions.

Acknowledgements

Research fundings from Universiti Sains Malaysia in the form of a Research University (RU) grant and a Short Term grant are gratefully acknowledged.

References

[1] Y.C. Sharma, B. Singh, J. Korstad, Advancements in solid acid catalysts for ecofriendly and economically viable synthesis of biodiesel, Biofuels, Bioprod. Biorefin. 5 (2011) 69-92.

[2] F. Chai, F. Cao, F. Zhai, Y. Chen, X. Wang, Z. Su, Transesterification of Vegetable Oil to Biodiesel using a Heteropolyacid Solid Catalyst, Adv. Synth. Catal. 349 (2007) 1057-1065.

[3] S. Zhang, Y.-G. Zu, Y.-J. Fu, M. Luo, D.-Y. Zhang, T. Efferth, Rapid microwave-assisted transesterification of yellow horn oil to biodiesel using a heteropolyacid solid catalyst, Bioresource Technol. 101 (2010) 931-936.

[4] A. Bielański, A. Micek-Ilnicka, Kinetics and mechanism of gas phase MTBE and ETBE formation on Keggin and Wells–Dawson heteropolyacids as catalysts, Inorg. Chim. Acta. 363 (2010) 4158-4162.

[5] J. Salimon, N. Salih, E. Yousif, Industrial development and applications of plant oils and their biobased oleochemicals, Arabian J. Chem. 5 (2012) 135-145.

[6] D.J. Murphy, Identification and characterisation of genes and enzymes for the genetic engineering of oilseed crops for production of oils for the oleochemical industry: a review, Ind. Crops Prod. 1 (1992) 251-259.

[7] H.-J. Kim, B.-S. Kang, M.-J. Kim, Y.M. Park, D.-K. Kim, J.-S. Lee, K.-Y. Lee, Transesterification of vegetable oil to biodiesel using heterogeneous base catalyst, Catal. Today, 93–95 (2004) 315-320.

[8] A.Z. Abdullah, B. Salamatinia, H. Mootabadi, S. Bhatia, Current status and policies on biodiesel industry in Malaysia as the world's leading producer of palm oil, Energ. Policy 37 (2009) 5440-5448.

[9] A.Z. Abdullah, N. Razali, K.T. Lee, Optimization of mesoporous K/SBA-15 catalyzed transesterification of palm oil using response surface methodology, Fuel Process. Technol. 90 (2009) 958-964.

[10] L.C. Meher, D. Vidya Sagar, S.N. Naik, Technical aspects of biodiesel production by transesterification—a review, Renew. Susta. Energ. Rev. 10 (2006) 248-268.

[11] M.Y. Koh, T.I. Mohd. Ghazi, A review of biodiesel production from Jatropha curcas L. oil, Renew. Susta. Energ. Rev. 15 (2011) 2240-2251.

[12] B.Y. Tao, Chapter 24 - Industrial Applications for Plant Oils and Lipids, in: Y. Shang-Tian (Ed.) Bioprocessing for Value-Added Products from Renewable Resources, Elsevier, Amsterdam, 2007, pp. 611-627.

[13] C.T. Hou, Biotransformation of unsaturated fatty acids to industrial products, in: Adv. Appl. Microbiol. Academic Press, 2000, pp. 201-220.

[14] C.F. Oliveira, L.M. Dezaneti, F.A.C. Garcia, J.L. de Macedo, J.A. Dias, S.C.L. Dias, K.S.P. Alvim, Esterification of oleic acid with ethanol by 12-tungstophosphoric acid supported on zirconia, Appl. Catal. A- Gen. 372 (2010) 153-161.

[15] C.S. Caetano, I.M. Fonseca, A.M. Ramos, J. Vital, J.E. Castanheiro, Esterification of free fatty acids with methanol using heteropolyacids immobilized on silica, Catal. Commun. 9 (2008) 1996-1999.

[16] D.Y.C. Leung, X. Wu, M.K.H. Leung, A review on biodiesel production using catalyzed transesterification, Appl. Energ. 87 (2010) 1083-1095.

[17] Y.C. Sharma, B. Singh, S.N. Upadhyay, Advancements in development and characterization of biodiesel: A review, Fuel, 87 (2008) 2355-2373.

[18] J.M. Marchetti, V.U. Miguel, A.F. Errazu, Possible methods for biodiesel production, Renew. Sust. Energ. Rev. 11 (2007) 1300-1311.

[19] M. Zabeti, W.M.A. Wan Daud, M.K. Aroua, Activity of solid catalysts for biodiesel production: A review, Fuel Process. Technol. 90 (2009) 770-777.

[20] M.K. Lam, K.T. Lee, A.R. Mohamed, Homogeneous, heterogeneous and enzymatic catalysis for transesterification of high free fatty acid oil (waste cooking oil) to biodiesel: A review, Biotechnol. Adv. 28 (2010) 500-518.

[21] M.N. Timofeeva, Acid catalysis by heteropoly acids, Appl. Catal. A-Gen. 256 (2003) 19-35.

[22] I.V. Kozhevnikov, Sustainable heterogeneous acid catalysis by heteropoly acids, J. Mol. Catal. A-Chem. 262 (2007) 86-92.

[23] S. Soled, S. Miseo, G.B. McVicker, J.E. Baumgartner, W.E. Gates, A. Gutierrez, J. Paes, Chapter 16 - Preparation of Bulk and Supported Heteropolyacid Salts, in: R.M. William (Ed.) Advanced Catalysts and Nanostructured Materials, Academic Press, San Diego, 1996, pp. 435-451.

[24] A.E.R.S. Khder, H.M.A. Hassan, M.S. El-Shall, Acid catalyzed organic transformations by heteropoly tungstophosphoric acid supported on MCM-41, Appl. Catal. A-Gen. 411–412 (2012) 77-86.

[25] S.K. Bhorodwaj, D.K. Dutta, Activated clay supported heteropoly acid catalysts for esterification of acetic acid with butanol, Appl. Clay Sci. 53 (2011) 347-352.

[26] Y. Liu, L. Xu, B. Xu, Z. Li, L. Jia, W. Guo, Toluene alkylation with 1-octene over supported heteropoly acids on MCM-41 catalysts, J. Mol. Catal. A-Chem. 297 (2009) 86-92.

[27] R. Heknatshoar, M.M. Heravi, S. Sadjadi, H.A. Oskooie, F.F. Bamoharram, Catalytic performance of Preyssler heteropolyacid, $[NaP_5W_{30}O_{110}]^{14-}$ in liquid phase alkylation of phenol with 1-octene, Catal. Commun. 9 (2008) 837-841.

[28] K.A. da Silva, I.V. Kozhevnikov, E.V. Gusevskaya, Hydration and acetoxylation of camphene catalyzed by heteropoly acid, J. Mol. Catal. A-Chem. 192 (2003) 129-134.

[29] B.Y. Giri, K.N. Rao, B.L.A.P. Devi, N. Lingaiah, I. Suryanarayana, R.B.N. Prasad, P.S.S. Prasad, Esterification of palmitic acid on the ammonium salt of 12-tungstophosphoric acid: The influence of partial proton exchange on the activity of the catalyst, Catal. Commun. 6 (2005) 788-792.

[30] M.R. Altiokka, A. Çıtak, Kinetics study of esterification of acetic acid with isobutanol in the presence of amberlite catalyst, Appl. Catal. A-Gen. 239 (2003) 141-148.

[31] S.R. Kirumakki, N. Nagaraju, K.V.R. Chary, S. Narayanan, Kinetics of esterification of aromatic carboxylic acids over zeolites Hβ and HZSM5 using dimethyl carbonate, Appl. Catal. A-Gen. 248 (2003) 161-167.

[32] J.A. Sánchez, D.L. Hernández, J.A. Moreno, F. Mondragón, J.J. Fernández, Alternative carbon based acid catalyst for selective esterification of glycerol to acetylglycerols, Appl. Catal. A-Gen. 405 (2011) 55-60.

[33] A. Corma, H. García, S. Iborra, J. Primo, Modified faujasite zeolites as catalysts in organic reactions: Esterification of carboxylic acids in the presence of HY zeolites, J. Catal. 120 (1989) 78-87.

[34] H. Atia, U. Armbruster, A. Martin, Dehydration of glycerol in gas phase using heteropolyacid catalysts as active compounds, J. Catal. 258 (2008) 71-82.

[35] V. Brahmkhatri, A. Patel, 12-Tungstophosphoric acid anchored to SBA-15: An efficient, environmentally benign reusable catalysts for biodiesel production by esterification of free fatty acids, Appl. Catal. A-Gen. 403 (2011) 161-172.

[36] A.I. Tropecêlo, M.H. Casimiro, I.M. Fonseca, A.M. Ramos, J. Vital, J.E. Castanheiro, Esterification of free fatty acids to biodiesel over heteropolyacids immobilized on mesoporous silica, Appl. Catal. A-Gen. 390 (2010) 183-189.

[37] L. Xu, X. Yang, X. Yu, Y. Guo, Maynurkader, Preparation of mesoporous polyoxometalate–tantalum pentoxide composite catalyst for efficient esterification of fatty acid, Catal. Commun. 9 (2008) 1607-1611.

[38] K.G. Georgogianni, M.G. Kontominas, P.J. Pomonis, D. Avlonitis, V. Gergis, Conventional and in situ transesterification of sunflower seed oil for the production of biodiesel, Fuel Process. Technol. 89 (2008) 503-509.

[39] M.G. Kulkarni, A.K. Dalai, Waste Cooking OilAn Economical Source for Biodiesel: A Review, Ind. Eng. Chem. Res. 45 (2006) 2901-2913.

[40] J.C. Juan, D.A. Kartika, T.Y. Wu, T.-Y.Y. Hin, Biodiesel production from jatropha oil by catalytic and non-catalytic approaches: An overview, Bioresource Technol. 102 (2011) 452-460.

[41] J. Jitputti, B. Kitiyanan, P. Rangsunvigit, K. Bunyakiat, L. Attanatho, P. Jenvanitpanjakul, Transesterification of crude palm kernel oil and crude coconut oil by different solid catalysts, Chem. Eng. J. 116 (2006) 61-66.

[42] J.A. Melero, L.F. Bautista, G. Morales, J. Iglesias, R. Sánchez-Vázquez, Biodiesel production from crude palm oil using sulfonic acid-modified mesostructured catalysts, Chem. Eng. J. 161 (2010) 323-331.

[43] Q. Shu, Z. Nawaz, J. Gao, Y. Liao, Q. Zhang, D. Wang, J. Wang, Synthesis of biodiesel from a model waste oil feedstock using a carbon-based solid acid catalyst: Reaction and separation, Bioresource Technol. 101 (2010) 5374-5384.

[44] P. Morin, B. Hamad, G. Sapaly, M.G. Carneiro Rocha, P.G. Pries de Oliveira, W.A. Gonzalez, E. Andrade Sales, N. Essayem, Transesterification of rapeseed oil with ethanol: I. Catalysis with homogeneous Keggin heteropolyacids, Appl. Catal. A-Gen. 330 (2007) 69-76.

[45] F. Cao, Y. Chen, F. Zhai, J. Li, J. Wang, X. Wang, S. Wang, W. Zhu, Biodiesel production from high acid value waste frying oil catalyzed by superacid heteropolyacid, Biotechnol. Bioeng. 101 (2008) 93-100.

[46] A.P.S. Chouhan, A.K. Sarma, Modern heterogeneous catalysts for biodiesel production: A comprehensive review, Renew. Sust. Energ. Rev. 15 (2011) 4378-4399.

[47] G. Sunita, B.M. Devassy, A. Vinu, D.P. Sawant, V.V. Balasubramanian, S.B. Halligudi, Synthesis of biodiesel over zirconia-supported isopoly and heteropoly tungstate catalysts, Catal. Commun. 9 (2008) 696-702.

[48] V.V. Bokade, G.D. Yadav, Synthesis of Bio-Diesel and Bio-Lubricant by Transesterification of Vegetable Oil with Lower and Higher Alcohols Over Heteropolyacids Supported by Clay (K-10), Process Saf. Environ. 85 (2007) 372-377.

[49] N. Katada, T. Hatanaka, M. Ota, K. Yamada, K. Okumura, M. Niwa, Biodiesel production using heteropoly acid-derived solid acid catalyst $H_4PNbW_{11}O_{40}/WO_3$–Nb_2O_5, Appl. Catal. A-Gen. 363 (2009) 164-168.

[50] J.S. Santos, J.A. Dias, S.C.L. Dias, F.A.C. Garcia, J.L. Macedo, F.S.G. Sousa, L.S. Almeida, Mixed salts of cesium and ammonium derivatives of 12-tungstophosphoric acid: Synthesis and structural characterization, Appl. Catal. A-Gen. 394 (2011) 138-148.

[51] J.H. Sepúlveda, J.C. Yori, C.R. Vera, Repeated use of supported H3PW12O40 catalysts in the liquid phase esterification of acetic acid with butanol, Appl. Catal. A-Gen. 288 (2005) 18-24.

[52] L. Pesaresi, D.R. Brown, A.F. Lee, J.M. Montero, H. Williams, K. Wilson, Cs-doped $H_4SiW_{12}O_{40}$ catalysts for biodiesel applications, Appl. Catal. A-Gen. 360 (2009) 50-58.

[53] K. Narasimharao, D.R. Brown, A.F. Lee, A.D. Newman, P.F. Siril, S.J. Tavener, K. Wilson, Structure–activity relations in Cs-doped heteropolyacid catalysts for biodiesel production, J. Catal. 248 (2007) 226-234.

[54] A. Zieba, L. Matachowski, J. Gurgul, E. Bielańska, A. Drelinkiewicz, Transesterification reaction of triglycerides in the presence of Ag-doped $H_3PW_{12}O_{40}$, J. Mol. Catal. A-Chem. 316 (2010) 30-44.

[55] A. Sivasamy, K.Y. Cheah, P. Fornasiero, F. Kemausuor, S. Zinoviev, S. Miertus, Catalytic Applications in the Production of Biodiesel from Vegetable Oils, ChemSusChem, 2 (2009) 278-300.

[56] Y.C. Sharma, B. Singh, J. Korstad, Latest developments on application of heterogenous basic catalysts for an efficient and eco friendly synthesis of biodiesel: A review, Fuel, 90 (2011) 1309-1324.

[57] A. Alsalme, E.F. Kozhevnikova, I.V. Kozhevnikov, Heteropoly acids as catalysts for liquid-phase esterification and transesterification, Appl. Catal. A-Gen. 349 (2008) 170-176.

[58] M.E. Chimienti, L.R. Pizzio, C.V. Cáceres, M.N. Blanco, Tungstophosphoric and tungstosilicic acids on carbon as acidic catalysts, Appl. Catal. A-Gen. 208 (2001) 7-19.

[59] Z. Obalı, T. Doğu, Activated carbon-tungstophosphoric acid catalysts for the synthesis of tert-amyl ethyl ether (TAEE), Chem. Eng. J. 138 (2008) 548-555.

[60] T. Alemdaroglu, Determination methods for the acidity of solid surfaces, Commun. Fac. Sci. Univ. Ank. Series B. 47 (2001) 27-35.

[61] J.G. Hernández-Cortez, L. Martínez, L. Soto, A. López, J. Navarrete, M. Manríquez, V.H. Lara, E. López-Salinas, Liquid phase alkylation of benzene with dec-1-ene catalyzed on supported 12-tungstophosphoric acid, Catal. Today, 150 (2010) 346-352.

[62] K. Nakajima, M. Hara, S. Hayashi, Environmentally benign production of chemicals and energy using a carbon-based strong solid acid, J. Am. Ceram. Soc. 90 (2007) 3725-3734.

Keyword Index

Author Index

Materials Science Forum

ISSN 0255-5476

Trans Tech Publications Ltd
Kreuzstr. 10 • 8635 Zurich-Durnten • Switzerland
Fax +41 (44) 922 10 33 • e-mail: ttp@ttp.net
http://www.ttp.net
http://www.scientific.net

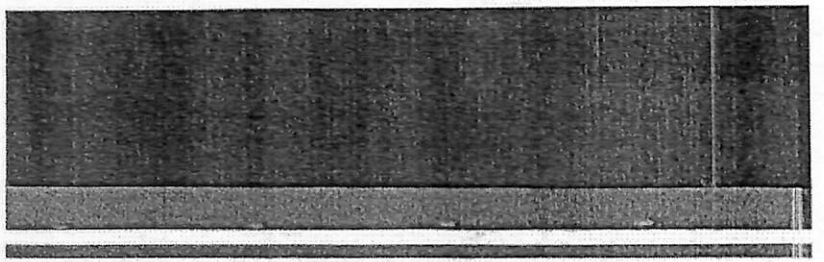

9 783037 857014

ISBN-13: 978-3-03785-701-4
Materials Science Forum Vol. 757
Electronically available at *http://www.scientific.net*

Energy 60 (2013) 283–291

Contents lists available at ScienceDirect

Energy

journal homepage: www.elsevier.com/locate/energy

Ultrasound-assisted transesterification of crude Jatropha oil using cesium doped heteropolyacid catalyst: Interactions between process variables

Ali Sabri Badday [1], Ahmad Zuhairi Abdullah*, Keat-Teong Lee [1]

School of Chemical Engineering, Universiti Sains Malaysia, 14300 Nibong Tebal, Penang, Malaysia

ARTICLE INFO

Article history:
Received 5 February 2013
Received in revised form
30 July 2013
Accepted 5 August 2013
Available online 27 August 2013

Keywords:
Biodiesel production
Jatropha oil
Ultrasound-assisted process
Cesium doped heteropolyacid catalyst
Optimization

ABSTRACT

Transesterification of crude Jatropha oil in the presence of cesium doped heteropolyacid catalyst and assisted by ultrasonic irradiation was investigated. Different Cs heteropolyacid catalysts with different levels of cesium exchange were synthesized and characterized for physical and chemical properties. They were subsequently tested in pre-elementary reaction conditions to identify the most active catalyst. $Cs_{1.5}H_{1.5}PW_{12}O_{40}$ catalyst showed the highest FAME (fatty acid methyl ester) yield of 81.3% in 60 min while higher Cs levels resulted in poorer activity. Four reaction variables i.e. reaction time (10–50 min), methanol to oil molar ratio (5:1–25:1), ultrasonic amplitude (30–90% of the maximum sonifier power) and catalyst amount (2.5–4.5 w/w oil) were optimized to generate mathematical representation of FAME yield. The highest yield of 90.5% was achieved in just 34 min under the optimum reaction conditions i.e. at an ultrasonic amplitude of ~60%, and a molar ratio of 25:1. The catalyst was also investigated for possible reusability and leaching under ultrasonic conditions. The reaction was mostly heterogeneous in nature and the catalyst also showed minimal reduction in the activity after three successive reaction runs under the optimum reaction conditions.

1. Introduction

As they are renewable in nature, environmentally friendly and can be mass produced, various vegetable oils are considered as promising potential feed stocks for biodiesel production. Currently, the main feed stocks for biodiesel production are such as sunflower oil, palm oil, rapeseed oil and soybean oil [1]. However, there have been worldwide rejections against the use of food sources for fuel industry. The demand for vegetable oils to be used for edible purposes as well as for feedstock in biodiesel production may lead to significant increase in their price [2]. The high cost of vegetable oils, which could be up to 75% of the production cost, has led to the manufacturing costs of biodiesel becoming approximately 1.5 times higher than that of petro-diesel [3]. As such, non-edible oils could provide interesting solution to this problem.

Non-edible vegetable oils such as, sea mango, castor and Jatropha curcas oils have been identified to be alternative feed stocks for biodiesel production [4]. These oils are not suitable for human consumption because of the presence of some toxic components. Among various non-edible oils, Jatropha oil is considered the most suitable source of triglycerides for biodiesel production since its seed possesses high oil content compared to other oils. It also has high productivity per hectare which is an important factor in selecting the most potential renewable source for biofuel. Its composition has no significant difference from edible oils [5]. However, crude Jatropha oil usually contains high water and free fatty acid contents that prevent its use with base catalysts which are the conventional method for biodiesel production [6]. Acid catalysts usually have better tolerance to high water and free fatty acid contents but the catalytic activity is generally low [7].

Among various acid catalysts, HPA (heteropolyacid) based catalysts usually receive great interest for application as either heterogeneous or homogeneous catalysts. Their high water and FFA (free fatty acid) tolerances and strong Brönsted acidity (approaching the superacid region) as well as high proton mobility and stability justify these materials as potential solid acid catalysts to be used [8]. Partial substitution of H^+ in HPA with alkaline cations is considered as an appropriate technique to create major effects on the surface area, pore structure, solubility and hydrophobicity of the parent HPA [9]. Reducing the solubility of HPA in either water or other polar solvents will improve its resistance towards

* Corresponding author. Tel.: +60 4 599 6411; fax: +60 4 594 1013.
E-mail addresses: azuhairi@yahoo.com, chzuhairi@eng.usm.my (A.Z. Abdullah).
[1] Tel.: +60 4 599 6411; fax: +60 4 594 1013.

0360-5442/$ – see front matter © 2013 Elsevier Ltd. All rights reserved.
http://dx.doi.org/10.1016/j.energy.2013.08.002

deactivation leading to an improvement in its potential for recycle and significantly contributes in achieving the objective of an eco-friendly process [10]. HPAs salts with large monovalent ions such as Cs^+, NH_4^+ and Ag^+ have attracted the interest due to dramatic increases in surface area and changes in solubility compared to the original HPAs [11]. Partial substitution of protons with these cations can also result in an increase in the number of available surface acidic sites for the reaction [9].

Ultrasonic irradiation has been successfully to enhance the emulsification of the immiscible reactants (oil and alcohol) to increase the low mass transfer rate during the reaction. This improvement might lead to reductions in the reaction time, alcohol to oil ratio, catalyst amount and reaction temperature causing a significant stenography in the production economics [12]. A wide range of homogenous [13] and heterogeneous catalysts [14,15] have been tested under ultrasonic irradiation and promising results have been demonstrated as compared to the conventional process. Esterification of PFAD (palm fatty acid distillate) with methanol in the presence of concentrated H_2SO_4 as a catalyst has been investigated by Deshmane et al. [16]. They recorded that mass transfer resistances under conventional approach appeared to be eliminated due to ultrasonication and conversions of more than 90% were achieved in about 150 min under ambient operating conditions. Meanwhile, conversions higher than 95% were obtained using ultrasonic irradiation for fatty acid (C8–C10) esterification in less than 180 min using H_2SO_4 as catalyst as reported by Kelkar et al. [17].

Like any other sound waves, ultrasound wave travels by a successive series of rarefaction and compression cycles vibrating the molecules of the carrier media, in this case the liquid reactants. When the attraction forces between the liquid molecules becomes less than the negative pressure of the cyclic rarefaction, a gap that is filled with vapor from the liquid will be generated [12]. At the beginning of its lifetime, it is only tiny but within other successive cycles, it grows to form an acoustic cavitation bubble. Yet, in the final stage of bubble compression, velocity of the bubble interface becomes tremendously fast i.e. close to or even faster than the sonic velocity in liquid [18].

Huge number of bubbles can be generated in the liquid during the ultrasonication. Some of them are stable and can stand for another cycle while others will undergo vigorous breakdown once reaching a certain critical size. The strong collapses will generate local pressure in the order of 2000 atm and the temperature could reach up to 5000 K [19]. Small hotspots that are generated from these collapses can offer the energy for some chemical reactions. These phenomena result in severe mixing between the two immiscible liquids close to the phase boundary and force the liquids to inspire micro jets which can reach a speed of up to 200 m/s. The cause for the micro jets generation is the asymmetric breakdown of the cavitation bubbles [20]. Besides that, the radial motion of bubbles creates an intimate mixing of the immiscible reactants causing the interfacial area between the reactants to increase enormously to allow faster reaction rates [21].

One of the advantages of these cavitations is that it causes a local increase in temperature near the boundary layer and this increment will modify the course of the reaction that consequently offset the requirement for external heating in the production process. On the other hand, the formation of micro jets eliminates the need for intense mechanical agitation to improve mass transfer between the two reactant phases [22]. Ultimately, significant improvement in the reaction rate will be achieved.

In the current study, the contribution of Cs doped HPA solid acid catalyst has been combined with the application of ultrasonic irradiation in accelerating the transesterification of crude Jatropha oil with high FFA and water contents. Until very recently, mature understanding on the ultrasound-assisted transesterification reaction catalyzed by heterogeneous acid catalyst is yet to be established. As such, the current research will contribute some improvement on the knowledge of ultrasound-accelerated chemical reactions as well as the application of solid acid catalysts for biodiesel production.

2. Materials and methods

2.1. Reagents and materials

Tungstophosphoric acid ($H_3PW_{12}O_{40}.nH_2O$), abbreviated as TPA in this manuscript, was supplied by Merck (Malaysia) while cesium chloride was purchased from Sigma–Aldrich (Malaysia). Crude Jatropha oil was supplied by Telaga Madu Resources (Malaysia) and the properties of the crude Jatropha oil used are tabulated in Table 1. Methanol that was used in the transesterification reaction was supplied by Thermo Fisher Scientific Inc. (USA) while ethanol (for catalyst preparation) and n-hexane (for product analysis) were purchased from Merck (Malaysia). Meanwhile, reference FAME (fatty acid methyl ester) standards were supplied by NuChek Prep. Inc. (Australia).

2.2. Catalyst synthesis

0.1 M of C_S solution was prepared by dissolving a pre-calculated amount of cesium chloride in 50:50 (ethanol/water) solution. Milky suspension solution was formed upon dropwise addition of the Cs solution to 0.08 M of TPA solution under constant stirring. The TPA solution was then prepared by dissolving appropriate amounts of TPA in 50:50 (ethanol/water) solution. Soon after the addition, the white solution was left for aging without stirring for 12 h at ambient temperature. Then, the solution was evaporated using a rotary evaporator to collect the white powder which was then washed with deionized water before drying in an oven at 110 °C for 4 h followed by calcination at 200 °C for 3 h. The general chemical representation of the reaction to generate the salts from cesium chloride is as follows;

$$3CsCl + H_3PW_{12}O_{40} \rightarrow Cs_3PW_{12}O_{40} + 3HCl \quad (1)$$

Meanwhile, various calculated amounts of Cs solution were prepared to achieve a partial substitution of the alkaline atom with H^+ ion in TPA. Catalysts with different cesium contents were represented as $Cs_xH_{3-x}PW_{12}O_{40}$ in which the x values were 1, 1.5, 2, 2.5 and 3. Here, x denotes the molar ratio of Cs^{1+} ion to $PW_{12}O_{40}^{3-}$ anion in the synthesized catalysts.

2.3. Catalyst characterization

The surface characteristics of the synthesized catalysts were determined based on nitrogen absorption–desorption by means of

Table 1
Properties of crude Jatropha oil.

Property	Value	Standard method/equipment/technique used
Density (kg/m³)	921	ASTM
Viscosity (cSt)	38.12	ASTM
Molecular weight (g/mol)	870	–
Water content (w %)	0.161	BP 2007 (Appendix IV C-Method III) (Karl Fisher Moisture Meter)
FFA content (w %)	10.5	MPOB P2.5

an Autosorb 1C system. FT-IR spectra of the Cs doped TPA catalysts were performed using a Perkin–Elmer FT-IR spectrophotometer. The X-ray diffraction patterns of the catalyst samples were determined using a Philips Goniometer PW 1820 system. The surface morphology was observed using an SEM unit (Oxford INCA/ENERGY-350) equipped with an EDAX (energy dispersive X-ray analysis) system. In addition; the catalysts acidity was calculated using an acid-base titration method [23].

2.4. Experimental setup

The experimental setup and the equipment used to conduct the ultrasound-assisted reactions can be found in our previous work [24]. In a typical experimental run, the desired amount of oil was charged into the reactor and placed in the water bath until it reached the reaction temperature. Then, the desired amount of the catalyst was added followed by the required amount of pre-heated methanol. Ultrasonification was then started and the condenser was turned on to recover the evaporated methanol. The water bath temperature was fixed at 54 °C and the heat generated by the ultrasonic probe combined with the heat gained from the water bath successfully maintained the reaction temperature at 65 ± 1 °C. After the desired reaction time, the reaction mixture was quenched and excess methanol was distilled out. The reaction mixture was then separated into two layers by centrifugation in an Eppendorf centrifuge at 3500 rpm for 25 min. The upper layer consisted of FAME was then collected for the chromatographic analysis.

Preliminary experiments were also carried out in the absence of ultrasonic irradiation or the catalyst. The absence of catalyst was tested by providing an ultrasonic irradiation at 75% of the maximum power with the reaction conditions of 60 min for the reaction time and with a methanol/oil ratio of 20. The experiment with zero ultrasonic amplitude (with vigorous mechanical stirring) was also conducted under the same reaction conditions in the presence of the catalyst. Testing of catalysts with different Cs contents was conducted under the same reaction conditions with the presence of catalyst at 4% (wt/wt oil).

2.5. Catalyst leaching and stability tests

With the purpose of studying the dissolution of the active component of catalyst in polar media and to investigate the influence of ultrasonic waves on the catalyst stability, an experiment similar to the "hot-filtration experiment" was conducted [25]. The catalyst was first allowed to have contact with methanol and then subjected to ultrasonication under the optimum reaction conditions. After the desired reaction time, the solid catalyst was filtered out and the desired amount of oil was added to this methanol. The reaction was then carried out without the presence of catalyst at the optimum reaction conditions in order to examine the contribution of leached catalyst on the reaction.

The catalyst reusability was tested by running the same batch of catalyst for several consecutive cycles or runs. First, the desired catalyst amount was used according the optimum reaction condition in the transesterification followed by filtration and washing. A filtration system consisted of 0.45 μm filter and a vacuum pump was used to extract the catalyst using n-hexane as solvent. Successive washing with n-hexane followed by washing with ethanol were performed to ensure the removal of any polar and non-polar components that were attached to the catalyst. The solid catalyst was then dried at 100 °C for 2 h before reuse and the method was repeated for up to three cycles after the fresh catalyst usage.

2.6. Product analysis

Analyses of the products were conducted using an Agilent GC (gas chromatograph) (7890A) system equipped with a FID (flame ionization detector) and a capillary column (Agilent Technologies, Inc. 19091 J-413 HP-5). The analyses of the reference materials (FAME standards) and the reaction products were carried out by dissolving the samples in n-hexane according to a desired dilution factor. The FAME standard used consisted of mixture of fatty acids with the following composition: Palmitic acid (25 wt. %), palmitoleic acid (5 wt. %), stearic acid (15 wt. %), oleic acid (30 wt. %) and linoleic acid (25 wt. %). 1 μl of the mixture was injected into the GC for the analysis.

2.7. Experimental design

A CCD (central composite design) was functionalized to establish the experimental design matrix with the application of four zero levels (center levels). The coded and actual reaction variables used in the experimental design are presented in Table 2. Reaction time (X_1), methanol to oil ratio (X_2), ultrasonic amplitude (X_3) and catalyst amount (X_4) were chosen with center values of 30 min, 15, 60% and 3.5% wt/wt oil, respectively. The selection of the center levels was made based on a previous work reported by Badday et al. [24]. Design Expert 6.0.6 software was employed to construct the experimental design by taking the FAME yield value as the response. The used third order polynomial for fitting the experimental data is expressed as follows:

$$Y = \lambda_0 + \sum_{i=1}^{n} \lambda_i X_i + \sum_{i=1}^{n} \lambda_{ii} X_i^2 + \sum_{i=1}^{n} \sum_{j=1}^{n} \lambda_{ij} X_i X_j + \sum_{i=1}^{n} \lambda_{iii} X_i^3 + \sum_{i=1}^{n} \times \sum_{j=1}^{n} \sum_{k=1}^{n} \lambda_{ijk} X_i X_j X_k + \varepsilon$$

where, Y: The response generated by the model; λ_0: Constant factor; λ_i: The linear effect coefficient; λ_{ii}, λ_{iii}: The quadratic and cubical effect coefficient; λ_{ij}, λ_{ijk}: The cross-product effect coefficients; X_i, X_j, X_k: Variables corresponding to the factors; ε: The error.

3. Results and discussion

3.1. Catalyst characteristics

The FT-IR spectra of the synthesized catalysts are presented in Fig. 1. The spectrum of the parent TPA shows major bands attributed to the vibration of oxygen attached to phosphorous and tungsten of the adsorption mode of the Keggin ion $(PW_{12}O_{40})^{3-}$. In Fig. 1, four major bands at 800 cm^{-1} (W–O–W in the edge), 890 cm^{-1} (W–O–W in the corner), 980 cm^{-1} (W=O) and at 1080 cm^{-1} (P–O) can be detected for the Keggin anion. Thus, the presence of Keggin anion could be confirmed as the obtained spectra could be clearly assigned to the typical vibrations of the parent TPA. The FT-IR results revealed that a good Keggin structure retention was achieved

Table 2
Coded and actual reaction variables used in the experimental design.

Real variables	Coded variables	Level		
		−α	0	+α
Reaction time (min)	X_1	10	30	50
Molar ratio	X_2	5:1	15:1	25:1
Ultrasonic amplitude (%)	X_3	30	60	90
Catalyst amount (w/w %)	X_4	2.5	3.5	4.5

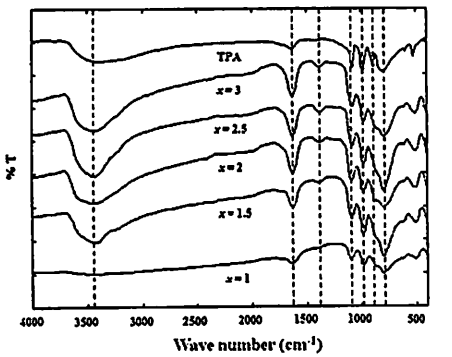

Fig. 1. FT-IR spectra of TPA and $Cs_xH_{3-x}PW_{12}O_{40}$ catalysts with different Cs to TPA ionic ratios.

after the incorporation of cesium into the heteropoly cage structure.

The XRD patterns of the prepared catalysts and that of the parent TPA are presented in Fig. 2. For pure TPA, diffraction peaks at 18°, 23°, 25°, 30°, 35° and 38° attributed to the triclinic phase of TPA can be detected. Even though the crystalline nature can be observed for all catalyst samples, the diffraction peaks become significantly weaker and broader with increasing Cs^+ content in the prepared catalysts. The shifts of the peaks toward higher angles in the $Cs_xH_{3-x}PW_{12}O_{40}$ samples are consistent with the presence of the body-centered cubic structure of the alkaline salts. This gave the indication for the reduction of the triclinic crystallites size of TPA and the shrinkage of the lattice cell due to the incorporation of Cs^+ ion replacing $H^+(H_2O)_{n/3}$ in the parent TPA [26].

The surface characteristics of the synthesized catalysts as well as the surface acidity are shown in Table 3. Tungstophosphoric acid itself has low surface area of about 1–2 m^2/g [27]. The surface area

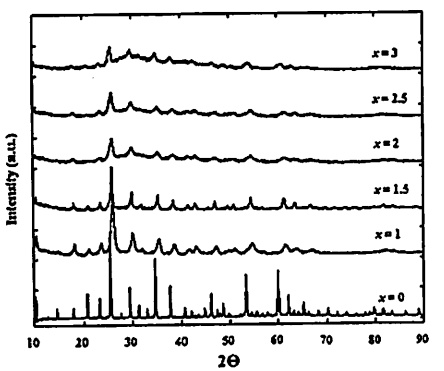

Fig. 2. XRD patterns of TPA and $Cs_xH_{3-x}PW_{12}O_{40}$ catalysts with different Cs to TPA ionic ratios.

Table 3
Surface properties and acidity of $Cs_xH_{3-x}PW_{12}O_{40}$ catalysts.

Sample	BET surface area (m^2/g)	Total pore volume (cm^3/g)	Average pore diameter (Å)	Surface acidity (μmol/g)
x = 1.0	17.0	0.034	80.9	1850
x = 1.5	32.7	0.087	106.9	1760
x = 2.0	110.7	0.170	63.1	1680
x = 2.5	95.8	0.180	76.8	1290
x = 3.0	64.5	0.100	65.5	1180

of the catalyst samples increased as the cesium content was increased for 'x' values smaller than 2. This increment was ascribed to the changes in the morphology due to the aggregation of fine particles in the structure and voids that were formed between the aggregates. As the cesium amount was increased beyond $x = 2$, the aggregates became denser and negatively affected the porous structure between the fine particles. Thus, a reduction in the specific surface area occurred. It could be concluded that the total pore volume of the prepared catalysts increased as the cesium content in the samples was increased. The increase in the pore volume could be attributed to increases in the voids that existed within the fine particles of the cesium doped catalysts.

Further information about the surface morphology of the prepared $Cs_xH_{3-x}PW_{12}O_{40}$ catalysts can be obtained from the SEM micrographs as presented in Fig. 3. The morphology of the catalysts was found to change as cesium ions successfully exchanged for hydrogen ion at an increasing ratio from 1 to 3. For an 'x' value of 1, the catalyst surface texture was more compact and smoother in its structure. As the cesium content was increased, the surface structure gradually changed to rather rough morphologies consisting of larger fine particles. A more porous structure was observed on the surface due to the aggregation of the fine particles. As the Cs ratio was increased to ratios exceeding 2, these fine particles became denser leading to increasing surface roughness. Enormous amount aggregates were formed with less voids and pores between them.

The mechanism of aggregates formation could consist of three successive steps i.e.: the nucleation of the fine particles due to the interaction between Cs^{1+} and $PW_{12}O_{40}^{3-}$ free ions, the formation of aggregates as a result of the combination of these fine particles, and the growth of the aggregates due to the agglumeration of different fine particles [28]. Thus, increasing the Cs content doped into TPA led to an increase the aggregation in the structure as it increased the nucleation activity of fine particles which affected its crystallinity nature as observed in XRD results. Besides that, the agglomeration of the massive number of aggregates reduced the amount of voids and pores on the structure to result in a decrease in the specific surface area as observed in Table 3.

The elemental compositions of the synthesized catalysts observed under EDAX are presented in Table 4 and the results proved the successful incorporation of Cs^{1+} ion into TPA structure. Discrepancies were also noticed between the stoichiometric tungsten to cesium ratio and the measured ratios. Nevertheless, the differences between the ratios were within an error range of ~6% which indicated good agreement between the experimental and calculated ratios.

The chemical composition of the produced FAME mixture after the reaction consisted of the following components; methyl palmitoleate (7.4 wt. %), methyl palmitate (19.0 wt. %), methyl linoleate (28.5 wt. %), methyl oleate (30.8 wt. %) and methyl stearate (11.4 wt. %). Other components were found to form 2.95 wt. % of the product mixture. It could be seen that the FAMEs consisted of five main compounds. Saturated and unsaturated C19 components were the dominant substances in the produced FAMEs. Further compositional analysis was not done as it was beyond the scope of this research work.

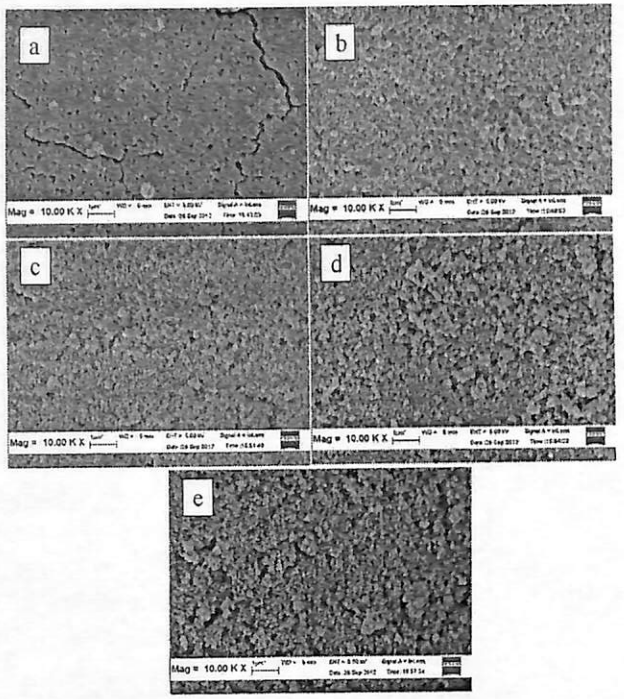

Fig. 3. SEM images of $Cs_xH_{3-x}PW_{12}O_{40}$ catalysts (a) $x = 1$ (b) $x = 1.5$ (c) $x = 2$ (d) $x = 2.5$ (e) $x = 3$.

3.2. Preliminary study

Blank experiments were carried out in order to investigate the effects of the absence of catalyst and the influence of ultrasonic irradiation on the reaction. The results revealed that for an ultrasound-assisted process without the presence of catalyst, significant transesterification reaction did not occur due to the absence of the catalytic active sites required. Besides that, no significant result was achieved with the presence of the solid acid catalyst under vigorous mechanical stirring process due to short reaction time. It was recorded that for this acid catalyzed transesterification process, reaction times of up to 5–6 h were required to achieve significantly high yield due to low reaction rate [29]. Choudhury et al. [30] reported that micro-mixing generated by ultrasound was capable of producing preferable emulsion compared to vigorous mechanical stirring (up to 600 rpm) and it resulted in much faster kinetics and higher conversion. About 90% of triglyceride conversion was achieved in just 1 h in the edible soybean oil transesterification process compared to 56% conversion in 5 h under optimized conditions using CaO catalyst.

Table 4
Elemental compositions of $Cs_xH_{3-x}PW_{12}O_{40}$ catalysts used in this study.

Sample	Elemental analysis (wt.%)					
	Cs	W	P	O	W/Cs calc.[a]	W/Cs measured
$x = 1.0$	6.98	78.69	3.09	11.24	12.0	11.3
$x = 1.5$	9.31	75.50	5.14	10.04	8.0	8.1
$x = 2.0$	12.72	73.03	5.64	8.60	6.0	5.7
$x = 2.5$	16.74	71.27	5.88	6.11	4.8	4.6
$x = 3.0$	18.47	70.46	5.36	5.70	4.0	3.8

[a] Calculated tungsten to cesium ratio according to the stoichiometry.

The effect of different Cs amounts doped into TPA on the transesterification yield under the preliminary reaction conditions are presented in Fig. 4. It can be observed that for Cs ratios lower than 2, the catalytic activity showed higher values compared with when $x > 2$. This could be attributed to high surface acidity of the catalysts due to the presence of less Cs amounts and the absence of available protons in the catalyst in the case of higher Cs content catalysts. Catalyst with $x = 1.5$ showed the best catalytic activity compared a catalyst with higher surface area when $x = 2$ and higher acidity with lower surface area catalyst when $x = 1$. The results revealed that the surface acidity played a more dominant role in the transesterification reaction rather than the catalyst surface area. For the catalyst with $x = 1.5$, both the catalyst acidity and the surface

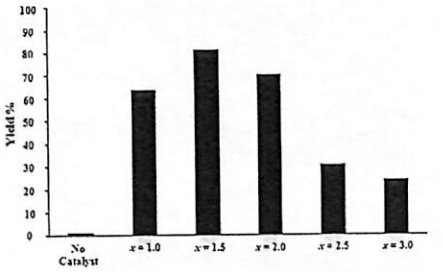

Fig. 4. Transesterification of Jatropha oil in an ultrasonic-assisted process over $Cs_xH_{3-x}PW_{12}O_{40}$ catalysts (reaction time 60 min, methanol/oil molar ratio 20:1, catalyst amount 4% (w/w) and ultrasonic power of 75%).

area contributed in the high catalytic activity so that the catalyst was chosen for further investigations.

3.3. Statistical analysis

The experimental design matrix including the un-coded values, point types and the experimental response values is presented in Table 5. The design consisted of 30 experiments according to 2^k+2k+6, where k is the number of independent variables [31]. Twenty four experiments were improved by six replications at the center points to evaluate the pure error. Third order polynomial equation based on the coded values was obtained using multiple regression analysis of the experimental data. The choice of a cubical polynomial equation to describe the design was attributed to the high value of determination coefficient (R^2) that was achieved. The polynomial equation describing the system is given as follows;

$$Y = -609.89 + 2.24X_1 - 3.79X_2 - 0.94X_3 + 477.65X_4 - 0.25X_1^2 + 0.01X_2^2 - 147.92X_4^2 + 0.12X_1X_3 + 1.65X_1X_4 + 0.79X_3X_4 + 2.65 \times 10^{-3}X_1^3 + 14.13X_3^3$$

where, Y is the response (yield of FAME), and X_1, X_2, X_3 and X_4 are the values in the coded form of the studied variables.

The Fisher F-test value of 18.49 combined with very small probability value (Prop. > F < 0.0001) as evaluated by the ANOVA statistical analysis of the design indicate high significance of the cubical equation to represent the experimental data. It can be concluded from the determination coefficient (R^2 = 93.76%) that the effect on the FAME yield could be mainly attributed to the variation in the independent variables and the remaining 6.24% could be explained as residues.

The significance of the reaction variables and interactions between them are summarized in Table 6. By virtue of experience, the larger the F-value and the smaller the Prob. > F, the more significant the corresponding variable was [32]. It can be observed that the molar ratio and catalyst amount had their significant effects on the reaction yield while the reaction time mostly had its influence in its single value. For a reversible reaction with low reaction rate such as the transesterification reaction, the presence of sufficient amounts of reactant had its noticeable influence on the reaction yield.

Molar ratio is the practical expression of the presence of reactants and in this study, it had significant influence on the studied design response. The catalyst amount was deemed to have a significant role in the current system as the presence of acid catalyst is generally required to drive the forward reaction, especially in the case of feed stocks with high FFA content. The interactions between reaction time and catalyst amount, between ultrasonic amplitude and catalyst amount as well as the triple interaction between the three variables had their significance influences. Besides that, the cubical forms of reaction time and catalyst amount showed positive influence on the reaction yield. The other interactions and the square forms as presented in Table 7 were also considered to establish the historical design for the experimental data.

Table 5
Central composite design matrix of four variables and respective responses.

Run	Point type	Real variables				Yield (%)
		Time (min)	M/O[a]	Amplitude (%)	Catalyst amount (w/w %)	
1	Fact	40	20	45	3.0	60.9
2	Fact	20	10	45	4.0	26.4
3	Fact	20	20	75	4.0	64.4
4	Fact	40	10	75	4.0	13.0
5	Fact	20	10	45	3.0	20.7
6	Fact	20	20	75	3.0	67.0
7	Fact	40	10	75	3.0	23.2
8	Fact	20	20	45	4.0	56.1
9	Fact	40	20	75	3.0	75.2
10	Fact	40	10	45	3.0	23.1
11	Fact	40	10	45	4.0	19.1
12	Fact	40	20	75	4.0	44.3
13	Fact	20	20	45	3.0	61.1
14	Fact	40	20	45	4.0	65.1
15	Fact	20	10	75	4.0	24.7
16	Fact	20	10	75	3.0	18.3
17	Axial	30	25	60	3.5	87.9
18	Axial	30	15	60	4.5	55.0
19	Axial	30	15	90	3.5	36.5
20	Axial	10	15	60	3.5	30.1
21	Axial	30	5	60	3.5	23.4
22	Axial	50	15	60	3.5	58.2
23	Axial	30	15	30	3.5	37.1
24	Axial	30	15	60	2.5	42.9
25	Center	30	15	60	3.5	41.7
26	Center	30	15	60	3.5	49.0
27	Center	30	15	60	3.5	42.4
28	Center	30	15	60	3.5	46.2
29	Center	30	15	60	3.5	44.1
30	Center	30	15	60	3.5	38.7

[a] Methanol to oil ratio.

3.4. Interaction between reaction parameters

Three dimension response surfaces for the representation of the FAME yield combined with the interaction of the reaction variables are represented in Fig. 5. The interaction between the reaction time

Table 6
Results of regression analysis for the third-order polynomial model and the estimated coefficients.

Model parameters	F-value	Prob. > F
X_1	2.51	0.1328
X_2	210.79	<0.0001
X_3	0.015	0.9039
X_4	3.20	0.0925
X_1^2	0.82	0.3778
X_2^2	5.88	0.0275
X_3^2	0.0073	0.9331
X_1X_3	0.79	0.3873
X_1X_4	3.19	0.0931
X_3X_4	2.22	0.1558
X_1^3	8.26	0.0110
X_3^3	3.66	0.0737
$X_1X_3X_4$	3.02	0.1012

Table 7
Predicted and experimental results at the optimum conditions for model validation.

Reaction conditions					Predicted yield (%)	Experimental yield (%)	Error (%)
Run	Time (min)	Molar ratio	Amplitude (%)	Catalyst loading (w/w)			
1	40.0	25.0	73	2.6	89.5	91.4	2.2
2	33.1	25.0	67	2.9	87.1	90.5	3.9
3	49.4	24.1	56	3.0	95.6	93.1	2.6

and the molar ratio while the other variables kept at their center values is presented in Fig. 5(a). It can be concluded that increasing the reaction time had its positive effects for all molar ratio values and vice versa. Low reaction yields with the presence of low methanol ratio for all reaction times were attributed to the insufficient methanol amount in the system to drive the forward reaction. For high reaction time and high molar ratios, the FAME yields showed maximum values attributed to the sufficient reaction time and adequate methanol amounts to support the reaction.

Unlike the response behavior at high reaction time, Fig. 5(b) shows a reduction in reaction response as ultrasonic amplitude was increased for high time values. It can be concluded that at low reaction time, increasing ultrasonic amplitude led to an increase in the yield. It was attributed to the positive ultrasonic mixing effects in enhancing the contact between the reactants at the initial stages of reaction time. Meanwhile, increasing amplitude under high reaction time levels led to a decrease in the yield after a certain level of amplitude (~60%). Subjecting the reacting mixture to high acoustic energy led to larger and stable cavitation bubbles which could act as barriers to the transfer of ultrasonic energy throughout the reaction mixture. So, poor mixing effects between the two immiscible layers resulted in low emulsification effects. Then, the transesterification reaction would take place at the boundary between the two layers. Similar behavior of ultrasound-assisted biodiesel production systems could be observed at high ultrasonic energy as reported in our previous work for an activated carbon-supported TPA catalyst [24]. Kumar et al. [33] and Stavarache et al. [22] also reported similar behavior for different ultrasound-assisted systems catalyzed by homogeneous catalysts.

The interaction between ultrasonic amplitude and the molar ratio presented in Fig. 5(c) indicates that for low reactant molar ratio, increasing the ultrasonic amplitude had negative effects on the response. This could be caused by severe mixing effect between the small FAME amounts (generated by low methanol amount) with the side product (glycerol). Meanwhile, slight increase in the reaction yield was observed when the ultrasonic amplitude was increased at high molar ratio. It was clear that at amplitude of ~60%, the reaction yield reached its maximum level with the presence of high methanol ratio. This could be explained on the basis of

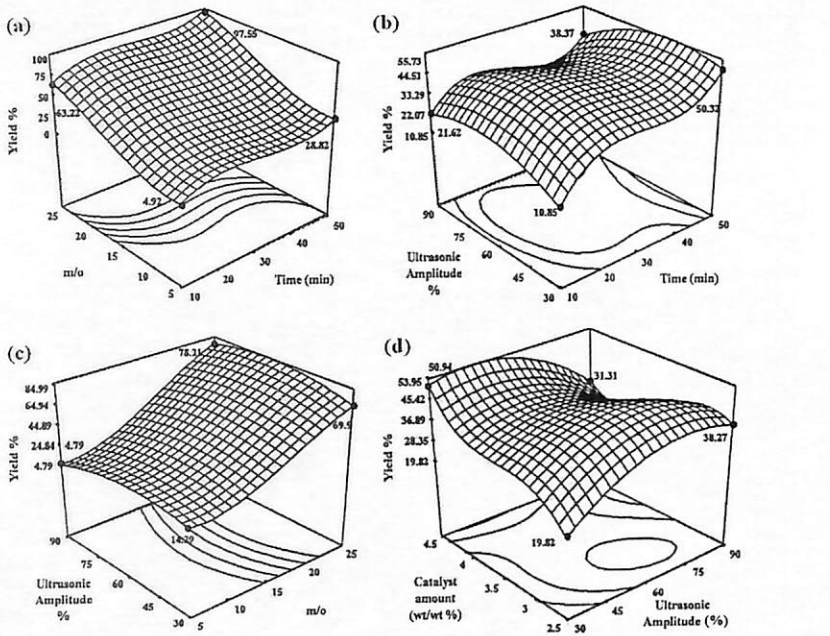

Fig. 5. Interactions between the reaction parameters. (a) between the reaction time and the methanol/oil ratio, (b) between the reaction time and the ultrasonic amplitude, (c) between the methanol/oil ratio and the ultrasonic amplitude, and (d) between the ultrasonic amplitude and the catalyst amount.

Author's personal copy

increment in the sizes and numbers of the droplets which led to an increase the available interface area between the reactants [22]. During the ultrasonic emulsification, coalescence phenomenon attributed to the collision of small droplets when the droplet concentration increased beyond a certain level and when the acoustic streaming strength was increase could also be observed [34].

Increasing ultrasonic amplitude had its positive effects on the reaction yield for all catalyst amounts to a level of 50–60%. However, negative effects were observed beyond these levels as can be observed in Fig. 5(d). For catalyst amounts above 3.5%, a decrease in the reaction yield was obtained when the ultrasonic amplitude was set beyond 60% level. The increasing trend in the reaction yield under low to moderate ultrasonic amplitude could be attributed to the enhancement in the heterogeneous catalyst reactivity due to the ultrasonic dispersion of the reactants on the catalytic active sites of the catalyst. As the crucial factor of any heterogeneous catalyzed system is the contact between the reactants and the catalyst, the cavitational shear force generated by the ultrasonic irradiation created much smaller reactant droplets to improve the interaction between the reactants and the catalyst. This, in turn, increased the available surface area for the reactants and led to the enhancement in the reaction yield. The role of moderate ultrasonic amplitude was also reported for different ultrasound-assisted catalytic processes [22,33,35]. In contrast, for high ultrasonic amplitude, the effects of large, long lived and stable cavitational bubbles had dominant negative influence on the emulsification process regardless of the presence of higher number of acid active sites in the catalyst system.

3.5. Process optimization

In order to identify the optimum reaction conditions and to investigate the validity of the proposed design, Design expert 6.0.6 software was used to fit the experimental data to the historical design. 10 possible solutions for the design were generated according to the order of suitability relating the proposed reaction variables value with the expected transesterification yield. Three solutions were chosen and the corresponding experimental runs were conducted as presented in Table 7. The experimental results were in good agreement with the predicted yields within ~4% of error.

It could be observed that the effect of catalyst combined with the ultrasonic mixing improved the transesterification for high FFA content crude Jatropha oil. $Cs_{1.5}H_{1.5}PW_{12}O_{40}$ solid acid catalyst powered by moderate ultrasonic amplitude of 67% was deemed to have its good influence on an acid catalyzed system to achieve 90.5% of FAME yield in just ~34 min of reaction. $Cs_{2.3}H_{0.7}PW_{12}O_{40}$ has been used for the esterification of palmitic acid and transesterification of tributyrin conducted at 6 h of reaction time under conventional process to achieve conversions of 100% and 50.2%, respectively [36]. In a related case, esterification of rice bran fatty acids conducted by Srilatha et al. [37] achieved 92.0% conversion using $Cs_1H_2PW_{12}O_{40}$ within 200 min of reaction. Low reaction yields were reported by Zieba et al. [38] for the transesterification of castor oil with methanol conducted for 180 min at a molar ratio 29:1 using $Cs_2H_1PW_{12}O_{40}$ and $K_2H_1PW_{12}O_{40}$ catalysts.

The significant role of ultrasound in allowing the transesterification reaction to be carried out at relatively low reaction temperature was also due to the generated heat during the collapses of the cavitation bubbles. Acid-catalyzed biodiesel production generally requires high reaction temperature to reduce the viscosity of the reactants in order to obtain an acceptable level of mixing due to the slow reaction rate [7]. Significant saving in the energy input of the process could be achieved as extra heating requirement was not needed in the current study. Significant reduction in the energy input requirements for the process was achieved due to short reaction time and low reaction temperature needed for the process.

3.6. Catalyst stability and reusability

The catalyst stability towards leaching is associated by the dissolution of the active component of the catalysts due to the contact with polar reaction mixture. The test revealed that 9.2% of reaction yield was obtained by the leached $PW_{12}O_{40}^{3-}$ anion from the catalyst structure. Shin et al. [39] reported different leaching levels for Cs doped TPA catalysts under super critical methanol process. Catalyst stability was also verified by Narasimharao et al. [36] who performed leaching tests in hot methanol. The results revealed that low Cs content catalysts showed higher tendency toward leaching while materials with higher Cs content were more stable which confirmed their heterogeneous mode of reaction. Low leaching amount of Cs salt of TPA in water was also reported by Yuan et al. [40].

Fig. 6 shows the FAME yields of successive reaction runs to reveal the potential for catalyst reusability. It can be concluded that only 3.8% of the catalytic activity was lost in the first run. For the second and third runs, 2.7% and 1.6% drops were observed, respectively. These reductions could be attributed to the heteropoly anion leaching and the washing process that was conducted between the cycles. Thus, under ultrasonic irradiation conditions and in polar reaction mixture, $Cs_{1.5}H_{1.5}PW_{12}O_{40}$ demonstrated good catalytic stability and low leaching behavior.

4. Conclusions

Transesterification of high FFA content crude Jatropha oil in the presence of Cs doped TPA solid acid catalyst in an ultrasound-irradiated reactor system was successfully conducted. Cs exchanged TPA catalyst at a molar ratio of 1.5 had its maximum effect on the reaction yield while further increase in the Cs amount was detrimental to the reaction. Four reaction variables were successfully optimized and the results revealed that moderate ultrasonic amplitude applied to the reaction mixture had a positive effect while high amplitudes could decrease the yield. Relatively short reaction time (~34 min), low reaction temperature (65 °C) and low catalyst amount (2.94 w/w) compared to those of other HPA salt catalyzed processes were demonstrated by the system. $Cs_{1.5}H_{1.5}PW_{12}O_{40}$ catalyst was also investigated for possible catalyst reusability and leaching of active component in the polar reaction mixture was evaluated. Major part of the catalytic activity was contributed by heterogeneous reaction and the catalyst showed

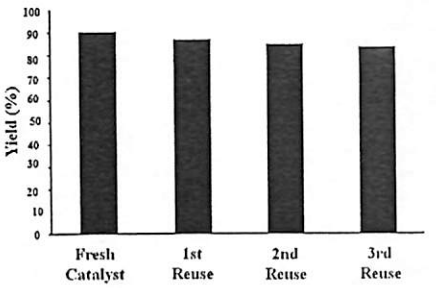

Fig. 6. Catalytic activity for successive reaction runs for $Cs_{1.5}H_{1.5}PW_{12}O_{40}$ catalyst under the optimum reaction conditions (reaction time 33 min, methanol/oil ratio 25, ultrasonic amplitude 67% and catalyst amount 2.94% wt/wt of oil).

minimal reductions in the reactivity when used in several successive reaction runs.

Acknowledgment

A Research University grant (814144) to support this work is gratefully acknowledged.

References

[1] Helwani Z, Othman MR, Aziz N, Kim J, Fernando WJN. Solid heterogeneous catalysts for transesterification of triglycerides with methanol: a review. Appl Catal A 2009;363(1–2):1–10.
[2] Jain S, Sharma MP. Prospects of biodiesel from Jatropha in India: A review. Renew Sust Energy Rev 2010;14(2):763–71.
[3] Uzun BB, Kilic M, Ozbay N, Pütün AE, Pütün E. Biodiesel production from waste frying oils: optimization of reaction parameters and determination of fuel properties. Energy 2012;44(1):347–51.
[4] Endalew AK, Kiros Y, Zanzi R. Heterogeneous catalysis for biodiesel production from Jatropha curcas oil (JCO). Energy 2011;36(5):2693–700.
[5] Lee HV, Taufiq-Yap YH, Hussein MZ, Yunus R. Transesterification of jatropha oil with methanol over Mg–Zn mixed metal oxide catalysts. Energy 2013;49:12–8.
[6] Peng-Lim D, Ganesan S, Mantam GP, Khairuddean M. Sequential conversion of high free fatty acid oils into biodiesel using a new catalyst system. Energy 2012;46(1):112–9.
[7] Lam MK, Lee KT, Mohamed AR. Homogeneous, heterogeneous and enzymatic catalysis for transesterification of high free fatty acid oil (waste cooking oil) to biodiesel: a review. Biotechnol Adv 2010;28(4):500–18.
[8] Chai F, Cao F, Zhai F, Chen Y, Wang X, Su Z. Transesterification of vegetable oil to biodiesel using a heteropolyacid solid catalyst. Adv Synth Catal 2007;349(7):1057–65.
[9] Santos JS, Dias JA, Dias SCL, Garcia FAC, Macedo JL, Sousa FSG, et al. Mixed salts of cesium and ammonium derivatives of 12-tungstophosphoric acid: synthesis and structural characterization. Appl Catal A 2011;394(1–2):138–48.
[10] Sepúlveda JH, Yori JC, Vera CR. Repeated use of supported H3PW12O40 catalysts in the liquid phase esterification of acetic acid with butanol. Appl Catal A 2005;288(1–2):18–24.
[11] Zhang S, Zu Y-G, Fu Y-J, Luo M, Zhang D-Y, Efferth T. Rapid microwave-assisted transesterification of yellow horn oil to biodiesel using a heteropolyacid solid catalyst. Biores Technol 2010;101(3):931–6.
[12] Badday AS, Abdullah AZ, Lee KT, Khayoon MS. Intensification of biodiesel production via ultrasonic-assisted process: a critical review on fundamentals and recent development. Renew Sust Energy Rev 2012;16(7):4574–87.
[13] Guo W, Li H, Ji G, Zhang G. Ultrasound-assisted production of biodiesel from soybean oil using Brunsted acidic ionic liquid as catalyst. Biores Technol 2012;125(0):332–4.
[14] Mootabadi H, Salamatinia B, Bhatia S, Abdullah AZ. Ultrasonic-assisted biodiesel production process from palm oil using alkaline earth metal oxides as the heterogeneous catalysts. Fuel 2010;89(8):1818–25.
[15] Salamatinia B, Mootabadi H, Bhatia S, Abdullah AZ. Optimization of ultrasonic-assisted heterogeneous biodiesel production from palm oil: a response surface methodology approach. Fuel Proc Technol 2010;91(5):441–8.
[16] Deshmane VG, Gogate PR, Pandit AB. Ultrasound-assisted synthesis of biodiesel from palm fatty acid distillate. Ind Eng Chem Res 2009;48(17):7923–7.
[17] Kelkar MA, Gogate PR, Pandit AB. Intensification of esterification of acids for synthesis of biodiesel using acoustic and hydrodynamic cavitation. Ultrason Sonochem 2008;15(3):188–94.
[18] Parkar PA, Choudhary HA, Moholkar VS. Mechanistic and kinetic investigations in ultrasound assisted acid catalyzed biodiesel synthesis. Chem Eng J 2012;187(0):248–60.
[19] De Castro ML, Capote FP. Analytical applications of ultrasound. Elsevier Science Limited; 2007.
[20] Ji J, Wang J, Li Y, Yu Y, Xu Z. Preparation of biodiesel with the help of ultrasonic and hydrodynamic cavitation. Ultrasonics 2006;44(Supplement 1):e411–4.
[21] Kalva A, Sivasankar T, Moholkar VS. Physical mechanism of ultrasound-assisted synthesis of biodiesel. Ind Eng Chem Res 2008;48(1):534–44.
[22] Stavarache C, Vinatoru M, Nishimura R, Maeda Y. Fatty acids methyl esters from vegetable oil by means of ultrasonic energy. Ultrason Sonochem 2005;12(5):367–72.
[23] Alemdaroglu T. Determination methods for the acidity of solid surfaces. Comm Fac Sci Univ Ank Series B 2001;47(2001):27–35.
[24] Badday AS, Abdullah AZ, Lee K- T. Optimization of biodiesel production process from jatropha oil using supported heteropolyacid catalyst and assisted by ultrasonic energy. Renew Energy 2013;50(0):427–32.
[25] Ferreira P, Fonseca IM, Ramos AM, Vital J, Castanheiro JE. Acetylation of glycerol over heteropolyacids supported on activated carbon Catal Comm 2011;12(7):573–6.
[26] Zhang J, Sun M, Cao C, Zhang Q, Wang Y, Wan H. Effects of acidity and microstructure on the catalytic behavior of cesium salts of 12-tungstophosphoric acid for oxidative dehydrogenation of propane. Appl Catal A 2010;380(1–2):87–94.
[27] Obali Z, Doğu T. Activated carbon–tungstophosphuric acid catalysts for the synthesis of tert-amyl ethyl ether (TAEE). Chem Eng J 2008;138(1–3):548–55.
[28] Okamoto K, Uchida S, Ito T, Mizuno N. Self-organization of all-inorganic dodecatungstophosphate nanocrystallites. J Am Chem Soc 2007;129(23):7378–84.
[29] Leung DYC, Wu X, Leung MKH. A review on biodiesel production using catalyzed transesterification. Appl Energy 2010;87(4):1083–95.
[30] Choudhury HA, Chakma S, Moholkar VS. Mechanistic insight into sonochemical biodiesel synthesis using heterogeneous base catalyst. Ultrason Sonochem 2013;20(7):561–8.
[31] Sen R. Response surface optimization of the critical media components for the production of surfactin. J Chem Technol Biotechnol 1997;68(3):263–70.
[32] Avramovic JM, Stamenkovic OS, Todorovic ZB, Lazic ML, Veljkovic VB. The optimization of the ultrasound-assisted base-catalyzed sunflower oil methanolysis by a full factorial design. Fuel Proc Technol 2010;91(11):1551–7.
[33] Kumar D, Kumar G, Poonam, Singh CP. Ultrasonic-assisted transesterification of Jatropha curcus oil using solid catalyst, Na/SiO_2. Ultrason Sonochem 2010;17(5):839–44.
[34] Gaikwad SG, Pandit AB. Ultrasound emulsification: effect of ultrasonic and physicochemical properties on dispersed phase volume and droplet size. Ultrason Sonochem 2008;15(4):554–63.
[35] Kumar D, Kumar G, Poonam, Singh CP. Fast, easy ethanolysis of coconut oil for biodiesel production assisted by ultrasonication. Ultrason Sonochem 2010;17(3):555–9.
[36] Narasimharao K, Brown DR, Lee AF, Newman AD, Siril PF, Tavener SJ, et al. Structure–activity relations in Cs-doped heteropolyacid catalysts for biodiesel production. J Catal 2007;248(2):226–34.
[37] Srilatha K, Sree R, Prabhavathi Devi BLA, Sai Prasad PS, Prasad RBN, Lingaiah N. Preparation of biodiesel from rice bran fatty acids catalyzed by heterogeneous cesium-exchanged 12-tungstophosphoric acids. Biores Technol 2012;116(0):53–7.
[38] Zicha A, Matachowski L, Lalik E, Drelinkiewicz A. Methanolysis of castor oil catalysed by solid potassium and cesium salts of 12-tungstophosphoric acid. Catal Lett 2009;127(1–2):183–94.
[39] Shin H-Y, An S-H, Sheikh R, Park YH, Bae S-Y. Transesterification of used vegetable oils with a Cs-doped heteropolyacid catalyst in supercritical methanol. Fuel 2012;96(0):572–8.
[40] Yuan C, Zhang F, Wang J, Ren X. 12-phosphotungstic acid and its Cs salt supported on various porous carriers as catalysts for the synthesis of fructone Catal Comm 2005;6(11):721–4.

Chemical Engineering and Processing 75 (2014) 31–37

Contents lists available at ScienceDirect

Chemical Engineering and Processing: Process Intensification

journal homepage: www.elsevier.com/locate/cep

Artificial neural network approach for modeling of ultrasound-assisted transesterification process of crude Jatropha oil catalyzed by heteropolyacid based catalyst

Ali Sabri Badday, Ahmad Zuhairi Abdullah*, Keat-Teong Lee

School of Chemical Engineering, Universiti Sains Malaysia, 14300 Nibong Tebal, Penang, Malaysia

ARTICLE INFO

Article history:
Received 23 June 2013
Received in revised form 26 August 2013
Accepted 25 October 2013
Available online 2 November 2013

Keywords:
Jatropha oil
Heteropolyacids
Ultrasound-assisted transesterification
Artificial neural network
Network training method

ABSTRACT

Transesterification of crude Jatropha oil to fatty acid methyl esters in an ultrasound-assisted process was conducted in the presence of different heteropolyacid-based catalysts. Tungstophosphoric acid immobilized on activated carbon and gamma alumina as well as cesium salt of the heteropoly acid were prepared and characterized for elucidation of their properties. The experimental data collected from the central composite design were used to establish artificial neural network (ANN) model in order to predict the response in the reaction. The models were also optimized to identify the suitable network topology and training method. The results obtained from ANN models were compared with the results of the regression analysis and good agreement was obtained to suggest the good potential of ANN in the FAME yield prediction.

1. Introduction

Transesterification is the most popular way to convert vegetable oils or animal fats to biofuel [1]. The main product is a mixture of fatty acid methyl esters (FAME) better known as biodiesel. Theoretically, 3:1 molar ratio of alcohol to triglyceride is needed to complete a transesterification process. Practically, the presence of excess alcohol in the reaction mixture and a catalyst (acid or base) could accelerate and control the equilibrium to achieve a high yield of the ester [2]. This reaction can be catalyzed by basic or acidic catalysts. However, basic catalysts can result in higher reaction rate while acid catalysts are more preferred in the case of significant impurities present in the reactants [1].

Due to their unique physicochemical properties, heteropolyacids have been widely used as acid catalysts in various chemical reactions and oxidation processes [3]. Yet, the solubility problem and low surface area of the HPAs (1–5 m^2/g) [4] are the main reasons for the immobilization of the active acidic component on appropriate porous support materials. An appropriate technique to create major effects on the surface area, pore and solubility of the parent HPA by partial substitution of H^+ in HPA with alkaline cations can also be conducted [5]. HPA-based catalysts generally show higher tolerance to water and FFA that will enable the use of cheap and readily available feed stocks for the transesterification reaction [6–10] to improve the overall economy of the FAME production process.

The methods for elucidating the effects of process parameters on the response have shifted from the costly and time consuming trial and error searches to powerful, elegant, and cost-effective statistical methods. Design of experiment (DOE) is a systematic approach used to investigate a system or process. It consists of a series of designed tests that subject planned changes to the input factors on a process to assess the effects on the process output. This method can achieve the identification of the "best" experimental conditions to be adopted in the experimentation [11]. On the other hand, artificial neural network (ANN) is a powerful mathematical modeling tool designed for complex systems. Since 1940s, ANN methods have been successfully applied in different areas of engineering and science [12].

Neural network is a parallel distributed processor consisting of simple processing units called neurons which have tendencies for storing experimental knowledge and make it ready to use. ANN resembles human brain in two respects i.e. gaining the knowledge from its environment by learning process and storing the acquired knowledge using the strength of interneuron connections known as synaptic weights. The process used to conduct the learning process is called the learning algorithm which has the function of modifying the weights via a systematic fashion to address the required purposes [13].

Rajković et al. [14] compared the use of ANN with the topology 4–10–1 with the response surface methodology (RSM) for ultrasound-assisted sunflower oil transesterification using KOH

* Corresponding author. Tel.: +60 4 599 6411; fax: +60 4 594 1013.
E-mail addresses: chzuhairi@eng.usm.my, azuhairi@yahoo.com (A.Z. Abdullah).

0255-2701/$ – see front matter © 2013 Elsevier B.V. All rights reserved.
http://dx.doi.org/10.1016/j.cep.2013.10.008

Table 1
Properties of the crude Jatropha oil.

Property	Value
Density (kg/m³)	921
Viscosity (cSt)	38.12
Molecular weight	870
Water content (wt.%)	0.161
FFA content (wt.%)	10.5

catalyst. Four input factors i.e. methanol/oil molar ratio, reaction temperature, catalyst loading and reaction time and one output response i.e. FAME yield were included into the optimization study. The ANN was proven to be a powerful tool for modeling and optimizing FAME production as less deviation between the experimental and simulated values was achieved compared to that in an RSM model.

In the present study, ultrasound-assisted transesterification process of crude Jatropha oil was studied. Particular focus has been given on the comparison between the regression analyses approach and ANN modeling to show the validity of the models in accurately expressing the process.

2. Experimental

2.1. Reagents and materials

Tungstophosphoric acid ($H_3PW_{12}O_{40}{\cdot}nH_2O$), abbreviated as TPA in this manuscript, was supplied by Merck (Malaysia) while cesium chloride was purchased from Sigma–Aldrich (Malaysia). Gamma alumina support was purchased from Merck (Malaysia) and activated carbon (AC) support was purchased from Galcon Carbon Corporation (USA). Crude Jatropha oil was supplied by Telaga Madu Resources (Malaysia) and the properties of the crude Jatropha oil are tabulated in Table 1. Methanol used in the transesterification reaction was supplied by Thermo Fisher Scientific Inc. (USA) while ethanol (for catalyst preparation) and n-hexane (for product analysis) were purchased from Merck (Malaysia). Meanwhile, reference FAME standards were supplied by NuChek Prep. Inc. (Australia).

2.2. Catalysts preparation

TPA supported on activated carbon and supported on gamma-alumina catalysts were synthesized as discussed in [6,7]. For preparation of Cs-doped heteropolyacid catalyst, 0.1 M of Cs_5 solution was first prepared by dissolving a pre-calculated amount of cesium chloride in 50:50 v/v of deionized water and ethanol solution. Milky suspension solution was formed during the drop wise addition of the Cs solution to 0.08 M TPA solution under constant stirring. The TPA solution was then prepared by dissolving a calculated amount of TPA in 50:50 v/v of deionized water and ethanol solution. After the addition, the white precipitate solution was left for aging without stirring for 12 h at ambient temperature. Then, the solution was evaporated in a rotary evaporator to collect the white powder which was then washed excessively using deionized water before drying in an oven at 110 °C for 2 h. The powder was then calcined at 200 °C for 4 h.

2.3. Catalysts characterization

Nitrogen adsorption–desorption isotherms and Brunauer–Emmet–Teller (BET) surface area for the synthesized catalysts were measured by means of an Autosorb 1C system. The BET surface area was calculated from the linear part of the adsorption plot between $0.0 < P/P_0 < 0.3$. The pore size distribution plots were obtained using the Barrett–Joyner–Halenda (BJH) model. The confirmation of the tungstophosphoric species after the catalyst preparation procedure was investigated by means of Raman spectroscopy. The Raman spectra of the supports and the synthesized catalysts were collected using a Raman Module (Jobin Yvon HR 800 UV) equipped with a CCD array detector. The samples were excited by an argon ion laser source with a wavelength of 514.55 nm. The catalyst samples were measured in the range of 200–1200 cm^{-1}. Surface acidity measurement for the prepared catalysts and the support materials was evaluated using titration method after a displacement reaction [15].

2.4. Transesterification reaction

The experimental setup and the equipment used to conduct the ultrasound-assisted reactions are described in detail elsewhere [6,7]. In a typical experimental run, the desired amount of oil was transferred into the reactor and placed in a water bath until it reached the desired reaction temperature. Then, a required preheated amount of methanol was added to the oil according to the desired molar ratio of the reactants followed by the desired amount of catalyst. At this point, ultrasonification was started and a condenser attached to the system was switched on to recover the evaporated methanol. Ultrasonic energy was supplied in a discrete pattern i.e. 10 s on and 3 s off at a certain percentage of the maximum power. After the required reaction time, the reaction mixture was quenched in cold water and the excess methanol was evaporated out. The reaction mixture was then separated into two layers by centrifugation at 3500 rpm for 25 min. The upper FAME layer was then collected for GC analysis. For all experimental runs, the water bath temperature was fixed at about 54 °C. In this system, the heat generated by the ultrasonic probe combined with the heat gained from the water bath successfully maintained the reaction temperature at 65 ± 1 °C. All the experiments were carried out in the presence of air under atmospheric pressure.

2.5. Product analysis

Analyses of the products were conducted using an Agilent gas chromatograph (GC) (7890 A). The GC unit was equipped with a flame ionization detector (FID) and fitted with a capillary column (Agilent Technologies, Inc. 19091J-413 HP-5) with dimensions of 30 m × 0.32 mm × 0.25 μm. The system was operated using an auto-injector mode and controlled with a PC.

2.6. Experimental design

In order to optimize the reaction conditions for ultrasound-assisted transesterification reaction, Design Expert 6.0.6 software was used. The software was employed to generate the design matrix (central composite design or CCD) for four reaction variables to analyze the data and to create mathematical expressions that can predict the reaction response by statistically fitting of the experimental responses on appropriate mathematical terminology. The selection of the center values for the reaction variables was accomplished as discussed previously [6,7]. Coded and actual reaction variables used in the experimental design are presented in Table 2.

2.7. Artificial neural network modeling

The data collected from the CCD matrix and the experimental yield values for the three catalysts were used for network training to establish the network model that could compute the predicted yield values from the input reaction conditions using MATLAB R2011b software. All experimental data were divided randomly into three groups i.e. training (70%), validation (15%) and testing data (15%). The results of different networks architecture

Table 2
Coded and actual reaction variables used in the experimental design.

Real variables	Coded variables	Level				
		−α	−1	0	+1	+α
Reaction time (min)	X_1	10	20	30	40	50
Molar ratio	X_2	5:1	10:1	15:1	20:1	25:1
Ultrasonic amplitude (%)	X_3	30	45	60	75	90
Catalyst amount (w/w %)	X_4	2.5	3	3.5	4	4.5

Table 3
Properties of the supports and the synthesized catalysts.

Sample	BET surface area (m^2/g)	Total pore volume (cm^3/g)	Average pore diameter (Å)	Surface acidity (μ mol/g catalyst)
AC	750	0.47	25.23	520
TPA20-AC	621	0.39	25	1570
Al	109.4	0.23	82.6	330
TPA25-Al	93.3	0.13	54.9	1300
Cs1.5HPW	32.72	0.087	106.9	1750

and training procedures were compared based on the coefficient of determination (R^2) and the standard deviation (σ). The number of hidden neurons in the hidden layer as well as the training algorithm was optimized to highlight the most effective network architecture and training procedure that would lead to the best predicted results. The number of neurons was optimized between 3 and 20 neurons in the hidden layer applying three different training algorithms for each catalyst. Levenberg–Marquardt backpropagation (trainlm), scaled conjugate gradient backpropagation (trainscg), and resilient backpropagation (trainrp) algorithms were chosen for training the designed networks.

Levenberg–Marquardt back propagation algorithm was designed to approach the second order training speed without the need for calculating the Hessian matrix as the matrix is approximated to a simplest form. The Jacobian matrix, which consisted of the first derivative of the network error was computed by back-propagation method used in the approximation as it was much less complex than the Hessian matrix [16]. In the conjugate gradient back propagation algorithm, the step size was regulated at each iteration and the search was conducted along the conjugate directions producing faster convergence comparing to steepest descent directions [17]. On the other hand, resilient back propagation algorithm could eliminate the harmful effects of the use of the steepest descent with sigmoid transfer functions in training the network that caused small changes in biases and weights even thought they were far from its optimal values [16].

The proposed network architecture is presented in Fig. 1 for the applicant feeds of the ultrasound assisted transesterification

Table 4
CCD matrix and the respective responses using the three catalysts.

Run	Point type	Real Variables				Yield (%)		
		Time (min)	M/O[a]	Amplitude (%)	Catalyst Amount (w/w %)	TPA 20-AC	TPA 25-Al	Cs1.5 HPW
1	Fact	40	20	45	3.0	82.31	60.49	60.94
2	Fact	20	10	45	4.0	40.74	37.55	26.43
3	Fact	20	20	75	4.0	63.55	53.27	64.43
4	Fact	40	10	75	4.0	46.50	35.16	12.95
5	Fact	20	10	45	3.0	42.19	38.16	20.67
6	Fact	20	20	75	3.0	56.3	49.34	66.96
7	Fact	40	10	75	3.0	42.13	43.74	23.21
8	Fact	20	20	45	4.0	57.46	58.45	56.09
9	Fact	40	20	75	3.0	88.23	61.22	75.15
10	Fact	40	10	45	3.0	42.32	45.4	23.14
11	Fact	40	10	45	4.0	44.72	41.55	19.13
12	Fact	40	20	75	4.0	90.60	84.16	44.26
13	Fact	20	20	45	3.0	54.04	51.89	61.14
14	Fact	40	20	45	4.0	88.96	61.15	65.06
15	Fact	20	10	75	4.0	48.42	36.03	24.70
16	Fact	20	10	75	3.0	35.53	37.7	18.27
17	Axial	30	25	60	3.5	89.33	83.74	87.89
18	Axial	30	15	60	4.5	75.60	66.52	54.96
19	Axial	30	15	90	3.5	71.06	68.78	36.50
20	Axial	10	15	60	3.5	37.68	48.33	30.07
21	Axial	30	5	60	3.5	28.31	33.57	23.37
22	Axial	50	15	60	3.5	70.80	54.18	58.18
23	Axial	30	15	30	3.5	63.32	42.67	37.09
24	Axial	30	15	60	2.5	69.97	46.05	42.88
25	Center	30	15	60	3.5	62.27	55.47	41.58
26	Center	30	15	60	3.5	75.10	62.95	48.04
27	Center	30	15	60	3.5	71.95	60.94	42.38
28	Center	30	15	60	3.5	67.11	57.31	46.18
29	Center	30	15	60	3.5	69.72	59.44	44.13
30	Center	30	15	60	3.5	70.47	51.38	38.68

[a] Methanol to oil ratio.

Table 5
Predicted and experimental results at the optimum conditions for the catalysts.

Catalyst	Reaction Conditions				Predicted yield %	Experimental yield %	Error %
	Time (min)	Molar ratio	Amplitude (%)	Catalyst amount (w/w)			
TPA20-AC	38	25	73	4.23	96.26	91.34	5.11
TPA25-Al	47.17	19.05	64.32	4.44	86.19	83.63	2.97
Cs1.5HPW	33.14	25.00	67	2.94	87.06	90.46	3.90

Table 6
Experimental and predicted FAME yields generated by neural network models using various number of neurons and training algorithms.

TPA20-AC				TPA25-Al				Cs1.5HPW			
Exp.	No. of neurons			Exp.	No. of neurons			Exp.	No. of neurons		
	5	4	19		10	8	19		7	8	14
	LM	RP	SCG		LM	RP	SCG		LM	RP	SCG
82.31	83.66	85.13	79.808	60.49	63.24	60.88	55.86	60.94	60.44	67.98	60.07
40.74	40.712	39.37	44.72	37.55	35.11	37.15	37.02	26.43	25.64	27.09	30.96
63.55	63.50	62.20	64.840	53.27	53.51	59.31	64.68	64.43	62.14	58.26	65.21
46.50	46.51	55.91	61.81	35.16	36.63	45.78	47.85	12.95	12.29	13.28	26.01
42.19	42.11	40.06	41.01	38.16	38.07	36.33	35.21	20.67	18.64	22.74	20.64
56.30	65.89	61.25	57.02	49.34	43.68	53.78	50.57	66.96	66.78	67.89	58.87
42.13	42.00	44.00	45.35	43.74	49.29	45.29	49.59	23.21	13.80	24.18	29.22
57.46	57.40	58.52	66.02	58.45	59.26	51.82	59.68	56.09	56.13	59.60	58.94
88.23	88.15	85.22	88.51	61.22	58.08	64.10	67.12	75.15	76.05	69.60	73.05
42.32	42.30	45.49	42.95	45.40	52.53	44.34	41.30	23.14	18.44	30.03	18.14
44.72	44.71	47.82	46.21	41.55	40.33	50.98	46.33	19.13	19.15	23.87	21.47
90.60	90.60	95.03	86.98	84.16	66.66	79.94	78.37	44.26	51.15	48.45	47.46
54.04	58.01	64.99	50.89	51.89	48.15	54.92	57.78	61.14	59.94	63.48	62.30
88.96	88.90	85.84	88.37	61.15	64.91	63.97	70.33	65.06	64.84	67.12	60.75
48.42	42.04	46.45	51.58	36.03	35.48	36.96	45.25	24.70	24.05	24.81	24.48
35.53	46.24	40.55	35.18	37.70	37.15	34.53	38.60	18.27	19.04	20.93	17.25
89.33	89.30	82.05	89.07	83.74	80.89	79.94	79.88	87.89	87.56	84.44	88.71
75.60	75.50	77.73	69.54	66.52	68.19	49.32	62.46	54.96	52.24	36.63	47.17
71.06	71.60	72.17	71.17	68.78	66.80	65.94	67.12	36.50	35.87	25.90	36.46
37.68	37.60	39.29	33.17	48.33	40.61	47.63	41.36	30.07	37.43	36.65	35.63
28.31	28.30	25.18	24.51	33.57	32.55	32.78	24.44	23.37	23.70	18.37	15.81
70.80	60.51	67.07	66.31	54.18	57.97	53.15	63.44	58.18	50.81	54.30	41.23
63.32	63.31	73.85	64.43	42.67	43.20	43.25	46.98	37.09	37.20	37.70	41.87
69.97	69.92	70.04	65.93	46.05	46.46	45.97	45.44	42.88	35.00	44.10	39.60
62.27	67.90	72.52	71.53	55.47	59.88	56.95	51.48	41.58	44.14	38.67	43.15
75.10	67.90	72.52	71.53	62.95	59.88	56.95	51.48	49.04	44.14	38.67	43.15
71.95	67.90	72.52	71.53	60.94	59.88	56.95	51.48	42.38	44.14	38.67	43.15
67.11	67.90	72.52	71.53	57.31	59.88	56.95	51.48	46.18	44.14	38.67	43.15
69.72	67.90	72.52	71.53	59.44	59.88	56.95	51.48	44.13	44.14	38.67	43.15
70.47	67.90	72.52	71.53	51.38	59.88	56.95	51.48	38.68	44.14	38.67	43.15
R^2	0.95	0.93	0.93	-	0.86	0.84	0.74	-	0.96	0.90	0.91
σ	4.14	4.70	4.69	-	4.91	5.26	6.75	-	3.86	3.88	5.69

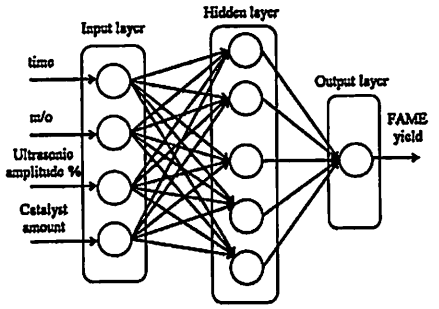

Fig. 1. Neural network architecture for the ultrasound-assisted process.

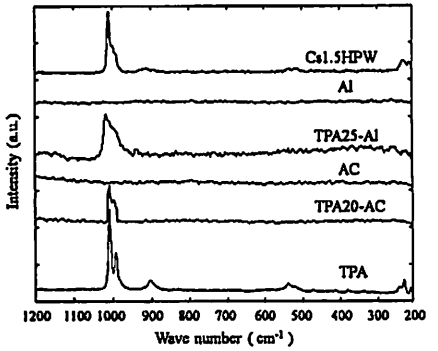

Fig. 2. Raman spectra for the TPA, supports, and the prepared catalysts.

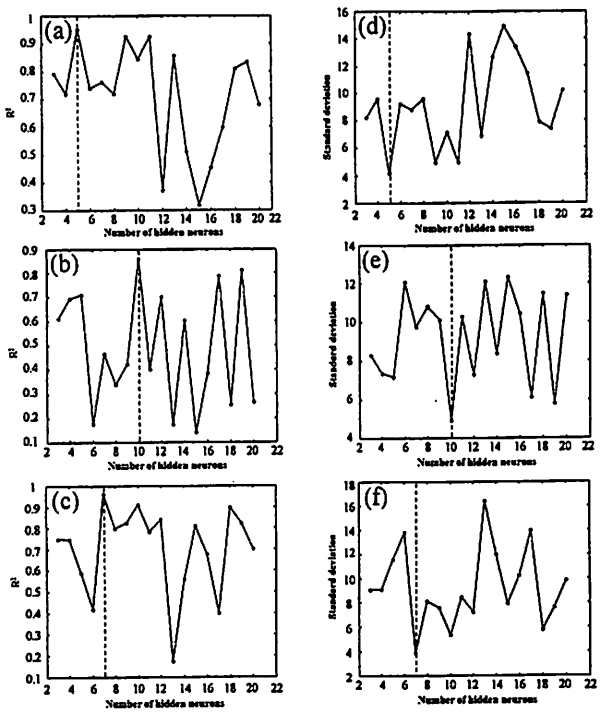

Fig. 3. Hidden neurons number based on R^2 for (a) TPA20-AC, (b) TPA25-Al, and (c) Cs1.5HPW, and based on σ for (d) TPA20-AC, (e) TPA25-Al, and (f) Cs1.5HPW.

process. The reaction time, reactants molar ratio, ultrasonic amplitude and catalyst amount were used as input parameters, while FAME yield was used as the output parameter.

3. Results and discussion

3.1. Catalysts characterization

The textural characterization results of TPA20-AC, TPA25-Al and Cs1.5HPW catalysts as well as the supported materials AC and Al combined with their surface acidity are shown in Table 3. Tungstophosphoric acid itself has low surface area of about 5 m^2/g [18]. The BET surface area of AC and Al supports used in this study were 750 m^2/g and 109.4 m^2/g, respectively. Effects of the inclusion the $PW_{12}O_{40}^{3-}$ anion in the mesoporous structure of the supported catalysts were seen as a reduction in the supports surface areas i.e. reductions of 17.2% in the case of AC supported catalyst and 14.6% in the case of Al supported catalyst. From the table, it can be concluded that immobilizing TPA on AC and Al resulted in reductions in surface area, microporous volume and total pore volume. This observation can be attributed to the partial blockage of pores by the active species. Similar reductions in the surface area and the pores of the catalyst were also reported in the work of Oball and Doğu [19] and Shringarpure and Patel [20]. The low surface acidity of the supports seemed to increase as the TPA immobilized on the catalysts.

Raman spectra of pure TPA, AC, Al and the catalysts are presented in Fig. 2. It can be seen that TPA shows strong characteristic bands at 1010 cm^{-1} attributed to the symmetric stretching (ν_s) of W=O_t and at 1000 cm^{-1} that was associated with the anti-symmetric stretching (ν_{as}) of W=O_t [21]. Low intensity bands appearing as shoulders are also noticed at 900 cm^{-1}, 532 cm^{-1} and 519 cm^{-1}. They are ascribed to W–O_b–W symmetric stretching vibration, W–O_c–W symmetric stretching vibration and O–P–O asymmetric deformation vibration, respectively [22,23].

No bands were detected for AC and Al samples while the presence of the Keggin anion can be easily proven by comparing the spectra of TPA20-AC and TPA25-Al with AC and Al. It can be noticed in TPA20-AC spectra that two bands appear at 1010 cm^{-1} and 1000 cm^{-1}. They are attributed to the strongest bands of (ν_s) W=O_t and (ν_{as}) W=O_t, respectively. The presence of $PW_{12}O_{40}$ anion in TPA25-Al could be proven as a band attributed to the strongest bands of (ν_s) W=O_t detected at 1010 cm^{-1}. The results also showed that the band at 1000 cm^{-1} appears as a shoulder in the figure as the intensity of (ν_{as}) W=O_t band was low compared to the symmetric stretching (ν_s) of W=O_t in the parent TPA. Low intensity bands were also detected by [24] who reported similar results for different TPA loadings on Al. High intensity bands were detected at 1010 cm^{-1} for Cs1.5HPW catalyst that is attributed to the symmetric stretching (ν_s) of W=O_t and that at 1000 cm^{-1} belongs to anti-symmetric stretching (ν_{as}) of W=O_t. Another band at 900 cm^{-1} was also noticed and it is attributed to W–O_b–W symmetric stretching at Cs1.5HPW catalyst. Meanwhile low intensity band appeared as a shoulder of W–O_c–W symmetric stretching vibration at 532 cm^{-1}. The results obtained from this test revealed the presence of TPA in the prepared catalysts as the relative bands related to the Keggin anion could be clearly detected.

3.2. RSM modeling

The design matrix generated by CCD for ultrasound-assisted crude Jatropha oil transesterification using the three catalysts is presented in Table 4. The table includes the point type, non-coded values of the reaction parameters and responses for the experiments. In order to identify the optimum reaction conditions and to investigate the validity of the proposed design, Design Expert 6.0.6 software was employed to fit the experimental data to a historical design. 10 possible solutions for each catalyst design were generated according to the order of suitability relating the proposed reaction variable values with the expected transesterification yield. Three solutions for each catalyst were chosen and the corresponding experimental runs were conducted as discussed in our published works [6,7] or in the complementary study for Cs salt catalyst. Table 5 presents the optimum reaction conditions for the three catalysts used in the current study.

3.3. Artificial neural network modeling

The results of the network models for the three catalysts for different neurons number in the hidden layer using different training algorithms for the optimum neuron number are presented in Table 6. It can be seen that for all the catalysts, Levenberg–Marquardt backpropagation algorithm was the best training procedure that achieved the highest R^2 and lowest σ. Levenberg–Marquardt algorithm is usually used for systems that contain moderate number of weights and have the fastest convergence. The advantage of this algorithm is especially noticeable if very accurate training is required. The algorithm can achieve the lowest standard deviation and mean square errors compared to any other algorithms [25]. However, as the number of network weights increases, the advantage of the algorithm decreases.

Using Levenberg–Marquardt backpropagation algorithm as the training process, Fig. 3 presents the calculated R^2 and σ values of the three catalysts networks versus the number of neurons in the hidden layer. It can be concluded from the values of R^2 that 5, 9 and 11 neurons in the hidden layer were suitable for TPA20-AC model as presented in Fig. 3(a). Combining these results with that for the minimum σ values in Fig. 3(d), it can be observed that the optimum number of neurons was 5 with R^2 value of 0.95 and σ value of 4.14. For TPA25-Al model, the optimum neurons number was 10 with R^2 and σ values of 0.86 and 4.91, respectively. Values of 0.96 of R^2 and 3.86 of σ confirmed that the optimum neurons number was 7 for Cs1.5HPW model. Thus, the optimum number of neurons was used for each model to create the network topologies which were 4–5–1 for TPA20-AC, 4–10–1 for TPA25-Al, and 4–7–1 for Cs1.5HPW. Here, the numbers in the expressions of the network topologies represent the neuron numbers in the input layer, the hidden layer and the output layer, respectively.

Fig. 4 shows the actual versus predicted yield values for the three catalysts. The figure illustrates that the predicted values comes in a good agreement with the experimental values inferring that the model was successfully developed to capture the correlation between reaction independent variables and FAME yield. The obtained R^2 values generated by the neural network models

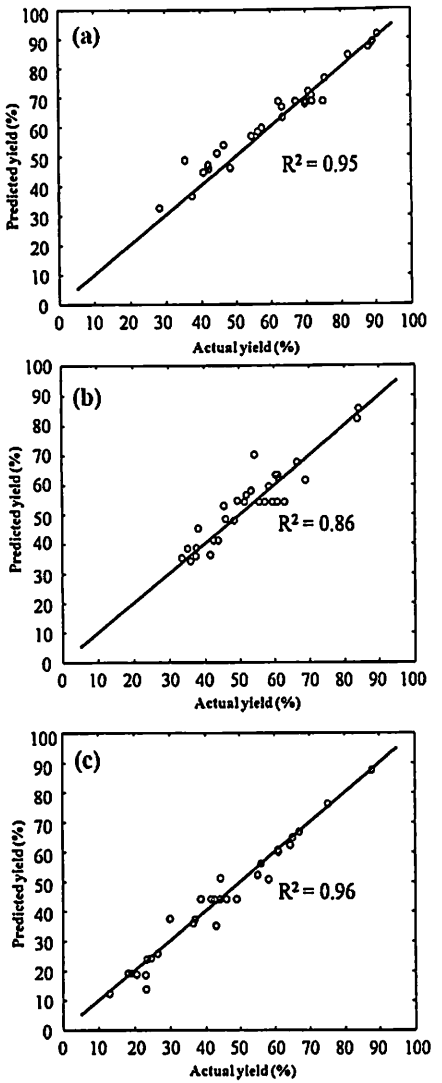

Fig. 4. Predicted vs. actual yield values for network models for (a) TPA20-AC, (b) TPA25-Al, and (c) Cs1.5HPW catalysts.

were compared with those generated by ANOVA analyses using regression model. The results revealed that R^2 values generated by regression analysis were 0.96, 0.90, and 0.94 for TPA20-AC, TPA25-Al, and Cs1.5HPW catalysts, respectively while R^2 values generated by the ANN were 0.95, 0.86, and 0.96 for the same three catalysts. It can be concluded that both procedures of modeling were efficiently able to accurately represent the experimental data and generate the suitable mathematical approach to predict the response of the reaction. However, two models for the studied catalysts generated by ANOVA analyses resulted in higher R^2 values than those obtained using ANN.

On the other hand, the mathematical representations of the models generated by ANN were too complicated in order to have good practical applicability. Thus, the use of the mathematical expressing would be difficult and it might require further programming steps. As such, comparison to identify a more suitable tool for representation the experimental data was actually in favor of the use of regression analysis.

4. Conclusions

The transesterification of crude Jatropha oil using ultrasound-assisted process was conducted in the presence of three heteropolyacid-based catalysts. Mathematical modeling was successfully accomplished for the three catalysts under respective optimum reaction conditions. The mathematical models developed based on ANN were able to accurately predict the reaction yields achieving results that were quite close approach to those of the mathematical representation obtained by the regression analyses. Optimizations for the neurons number in the hidden layer as well as the training method used revealed that Levenberg–Marquardt back propagation algorithm was the best method for the network training step.

Acknowledgements

Research grants in the form of a Short Term (60312010), an FRGS (6071205) and a Research University (814144) grants to support this research work are gratefully acknowledged.

References

[1] D.Y.C. Leung, X. Wu, M.K.H. Leung, A review on biodiesel production using catalyzed transesterification, Applied Energy 87 (2010) 1083–1095.
[2] X. Yin, H. Ma, Q. You, Z. Wang, J. Chang, Comparison of four different enhancing methods for preparing biodiesel through transesterification of sunflower oil, Applied Energy 91 (2012) 320–325.
[3] A. Towata, M. Sivakumar, K. Yasui, T. Tuziuti, T. Kozuka, Y. Iida, Ultrasound induced formation of paraffin emulsion droplets as template for the preparation of porous zirconia, Ultrasonics Sonochemistry 14 (2007) 705–710.
[4] H. Atia, U. Armbruster, A. Martin, Dehydration of glycerol in gas phase using heteropolyacid catalysts as active compounds, Journal of Catalysis 258 (2008) 71–82.
[5] J.S. Santos, J.A. Dias, S.C.L. Dias, F.A.C. Garcia, J.L. Macedo, F.S.G. Sousa, L.S. Almeida, Mixed salts of cesium and ammonium derivatives of 12-tungstophosphoric acid: synthesis and structural characterization, Applied Catalysis A: General 394 (2011) 138–148.
[6] A.S. Badday, A.Z. Abdullah, K.-T. Lee, Ultrasound-assisted transesterification of crude Jatropha oil using alumina-supported heteropolyacid catalyst, Applied Energy 105 (2013) 380–388.
[7] A.S. Badday, A.Z. Abdullah, K.-T. Lee, Optimization of biodiesel production process from Jatropha oil using supported heteropolyacid catalyst and assisted by ultrasonic energy, Renewable Energy 50 (2013) 427–432.
[8] F. Chai, F. Cao, F. Zhai, Y. Chen, X. Wang, Z. Su, Transesterification of vegetable oil to biodiesel using a heteropolyacid solid catalyst, Advancement in Synthesis and Catalysis 349 (2007) 1057–1065.
[9] N. Katada, T. Hatanaka, M. Ota, K. Yamada, K. Okumura, M. Niwa, Biodiesel production using heteropoly acid-derived solid acid catalyst $H_4PNbW_{11}O_{40}/WO_3$–Nb_2O_5, Applied Catalysis A: General 363 (2009) 164–168.
[10] G. Sunita, B.M. Devassy, A. Vinu, D.P. Sawant, V.V. Balasubramanian, S.B. Halligudi, Synthesis of biodiesel over zirconia-supported isopoly and heteropoly tungstate catalysts, Catalysis Communications 9 (2008) 696–702.
[11] F. Galvanin, M. Barolo, F. Bezzo, Towards on-line model-based design of experiments, In: B. Bertrand, J. Xavier (Eds.), Computer Aided Chemical Engineering, Elsevier, 2008, pp. 349–354.
[12] E. Jorjani, S. Chehreh Chelgani, S. Mesroghli, Application of artificial neural networks to predict chemical desulfurization of Tabas coal, Fuel 87 (2008) 2727–2734.
[13] S. Haykin, Neural Networks: A Comprehensive Foundation, Prentice Hall, New Jersey, 1994.
[14] K.M. Rajković, J.M. Avramović, P.S. Milić, O.S. Stamenković, V.B. Veljković, Optimization of ultrasound-assisted base-catalyzed methanolysis of sunflower oil using response surface and artificial neural network methodologies, Chemical Engineering Journal 215–216 (2013) 82–89.
[15] T. Alemdaroglu, Determination methods for the acidity of solid surfaces, Communications Faculty of Sciences University of Ankara Series B: Chemistry and Chemical Engineering 47 (2001) 27–35.
[16] O. Kisi, E. Uncuoglu, Comparison of three back-propagation training algorithms for two case studies, Indian Journal of Engineering and Materials Sciences 12 (2005) 434–442.
[17] H. Adeli, S.L. Hung, Machine Learning: Neural Networks, Genetic Algorithms and Fuzzy Systems, John Wiley and Sons, Inc., New Jersey, 1994.
[18] H.-Y. Shin, S.-H. An, R. Sheikh, Y.H. Park, S.-Y. Bae, Transesterification of used vegetable oils with a Cs-doped heteropolyacid catalyst in supercritical methanol, Fuel 96 (2012) 572–578.
[19] Z. Obali, T. Doğu, Activated carbon-tungstophosphoric acid catalysts for the synthesis of tert-amyl ethyl ether (TAEE), Chemical Engineering Journal 138 (2008) 548–555.
[20] P.A. Shringarpure, A. Patel, Supported undecatungstophosphate: an efficient recyclable bi-functional catalyst for esterification of alcohols as well as selective oxidation of styrene, Chemical Engineering Journal 173 (2011) 612–619.
[21] E. Caliman, J.A. Dias, S.C.L. Dias, F.A.C. Garcia, J.L. de Macedo, L.S. Almeida, Preparation and characterization of $H_3PW_{12}O_{40}$ supported on niobia, Microporous and Mesoporous Materials 132 (2010) 103–111.
[22] I. Holclajtner-Antunović, U.B. Mioč, M. Todorović, Z. Jovanović, M. Davidović, D. Bajuk-Bogdanović, Z. Lausević, Characterization of potassium salts of 12-tungstophosphoric acid, Materials Research Bulletins 45 (2010) 1679–1684.
[23] K. Mohan Reddy, N. Seshu Babu, P.S. Sai Prasad, N. Lingaiah, Aluminium-exchanged tungstophosphoric acid: an efficient catalyst for intermolecular hydroarylation of vinyl arenes, Catalysis Communications 9 (2008) 2525–2531.
[24] E. Caliman, J.A. Dias, S.C.L. Dias, A.G.S. Prado, Solvent effect on the preparation of $H_3PW_{12}O_{40}$ supported on alumina, Catalysis Today 107–108 (2005) 816–825.
[25] G.R. Moradi, S. Dehghani, F. Khosravian, A. Arjmandzadeh, The optimized operational conditions for biodiesel production from soybean oil and application of artificial neural networks for estimation of the biodiesel yield, Renewable Energy 50 (2013) 915–920.

Applied Energy 105 (2013) 380–388

Contents lists available at SciVerse ScienceDirect

Applied Energy

journal homepage: www.elsevier.com/locate/apenergy

Ultrasound-assisted transesterification of crude Jatropha oil using alumina-supported heteropolyacid catalyst

Ali Sabri Badday [1], Ahmad Zuhairi Abdullah [*,1], Keat-Teong Lee [1]

School of Chemical Engineering, Universiti Sains Malaysia, 14300 Nibong Tebal, Penang, Malaysia

HIGHLIGHTS

- Fatty acid methyl esters synthesis from crude Jatropha oil.
- Ultrasound-assisted transesterification system.
- Tungstophosphoric acid on gamma alumina catalysts.
- Effects of four reaction variables were investigated and optimized.
- Catalyst reusability and leaching of the active component.

GRAPHICAL ABSTRACT

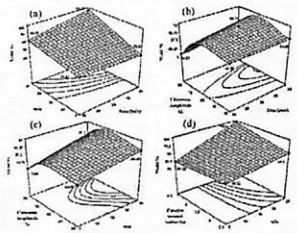

ARTICLE INFO

Article history:
Received 12 July 2012
Received in revised form 13 November 2012
Accepted 7 January 2013

Keywords:
Biodiesel
Ultrasound-assisted transesterification
Heteropolyacid
Alumina support
Jatropha oil

ABSTRACT

Fatty acid methyl esters synthesis from crude Jatropha oil using an ultrasound-assisted process was investigated. Several gamma alumina (Al) supported tungstophosphoric acid (TPA) catalysts were synthesized and characterized to elucidate their catalytic behaviors. TPA loadings on the support between 15% and 35% were investigated. The catalyst with 25% loading achieved the highest yield of 64.3% in 60 min. Effects of reaction time (10–50 min), reaction molar ratio (5:1–25:1), ultrasonic amplitude (30–90% of the maximum sonifier power) and catalyst amount (2.5–4.5 w/w oil) were investigated and optimized. Mathematical representation of FAME yield was successfully generated and statistically validated. A highest reaction yield of 84% was achieved under the optimum conditions i.e. at an ultrasonic amplitude of ~60%, a molar ratio of 19:1 and a reaction temperature of 65 °C in just 50 min. Interactions between the reaction variables were also statistically validated. The catalyst was also investigated for possible reusability.

1. Introduction

The world's energy demand still depends extensively on finite fossil resources [1,2]. Recently, the world wide concerns have been dedicated to the search for appropriate solutions to these serious issues and oleochemicals such as biodiesel are promising alternatives [3]. Transesterification of the vegetable oil is the most popular method for biodiesel production [4]. Triglycerides that exist in the oil will undergo successive reactions by generating one mol of fatty acid ester and an intermediate co-product in each step. These mono-alkyl esters of long-chain fatty acids i.e. biodiesel are considered the most potential alternative fuel [5]. Usually, edible oils are used as the sources of triglyceride for biodiesel production [6]. Non-edible oils such as Karanja oil, Polanga oil and Jatropha oil also attract great attention as they do not affect food industry when used as feedstock for fuel production [7].

Crude Jatropha oil usually contains high water and free fatty acid contents that prevent its use in base catalyzed transesterification process [8]. As such, acid catalysts should be used. Among various acid catalysts, heteropolyacids (HPAs) offer some advantages to be used in this application as either heterogeneous or homogeneous catalysts depending on their composition and the nature of

* Corresponding author.
E-mail address: chzuhairi@eng.usm.my (A.Z. Abdullah).
[1] Tel.: +60 4 5996411; fax: +60 4 5941013.

0306-2619/$ - see front matter
http://dx.doi.org/10.1016/j.apenergy.2013.01.028

the reaction medium [9]. HPAs with Keggin structures such as $H_3PW_{12}O_{40}$, $H_4SiW_{12}O_{40}$, $H_3PMo_{12}O_{40}$ and $H_4SiMo_{12}O_{40}$ have been successfully used to catalyze a wide range of acid-catalyzed reactions. They usually have high water and FFA tolerance, fewer side reactions, strong Brönsted acidity (approaching that of superacid region) as well as high proton mobility and stability [10] to justify their use as potential solid acid catalysts. Despite these advantages, the solubility of HPA in polar reaction mixtures and low surface area (1–5 m^2/g) are the main drawbacks [11]. This justifies the need for immobilizing these acidic active components on appropriate porous support materials. Different supports have been used such us zeolites [12], silica [13] and activated carbon [14]. However, slow reaction rate in conventional transesterification process requires extreme reaction conditions [15].

Application of ultrasonic energy in biodiesel production is an attractive and effective approach to solve the problem of poor reaction rate [16]. Poor mass transfer due to poor contact between the reactants causes low reaction rate. Subjecting ultrasonic waves to the reaction mixture forces the fluids to generate huge number of cavitation bubbles which grow rapidly and subsequently undergo vigorous collapses. The collapses will lead to the formation of microjets that can create fine emulsion between the reactants. Besides that, these collapses also generate local temperature increase within the reaction mixture [17]. The use of ultrasonic energy in biodiesel production has been investigated for homogenous [18,19] or heterogeneous [20–22] base catalyzed process. However, report on the use of heterogeneous acid catalyst in an ultrasound-assisted process is still hardly found.

In this study, the transesterification of crude Jatropha oil has been conducted in the presence of alumina-supported heteropolyacid supported catalyst to demonstrate the effects of ultrasound-assisted process in conjunction with an acid catalyst for FAME synthesis. Various process variables were studied for their effects in the product yield. A historical design was applied to the obtained experimental data to evaluate the optimum reaction conditions. The catalyst was also investigated for its stability and leaching of active component.

2. Experimental

2.1. Materials

Tungstophosphoric acid ($H_3PW_{12}O_{40}{\cdot}nH_2O$) (TPA) and gamma alumina support were purchased from Merck (Malaysia) while crude Jatropha oil was supplied by Telaga Madu Resources (Malaysia). The properties of the oil are given in Table 1. Methanol was supplied by Thermo Fisher Scientific Inc. (USA) while ethanol and *n*-hexane were purchased from Merck (Malaysia). Meanwhile, FAME standards were supplied by NuChek Prep. Inc. (Australia).

2.2. Catalyst preparation

The catalysts were synthesized by dissolving the desired amounts of TPA in (50:50 v/v) deionized water and ethanol solution. Wet impregnation method was adopted by contacting the support with the solution (4 ml/g support) for 20 h under constant stirring. Excess solution was then removed using a rotary evaporator and the catalyst was washed with deionized water followed by drying for 2 h. The dry catalyst was then calcined at 400 °C in an air flow for 4 h.

2.3. Catalyst characterization

Surface properties of the catalysts were determined by means of an Autosorb 1C system. FT-IR spectra of the catalysts were obtained using a Perkin–Elmer FT-IR spectrophotometer while X-ray diffraction patterns were obtained using an XRD system (Philips Goniometer PW 1820) with a scanning range from 10° to 90°. Transmission electron microscope (TEM) equipped with an image analyzer and operated at 120 kV was also used to characterize the catalysts. Raman Module (Jobin Yvon HR 800 UV) equipped with a Peltier-cooled CCD array detector was used to obtain Raman spectra of the samples.

Table 1
Properties of the Jatropha oil used.

Property	Value
Density (kg/m³)	921
Viscosity (cSt)	38.12
Molecular weight	870
Water content (wt.%)	0.161
FFA content (wt.%)	10.5

2.4. Equipment

The setup for the transesterification process consisted of a three-neck glass reactor partially submerged in a water bath to regulate the temperature. A condenser was fitted to the reaction vessel to return the evaporated methanol back to the reaction vessel. Ultrasonic energy was supplied using a Branson (USA) ultrasonic processor capable of generating a frequency of 20 kHz with the highest power of 400 W (at 100% level).

In a typical run, the desired amount of oil was transferred into the reactor and it was placed in the water bath until the reaction temperature was reached. Then, the desired amount of the catalyst was added followed by pre-heated methanol at appropriate ratios. A condenser was then used to recover the evaporated methanol. The ultrasonic energy was then applied in a discrete pattern with 10 s on and 3 s off. The water bath temperature was fixed at 56 °C and the heat generated by the ultrasonic probe would maintain the temperature at 65 ± 1 °C. After the reaction, the reaction mixture was quenched and excess methanol was distilled out. The reaction mixture was then separated into two layers by centrifugation at 3500 rpm for 20 min. The upper layer was then collected for analysis.

Blank experiments were also carried out in the absence of catalyst or ultrasonic irradiation. The absence of catalyst was tested by providing ultrasonic irradiation at 75% of the maximum power for 60 min with a methanol/oil ratio of 20. The same conditions were also tested in the absence of TPA on alumina and for testing the effect of HPA loading on the support. The same experimental run under mechanical stirring was also tested under the same conditions.

Analyses of the reaction products were conducted using a gas chromatograph (GC) (Agilent 7890 A system). The GC unit was equipped with a flame ionization detector (FID) and fitted with a capillary column (Agilent Technologies, Inc. 19091J-413 HP-5).

2.5. Catalyst leaching and stability

In order to study the leaching of Kiggin anion from the supported catalyst and to examine the influence of ultrasonic waves on the catalyst stability, an experiment similar to the "hot-filtration experiment" was conducted [13,14]. The catalyst was first added to methanol and then subjected to ultrasonication under the optimum reaction conditions. After the desired reaction time, the solid catalyst was filtered out and the desired amount of oil was added to the methanol. The reaction was then carried out without the presence of the catalyst at the optimum reaction conditions in order to examine the contribution of any leached anion on the reaction.

Table 2
Coded and actual reaction variables used in the experimental design.

Real variables	Coded variables	Level		
		−1	0	+1
Reaction time (min)	X_1	10	30	50
Molar ratio	X_2	5:1	15:1	25:1
Ultrasonic amplitude (%)	X_3	30	60	90
Catalyst amount (w/w %)	X_4	2.5	3.5	4.5

The catalyst reusability was tested by running the same batch of catalyst for several successive runs. First, the desired amount of catalyst was used at optimum reaction conditions of the transesterification process followed by filtration and washing. A filtration system with 0.45 μm membrane filter and a vacuum pump were used to extract the catalyst using *n*-hexane as solvent. Successive washing with *n*-hexane followed by washing with ethanol were performed to ensure the removal of most polar and non-polar compounds that were attached to the catalyst. The solid catalyst was then dried at 100 °C for 2 h before reuse.

2.6. Experimental design

Four zero levels (center levels) were selected and applied in a central composite design (CCD) in order to establish the experimental design matrix. Reaction time (X_1), methanol to oil ratio (X_2), ultrasonic amplitude (X_3) and catalyst amount (X_4) were chosen with center values of 30 min, 15%, 60% and 3.5 wt/wt oil, respectively (Table 2). For the ultrasonic amplitude, 60% of the total power was selected as the central level as early observations suggested that levels lower than 30% were too low to create any positive effect. Meanwhile, 100% was also avoided due to the very intense cavitation effect. Reaction time center level was selected based on the results of the reaction time effect tests while zero levels of other variables were selected based on the most suitable levels reported for acid catalyzed transesterification [23]. Design Expert 6.0.6 software was employed for constructing the design and the production yield was taken as the response.

3. Results and discussion

3.1. Catalysts characterization

Surface characteristics of Al and the TPA–Al catalysts are shown in Table 3. It can be observed that the surface area, total pore volume and pore diameter decreased with increasing TPA loading. The diameter of the TPA molecule is about 12 Å [24] to suggest its possible inclusion inside the mesopores of the support. Similar observation was recorded upon 20 wt.% TPA loading into alumina [25]. The possibility of TPA multilayer formation on the support surface at high loadings (30 and 35 wt.%) could not be ruled out. The partial blockage of the pores by the multilayer TPA deposition could be responsible for a decrease in the surface area [26].

Fig. 1 shows the FT-IR spectra for TPA, Al and the supported catalysts. For the pure TPA, it can be seen that four major bonds are

Table 3
Physical properties of Al and the TPA catalysts.

Sample	BET surface area (m^2/g)	Total pore volume (cm^3/g)	Average pore diameter (Å)
Al	109.4	0.23	82.6
TPA25–Al	93.3	0.13	54.9
TPA30–Al	83.4	0.10	52.0
TPA35–Al	71.9	0.09	49.8

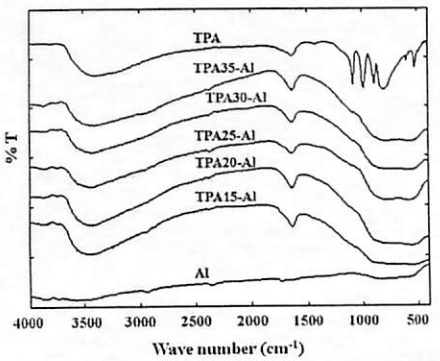

Fig. 1. The FT-IR spectra of Al and the supported catalysts.

attributed to the stretching modes of oxygen to phosphorous and tungsten of the adsorption mode of the Keggin ion $(PW_{12}O_{40})^{-3}$. Bands at 800 cm^{-1} (W—O—W in the edge), 890 cm^{-1} (W—O—W in the corner), 980 cm^{-1} (W=O) and at 1,080 cm^{-1} (P—O) can be detected for the Keggin anion. For the supported catalysts, a shoulder at 910 cm^{-1} was attributed to the symmetric stretching of (W=O) bond. The difference between the anion area (1.1 nm^2) and the surface area of the support (109 m^2) suggested a high dispersion on the surface [27]. The existence of Keggin anion was not evident for TPA loadings on alumina below 40 wt.%.

Analysis done on the TEM images revealed some information about the dispersion of the active species (Fig. 2). A wormhole-like mesostructure of Al sample can be observed in Fig. 2a. The images of the loaded catalysts revealed the presence of the Kiggin anion as small round particles that were distributed over the support. The difference in the diameters between the TPA and the support mesopores provided the opportunity for TPA anions to be trapped inside the pores. This was substantiated by the presence of dark particles in Fig. 2b–d.

It is noted that reductions in diffraction peaks of the support in XRD patterns and the magnitude of these reductions increased with increasing TPA loading (Fig. 3). None of the catalysts showed peaks that could be assigned to the active phase which indicated a good dispersion of TPA on the support. Similar result has been observed for TPA supported on alumina [25,26], silica, zirconia and activated carbon [25] and for different HPAs immobilized on alumina [11]. This good dispersion could be related to the difference in the mean pore diameter of the supports (about 80 Å) and the diameter of the HPA molecule which allowed more uniform distribution of TPA on the surface [25].

Raman IR spectrum is considered a suitable technique for observation of the Keggin structures to prove the presence of TPA in the synthesized catalysts [11]. The spectra of TPA, Al and TPA25–Al are shown in Fig. 4. TPA shows characteristic bands at 1010 cm^{-1} attributed to the symmetric stretching (ν_s) of $W{=}O_d$ while the band at 1000 cm^{-1} is attributed to anti-symmetric stretching (ν_{as}) of $W{=}O_d$ which was considered the strongest bands of TPA [28]. Low intensity bands that appear as shoulders are also noticed at 532 cm^{-1} and 519 cm^{-1}. They are ascribed to W—O—W symmetric stretching vibration and O—P—O asymmetric deformation vibration, respectively [29]. No band was detected for Al sample while the presence of the Keggin anion can be confirmed by comparing the spectra of Al with TPA25–Al. It can be noticed in

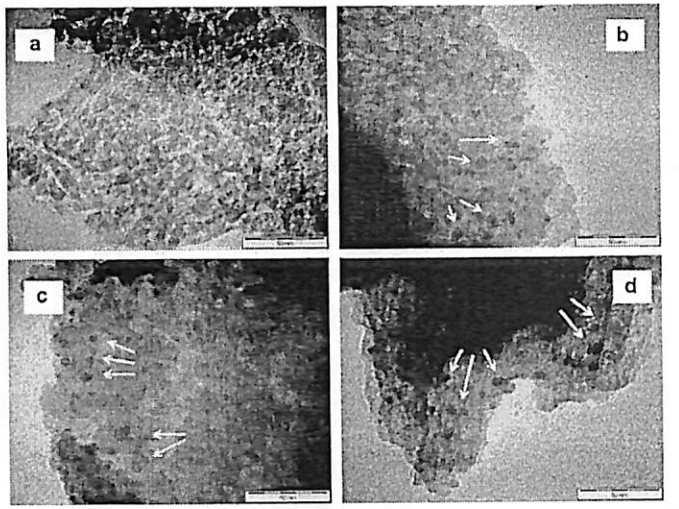

Fig. 2. TEM images of (a) Al, (b) TPA25–Al, (c) TPA30–Al, and (d) TPA35–Al catalysts.

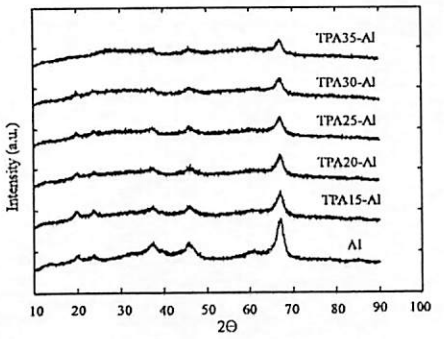

Fig. 3. XRD patterns of Al and the supported catalysts.

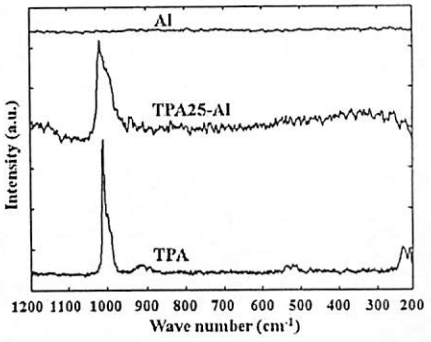

Fig. 4. Raman spectra of TPA, Al and TPA25–Al samples.

TPA25–Al spectra that two bands are detected at 1010 cm^{-1} and 1000 cm^{-1}. They are attributed to the strongest bands of (ν_s) $W{=}O_d$ and (ν_{as}) $W{=}O_d$, respectively. Ca iman et al. [27] reported similar results for different TPA loadings on Al.

3.2. Preliminary study

The results of blank runs revealed that significant reaction did not occur with the presence of alumina only or without the presence of catalyst (reactants alone) (Fig. 5). This was mainly due to the absence of acidic active sites to catalyze the reaction. The run without the use of ultrasound (mechanically stirred) also resulted in no significant reaction. Conventional acid catalyzed reactions require long reaction time (5–6 h) due to the slow reaction rate [4] compared to base-catalyzed ones (2–3 h) [8]. However, base catalysts are not suitable in this study due to high FFA content in the oil.

The reaction yield increased with increasing TPA content in the catalyst and reached the highest value with TPA25–Al (Fig. 5). The presence of active sites on the catalyst promoted the reactants' conversion and promoted the forward reaction. High TPA loadings (above 25 wt.%) led to a decrease in the reaction yield due to the reduction in the accessibility of the reactants to the active sites. This was caused by the blockage of the catalyst pores by the acidic active sites leading to internal diffusion limitation. Low accessibility of the reactants to the active sites resulted in negative effects on the reaction yield.

Fig. 5. Transesterification of Jatropha oil using an ultrasound-assisted process over TPA immobilized on alumina (reaction time 60 min, methanol/oil molar ratio 20:1, catalyst amount 4% (w/w) and ultrasonic power 75%).

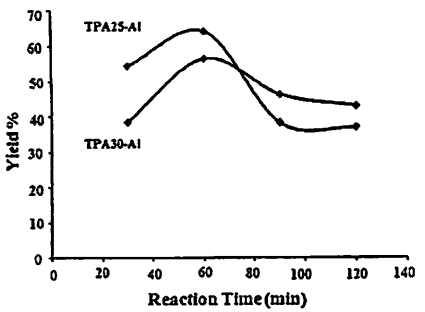

Fig. 6. Effect of reaction time on FAME yield (methanol/oil molar ratio 20:1, catalyst amount 4% (w/w), and ultrasonic power 75%).

Changes in FAME yield with reaction time can be seen in Fig. 6 for both TPA25–Al and TPA30–Al catalysts under ultrasonic condition. For short reaction time, insufficient contact time between the reactants led to low reaction yield. The yields increased with increasing reaction time, reaching their maximum levels in about 60 min for both catalysts. The highest reaction yields were 64.3% and 56.6% for TPA25–Al and TPA30–Al, respectively. Meanwhile, FAME yield decreased for both catalysts after 60 min probably due to FAME glycerolysis and other side reactions. It has been reported that beyond 60 min for the ultrasound-assisted transesterification, monoglycerides content was high due to the slow reaction rate to convert it to glycerol and FAME [30]. Sufficient amounts of monoglycerides accumulated in the reaction mixture could lead to enhancement in the solubility of FAME in the glycerol. Side reaction between FFA and glycerol, mono and glycerides could also generate triglycerides that negatively affected the yield [31].

3.3. Statistical analysis

Without the use of any statistical method, a wide range of experimental runs would be required to characterize the interaction between the process variables [16]. Different design models such as full factorial design, Taguchi's algorithm and response surface methodology have been established for optimizing the data. The experimental design matrix including the un-coded values, point types and the experimental responses values is presented in Table 4. It consisted of 30 experiments according to $2^k + 2k + 6$, where k is the number of independent variables [32]. Twenty four experiments were improved by six replications at the center points to evaluate the pure error. The third order polynomial equation based on the coded values obtained using multiple regression analysis of the experimental data is:

$$Y = 67.99 + 1.82X_1 + 0.85X_2 - 3.11X_3 - 13.27X_4 + 0.1X_3^2 - 0.14X_1X_2 - 0.04X_1X_3 - 0.07X_2X_3 + 1.22X_2X_4 - 7.19 \times 10^{-4}X_3^2 - 3.13 \times X_1X_2X_3 \quad (1)$$

Here, Y is the response (FAME yield) while X_1, X_2, X_3 and X_4 are the coded forms of the studied variables. The choice of a cubical polynomial equation to describe the design was made on the basis of the high value of determination coefficient (R^2) that was achieved.

The ANOVA statistical analysis (Table 5) shows high significance of the cubical equation to represent the experimental data as expressed by the Fisher F-test value (13.44) combined with a very small probability value (Prop. > F < 0.0001). Based on an R^2 value of 89.69%, the effect on the FAME yield could be attributed to the variation in the independent variables while the remaining 10.31% could be explained by residues.

Generally, larger F-value and smaller the Prob. > F value indicate more significant corresponding variable [33]. It is noted in Table 6 that reaction time, molar ratio and catalyst amount had significant effects on the yield while ultrasonic amplitude mostly had its influence in its square value. Two interactions between the molar ratio with reaction time and catalyst amount as well as the triple interaction between the reaction time, molar ratio and the ultrasonic amplitude showed significant effects on the response. The other interactions and the cubical form of the ultrasonic amplitude (Table 7) were also considered to establish a historical design based on the experimental data.

3.4. Interaction between parameters

The possible interactions between the reaction variables should be more observable if 3D surfaces are established from the experimental data. Fig. 7a shows the interaction between reaction time and molar ratio while the other parameters are kept at their center values. It can be concluded that an increase in reactants' molar ratio had positive effects on the reaction yield for both low and high reaction times, while increasing the reaction time had its positive influence only at high molar ratio. Insufficient amounts of methanol to drive the forward reaction at low molar ratio of 5:1 resulted in low yield. Subjecting the reaction mixture to ultrasonic irradiation for the maximum reaction time in the presence of low methanol amounts led to a decrease in the yield. This could be attributed to severe mixing effects between the small FAME amounts (produced by low methanol amount) with the by-product (glycerol). For high reaction times and high molar ratios, the FAME yields showed maximum values due to the sufficient reaction time and adequate methanol amounts to support the reaction.

The inter-dependence between ultrasonic amplitude, reaction time and reactants' molar ratio are presented in Fig. 7b and c, respectively. For low and high reaction times and molar ratios, the reaction yield was found to increase with increasing ultrasonic amplitude and it reached the maximum values at moderate levels (~60–70%). For all reaction times and molar ratio values, the reaction yields showed a decreasing trend at high ultrasonic amplitudes due to the formation of large number of cavitation bubbles in the liquid. The combination of these bubbles forming larger and more stable bubbles could create a barrier to the acoustic energy transmission throughout the reaction mixture leading to poor mixing effects between the two immiscible layers. Similar behaviors of ultrasonic-assisted biodiesel production systems at high ultrasonic energy have been reported [22,34]. In Fig. 7c, increasing molar ratio visibly improved the reaction yield at the minimum and maximum ultrasonic amplitude levels due to the increase in the number of cavitation bubbles that would collapse to form an emulsion between the two layers.

It can be observed in Fig. 7d that increasing catalyst amount with the presence of low methanol amount negatively affected the yield but it showed an increasing trend in the yield when high methanol amounts were used. Thus, increasing the catalyst amount led to an increase in the available active sites for the reactants to undergo the chemical reaction.

3.5. Process optimization

Optimization of the reaction variables by fitting the experimental data to the historical design using the Design Expert 6.0.6 software was also attempted. The software suggested 10 possible

Table 4
Central composite design matrix of four variables and the respective responses.

Run	Point type	Real variables				Yield (%)
		Time (min)	M/O[a]	Amplitude (%)	Catalyst amount (w/w %)	
1	Fact	40	20	45	3.0	60.49
2	Fact	20	10	45	4.0	37.55
3	Fact	20	20	75	4.0	53.27
4	Fact	40	10	75	4.0	35.16
5	Fact	20	10	45	3.0	38.16
6	Fact	20	20	75	3.0	49.34
7	Fact	40	10	75	3.0	43.74
8	Fact	20	20	45	4.0	58.45
9	Fact	40	20	75	3.0	61.22
10	Fact	40	10	45	3.0	45.40
11	Fact	40	10	45	4.0	41.55
12	Fact	40	20	75	4.0	84.16
13	Fact	20	20	45	3.0	51.89
14	Fact	40	20	45	4.0	61.15
15	Fact	20	10	75	4.0	36.03
16	Fact	20	10	75	3.0	37.70
17	Axial	30	25	60	3.5	83.74
18	Axial	30	15	60	4.5	66.52
19	Axial	30	15	90	3.5	68.78
20	Axial	10	15	60	3.5	48.33
21	Axial	30	5	60	3.5	33.57
22	Axial	50	15	60	3.5	54.18
23	Axial	30	15	30	3.5	42.67
24	Axial	30	15	60	2.5	46.05
25	Center	30	15	60	3.5	55.47
26	Center	30	15	60	3.5	62.95
27	Center	30	15	60	3.5	60.94
28	Center	30	15	60	3.5	57.31
29	Center	30	15	60	3.5	59.44
30	Center	30	15	60	3.5	51.38

[a] Methanol to oil ratio.

Table 5
Analysis of variance (ANOVA) for the cubic model representing the ultrasound-assisted biodiesel production process.

Sources of variations	Sum of squares	Degrees of freedom	Mean square	F-value	Prob. > F
Model	4198.29	11	381.66	13.44	<0.0001
Residual	482.62	17	28.39	-	-
Lack of fit	396.74	12	33.06	1.92	0.2428
Pure error	82.88	5	17.18	-	-
Total	4680.91	28			

R^2 = 0.8969, Adj. R^2 = 0.8302, C.V. = 10.18, SD = 5.33.

Table 6
Results of regression analysis for the full second-order polynomial model and the estimated coefficients.

Model parameters	F-value	Prob. > F
X_1	9.91	0.0059
X_2	103.08	<0.0001
X_3	1.48	0.2411
X_4	5.34	0.0336
X_3^2	11.68	0.0033
X_1X_2	3.12	0.0952
X_1X_3	1.42	0.2497
X_2X_3	1.49	0.2385
X_2X_4	5.24	0.0351
X_3^2	2.49	0.1328
$X_1X_2X_3$	3.10	0.0961

Table 7
Predicted and experimental results under the optimum conditions for model validation.

Run	Reaction Conditions				Predicted yield (%)	Experimental yield (%)	Error (%)
	Time (min)	Molar ratio	Amplitude (%)	Catalyst amount (w/w)			
1	37.00	22.69	72.12	4.26	87.54	89.32	2.04
2	47.17	19.05	64.32	4.44	86.19	83.63	2.97
3	48.13	23.41	46.86	4.44	85.56	88.14	3.01

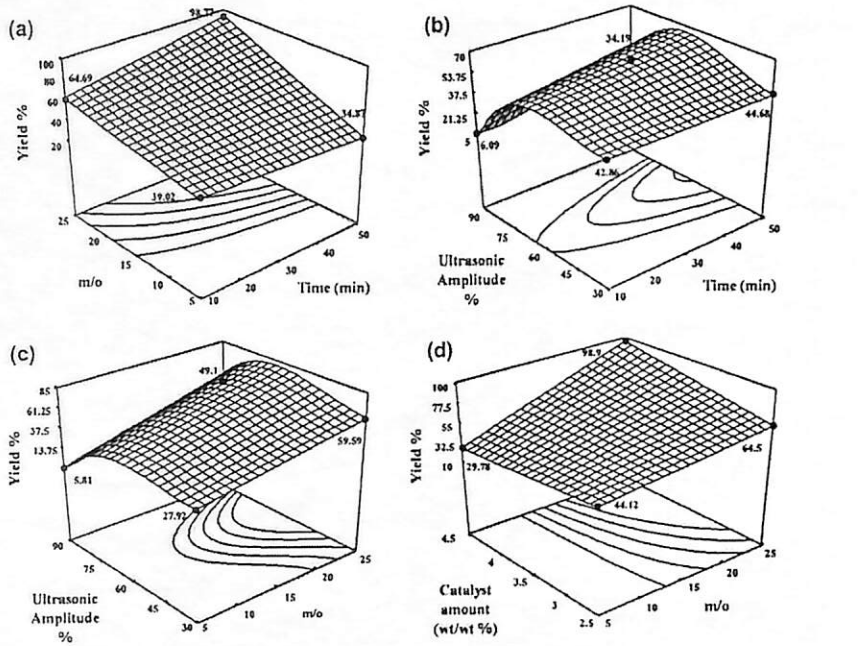

Fig. 7. Interactions between reaction parameters, (a) between reaction time and methanol/oil ratio, (b) between reaction time and ultrasound amplitude, (c) between methanol/oil ratio and ultrasound amplitude, and (d) between molar ratio and catalyst amount.

solutions according to the order of suitability. Table 7 presents three selected solutions and the corresponding values of the experimental yield to validate the proposed reaction conditions. The experimental results showed good agreement with the predicted ones within 3% error. Besides that, an experiment was also conducted using TPA25–Al catalyst under the optimum reaction conditions. In this experiment, vigorous mechanical stirring was used instead of ultrasonic irradiation. The absence of FAME in the product layer confirmed the positive role of ultrasonic energy to accelerate the transesterification reaction under the optimum reaction conditions. This results confirmed our findings reported in earlier works [20,21].

It can be concluded that the reaction time for the ultrasound-assisted process below 50 min achieved ~85% of FAME yield in the presence of the solid acid catalyst. This observation suggested the contribution of ultrasonic energy in enhancing the reaction rate compared to other conventional transesterification processes that require relatively longer reaction time. The use of TPA either homogenously [35] or supported on a support material [36] recorded high reaction yield of ~90% within 5 h. Another enhancement in terms of reactant molar ratio achieved in this reaction system was seen based on the methanol to oil ratio of ~22 compared to 70:1 as reported for a conventional stirring reactor system using the same type of catalyst [35,36]. Low acid value crude Jatropha oil was transesterified using an ultrasound-assisted process in the presence of Na/SiO_2 catalyst and the system achieved 98% yield with a molar ratio of 9:1 [22]. The significant contribution of the solid acid catalyst in converting crude oil with high FFA and water content could be observed in this work.

The significant role of ultrasound in decreasing the required reaction temperature due to the generated heat during the collapse of the cavitation bubbles was also proven. Acid catalyzed biodiesel processes generally require high reaction temperature to reduce the viscosity of the reactants to achieve an acceptable level of mixing due to the slow reaction rate [37]. Without the need of extra heating equipments in the current study, significant saving

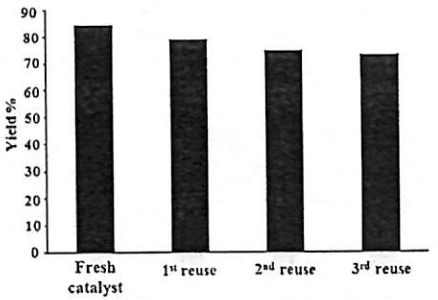

Fig. 8. Catalytic activity of TPA25–Al in successive reaction runs under the optimum reaction conditions.

in the energy input of the process could be achieved. Significant reduction in the energy input requirements for the process due to low reaction time and reaction temperature is considered a critical issue that has positive effect on the overall process economy.

3.6. Catalyst stability

Investigation on the stability of the catalyst under the ultrasonic reaction conditions in polar reaction mixture revealed that 9.6% of the FAME yield was achieved under the optimum conditions due to the minimal leaching of $PW_{12}O_{40}^{3-}$ anion. Thus, the reaction was mostly heterogeneous in nature. Leaching of the active component from the catalyst occurred due to the partial dissolution of TPA in the polar reaction mixture and the exposure of the solid catalyst to direct ultrasonic effects. Compared with other immobilized TPA catalysts on different supports such as zirconia and silica [15], this catalyst showed minimal leaching attributed to the strong absorption of TPA on the alumina. The TPA catalyst stability towards leaching has also been demonstrated for the esterification of *n*-butanol with different alcohols [38] and alkylation of phenol [39].

The yields achieved in the successive reaction runs to investigate the potential for catalyst reusability are shown in Fig. 8. It can be concluded that a reduction of about 6.6% of the optimum reaction yield was recorded for the first reuse. Second reuse of the catalyst showed a reduction of 5.3% in the yield while almost similar reaction yields were achieved between the second and the third reaction runs. This reduction in activity could be attributed to the heteropoly anion leaching, bearing in mind that a washing step was conducted between the reuse cycles.

In this study, thorough cleaning of the recovered catalyst after the reaction could not be achieved. Washing with *n*-hexane and ethanol was expected to remove most of the polar and non-polar compounds that were stuck on the catalyst surface. However, as the composition of the reaction mixture was about the same with the earlier reaction run, significant effect of the catalytic activity was unlikely. Unfortunately, the unidentified organic compounds could decompose during the degassing step at 300 °C during the surface analysis based on N_2 adsorption so that reliable surface area results could not be achieved. As such, surface area of the used catalyst was not reported in this work.

4. Conclusions

Ultrasound-assisted transesterification of crude Jatropha oil in the presence of TPA supported by Al catalysts was successfully studied. The catalysts were tested to show the activity in FAME production from crude Jatropha oil with high FFA content. A loading of 25 wt.% of the heteropolyacid in the catalyst had its maximum effects on the reaction yield. TPA25–Al and TPA30–Al catalysts showed that increasing the reaction time beyond 60 min had negative effects on the yield due to side reactions. Moderate ultrasonic amplitude had positive effects while high amplitudes were detrimental to the process. Short reaction time (~50 min), low reaction temperature (65 °C) and moderate molar ratio (~19) compared to other HPA catalyzed processes were demonstrated by the system. TPA25–Al catalyst was also investigated for possible catalyst reusability and leaching of active component and positive results were demonstrated.

Acknowledgment

A Research University (RU) grant to support this work is gratefully acknowledged.

References

[1] Abdullah AZ, Salamatinia B, Mootabadi H, Bhatia S. Current status and policies on biodiesel industry in Malaysia as the world's leading producer of palm oil. Energy Policy 2009;37:5440–8.
[2] Abdullah AZ, Razali N, Lee KT. Optimization of mesoporous K/SBA-15 catalyzed transesterification of palm oil using response surface methodology. Fuel Process Technol 2009;90:958–64.
[3] Kim HJ, Kang BS, Kim MJ, Park YM, Kim DK, Lee JS, et al. Transesterification of vegetable oil to biodiesel using heterogeneous base catalyst. Catal Today 2004;93–95:315–20.
[4] Leung DYC, Wu X, Leung MKH. A review on biodiesel production using catalyzed transesterification. Appl Energy 2010;87:1083–95.
[5] Yin X, Ma H, You Q, Wang Z, Chang J. Comparison of four different enhancing methods for preparing biodiesel through transesterification of sunflower oil. Appl Energy 2012;91:320–5.
[6] Santori G, Di Nicola G, Moglie M, Polonara F. A review analyzing the industrial biodiesel production practice starting from vegetable oil refining. Appl Energy 2012;92:109–32.
[7] Juan JC, Kartika DA, Wu TY, Hin TYY. Biodiesel production from Jatropha oil by catalytic and non-catalytic approaches: an overview. Bioresour Technol 2011;102:452–60.
[8] Koh MY, Mohd TI. A review of biodiesel production from *Jatropha curcas* L. oil. Renew Sust Energy Rev 2011;15:2240–51.
[9] Sharma YC, Singh B, Korstad J. Advancements in solid acid catalysts for ecofriendly and economically viable synthesis of biodiesel. Biofuels Bioprod Biorefin 2011;5:69–92.
[10] Chai F, Cao F, Zhai F, Chen Y, Wang X, Su Z. Transesterification of vegetable oil to biodiesel using a heteropolyacid solid catalyst. Adv Synth Catal 2007;349:1057–65.
[11] Atia H, Armbruster U, Martin A. Dehydration of glycerol in gas phase using heteropolyacid catalysts as active compounds. J Catal 2008;258:71–82.
[12] Mukai SR, Lin L, Masuda T, Hashimoto K. Key factors for the encapsulation of Keggin-type heteropoly acids in the supercages of Y-type zeolite. Chem Eng Sci 2001;56:799–804.
[13] Tropecêlo AI, Casimiro MH, Fonseca IM, Ramos AM, Vital J, Castanheiro JE. Esterification of free fatty acids to biodiesel over heteropolyacids immobilized on mesoporous silica. Appl Catal A 2010;390:183–9.
[14] Ferreira P, Fonseca IM, Ramos AM, Vital J, Castanheiro JE. Acetylation of glycerol over heteropolyacids supported on activated carbon. Catal Commun 2011;12:573–6.
[15] Vyas AP, Verma JL, Subrahmanyam N. A review on FAME production processes. Fuel 2010;89:1–9.
[16] Veljković VB, Avramović JM, Stamenković OS. Biodiesel production by ultrasound-assisted transesterification: state of the art and the perspectives. Renew Sust Energy Rev 2012;16:1193–209.
[17] Badday AS, Abdullah AZ, Lee KT, Khayoon MS. Intensification of biodiesel production via ultrasonic-assisted process: a critical review on fundamentals and recent development. Renew Sust Energy Rev 2012;16:4574–87.
[18] Hingu SM, Gogate PR, Rathod VK. Synthesis of biodiesel from waste cooking oil using sonochemical reactors. Ultrason Sonochem 2010;17:827–32.
[19] Kumar D, Kumar G, Singh CP. Fast, easy ethanolysis of coconut oil for biodiesel production assisted by ultrasonication. Ultrason Sonochem 2010;17:555–9.
[20] Mootabadi H, Salamatinia B, Bhatia S, Abdullah AZ. Ultrasonic-assisted biodiesel production process from palm oil using alkaline earth metal oxides as the heterogeneous catalysts. Fuel 2010;89:1818–25.
[21] Salamatinia B, Mootabadi H, Bhatia S, Abdullah AZ. Optimization of ultrasonic-assisted heterogeneous biodiesel production from palm oil: a response surface methodology approach. Fuel Process Technol 2010;91:441–8.
[22] Kumar D, Kumar G, Singh CP. Ultrasonic-assisted transesterification of *Jatropha curcus* oil using solid catalyst, Na/SiO_2. Ultrason Sonochem 2010;17:839–44.

Energy Policy 62 (2013) 456–462

Contents lists available at ScienceDirect

Energy Policy

journal homepage: www.elsevier.com/locate/enpol

Prospects and current status of B5 biodiesel implementation in Malaysia

Mohd.Hizami Mohd. Yusoff [a], Ahmad Zuhairi Abdullah [a,*], Shazia Sultana [a], Mushtaq Ahmad [a,b]

[a] School of Chemical Engineering, Engineering Campus, Universiti Sains Malaysia, 14300 Nibong Tebal, Malaysia
[b] Biofuel Laboratory, Quaid-i-Azam University, Islamabad 45320, Pakistan

HIGHLIGHTS

- Prospects of B5 biodiesel implementation in Malaysia.
- National Biofuel Policy thrusts pertinent to B5 program.
- Successful application of B5 in government and industrial sectors.
- Challenges in CPO production, weak domestic demand and export tax.
- Reassessment of national policy according to global issues.

ARTICLE INFO

Article history:
Received 8 May 2013
Accepted 1 August 2013
Available online 24 August 2013

Keywords:
Malaysian B5 biodiesel status
National policy
Challenges and sustainability

ABSTRACT

This paper addresses B5 biodiesel programs in Malaysia, global challenges on the production of palm oil. Protective measures for future efficiency as well as continued viability of this renewable energy sector are also discussed. Crude palm oil (CPO) prices are currently suppressed because of high palm oil inventory. Malaysian government has taken a pro-active step in implementing the B5 biodiesel for transportation and industrial sectors through the introduction of B5 biodiesel. The B5 Biodiesel Program which was initially targeted at selected government agencies has been fully implemented for subsidized sectors in the Central Region. The promotion of B5 development is highly attractive due to its potential local feedstock from palm oil industry and the availability of production technologies that offer opportunities for the sustainable development in energy entrepreneurships. Nationally, produced B5 will improve the access to alternative energy services and is expected to help in improving productivity and sustainability. Despite successful local B5 implementation, Malaysia is recently facing global challenges on the biodiesel production which currently remains stagnant due to weak domestic demand and uncompetitive export tax structure.

1. Introduction

1.1. Energy vision statement by Malaysian government

Energy is one of the essential inputs for economic, social and industrial development of any nation. A sustainable and continuous supply of energy resources is essential to maintain and improve the socio-economic conditions. However, in current era of energy shortage, the conventional energy sources which are mainly derived from fossil fuels are depleting at very fast rate and facing the major challenges of high price and environmental problems such as emission of green house gases (GHG). Environmental concern about the effect of green house gas (GHG) emissions on climate change is pushing particularly the developing nations, international community and policy makers to achieve sustainable development by utilizing alternate sources of energy with less carbon emission (the vision that is usually termed as "Clean Development Mechanism" (CDM)). Energy policies of any developing nation usually aim at promoting the penetration of these technologies into the society and they usually address aspects such as energy resources, feedstock availability, conversion technologies and energy demand sectors (Nakata et al., 2011). To address these concerns, Malaysian government is trying to implement energy technology and policy by using palm oil biodiesel as the most significant eco-friendly source of energy. This is due to the availability of this feedstock which is caused by the surplus production of palm oil industry locally.

* Corresponding author. Tel.: +604 599 6411; fax: +604 594 1013.
E-mail addresses: chzuhairi@eng.usm.my, azuhairi@yahoo.com (A.Z. Abdullah).

0301-4215/$ - see front matter © 2013 Elsevier Ltd. All rights reserved.
http://dx.doi.org/10.1016/j.enpol.2013.08.009

1.2. Current energy scenario in Malaysia

In Malaysia, the major sectors that are the main users of energy include transportation (40.3%) and industries (38.6%). According to an estimate, the energy demand is expected to increase at a rate of 5–7% per year during next 20 years from 2004 (Lau et al., 2009). Meanwhile, to cope up with this high energy requirements, Malaysia still heavily relies on non-renewable energy sources like oil, natural gas, hydro power and coal (Poh and Kong, 2002). However, these sources are depleting in very fast rate due to increasing demands in almost all energy sectors.

Malaysian economy should not be totally dependent or expected to sustain on its oil resources even though it is the 3rd largest oil reserve country in the Asia Pacific Region. It is estimated that the oil and gas reserves will be available only for the next 15 and 30 years, respectively (Ahmad et al., 2011). Meanwhile, over the next 20 years, the demand for energy is expected to double especially in fast developing countries like Malaysia where there is a rapid urbanization and economic growth nationwide. In addition, the use of more petroleum-based fuel also contributes to very high emissions of green house gasses (GHGs) and other pollutants that may lead to negative impacts on indigenous biodiversity and ecosystem of the country (Shahid and Jamal, 2008). In the light of current and future status of energy demand in Malaysia coupled with the availability of fossil fuel resources and their environmental impacts, Malaysia along with international communities are in urgent search of alternative energy resources. Biofuels like biodiesel which comes from renewable resource can be used as an option for supporting sustainable development in many regions of the world including Malaysia.

1.3. Palm oil biodiesel: a promising option for Malaysia

Biodiesel is defined as a clean-burning alternative to diesel fuel. It consists of mono-alkyls esters of long chain fatty acid (FAMEs) and can be used in compression–ignition (CI) engines and for generation of electricity. It is mainly synthesized from renewable, non-petroleum-based sources of vegetable oils (such as palm, pongame, jatropha, rapeseeds, soy etc.), animal fats (such as poultry, tallow, fish etc.), waste cooking oils and trap grease (Meher et al., 2006).

The quality standards and fuel properties of biodiesel may differ in each country due to its geographical location, nature of its feedstock and the production technology available locally. In literature, a number oil bearing crops are listed and identified as potential feedstock for biodiesel production including soybean, palm, sunflower, safflower, cottonseed, rapeseed and peanut oils (Mofijur et al., 2012). However, to date, biodiesel production in Malaysia mainly utilizes palm oil as primary oil on the basis of the availability of this feedstock, low price and desirable characteristics of the oil. Palm oil is considered as a promising option for Malaysia and many countries in this region and it is believed to be a sustainable long-term feedstock. It is due to its continuous growth behavior, high production rate and shorter time for harvest as compared to fossil fuels which need millions of years to be produced.

According to an estimate, Malaysia is one of the most productive countries for palm oil (42.3%) in the world. To ensure sustainability and further development of this industry, the government has set up agencies such as Malaysians Palm Oil Board (MPOB). Among other functions, it is meant for developing bio-resources production through this industry and biodiesel is one of them. Based on these strategies, Malaysia has become one of the largest countries in biomass production particularly with respect to the application of palm oil as major feedstock for biofuel production (Goh et al., 2010).

As the world's largest crude palm oil (CPO) exporter and the second largest CPO producer, Malaysia moves forward in the development of biofuel technology through the introduction of National Biofuel Policy which was launched in 2006. Currently, it is looking forward to improving the implementation program of B5 using palm oil as its primary feedstock. B5 is a blend of 5% palm methyl ester (PME) and 95% petroleum diesel. Even though there are other biodiesel blends such as B2, B10 and B20 which are currently produced in many countries, B5 is the one that Malaysian government has mandated for initial implementation as a part of the national policy (Bernama, 2011). In the same year, Malaysia started the production of B5 biodiesel which was implemented in stages at retail stations in the Central Region of Peninsular Malaysia involving Putrajaya, Malacca, Negeri Sembilan, Kuala Lumpur and Selangor (MPIC, 2011e). The initiative taken by the government would reflect the commitment to maintain the stability, prosperity and well-being of the nation's oil palm industry. At the same time, it serves in promoting the use of palm biodiesel as a source of renewable energy that contributes to a cleaner environment which is in line with the National Biofuel Policy.

After launching the National Biofuel Policy, the ambition has been noted at national level to make the sale of B5 mandatory as soon as possible throughout the country, with legislation currently being considered (Bernama, 2011). With the currently announced biodiesel capacity, Malaysia would be able to support B5 in transport fuels in coming years and it is expected that small quantity of biodiesel will also be available for export in addition to the export of palm oil. Despite being successful in the B5 implementation locally, Malaysia is still facing some global challenges in terms of the CPO pricing, weak domestic demand as well as uncompetitive export structure (Lee, 2012).

Several articles have been published on biodiesel production, feedstock availability and role of biodiesel industry in Malaysia. However, to best of our knowledge, the status of the B5 implementation nationwide and the success of the biofuel policy have not been discussed in detail to evaluate the potential role of palm oil industry for production of B5 in ensuring sustainable development in Malaysia. The assessment of such biofuel policy is the subject of this article. The analysis will take into account the rapidly growing market of palm oil which implies the need for efficient implementation to overcome energy crises. This article is written with the objective of assessing the strengths and weaknesses of Malaysian National Biofuel Policy. Most discussion will circulate around the current implementation status in transport and fishery sectors based on comprehensive review to explore scenarios for the possible impacts in the long-term application and challenges facing the palm oil industry.

2. Biodiesel policy paradigms in Malaysia

The key challenges facing the Malaysian nation is how to meet its growing energy needs and sustain economic growth without contributing to climate change and to solve the shortage problems of fossil fuels. To address these challenges, B5 Biodiesel Program was introduced in an attempt to test the readiness of local infrastructures for a complete switch to the new alternative fuel. The main objective of the program is to encourage the use of biodiesel to reduce the country's dependence on depleting fossil fuels while at the same time promoting the demand for palm oil which coincides with the National Biofuel Policy that was launched on 21st March 2006. This policy also supports the increasing use of indigenous biofuel for energy security as the most potential alternative which is usually termed as 'future fuel' among public in line with the Malaysia's Five-Fuel Diversification Policy. As shown in Fig. 1, there are five key thrusts decided as the major components of this policy (Abdullah et al., 2009).

Concurrent with the biofuel policy and larger biofuel promotion program undertaken by the Malaysian government at the national level is a more serious effort to support biodiesel use for

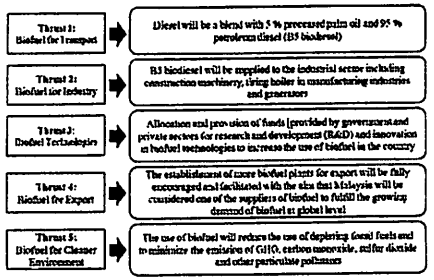

Fig. 1. Key thrusts of Malaysian Biofuel Policy 2008.

clean environment and green technology. First, it can be seen in the replacement of the Ministry of Energy, Communications and Multimedia with the new ministry i.e., the Ministry of Energy, Green Technology and Water a few years ago. In April 2009, the National Green Technology Policy was also launched with the main objectives of providing guidance toward acceleration of the national economy and to promote sustainable development. The policy is built on four main pillars i.e., energy, environment, economy and social (Oh et al., 2010).

- Energy—seeks to attain energy independence and promote efficient utilization.
- Environment—conserves and minimizes the impact on the environment.
- Economy—enhances the national economic development through technology.
- Social—improves the quality of life for all.

With the introduction of the National Biofuel Policy that consists of five strategic thrusts, it is believed that the policy will form a comprehensive framework detailing concrete initiatives that could encourage the use of biodiesel in Malaysia. Efforts should also be directed toward promoting government, private and community participations and entrepreneurship through higher participation of R&D institutions in the process of biofuel development. Recognizing the importance of continuous R&D on biofuel technology is one of the major mandates of the National Biofuel policy. It is stated in the policy that R&D efforts would be focused on palm oil research, production and conversion technologies of biodiesel besides maximizing the efficient use of B5 in industrial and transport sectors (Abdullah et al., 2009). The policy provides high priority on R&D and technology development based on the indigenous feedstock and needs which will be benchmarked against international efforts.

Above all, it is important for the National Biofuel Policy to be comprehensive enough and it should be based on the pillars of energy, environment sustainability, economic, social, technological development and trade for export. This type of policy is considered to be encouraging for developing Malaysia which ensures its energy security, clean environment and sustainable development using eco-friendly biofuel as an alternate source of energy (Ahmad et al., 2011).

3. B5 biodiesel development, potential and implementation in Malaysia

Globally, Malaysia is second largest producer of palm oil after Indonesia and has great potential to play a key role in the world biodiesel market due to its well-established palm oil industry (Kalam et al., 2008). The abundance of the raw feedstock had led the Malaysian government to begin biodiesel production program by the establishment of the governmental agency namely Malaysian Palm Oil Board (MPOB) which is known as the pioneer in developing the palm oil biodiesel and to subsequently develop a road map for the use of biofuels in petrol and diesel engines. The idea of utilizing palm oil for biodiesel production was developed since 1982 considering the depleting fossil fuel resources. At that time, it was expected that Malaysian industries and vehicles would be using B5 biodiesel in the near future (Adnan, 2012). Since then, extensive research and development using palm oil and its products have been directed toward biodiesel production.

Fig. 2 summarizes the development of B5 biodiesel implementation in Malaysia from 2006 until 2013. According to the third thrust of the biofuel policy i.e., regarding the biofuel technology, the government has allocated about RM 300 million of grants for the development of biodiesel technologies including blending facilities nationwide (Adnan, 2013). To date, about RM 80 million was spent by oil companies and biodiesel producers to build the B5 blending facilities and for biodiesel subsidies which can then be easily upgraded to B10. As of October 2011, a total of 60 palm oil-based biodiesel manufacturing licenses had been approved by the Malaysia's Ministry of Plantation Industries and Commodities (MPIC) with a total annual capacity of 6.79 million t. A total of 20 biodiesel plants have been commissioned since 2006. The status of the approved biodiesel licenses is summarized in Table 1. Until recently, there are 11 active biodiesel plants in the country with the total annual capacity of 1.65 million t per year (Kheang and May, 2012). Table 2 presents the list of the active biodiesel plants in Malaysia as of 2008.

3.1. Introduction of the first B5 Envo Diesel

The development of biodiesel in Malaysia was solidified with the introduction of the first B5 biodiesel in 2006 by the former

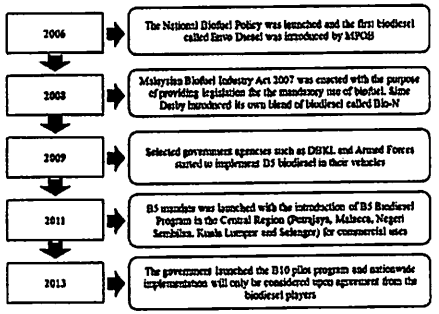

Fig. 2. Development of B5 biodiesel implementation program in Malaysia.

Table 1
Recent status of approved biodiesel licenses (Kheang and May, 2012).

Implementation phase	No.	Production capacity (million t/year)
Commercial production	20	2.62
Completed construction	12	1.20
Under construction	5	0.90
Pre-construction/planning	23	2.07
Total approved	60	6.79

Prime Minister Tun Abdullah Ahmad Badawi. It was made right after the launching of National Biofuel Policy which was initially implemented on selected government vehicles (Lim and Lee, 2010). At that time, the targeted agencies were the Defense Ministry, Selangor Public Works Department, Kuala Lumpur City Hall (DBKL) and agencies under MPIC (Bernama, 2005). MPOB introduced the B5 with the brand name of Envo Diesel which is a mixture of 5% processed palm oil and 95% petroleum diesel. This was the initiative that acted as a starting catalyst for changing the people's perception on the palm oil industry as an agro-based industry for future foundation for sustainable development in energy as well as for ensuring cleaner environment.

However, the implementation of Envo Diesel in diesel vehicles encountered some obstacles due to apprehension from engine manufacturer. Japan Automobile Manufacturers Association (JAMA) refused to extend the engine warranty on the Envo Diesel usage due to several problems that could occur in the engine such as engine clogging, fuel system corrosion as well as material incompatibility (Petrolworld, 2008). Due to this refusal, the government has shifted the use of refined palm oil with palm methyl esters which was known as B5. Since then, government of Malaysia has undertaken several policy measures for practical actions in developing biodiesel industry. They are based on extensive research works and continuous development on palm oil based biodiesel production technologies and biodiesel quality improvement.

3.2. Bio-N biodiesel by Sime Darby

In order to reflect the policy which envisages utilization of environmental friendly fuel, Sime Darby Plantation Sdn. Bhd. has also introduced its own biodiesel blend. Despite the high processing cost of biodiesel, the Sime Darby Group has taking the lead in this initiative to declare biodiesel a future fuel in Malaysia through the introduction of its new biodiesel blend called Bio-N (Motor Trader, 2010). Bio-N was an initiative of Sime Darby in response to the government's call for public usage of biodiesel in Malaysia. It was produced at a plant located at Teluk Panglima Garang and was initially used by Sime Darby's upstream operations vehicles since March 2008. Its was demonstrated confidently by the Sime Darby President and Group Chief Executive himself by pumping it into his BMW 730 LD, executives cars as well as the company's tractors and motorbikes in order to show full support on the government policy. At the same time, this effort reflected their commitment toward the use of eco-friendly fuel (Sime Darby, 2010).

Even though the cars fueled with Bio-N generally run smoothly without major problem, there are no standards for the fuel established and no approval have been made by the Malaysia's Ministry of Domestic Trade and Consumer Affairs as well as the Department of Environment and Standards and Industrial Research Institute of Malaysia (SIRIM). Until the standards of the biodiesel are issued, it is actually not recommended to use Bio-N for public cars (Tan, 2011; Adnan, 2013). However, the issue came to light when the standards of the biodiesel blends was finally accepted and approved by Malaysian Automotive Association (MAA).

In order to ensure that the fuel is suitable for any local motor manufacturers, the B5 biodiesel must meet the new standards regulated by the Department of Standards Malaysia namely the MS2008 standards which are derived from the international standards (EN14214). The standards were developed with an Industry Standards Committee involving 17 organizations, and a Technical Committee consisting of 16 organizations that include fuel retailers in Malaysia, SIRIM, Automobile Association Malaysia (AAM) and Malaysian Road Transport Department (Tan, 2011). The simple data on comparative analysis of fuel compatibility of MS2008 standards and EN14214 standards are given in Table 3. The establishment of the biodiesel standards has led the government to take a few steps ahead. They were done by utilizing the B5 biodiesel in the transport and industrial sectors that coincided with the National Biofuel Policy which highlighted the priority options of B5 implementation in these sectors (Ahmad et al., 2011).

3.3. B5 biodiesel implementation in Peninsular Malaysia

The implementation of B5 biodiesel is mainly divided into three phases involving selected government agencies (Phase I), retail stations in the Central Region (Phase II) and subsequently nationwide (Phase III). In February 2009, the first phase of the implementation started with the involvement of 3900 diesel engine vehicles from various government agencies such as the Kuala Lumpur City Council (DBKL) and Armed Forces. Until October 2011, 14.54 million l of B5 had been supplied and it utilized about 639 t of palm biodiesel. The implementation of B5 for transportation sector was seen to be successful with an increase in biodiesel production in Malaysia by 48%. 173, 220 t of palm biodiesel was produced in 2011 compared to 2010 which saw only 117,173 t of biodiesel produced (Mamat, 2012).

In conjunction with the success of the B5 implementation in the government vehicles, the government has widened the B5 program in the Central Region to also involve retail stations as well as fisheries sector. The B5 Biodiesel Program was officially launched by the Plantation Industries and Commodities Minister, Tan Sri Bernard Dompok in June 2011 and Putrajaya became

Table 3
Comparison between Malaysian and European biodiesel standards (Tan, 2011).

Properties	MS2008	EN14214
Carbon residue (%) (m/m)		
(On 10% distillation residue)	0.30 (max)	0.30 (max)
(On 100% distillation sample)	0.05 (max)	-
Iodine value (g Iodine/100 g)	110 (max)	120 (max)
Cold filter plugging point (CFPP) (°C)	15 (max)	Not available

Table 2
List of active biodiesel plants in Malaysia as in 2008 (Lim and Lee, 2010).

No.	Company	Location	Plant capacity (t/year)
1	Carotino Sdn. Bhd.	Pasir Gudang, Johor	200,000
2	Malaysia Vegetable Oil Refinery Sdn. Bhd.	Pasir Gudang, Johor	110,000
3	PGEO Bioproducts Sdn. Bhd.	Pasir Gudang, Johor	100,000
4	Vance Bioenergy Sdn. Bhd.	Pasir Gudang, Johor	200,000
5	Mission Biotechnology Sdn. Bhd.	Kuantan, Pahang	200,000
6	Carotech Bio-Fuel Sdn. Bhd.	Ipoh, Perak	150,000
7	Lereno Sdn. Bhd.	Setiawan, Perak	60,000
8	Golden Hope Biodiesel Sdn. Bhd.	Teluk Panglima Garang, Selangor	150,000
9	Global Bio-Diesel Sdn. Bhd.	Lahad Datu, Sabah	200,000
10	SPC Bio-Diesel Sdn. Bhd.	Lahad Datu, Sabah	100,000

Table 4
Launching of B5 Biodiesel Program in the Central Region of Malaysia in 2011.

Location	Date	Remarks
Putrajaya	June	Six petrol stations participated in this program (five from Petronas and one from Shell) (MPIC, 2011a).
Malacca	July	Being the second state to supply B5 biodiesel, 107 petrol stations were involved in this program which could supply about 664,000 l of palm biodiesel monthly in Malacca (MPIC, 2011b).
Negeri Sembilan	August	156 Petrol stations participated in this program and it was expected that 1.1 million l of palm biodiesel would be consumed monthly in this state which could save up 13 million l of fossil-diesel per year (MPIC, 2011c).
Kuala Lumpur	October	In Kuala Lumpur, 247 petrol stations participated in the B5 Program and it was expected that 1.03 million l of biodiesel would be consumed every month (saving about 12.4 million l of fossil-diesel every year) (MPIC, 2011d).
Selangor	November	634 pump stations were involved in the B5 Program in Selangor in which were about 4.85 million l of palm biodiesel would be supplied every month (saving about 58 million l fossil diesel every year) (MPIC, 2011e).

the first location to see the implementation of this fuel. With this initiative, Malaysia became the second country in world to implement the use of B5 which is higher than biodiesel blends in Thailand (B2) and Philippines (B1). After this, it was replicated to Malacca, Negeri Sembilan, Kuala Lumpur and Selangor (Ismail, 2011). Table 4 illustrates the chronology of the B5 biodiesel program implementation history in the Central Region involving 5 major petroleum companies including Petronas, Shell, BHPetrol, Esso and Caltex.

The highest usage of B5 was recorded in Selangor in which the B5 was supplied to 634 stations followed by Kuala Lumpur (247 stations), Negeri Sembilan (156 stations), Malacca (107 stations) and Putrajaya (6 stations). In this regard, the most successful mandatory B5 implementation in the Central Region was achieved in Selangor state. The use of palm oil-based B5 biodiesel in the Central Region was expected to see 6587 t of palm oil mixed with petroleum diesel monthly in 1150 petrol stations (The Star, 2011). In order to achieve this target, the government through the MPOB had allocated RM 43.1 million of fund for construction of B5 in-line blending facilities at six petroleum depots in Port Klang, Klang Valley Distribution Terminal (KVDT), Port Dickson and Tangga Batu which belong either to Petronas Dagangan, Shell Malaysia Trading, Esso Malaysia, Chevron Malaysia or Bousted Petroleum Marketing (Lim, 2011). Overall, the main aim of this initiative as taken by the government was to maximize the usage of B5 to reduce the country's huge palm oil inventory to stabilize the CPO price as well as to increase the income of palm oil farmers.

This program initially covered land transport sector including private cars and commercial vehicles. However, the B5 biodiesel was further implemented in the fisheries sector in order to increase the consumption CPO in the country. Fisheries sector plays an important role in the development of the Malaysian economy which contributes significantly to the national gross domestic product (GDP) as well as the source of cheap animal protein to the people. It also generates employment and foreign exchange.

In the meantime, this sector could also be considered as one of the major diesel consuming industries after transportation sector to become among the contributors of GHG, water pollution and fuel spill. Thus, many boaters have considered switching to biodiesel because of the reduced smoke as well exhaust odor. These factors have led the government to start implementing the biodiesel on the fishing boat engines as an effort to reduce GHG emissions toward a cleaner environment while at the same time reduces dependency on the depleting petroleum diesel (Ahmad et al., 2011).

In February 2012, Malaysian government launched the implementation of B5 program in fishery sectors in the Central Region under the umbrella of the National Biofuel Policy. At the same time, B5 biodiesel was declared as safe for use in fishing boat engines and engine warranty was also given by the petroleum companies and engine manufacturers in order to encourage the positive perception among people involved in this sector. In addition, it could also enhance engine performance and reduce smoke emissions along with other GHG.

MPOB and The Fisheries Development Authority of Malaysia (LKIM) had jointly conducted a trial project involving the use of 30,000 l B5 by boats owned by the Persatuan Nelayan Kawasan, Bagan Pasir, Tanjung Karang (MPIC, 2012). The results of this study indicated that, by using B5 biodiesel, the engine power was found to be compatible with that ran by fossil diesel and also more beneficial in lowering smoke emission as well as reducing engine knocking. Furthermore, none of any adverse effect on the engine was reported. According to an estimate, the launching of this program would result in the use of 39 million l of biodiesel every year which contributes to the saving of 30.51 million l diesel in fleet card sector, 5.77 million l in fisheries sector and 2.28 million l in skid tank sector (Mamat, 2012).

In the meantime, the initiation of this new B5 fuel program was not expected to bring about any negative impact with respect to the operating cost of the targeted consumers as the government would continue to keep the price at RM 1.80/l which is similar to that of regular diesel (Bernama, 2011). Thus, consumers still have a little incentive to switch to B5 since it does not require any engine modification. Furthermore, B5 biodiesel offers several benefits especially toward a greener and cleaner environment. Utilization of palm biodiesel is reported to be environment friendly as contributes to 50% reduction in GHG emission compared to fossil fuels (MPIC, 2011e). However, the combustion of palm oil biodiesel can still release considerable amount of NO_x emission (which is still below regulated level) to the atmosphere (Lim and Lee, 2010). Luckily, it can still be reduced with the installation of catalytic converters in biodiesel powered vehicles (Lozada and Islas, 2010). Regarding engine performance, smoke emission and volatility levels of B5 are lower as compared to those in regular diesel engines due to a presence of oxygen in the fuel (Kalam et al., 2008).

Even though the B5 program still has yet to be fully implemented nationwide, the government has taken a new step forward by migrating to B10 from the existing B5 biodiesel in line with the decision to upgrade the existing B5 program. This is due to the increasing CPO stock levels which was 2.63 million t as of December 2012 (Thean, 2013). In order to reduce the high palm oil inventory while promoting the green alternative fuel, MPOB has introduced the B10 biodiesel pilot program which was officially launched on 7th February 2013 by the MPIC Minister Tan Sri Bernard Dompok (Aziz, 2013). It was expected that 1 million t of CPO and 2.6 million t of palm oil inventory would be reduced with the introduction of this program. The implementation of B10 biodiesel initially involved vehicles from Ministry of Plantation Industries and Commodities (MPIC) in order to convince the petroleum companies and engine manufacturers.

According to recent studies by MPOB, B10 would not give negative impact to the diesel engine vehicles in which 10% in B10 is too small to pose significant effect. However, some of the participants in the biodiesel program were not convinced with the implementation of B10 in diesel engine vehicles because of the unknown properties of the B10 biodiesel (Adnan, 2013). This matter has forced the government to cooperate with SIRIM and Department of Standard Malaysia in order to develop a new set of standards specifically for B10 biodiesel as the existing biodiesel standards are only applicable to B5 biodiesel. Full implementation of B10 will be carried out after the new standards for B10 have established and subsequently, the B5 program will be gradually terminated (Thean, 2013).

4. Global and local challenges to biodiesel production in Malaysia

Malaysia is known as the leading producer of palm methyl esters (PME) back in 2005. However, this country is currently having a competitive edge over the global biodiesel producers as its local biodiesel production still remains stagnant due to weak domestic demand and also uncompetitive export tax structure. According to Carotino Sdn. Bhd. Executive Director, only 170,000 t of biodiesel was produced in 2011 which represented only 6% of the total installed capacity which was then 2.7 million t from 29 biodiesel plants nationwide (The Star, 2012). Thus, now Malaysia is unfortunately losing its position and considered to be a small biodiesel producer as compared to the other vegetable oil producing countries like Europe, United State (US), Brazil, Argentina, Indonesia, Thailand or even Colombia. Compared to Indonesia, Malaysia has been using less than 1% of its CPO for biodiesel production for the last five years while Indonesia significantly increased its consumption of CPO to 9% by the end of 2011 (Lim, 2012).

4.1. Biodiesel export market

As discussed earlier, Malaysia was declared as the world's largest palm oil exporter in 2006. This can be observed from its revenue generation due to high export rate compared to other countries. MPOB reported that the total revenue generated from the biodiesel export had reached up to 172 USD million in 2008 (Lim and Lee, 2010). Very recently, Malaysia contributed about 42.3% of palm oil production and 48.3% of world's palm oil export in 2012 (Hosseini and Wahid, 2012). Current trends of the exports and domestic consumption conclude that Malaysia is currently losing out to its competitors like Indonesia, Thailand and Colombia. It can be seen by the reduction of the biodiesel export in 2011 which was only 50,000 t compared to 86,000 t in 2010. Malaysia's biodiesel exports were found to be still lower as compared to those of Indonesia and Argentina that successfully exported 62% and 73% of their total biodiesel production, respectively in 2011 (Adnan, 2012). This weak export performance was believed to be due to the lack of competitiveness among the biodiesel producers. In view of its current domestic production and high export duty, it is expected that Malaysia's biodiesel export would further reduce in the future. In an effort to curb this problem, the government will continue to encourage the export of biodiesel to several countries including the European Union, United States and Australia with the objective of recovering and sustaining its strong position versus other key players (Abdullah et al., 2009).

Another factor that is seriously affecting the Malaysia's biodiesel export market is the export duty differential. Indonesia has been structuring their CPO and biodiesel differential duties in order to stimulate their biodiesel downstream activities. To date, Indonesia's duty for CPO is 16.5% and the duty on biodiesel is 2%. The strategy taken by Indonesia has brought about positive impact on their biodiesel market. This can be seen by an increase in the Indonesia's biodiesel export which was about 62% of its total production in 2011 compared to that in the previous year which was only 28% (Lim, 2012).

In order to improve the competitiveness of Malaysian palm oil and regain the market share from Indonesia, the export duty of Malaysia's CPO should to be revised and restructured. For that reason, Palm Oil Refiners Association of Malaysia (PORAM) has proposed to the government to cut the export tax to between 8% and 10% (Ching, 2012) as the current export tax structure is considered to be not sufficiently attractive for export purposes. This measure seems to enlighten the palm oil players following the government's announcement on the palm oil duty reforms. On 12 October 2012, Malaysian Cabinet approved to cut the CPO export duties to between 4.5% and 8.5% from the earlier level of 23% and also abolished the duty-free export quota from January 2013 onward (Ching-Ling and Foon, 2012). Even though the proposed rate is still far from ideal, the rate announced by the government was still more practical and bearable for planters. It is expected that by lowering the CPO export tax, the refineries in Malaysia will be able to market their products to the global markets at competitive prices (Ching, 2012).

4.2. CPO stocks consumption

Despite lower yearly production, Malaysian CPO stocks have increased to a record level recently compared to that of the earlier year as the exports failed to keep up with the production rate. This can be seen by the official monthly data release which showed that Malaysia's palm oil stocks increased by 17.43% from August 2012 to 2.48 million t in September 2012 (Shen and Yeap, 2012). Even though Malaysia has started implementing the B5 biodiesel programs in some of the land transport sectors, the progress was still slow, due to the limited availability of the product in certain regions. As a consequence, the CPO stock level continued to increase recently (Bernama, 2011).

The full implementation of the B5 is expected to reach other regions in Peninsular Malaysia including Sabah and Sarawak by 2013 with a goal of about 570,000 t of CPO to be used to produce 500,000 t biodiesel (Wahab, 2012). However, the local consumption of CPO declined by 20% and not increased as expected upon the implementation of B5 mandate (Lane, 2012). Thus, Malaysian biodiesel players must rely on the government to communicate and consult with the relevant parties to successfully implement the B10 (blending of 10% PME) or B20 (blending of 20% PME) program as soon as possible since several countries have taken a step forward in implementing higher PME blend in their diesel. Argentina has mapped out the implementation of B10 by 2015 replacing the current B5 while elsewhere, Colombia is even aiming for the migration from the current B10 to B20 by 2015 (The Star, 2012). By implementing the B10 or B20 program in Malaysia, it is expected that the CPO consumption would increase by another 300,000 t a year to effectively reduce the inventory of palm oil while at the same time contributes to the successful implementation of biodiesel program.

5. Conclusions

Like other developing nations, Malaysia realizes that energy shortage will be the main problem facing its sustainable development in the near future. As such, Malaysian government is highly enthusiastic for expanding and improving access to clean and indigenous palm oil based biofuel energy services. The potential renewable energy resource in the form of palm oil biodiesel (B5) in Malaysia provides great opportunities to develop the local palm oil industry while at the same time meeting the future energy demands. Implementation programs have been initiated at the local, national and regional levels to expand B5 access and meet its developmental challenges. Various financial instruments and funds toward successful biodiesel implementation as well as the scenario with respect to the availability

of feedstock for biodiesel production in Malaysia are reviewed. These include government, domestic, private, multilateral and bilateral sources to fulfill its energy requirement for industrial and transport sectors. Successfully implementations of B5 program in the government agencies and in the Central Region involving transportation and fisheries sectors are particularly discussed. As the progress of the program is quite slow, the B5 implementation has been planned to extend nationwide in stages including to unsubsidized sectors by 2014. The government has also introduced a pilot B10 program which is expected to be fully implemented in mid 2014 upon agreement from parties involved. The initiatives would indirectly be beneficial to consumers while conserving the environment. In addition to better performance in the engine, the implementation of B5 and B10 biodiesel in the subsidized and unsubsidized sectors would contribute to reductions in fossil fuel consumption and emission level which is in line with the global efforts to reduce the GHG emission. In order to overcome the global challenges, several measures on the biodiesel usage as planned by the government by extending it to power plants or diesel engine vehicles in the major plantation companies nationwide are also highlighted.

Acknowledgment

The Research University (814144) grant to support biodiesel research at the School of Chemical Engineering, Universiti Sains Malaysia is gratefully acknowledged.

Appendix A. Supporting information

Supplementary data associated with this article can be found in the online version at http://dx.doi.org/10.1016/j.enpol.2013.08.009.

References

Abdullah, A.Z., Salamatinia, B., Mootabadi, H., Bhatia, S., 2009. Current status and policies on biodiesel industry in Malaysia as the world's leading producer of palm oil. Energy Policy 37, S460–S448.

Adnan, H., 2012. Malaysian dilemma on biodiesel exports. Available from: ‹http://biz.thestar.com.my/news/story.asp?file=/2012/4/17/business/11114257›. (accessed 24.12.12).

Adnan, H., 2013. Malaysia's B10 biodiesel programme and its benefits. Available from: ‹http://biz.thestar.com.my/news/story.asp?file=/2013/2/12/business/12699472&sec=business›. (accessed 22.02.13).

Ahmad, S., Kadir, M.Z.A.A., Shafie, S., 2011. Current perspective of the renewable energy development in Malaysia. Renewable and Sustainable Energy Review 15, 897–904.

Aziz, M.A., 2013. B10 tingkat industri biodiesel. Available from: ‹http://www.bharian.com.my/articles/B10tingkatindustribiodiesel/Article/›. (accessed 20.02.13).

Bernama, 2006. PM launches "Envo Diesel" Biofuel. Available from: ‹http://www.bernama.com/bernama/v3/news_litr.php?id=187164›. (accessed 23.02.13).

Bernama, 2011. B5 biodiesel supply nationwide by 2013: Dompok. Available from: ‹http://www.theborneopost.com/2011/10/07/b5-biodiesel-supply-nationwide-by-2013-dompok-latest/›. (accessed 26.12.12).

Ching, O.T., 2012. Green light for CPO export tax cut. Available from: ‹http://www.btimes.com.my/Current_News/BTIMES/articles/20121011011000/Article/index_html›. (accessed 26.12.12).

Ching-Ling, H., Foon, H.W., 2012. Palm oil duty reforms create 'feel-good factor'. Available from: ‹http://www.theedgemalaysia.com/in-the-financial-daily/223607-palm-oil-duty-reforms-create-feel-good-factor.html›. (accessed 26.12.12)

Goh, C.H. Tan, K.T., Lee, K.T., Bhatia, S., 2010. Bio-ethanol from lignocellulose: status, perspectives and challenger in Malaysia. Bioresource Technology 101, 4834–4841.

Hosseini, S.E., Wahid, M.A., 2012. Necessities of biodiesel utilization as a source of renewable energy in Malaysia. Renewable and Sustainable Energy Reviews 16, 5732–5740.

Ismail, M.N., 2011. B5 biodiesel debuts in Kuala Lumpur, at 247 stations. Available from: ‹http://palmnews.mpob.gov.my/palmnewsdetails/palmnewsdetail.php?idnews=8873›. (accessed 24.12.11).

Kalam, M.A., Masjuki, H.H., Saifullah, M.G., Seng, T.B., 2003. Envo Diesel test on automotive engine—an analysis of its performances and emission results. International Journal of Mechanical and Materials Engineering 3 (1), 55–60.

Kheang, L.S., May, C.Y., 2012. Malaysia: achievement and challenges in adoption of Biofuels and Bio-energy. In: Proceedings of the 3rd International Symposium on Biofuels and Bioenergy, New Delhi, India.

Lane, L., 2012. Palm oil demand drops despite Malaysia's B5 biodiesel mandate. Available from: ‹http://www.biofuelsdigest.com/›. (accessed 24.12.12)

Lau, L.C., Tan, K.T., Lee, K.T., Mohamed, A.R., 2009. A comparative study on the energy policies in Japan and Malaysia in fulfilling their nations' obligations towards the Kyoto Protocol. Energy Policy 37, 4771–4778.

Lee, J., 2012. Fuelled by passion. Available from: ‹http://thestar.com.my/news/story.asp?file=/2012/4/30/metrobiz/11200876&sec=metrobiz›. (accessed 27.02.13).

Lim, A., 2011. B5 biodiesel programme begins-Putrajaya kicks things off. Available from: ‹http://paultan.org/2011/06/01/b5-biodiesel-programme-begins-putrajaya-kicks-things-off/›. (accessed 24.12.12).

Lim, B.S., 2012. Malaysian palm biodiesel losing out against rivals. Available from: ‹http://www.theedgemalaysia.com/highlights/210019-malaysian-palm-biodiesel-losing-out-against-rivals.html›. (accessed 25.12.12).

Lim, S., Lee, K.T., 2010. Recent trends, opportunities and challenges of biodiesel in Malaysia. Renewable and Sustainable Energy Reviews 14, 938–954.

Lozada, L., Islas, J., 2010. Environmental and economic feasibility of palm oil biodiesel in Mexican transportation sector. Renewable and Sustainable Energy Reviews 14, 486–492.

Mamat, C.J., 2012. Sektor Perikanan Wilayah Tengah guna B5. Available from: ‹http://www.bharian.com.my/bharian/articles/SektorPerikananWilayahTengahgunaB5/Article›. (accessed 22.02.12).

Meher, L.C., Vidya-Sagar, D., Naik, S.N., 2006. Technical aspects of biodiesel production by transesterification—a review. Renewable and Sustainable Energy Reviews 10, 249–268.

Mofijur, M., Masjuki, H.H., Kalam, M.A., Hazrat, M.A., Liaquat, A.M., Shahabuddin, M., Varman, M., 2012. Prospects of biodiesel from Jatropha in Malaysia. Renewable and Sustainable Energy Reviews 16, 5007–5020.

Motor Trader, 2010. Introduction to B5 biodiesel. Available from: ‹http://www.motortrader.com.my/news/introduction-to-b5-biodiesel/›. (accessed 05.02.13).

MPIC, 2011a. Ministry of Plantation Industries and Commodities Malaysia (MPIC) press release. Majlis pelancaran penggunaan biodiesel sawit adunan B5 peringkat wilayah tengah di Putrajaya. Available from: ‹http://www.kppk.gov.my/›. (accessed 24.12.12).

MPIC, 2011b. Ministry of Plantation Industries and Commodities Malaysia (MPIC) press release. Majlis pelancaran penggunaan biodiesel sawit adunan B5 peringkat negeri Melaka. Available from: ‹http://www.kppk.gov.my/›. (accessed 24.12.12).

MPIC, 2011c. Ministry of Plantation Industries and Commodities Malaysia (MPIC) press release. Majlis pelancaran program B5 (penggunaan adunan 5% metal ester wasit dengan 95% diesel petroleum) peringkat Negeri Sembilan. Available from: ‹http://www.kppk.gov.my/›. (accessed 24.12.12).

MPIC, 2011d. Ministry of Plantation Industries and Commodities Malaysia (MPIC) press release. Majlis pelancaran program B5 (penggunaan adunan 5% metal ester sawit dengan 95% diesel petroleum) peringkat Kuala Lumpur. Available from: ‹http://www.kppk.gov.my/›. (accessed 24.12.12).

MPIC, 2011e. Ministry of Plantation Industries and Commodities Malaysia (MPIC) press release. Launching of the B5 programme in Selangor and the commemoration of the successful mandatory implementation in the central region. Available from: ‹http://www.kppk.gov.my/›. (accessed 24.12.12).

MPIC, 2012. Ministry of Plantation Industries and Commodities Malaysia (MPIC) press release. Launching of the B5 programme in fisheries sector in the central region. Available from: ‹http://www.mpic.gov.my/›. (accessed 24.02.13).

Nakata, T., Silva, D., Rodionov, M., 2011. Application of energy system models for designing a low-carbon society. Progress in Energy and Combustion Science 37, 462–502.

Oh, T.H., Pang, S.Y., Chua, S.C., 2010. Energy policy and alternative energy in Malaysia: issues and challenges for sustainable growth. Renewable and Sustainable Energy Reviews 14, 1241–1252.

Petrolworld, 2008. Malaysia: Envo Diesel biofuel to be replaced with methyl ester. Available from: ‹http://www.petrolworld.com/alternative-fuels/malaysia-envo dieselbiofuel-to-be-replaced-with-methyl-ester.html›. (accessed 27.02.13).

Poh, K.M., Kong, H.W., 2002. Renewable energy in Malaysia: a policy analysis. Energy for Sustainable Development IV (3), 31–39.

Shahid, E.M., Jamal, Y., 2008. A review of biodiesel as vehicular fuel. Renewable and Sustainable Energy Reviews 12, 2484–2494.

Shen, C.K., Yeap, C., 2012. Malaysia can have B5 biodiesel nationwide by Dec to cut CPO stocks. Available from: ‹http://www.theedgemalaysia.com/business-news/222655-malaysia-can-have-b5-biodiesel-nationwide-by-dec-to-cut-cpo-stocks.html›. (accessed 26.12.12).

Sime Darby, 2010. Sime Darby Plantation press release. Sime Darby plantation responds to government's call for use of biodiesel in private sector. Available from: ‹http://www.simedarbyplantation.com/›. (accessed 05.02.13)

Tan, P., 2011. Malaysian B5 biodiesel at pumps to comply with MS2008 based on EN14214 biodiesel standard. Available from: ‹http://paultan.org/›. (accessed 05.02.13).

The Star, 2011. Govt. aims for biodiesel use to reach 500,000 t per month. Available from: ‹http://biz.thestar.com.my/news/story.asp?file=/2011/11/1/business/20111101134511›. (accessed 25.12.12)

The Star, 2012. B10 biofuel programme to help reduce inventory. Available from: ‹http://biz.thestar.com.my/news/story.asp?file=/2012/10/13/business/12160822&sec=business›. (accessed 25.12.12).

Thean, J.N., 2013. B10 to be launched tomorrow to remove 1 million t of CPO. Available from: ‹http://theedgemalaysia.com›. (accessed 20.02.13).

Wahab, A.G., 2012. Malaysia biofuels annual reports 2012. Available from: ‹http://www.fas.usda.gov/›. (accessed 24.12.12).

Contents lists available at ScienceDirect

Applied Catalysis A: General

journal homepage: www.elsevier.com/locate/apcata

Ultrasound-assisted biodiesel production from waste cooking oil using hydrotalcite prepared by combustion method as catalyst

Mohd Razealy Anuar, Ahmad Zuhairi Abdullah*

School of Chemical Engineering, Universiti Sains Malaysia, 14300 Nibong Tebal, Penang, Malaysia

ARTICLE INFO

Article history:
Received 11 November 2015
Received in revised form 15 January 2016
Accepted 19 January 2016
Available online 22 January 2016

Keywords:
Ultrasound-assisted system
Biodiesel
Transesterification
Hydrotalcite
Combustion method

ABSTRACT

Ultrasound-assisted biodiesel production from waste cooking oil catalyzed by hydrotalcite (HT) catalyst prepared using combustion method was studied. Two important parameters in the HT synthesis i.e., calcination temperature (550–850 °C) and fuel type (saccharose, glucose and fructose) were particularly investigated. The dependence of HT's characteristics on the synthesis parameters and correlations with their catalytic performance under ultrasound condition were successfully elucidated. The HT catalyst prepared using saccharose and calcined at 650 °C was the best catalyst to be used in the transesterification reaction. It showed high biodiesel yield (about 76.45%) in just 60 min in the presence of low ultrasound amplitude (~11 kHz). The enhancement effect of ultrasound was successfully demonstrated. The reaction only needed short reaction time (about 1 h) to give a biodiesel yield of up to 76.45% compared to conventional stirring method that needed about 5 h to achieve the same yield.

1. Introduction

Sustainable energy supply in the future is of great concern due to the depletion of petroleum fuel resources. The quest for replacement fuel is currently underway. The use of vegetable oil as biodiesel feedstock provides interesting alternative as sustainable carbon cycle and environmentally friendly objectives are guaranteed. Meanwhile, the enhancement of biodiesel production process can be achieved through the use of sophisticated equipment such as membrane reactor, reactive distillation column, high frequency magnetic impulse cavitation reactor, centrifugal contact separator and ultrasound-assisted system [1]. However, mature understanding and the full potential of these systems are yet to be achieved. Development of advanced technologies that can stimulate an economical biodiesel production is highly needed. Therefore, it has motivated this present study on the use of an efficient and novel catalytic reaction system for biodiesel production.

Feedstock is an important aspect that can affect the economic viability of biodiesel production process. Atabani et al. [2] have reviewed various feedstock consisting of both edible and non-edible oils suitable for biodiesel production. However, edible feedstock might face the fuel vs food dilemma as well as the deforestation issue [3]. Meanwhile, non-edible feedstock usually encounter limitations with regards to impurities that can affect the production process [4]. However, such problems motivate researchers to come out with new inventions and solutions. Research on waste cooking oil as the non edible feedstock has enticed many researchers to come up with new ideas [5–7] to ensure the future relevance of biodiesel industry. In line with that, the present study evaluates the prospects of waste cooking oil in a positive way for commercial use in biodiesel industry. However, the use of waste cooking oil as feedstock is rather challenging as it basically contains high concentrations of 2 major impurities i.e., free fatty acid and moisture. However, with the available technology, the problem can be solved with several pre-treatment techniques and the use of specific types of catalyst [8,9]. Based on such concerns, this work has been designed to demonstrate an innovative and suitable catalytic reaction system that could possibly address the challenges of using waste cooking palm oil as the feedstock.

Biodiesel production process has been successfully intensified with recently developed processing technologies including pyrolysis, dilution, micro-emulsion, transesterification and esterification [2]. In recent years, most of the studies have been focusing on the role of heterogeneous catalysts in transesterification or esterification reaction. The conventional production processes of biodiesel i.e., through the use of homogeneous acid and base catalysts such as sulfuric acid and potassium hydroxide have been successfully performed [10–13]. The main drawback experienced when dealing with homogeneous catalyst with regards to the product separation has enticed the study on the application of heterogeneous catalysts

* Corresponding author. Fax: +60 45941013.
E-mail address: chzuhairi@usm.my (A.Z. Abdullah).

http://dx.doi.org/10.1016/j.apcata.2016.01.023
0926-860X/

such as CaO, hydrotalcite, dolomite, silica, SiO_2 etc. [14] which are sufficiently active and the need for further product purification can be avoided.

Conventional biodiesel production processes based on heterogeneous catalysis still show some drawbacks with regards to long processing time and poor rate of reaction. Many factors should also be considered when dealing with the immiscible reactants i.e., oil and alcohol. The reactants usually experience mass transfer limitation and emulsification problem so that longer time is needed for the reaction to complete. These problems can be effectively solved by conducting the biodiesel production process in the presence of ultrasound and solid catalysts. Badday at al. [15,16] have performed various studies on the enhancement of biodiesel processing using an ultrasound system. The reaction period was efficiently shortened to 60 min and the function of ultrasound had been technically elucidated. Poor mass transfer and emulsification limitation are no longer the issues toward achieving high transesterification rate to achieve high yield of biodiesel. Super vigorous effect due to high mechanical agitation provided by ultrasound can facilitate the contact between oil and alcohol. Besides, the boundary limitation between both reactants can be eliminated to force the reaction to occur mostly inside the catalyst pores. Therefore, this pivotal role of ultrasound could efficiently assist the catalytic reaction system and it is thoroughly addressed in this study.

Hydrotalcite (HT) is commercially recognized as an applicable catalyst in many reactions. HT generally possesses layered structure and its properties are often differentiated based on the composition with respect to the type of cation and the intercalated anion [17]. HT is predominantly basic in which the cations (usually Mg) in the layered structure belong to alkaline earth metals and the intercalated anions are basic (usually CO_3^{2-}). Besides, HT catalyst is relatively robust where it shows no leaching problem during transesterification reaction [18]. These desired properties of HT justify its suitability to be used as high mechanical strength catalyst in an ultrasound-assisted system. In previously reported works, HT has shown good performances in catalyzing transesterification reaction for biodiesel production in which the highest FAME conversions and yields were recorded to be up to 77% [18,19] and 95.2% [20,21], respectively. HT might provide adequate hydroxyl and carbonate ions to create highly basic condition to initiate the transesterification reaction. The reaction starts when the carbonyl carbon of triglyceride is attacked by alkoxide ion from alcohol producing intermediates with the aid of hydroxyl ions from HT [22]. Then, further reaction between these intermediates would form methyl ester (biodiesel). The presence of sufficient ions provided by HT would speed up the reaction rate. Thus, by considering all the chemical and physical properties as well as the mechanistic advantages of HT, this catalyst has been chosen to be used in this study.

There are 8 general methods identified to be possibly used in preparing HT including co-precipitation, urea hydrolysis, hydrothermal treatment, combustion method, sol–gel, microwave irradiation, steam activation and solvothermal methods [23]. From all methods reviewed, the method that needs close attention is combustion method as significantly shorter preparation time is needed. In this study, by considering all advantages and disadvantages of each HT preparation method, combustion method has been selected. There are 2 major determinants that should be focused on in the combustion method which are the calcination temperature and fuel type. HT is activated by thermal decomposition and this stage is critical and needs to be emphasized. Suitable calcination conditions should be provided in order to achieve complete decomposition of interlayer anions and to avoid detrimental effects of periclase-like phases (MgO segregated phases) on the HT structure [24]. Heating of HT to a certain high temperature usually causes dehydration, decomposition of anions and segregation of oxides.

Fuel is needed in the synthesis of HT to initiate and influence the reaction. The types of fuel used in previously reported studies include sugars, glycine and urea [24–26]. The combustion process generally takes less than 5 min to complete and the reaction is actually based on the principle of explosive decomposition of fuel mixtures [25,26]. Fuel is important in producing CO_2 and H_2O compounds that are highly required for the formation of layered structure by means of various forms of probe molecules such as monodentate, bidentate and bridge [25,27]. Thus, a good preparation method would ideally result in proper layered structure of HT catalyst that is desirable in the transesterification reaction.

In this study, the production of biodiesel from waste cooking oil has been conducted in the presence of hydrotalcite as the catalyst coupled with the application of ultrasound to further enhance the transesterification reaction. Particular focus has been given to the capability of HT synthesized using combustion method. Two major important parameters i.e., calcination temperature and fuel type have been investigated. Effects of those parameters on HTs' characteristics and their catalytic performance (biodiesel yield) under ultrasound system have been elucidated. Comparison between ultrasound and conventional stirring methods has been technically performed in order to demonstrate on the benefits of an ultrasound-assisted system in producing biodiesel.

2. Experimental

2.1. Materials and reagents

Magnesium nitrate hexahydrate (Merck), aluminum nitrate nonahydrate (Ridel de Hein), sodium carbonate (Fischer Scientific), D-glucose (R&M Chemical), saccharose (Merck), fructose (Merck) were used to synthesize the hydrotalcite. Waste palm oil (from the campus's cafeteria) and methanol (Merck) were used as the reagents for the transesterification reaction. Meanwhile, *n*-hexane (Merck), methyl heptadecanoate (Fluka), fatty acid methyl esters (FAME) standards (Sigma and Fluka) were used for fatty acid methyl ester (FAME) analysis.

2.2. Catalyst preparation

Hydrotalcite was synthesized using combustion method in which the preparation of MgAlO oxide mixture was adapted from Anuar et al. [24] and Davilla et al. [25]. The Mg/Al ratio was maintained at 3. Pre-calculated amounts of magnesium nitrate and aluminum nitrate were first suspended in 80 ml of deionized water that was placed in two different beakers for better suspension and then heated to 80 °C. Then, it was thoroughly mixed in a beaker and kept at 80 °C. 20% wt of Na_2CO_3 and 10 wt% of fuel (sugars) from the total weight of sample were then added. Next, the mixture was stirred vigorously and maintained at 80 °C until all water had evaporated. The resulting solid was then calcined in a furnace for 5 min. Calcination of MgAlO was then carried out at 4 different temperatures i.e., 550 °C, 650 °C, 750 °C and 850 °C. The fuels used in the catalyst preparation were saccharose, glucose and fructose. The amount of fuel used was kept constant at 10 wt% of the total mixture. The effects on the catalytic reaction were studied. Then, the resulting MgAlO catalysts were ground into powder form and put in contact with 60 ml of 0.05 M anion solution for 5 min at room temperature. The solid products were then filtered and washed 2 times with deionized water and dried in an oven at 100 °C.

2.3. Catalyst characterization

The analysis of surface area was carried out using a Micromeritics ASAP 2020 V3.02 H surface analyzer based on nitrogen adsorption/desorption. X-ray diffraction (XRD) was used to study

the crystallinity of HT. The analysis was carried out using a Siemens D5000 diffractometer with monochromatized CuKα radiation and the diffraction was recorded in the 2θ range of 10–70°. The structure and surface morphology analysis of HT samples were performed using a scanning electron microscope (SEM) (Leo Supra 50 VP (Germany)). The SEM unit was equipped with EDX system for determination of the chemical composition of a certain particular spots on the sample. The microanalysis was performed by means of an Oxford INCA 400 EDX. FTIR spectra of HT catalysts were obtained using a Shimadzu IR Prestige-21 FTIR spectrophotometer. The decomposition analysis of HT catalysts was performed using a thermal gravimetric analyzer (PerkinElmer TGA 7, USA).

2.4. Ultrasound-assisted catalytic reaction

The ultrasound-assisted reaction was conducted in a three-necked glass reactor equipped with a condenser and a thermocouple. For this reaction, the thermocouple was used to monitor changes in temperature before and after reaction. Ultrasonication effect was achieved by means of a probe type ultrasonic transducer connected to an ultrasonic processor (Branson, USA). The ultrasonic processor was operated at a frequency of 20.050 kHz.

In a typical experimental run, the desired amount of waste cooking oil was measured and preheated prior to mixing for 5 min with the desired amount of catalyst (0.08 g catalyst/g oil). Then, the required amount of methanol at an appropriate ratio (15:1) was added and the mixture was heated in a water bath until it achieved a temperature of 57 °C. The ultrasonic energy was then applied in a discreet pattern with 10s pulse on and 3s pulse off. The pattern was maintained in all the experimental runs. The ultrasonic amplitude was set at 55% for a total reaction time of 60 min.

In order to investigate the benefit of ultrasound, the transesterification process without ultrasound was also carried out. The conventional method of biodiesel production was performed by using a stirring method in a two-necked glass reactor of the same volume. The reactor was attached to a condenser for methanol recovery. Besides, the reactor was also equipped with a thermocouple to monitor the temperature during the reaction. During the reaction, the reactor vessel was partially submerged in a water bath in order to maintain the required reaction temperature. The water bath was equipped with a stirrer to provide stirring effect for the reaction mixture. The reaction temperature was maintained at 65 °C for the whole reaction time.

The reusability test of HT catalyst was carried out by running the successive reaction runs under the same reaction conditions using the most active HT catalyst. The experimental run was repeated for up to 3 cycles. After every cycle, the catalyst was centrifuged out of the product mixture at 3500 rpm for 30 min. The catalyst was then recollected and washed with *n*-hexane to remove the remaining glycerol. It was then filtered and recalcined at 300 °C for 3 h in order to remove any remaining glycerol that adhered on its surface. After that, the calcined catalyst was put in contact with sodium carbonate solution and dried before use in the next experimental cycle.

2.5. Product analysis

Fatty acid methyl ester (FAME) analyses were performed using a gas chromatograph (Agilent Technologies) equipped with an FID (Agilent technologies Inc. 19091J-413HP-5). It was also equipped with a silica capillary column manufactured by Agilent Technologies and nitrogen was used as the carrier gas. The sample analysis was carried out using of an internal standard (methyl heptadecanoate). The samples were first dissolved in *n*-hexane and the dilution factor was fixed at 50. Then, 1 μl of the mixture was injected into the gas chromatograph. The yield of FAME was calculated based on the equation derived from the ratio of FAME samples and the internal standard.

3. Results and discussion

3.1. Characterization of HT

The characteristics of HT based on nitrogen adsorption-desorption analysis are presented in Table 1. It can be observed that, the increase in the calcination temperature did not directly affect the surface characteristics as no clear trend to indicate an increase or decrease in the surface area was obtained. An increase in the calcination temperature to 650 °C resulted in an increase in the surface area (77.46 m^2/g). However, further increase beyond that brought about a detrimental effect. The surface areas obtained in this study were lower compared to those reported in previous works [18,26] in which the surface areas recorded were generally higher than 100 m^2/g. The surface area showed a descending trend with the increase in the calcination temperature beyond 650 °C. This might be due to partial pore framework collapse that inhibited the diffusion of nitrogen gas to reach the internal pores. Thus, less surface area was recorded. The use of saccharose resulted in the highest surface area compared to that of glucose and fructose.

In the combustion method, fuel would assist by providing enough energy due to the enthalpy release from the fuel used. Adequate source of enthalpy would result in good development of layered double hydroxide in which the octahedral arrangements of divalent and trivalent cations are well constructed. HT sample prepared using saccharose demonstrated the largest surface area while the other catalysts recorded slightly lower surface areas. Anuar et al. [24] also discovered that saccharose could provide the largest amount of energy as the enthalpy given is 5646.7 kJ/mol due to relative high number of C and H compared to the other fuels used. This factor is very useful in assisting the combustion process. Glucose and fructose belong to monosaccharide group that possess lower number of combustible components so that the creation of pore framework could not be satisfactorily achieved. Consequently, slightly lower surface areas were recorded. Fortunately, the textural characteristics might not be the sole determinant for the catalyst's performance in its reaction as it is also determined by the conditions of the reaction.

In tandem with surface area, the total pore volume also demonstrated the same trend. Large surface area and pore volume would be obtained when the calcination was conducted at a suitable temperature so that the heat treatment on hydrotalcite would occur adequately. As the temperature was increased to 650 °C, the formation of mixture of oxides in the layered structure successfully took place. The porous network developed did not experience significant collapse and the formation of segregated phases of magnesium oxide (MgO) would also be avoided. An increase in the temperature beyond that would lead to major collapse in the layered hydroxide structure and porous network. As the water molecules in the interlayer had been totally removed, the arrangement between divalent and trivalent cations started to vibrate to the critical point. Thus, it might affect the octahedral arrangement between the LDH components and sequentially dislocated any species from the layered structure. Thus, the structure could loose its robustness and experienced a major collapse in the main structure of HT. Consequently, the collapsed structure might affect the pore structure leading to deteriorated texture of HT.

Based on Fig. 1, HT was successfully synthesized using combustion method as indicated by the diffraction peaks at 11.792°, 23.561°, 34.312°, 35.540°, 39.223°, 47.015°, 48.010°, 56.514°, 61.518°, 63.693°. The result is consistent with previously reported ones [26,28]. Calcination below 650 °C caused the LDH network

Table 1
Surface characteristics of HT catalysts.

Sample	Surface[a] area (m^2/g)	Total[b] pore volume (cm3/g)	Average[c] pore diameter (nm)
MgAl SAC 550	30.3	0.16	12.77
MgAl SAC 650	77.5	0.33	14.75
MgAl SAC 750	34.5	0.13	25.32
MgAl SAC 850	20.2	0.09	29.26
MgAl GLU 650	72.7	0.26	12.48
MgAl FRU 650	60.5	0.27	16.43

[a] BET surface area.
[b] BJH cumulative pore volume.
[c] BJH average pore diameter (4 V/A).

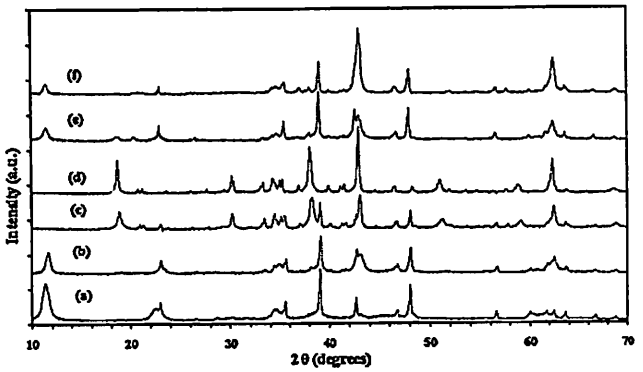

Fig. 1. XRD patterns of (a) MgAl SAC 550 (b) MgAl SAC 650 (c) MgAl SAC 750 (d) MgAl SAC 850 (e) MgAl GLU 650 and (f) MgAl FRU 650.

to be successfully constructed as high intensity diffraction peaks appear at 11.792° and 23.561° to indicate a layered structure [19,24]. However, samples calcined at 750 °C and 850 °C did not show peaks that are associated with structural collapse. Treatment of HT at excessively high temperatures caused the main components of the material to partially collapse due to high vibration effect to produce additional phases. As expected, the use of saccharose led to better intensity of HT peaks compared to those of glucose and fructose. Thus, it must have provided the highest and optimal enthalpy as required for complete reconstruction of the LDH structure. All of the samples demonstrated sharp and symmetrical peaks that are attributed to (003), (006), (012), (015), (018) and (113) planes [29]. The XRD diffraction patterns are generally consistent with that of HT with the composition of $[Mg_4Al_2(OH)_{12}(CO_3)(H_2O)_3]_{as}$ [29].

The reflections at 18.5° and 20.5° are attributed to $MgAl_2(OH)_8$ while those at 15.2° and 30.2° are attributed to $Mg_5(CO_3)_4(OH)_2{\cdot}4(H_2O)$ and these components are categorized as impurities [29]. HTs that were prepared at higher temperatures and using glucose as fuel demonstrated the appearance of these impurities. Supposedly, fuel generated enough energy to create decomposition explosion for the metals to merge octahedrally as brucite-like layers. However, the non-optimal enthalpies provided by glucose and fructose caused an incomplete and partial reconstruction of the layered structures. Consequently, isolated phases were formed to coat the external surface leading to the deterioration of the pore dispersion of the catalysts. HT samples calcined above 650 °C and prepared using fructose significantly showed the presence of periclase phase or MgO peaks at 36.9°, 43.167° and 62.534°. The non-optimal heat provided caused the existence of divalent metal oxide phases (MgO) with periclase structures that were also attributed to partial surfacial reconstruction [24].

The morphology study of HT was conducted using a scanning electron microscope. The SEM images were obtained from the fresh sample before use in the reaction. The difference can clearly noticed by monitoring the presence of the porous network in Fig. 2. Images (a) and (b) show surface morphology of samples calcined below 650 °C with irregular shaped particles and less compact agglomerates of porous network. The pore sizes are estimated to be less than 1 μm and they are consistent with the pore diameters analyzed based on N_2 adsorption-desorption that are ranging from 12.48 nm to 29.26 nm. However, images (c) and (d) reveal irregular shape particles with compact agglomeration of porous network and densely packed meso-structure. They also indicate that the external surface areas were made up of amorphous conglomeration of MgO periclase due to the extreme heat treatments (750–850 °C). The results are in good agreement with XRD patterns. Calcination temperature of 750 °C and 850 °C evidently caused the existence of periclase phases. This might also suggest that the most ideal heat treatment for the HT preparation was 650 °C.

HT catalyst prepared using saccharose as fuel demonstrated the most evenly distributed pore structure. The adequate heat provided by saccharose successfully created a significant porous network that could be clearly seen from the outer surface of HT. Meanwhile, HTs prepared using glucose and fructose showed compact agglomeration of particles with small porous network. The external surfaces of the catalysts were likely to have been coated with non-homogeneous phases (impurities). Glucose and fructose belong to the monosaccharide group so that the enthalpy energies given are

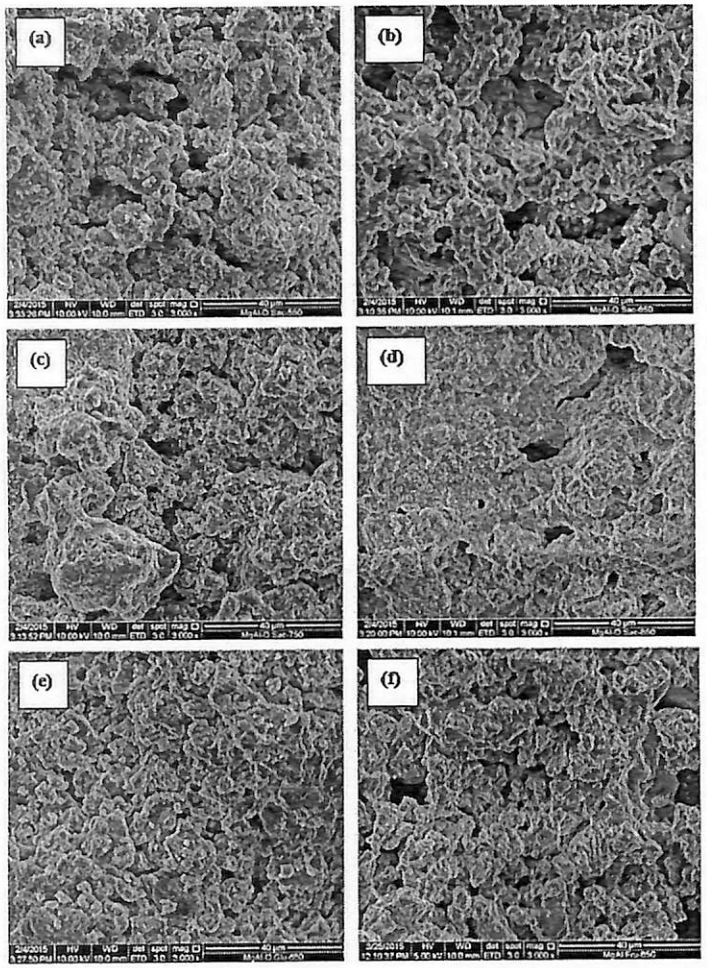

Fig. 2. SEM images of (a) MgAl SAC 550 (b) MgAl SAC 650 (c) MgAl SAC 750 (d) MgAl SAC 850 (e) MgAl GLU 650 and (f) MgAl FRU 650.

about the same. In line with that, the surface morphologies of both HT samples were quite similar.

The elemental compositions of the main components in HT were obtained using EDX and they are summarized in Table 2. From the result, the Mg/Al ratio of each HT sample is close to the desired ratio of 3. These results are somewhat comparable with a reported work [26]. O is the most predominant element that existed in every HT sample (55.84–64.46%). For samples calcined in the range of 550–750 °C, the compositions of Mg and Al were supposed to be identical. However, the composition of Mg for the sample calcined

Table 2
Chemical composition of HT catalysts based on EDX results.

Samples	Mg/Al	Chemical composition (wt%)				
		Mg	Al	O	C	Na
MgAl SAC-550	2.96	9.55	3.23	64.2	10.46	12.56
MgAl SAC-650	2.98	9.73	3.26	64.46	10.47	12.08
MgAl SAC-750	2.87	8.42	2.93	63.02	10.41	15.22
MgAl SAC-850	3.21	17.87	5.56	55.84	10.69	10.04
MgAl GLU-650	3.2	9.47	2.96	63.76	10.2	13.61
MgAl FRU-650	3.19	9.5	2.98	63.56	11.62	12.34

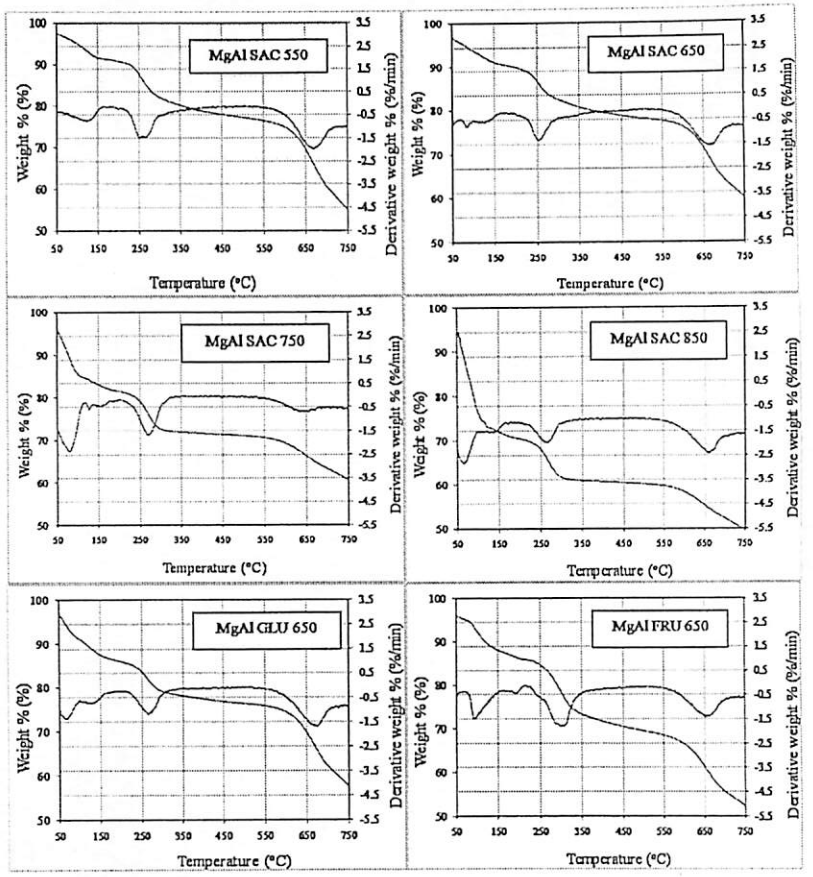

Fig. 3. TGA-DTG profiles of HT catalysts.

at 850 °C (17.87%) was significantly different compared to that of the other catalysts. This might be due to the presence of MgO phases that could have segregated out to the external surface of the catalyst. At high temperature, Mg from Mg–O and Al–O bondings were partially destroyed to form MgO as a new phase. This could confirm the conglomeration of amorphous phases in the SEM images and agreed with the XRD patterns where MgO peak was significantly detected for the sample calcined at 850 °C. The difference in the fuel used did not significantly influence the composition of HT. In this case, the structures of HT were uniformly constructed. The presence of Mg and high composition of O that belongs to carbonate species could confirm the existence of basic sites in HT that are highly required to conduct the transesterification reaction efficiently.

Thermogravimetric (DTG-TGA) profiles of HT are shown in Fig. 3. All samples show quite similar weight losses of about 40–49% and characterized by 3 major steps of decomposition. The decomposition before reaching 250 °C was due to the removal of interparticle water that was physically and chemically adsorbed in the pores as well as interlayer water molecules [30]. The samples calcined below 650 °C (MgAl SAC 550 and MgAl SAC 650) showed the same trend with initial decay temperatures at about 250 °C. Higher calcination temperatures caused higher decomposition rate due to lower amount of water in the LDH structure. The second stage represents the removal of hydroxyl component at brucite like layers and the remaining components of the interlayer including CO_3^{-} and OH^{-} in the form of H_2O and CO_2 [19,30]. At 650 °C, all water molecules, hydroxyl and interlayer components had been totally removed from the LDH structure. The samples calcined above 650 °C demon-

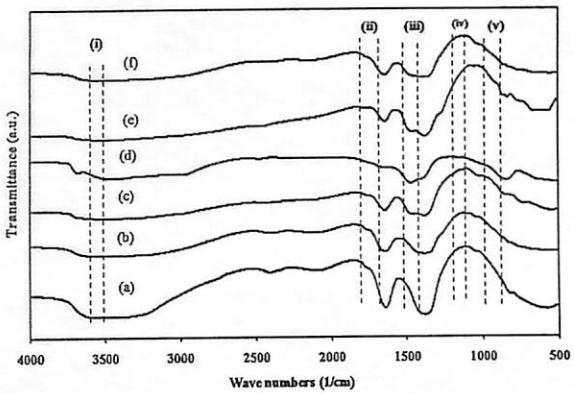

Fig. 4. FTIR spectra of (a) MgAl SAC 550 (b) MgAl SAC 650 (c) MgAl SAC 750 (d) MgAl SAC 850 (e) MgAl GLU 650 (f) MgAl FRU 650 (i) 3450–3500 cm^{-1} (ii) 1640–1660 cm^{-1} (iii) 1375–1400 cm^{-1} (iv) 1015–1210 cm^{-1} and (v) 870–900 cm^{-1}.

strated high rates of decomposition in which the removal of adsorbed water and weight loss were highly significant. This might be due to the higher heat treatment temperatures that caused lower amounts of water molecules in the LDH network. Thus, the decomposition process occurred very fast even at low temperature. The HT prepared with saccharose as fuel showed the least removal of water molecules (10.87%) in the first stage of decomposition. It might be due to massive enthalpy provided during heat treatment to cause more rapid water loss during the decomposition. Besides, the chemical interaction between adsorbed carbon dioxide or other volatile gaseous with cations could hinder their physical desorption.

The second stage of decomposition (>250 °C) represents the removal of hydroxyl group in the interlayer gallery and the brucite-like layers. The HT catalyst calcined with fructose showed the highest weight loss of about 23.27%. It might confirm the fact that the non-optimal enthalpy given off during calcination will produce less thermostable HT structure. The interaction between the divalent and trivalent cations with hydroxyl group made the material unstable so that the dehydroxylation was relatively easy to occur. Besides, the decomposition at this stage also involved the removal of CO_3^- anion in the interlayer. The third stage of decomposition started when temperature exceeded 650 °C. The divalent and trivalent cations (Mg and Al) are the main components that construct the infinite layered structure and they were the only species that remained at the end of the decomposition process.

The existence of the elements constructing the LDH structure was also verified by FTIR spectra (Fig. 4). The band between 3450–3500 cm^{-1} is attributed to the OH ions located between the brucite like layers, thus, confirming the development of layered structure [26,30]. The presence of H_2O molecules in the interlayer is indicated by the 1634–1643 cm^{-1} band. The band seems to be weakening with elevated calcination temperature to indicate that high temperature indeed caused the interlayer water molecules to diminish. The peak at 1374–1385 cm^{-1} represents the vibration of carbonate ions (CO_3^- anion) [30]. This anion species were located in the interlayer gallery and functioned as the connector between the cations forming the layered structure. The covalent carbonate is also represented by the bands at 1042–1092 cm^{-1} and 810–825 cm^{-1} [26]. The increase in the calcination temperature caused the structure to collapse partially and trapped the CO_3^- species inside the solid. This confirmed the significant intensity of the band at 810–820 cm^{-1} due to the collapse of HT structures that were treated at high temperatures. With the HT calcined at optimal temperature (650 °C), no such phenomenon occurred in the layered structure. This might also indicate that the structure of HT was constructed very well without significant internal structural collapse. Above all, the fuel presented an insignificant effect to the structure and bonding characteristics of HT as long as the heat treatment was carried out at optimal temperature.

3.2. Catalytic activity of HT

3.2.1. Effect of calcination temperature

Catalytic activity of the as-synthesize HT catalysts was demonstrated based on ultrasound-assisted biodiesel production process. The expected reactions to take place in reactor system were both transesterification and esterification. As HT catalyst mainly comprises of divalent and trivalent cations, the reaction could take place in both acidic and basic conditions depending on the reactants involved. However, HT is predominantly categorized as a basic catalyst and the main reaction was a base-catalyzed transesterification reaction. The reaction was conducted for up to 60 min with the ultrasonic amplitude fixed at 55%.

The characteristics and the catalytic activity of HT in ultrasound-assisted condition are expected to be different. The results are presented in Fig. 5 in which the performance is shown based on fatty acid methyl ester (FAME) yield. The waste cooking oil produced FAME that comprised of mainly methyl palmitate, methyl stearate, methyl linoleate and methyl oleate. From figure, the sample calcined at 650 °C gave the highest FAME yield of about 76.45%. The present study showed a somewhat lower FAME yield compared to that of Badday et al. [16] which was 84%. However, there were some improvements in which the reaction was conducted in just moderate ultrasonic amplitude (55%) with only 15:1 methanol to oil ratio. Besides, this result was consistent with the characterization results that suggested that the HT was synthesized at optimal temperature. Otherwise, further increase in the calcination temperature caused the yield to experience slight drops to 66.35% and 68.41% for calcination temperatures of 750 °C and 850 °C, respectively.

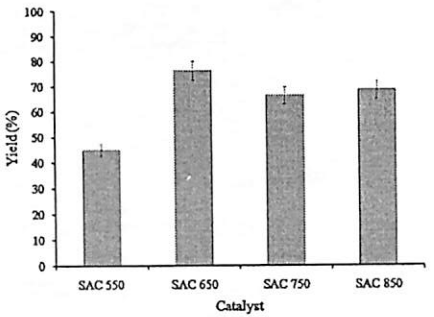

Fig. 5. Catalytic activity of HT with different calcination temperatures in the transesterification reaction of waste cooking oil under ultrasound-assisted condition (reaction time 60 min, methanol to oil ratio 15:1, catalyst amount 0.08 g catalyst/g oil and ultrasound amplitude 55%).

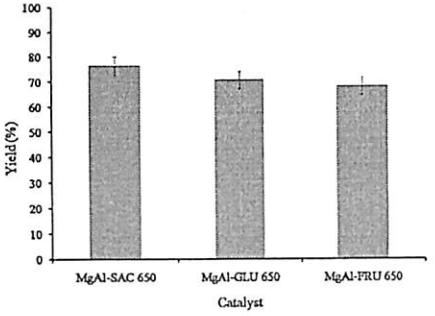

Fig. 6. Catalytic activity of HT with different fuel types in the transesterification reaction of waste cooking oil under ultrasound-assisted condition (reaction time 60 min, methanol to oil ratio 15:1, catalyst amount 0.08 g catalyst/g oil and ultrasound amplitude 55%).

The transesterification reaction was conducted in short reaction time (60 min) compared to the system with conventional stirring in which the reaction could take up to 6 h [18]. This might suggest that the transesterification reaction was significantly intensified due to the effects of ultrasound. The cavitation bubbles produced from the ultrasonic irradiation principally led to a highly reactant mixing effect by providing enough energy in overcoming the emulsification and mass transfer limitation [31]. The energy generated from the breakdown of the cavitation bubbles produced acoustic cavitation that provided internal heat that minimized the immiscibility limitation at the boundary layer of oil and alcohol molecules [32]. This might also facilitate the contact between reactants and the catalyst active sites so that the reaction would be more efficient. Thus, high reaction rate gave rise to high yield of FAME.

The LDH network with brucite-like layers is made up of octahedrally amalgamated divalent and trivalent cations. In this study, it was successfully created at 650 °C with highly suitable catalyst characteristics for the transesterification reaction. The ideal formation of HT might promote the existence of hydroxyl and carbonate ions which were highly required to initiate the transesterification reaction when the carbonyl carbons of triglycerides are attacked by alkoxide ions [22]. The assistance from the super vigorous effect could increase the production of alkoxide ions when the hydroxyl groups of alcohol were deprotonated by negative ions of the catalyst. Thus, the conversion of oil into methyl ester could rapidly occur in short reaction times so that increased FAME yields could be achieved. Calcination at 850 °C caused the formation of segregated phase of magnesium oxide (MgO) on the outer surface of the catalyst as verified by the SEM images. In line with that, the reaction did not occur in the porous framework structure of the catalyst but only catalyzed by the basic condition provided by the MgO phase. Besides, the acid-base bifunctionalized during the reaction was not effectively applied and subsequently caused significant formation of soap. However, for calcination carried out below 650 °C, the LDH network was partially created and the construction of pores was still incomplete so that it might limit the reaction.

3.2.2. Effect of fuel type

The study was further conducted by varying the type of fuel used in synthesizing HT. Fuel was the last chemical added into the mixture of Mg, Al and Na_2CO_3 to allow a better mixing of these brucite-like layer components. In the combustion method, sugar is important to ensure the development of MgAlO structure during calcination. Three different fuels used were saccharose, glucose and fructose. They are differentiated by their molecular structure and the number of C and H in the molecule. It can be observed that, different types of sugar led to different catalytic performance of HT. From Fig. 6, saccharose seems to be the most effective fuel to synthesize the best HT to catalyze the transesterification reaction. This result was somewhat consistent with those of Martunus et al. [26] and Helwani et al. [18] where both of these works demonstrated the positive role of saccharose. HT samples using glucose and fructose as fuels showed slightly lower yields of FAME which were 70.75% and 68.1%, respectively. As highlighted from a previous work [24], saccharose could provide sufficient enthalpy to allow the construction the desired LDH network that could fulfill the needs in the transesterification reaction.

Sugars contain C and H atoms that will function in enhancing the combustion process. This process produces CO_2 which is the combustion product that will play a role as the probe molecule to the oxide surfaces to favor the construction of layered framework [25]. High enthalpy provided by saccharose in this study would cause the production of more CO_2 that would eventually lead to the formation of larger surface area in HT. Glucose and fructose belong to monosaccharide group in which the number of combustible components is lower compared to saccharose (disaccharide group). Thus, less thermal explosion was expected to occur to create large surface area material. Larger surface area could provide better opportunity for the reaction to occur especially when in contact with active sites that were rich with hydroxyl and carbonate ions. It would mechanistically create a pool of negative ions that promoted the formation of alkoxide ions from alcohol that were highly needed to initiate the transesterification reaction. The tetrahedral intermediates would be rapidly produced from the deprotonation of carbonyl carbons of triglycerides and reacted with each other to form methyl esters [22]. Thus, it resulted in an increase in the formation of FAME.

Waste cooking oil used as the reactant might contain some impurities including free fatty acid and water molecule. Based on HT unique property called the memory effect, the reconstruction of LDH network is favored when contacted with water. Davila et al. [25] highlighted that the combustion process might cause an extraction of Al from the brucite-like layer to present as spinel. The brucite-like layers might recover itself when Al-spinel is susceptible with water molecule and reconstructed in octahedral arrangement of Mg–Al cations network. Thus, the layered structure

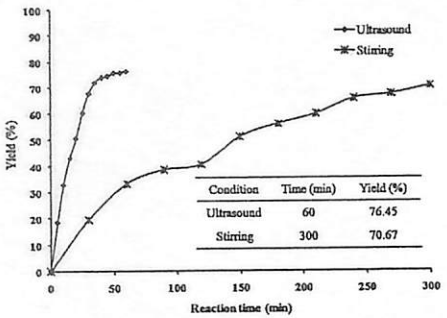

Fig. 7. Transesterification reaction of waste cooking oil using MgAl SAC 650 catalyst conducted under ultrasound-assisted and mechanical stirring conditions.

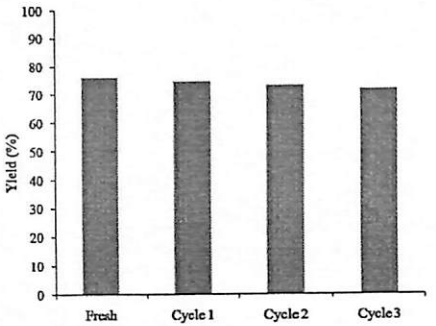

Fig. 8. Catalytic activity of MgAl SAC 650 in successive reaction cycles (reaction time 60 min, methanol to oil ratio 15:1, catalyst amount 0.08 g catalyst/g oil and ultrasound amplitude 55%).

became stable and the active sites became widely exposed to the reactants to speed up the reaction. This might explain the flexibility of HT catalyst with various kinds of feedstock and highly applicable for the transesterification reaction assisted by ultrasound. In a short reaction time of 60 min and low ultrasound amplitude (55%), the yield achieved was up to 76.45%.

3.2.3. Comparison with mechanical stirring method

Comparison between biodiesel production using ultrasound system and the conventional stirring method is shown in Fig. 7. In 60 min, the reaction operated under ultrasound condition demonstrated a marked increase in the FAME yield. Due to strong mechanical agitation provided by ultrasound, the mass transfer limitation of the reactants was minimized. The sufficient emulsification effect caused the reactants to have efficient contact with the catalyst surface and ultrafine mixing dispersion was created [33]. Therefore, high biodiesel yield could be achieved in shorter reaction time. Meanwhile, the reaction operated under stirring method showed relatively poor yields and longer time was needed to achieve high biodiesel yield. A biodiesel yield of only 33.7% was achieved by the stirred reaction in 60 min while for the ultrasound-assisted system, the yield obtained was nearly double under the same conditions. Then, when the reaction was extended to 300 min (5 h), the highest yield achieved was only about 70.66% which was significantly lower than that of ultrasound-assisted system. From the behavior demonstrated by these two biodiesel production methods, it is conducted that the ultrasound-assisted system was clearly more superior. Obviously, ultrasound could be beneficially applied to reduce the reaction time to achieve higher FAME yield due to strong mechanical agitation effect that consequently led to significantly faster reaction.

Both ultrasound and stirring methods showed increasing trends of FAME yield throughout the reaction time. It means, net forward reaction took place during the reaction so that the yield did not show any decrement. For the system using ultrasound, a sharp increase in biodiesel yield was observed in the first 30 min. After that, the reaction occurred steadily with a slight increase in the biodiesel yield. Therefore, ultrasound was efficiently used to accelerate the reaction. Super vigorous effect by ultrasound created reactants emulsification and facilitated their diffusion to the active sites inside the catalyst pores. Liquid phase reactants could also cause the HT catalyst to slightly swell up to form larger pore structure so that more triglyceride molecules could diffuse and react. After 30 min, the reaction leveled off due to low reactants concentration and high FAME content in the reaction mixture. These factors explain the slight increase in the biodiesel yield with time. For the stirring reactor, the yield increased steadily in the period of 300 min. The insufficient reactants contact with the catalyst due to inadequate agitation made the reaction to experience significant mass transfer limitation. Thus, low activity was demonstrated due to slow progress of reaction so that more time was needed to achieve sufficiently high biodiesel yield.

3.2.4. Reusability of catalyst

Fig. 8 shows the catalytic activity of MgAl SAC 650 in successive runs of transesterification reaction under the same reaction conditions. The FAME yield experienced a slight reduction from the first cycle to the third cycle. It can be concluded that, the system suffered only 4.02% of FAME yield reduction throughout these successive runs. Compared to a previously reported work [15], the HT catalyst demonstrated a relatively lower reduction in the FAME yield, thus, confirming the robustness of the catalyst as claimed by Helwani et al. [18]. In short, the HT catalyst showed a good potential in catalyzing several reaction cycles that resulted in considerably high FAME yield in every cycle. A slight reduction in catalytic activity could be attributed to minor internal pore structure collapses that affected the contact between reactants and the catalyst active sites. The collapses could be due to the repeated calcination step that was carried out between the cycles. However, the layered structure was still maintained and CO_3^{2-} was still intercalated into the interstitial positions after the calcination process as the MgAlO (calcined sample) was placed in contact with carbonate solution before every subsequent reuse cycle. This might be attributed to the unique memory effect of HT [25]. The results prove that the HT catalyst was highly stable and suitable to be used in the ultrasound-assisted reactor system to produce FAME.

3. Conclusions

Catalytic transesterification reaction of waste cooking oil producing biodiesel in an ultrasound-assisted reactor system was successfully carried out. The capability of HT catalyst synthesized using combustion method was demonstrated. The catalyst prepared using saccharose and subsequently calcined at 650 °C (MgAl SAC 650) was the most active catalyst to give the highest biodiesel yield of about 76.45% in just 60 min with the use of low ultrasound amplitude (55%). The catalytic performance of MgAl SAC 650 was successfully correlated with its characteristics. It was found to be well synthesized with complete reconstruction of layered double hydroxide network. The performance of conventional reaction using mechanical stirring was significantly improved when ultrasound was used where it resulted in intensed reaction due to good emulsification effect between reactants. The reaction time was significantly reduced where high biodiesel yield (76.45%) could be achieved in only 60 min compared to conventional mixing method that needed longer reaction times of up to 300 min to achieve the same yield.

Acknowledgment

A Research University grant (814144) from USM is gratefully acknowledged.

References

[1] P.P. Oh, H.L.N. Lau, J. Chen, M.F. Chong, Y.M. Choo, Renew. Sustain. Energy Rev. 16 (2012) 5131–5145.
[2] A.E. Atabani, A.S. Silitonga, I.A. Badruddin, T.M.I. Mahlia, H.H. Masjuki, S. Mekhilef, Renew. Sustain. Energy Rev. 16 (2012) 2070–2093.
[3] S. Lim, L.K. Teong, Renew. Sustain. Energy Rev. 14 (2010) 938–954.
[4] A. Javidialesaadi, S. Raeissi, APCBEE Procedia 5 (2013) 474–478.
[5] L.F. Chuah, S. Yusup, A.R. Abd Aziz, A. Bokhari, J.J. Klemeš, M.Z. Abdullah, Chem. Eng. Process. 95 (2015) 225–240.
[6] M.K. Lam, K.T. Lee, Fuel Process. Technol. 92 (2011) 1639–1645.
[7] M.K. Lam, K.T. Lee, A.R. Mohamed, Biotechnol. Adv. 28 (2010) 500–518.
[8] C.D. Mandolesi de Araújo, C.C. de Andrade, E. de Souza e Silva, F.A. Dupas, Renew. Sustain. Energy Rev. 27 (2013) 445–452.
[9] M. Niu, X. Kong, RSC Adv. 5 (2015) 27273–27277.
[10] V.G. Deshmane, P.R. Gogate, A.B. Pandit, Ind. Eng. Chem. Res. 48 (2008) 7923–7927.
[11] W. Guo, H. Li, G. Ji, G. Zhang, Bioresour. Technol. 125 (2012) 332–334.
[12] F.F.P. Santos, J.Q. Malveira, M.G.A. Cruz, F.A.N. Fernandes, Fuel 89 (2010) 275–279.
[13] L.T. Thanh, K. Okitsu, Y. Sadanaga, N. Takenaka, Y. Maeda, H. Bandow, Bioresour. Technol. 101 (2010) 639–645.
[14] M.E. Borges, L. Díaz, Renew. Sustain. Energy Rev. 16 (2012) 2839–2849.
[15] A.S. Badday, A.Z. Abdullah, K.-T. Lee, Energy 60 (2013) 283–291.
[16] A.S. Badday, A.Z. Abdullah, K.-T. Lee, Appl. Energy 105 (2013) 380–388.
[17] R. Salomão, L.M. Milena, M.H. Wakamatsu, V.C. Pandolfelli, Ceram. Int. 37 (2011) 3063–3070.
[18] Z. Helwani, N. Aziz, M.Z.A. Bakar, H. Mukhtar, J. Kim, M.R. Othman, Energy Convers. Manag. 73 (2013) 128–134.
[19] I. Reyero, I. Velasco, O. Sanz, M. Montes, G. Arzamendi, L.M. Gandía, Catal. Today 216 (2013) 211–219.
[20] X. Deng, Z. Fang, Y.-h. Liu, C.-L. Yu, Energy 36 (2011) 777–784.
[21] C.C.C.M. Silva, N.F.P. Ribeiro, M.M.V.M. Souza, D.A.G. Aranda, Fuel Process. Technol. 91 (2010) 205–210.
[22] L.C. Meher, D. Vidya Sagar, S.N. Naik, Renew. Sustain. Energy Rev. 10 (2006) 248–268.
[23] M.R. Othman, Z. Helwani, F. Martunus, W.J.N. Fernando, Appl. Organomet. Chem. 23 (2009) 235–246.
[24] M.R. Anuar, A.Z. Abdullah, M.R. Othman, Catal. Commun. 32 (2013) 67–70.
[25] V. Dávila, E. Lima, S. Bulbulian, P. Bosch, Microporous Mesoporous Mater. 107 (2008) 240–246.
[26] Martunus, M.R. Othman, W.J.N. Fernando, Microporous Mesoporous Mater. 138 (2011) 110–117.
[27] D.P. Debecker, E.M. Gaigneaux, G. Busca, Chem. Eur. J. 15 (2009) 3920–3935.
[28] C. García-Sancho, R. Moreno-Tost, J.M. Mérida-Robles, J. Santamaría-González, A. Jiménez-López, P.M. Torres, Catal. Today 167 (2011) 84–90.
[29] R. Rahul, J.K. Satyarthi, D. Srinivas, Indian J. Chem. Sect. A 50A (2011) 1017–1025.
[30] M. Dixit, M. Mishra, P.A. Joshi, D.O. Shah, J. Ind. Eng. Chem. 19 (2013) 458–468.
[31] A. Kalva, T. Sivasankar, V.S. Moholkar, Ind. Eng. Chem. Res. 48 (2009) 534–544.
[32] M. Toda, A. Takagaki, M. Okamura, J.N. Kondo, S. Hayashi, K. Domen, M. Hara, Nature 438 (2005) 178.
[33] A.S. Badday, A.Z. Abdullah, K.-T. Lee, Renew. Energy 62 (2014) 10–17.

Chemical Engineering Communications, 203:496–504, 2016

ISSN: 0098-6445 print/1563-5201 online
DOI: 10.1080/00986445.2015.1039120

Taylor & Francis

Selective Monolaurin Synthesis through Esterification of Glycerol Using Sulfated Zirconia-Loaded SBA-15 Catalyst

AHMAD ZUHAIRI ABDULLAH[1], ZAHRA GHOLAMI[2], MUHAMMAD AYOUB[3], and FATEMEH GHOLAMI[1]

[1]*School of Chemical Engineering, Universiti Sains Malaysia, Nibong Tebal, Penang, Malaysia*
[2]*Centralized Analytical Laboratory, Universiti Teknologi PETRONAS, Tronoh, Perak, Malaysia*
[3]*Department of Chemical Engineering, Universiti Teknologi PETRONAS, Tronoh, Perak, Malaysia*

The selective conversion of lauric acid to glycerol monolaurin over sulfated zirconia SBA prepared under various conditions was investigated in this study. The structural properties of the prepared catalysts were characterized using different characterization techniques. Sulfated zirconia was successfully incorporated with improved properties, such as larger mesopore surface area; the mesoporous structure was preserved as well. The highest yield of 79.1% was obtained during reaction over SZSBA-15 catalyst with 16 wt.% zirconium oxychloride loading and 3 h of reflux time. About 83.4% selectivity toward monolaurin was achieved at a high conversion of lauric acid (94.9%), a lauric acid-to-glycerol molar ratio of 4.0, within 6 h, and at 160°C. Product distribution was successfully elucidated. High selectivity to monolaurin was influenced by molecular sieving effects.

Keywords: Esterification; Lauric acid; Mesoporous catalyst; Molecular sieving effect; Monolaurin selectivity; Sulfated zirconia

Introduction

Lauric acid (also known as dodecanoic acid) is a saturated fatty acid that is mostly found in coconut and palm kernel oils. The low toxicity of lauric acid enables its use in numerous types of consumer products. This fatty acid possesses a nonpolar hydrocarbon tail and a polar carboxylic acid head, which allows them to interact with polar solvents and fats, thereby allowing water to dissolve fats. Meanwhile, monolaurin (also known as glycerol monolaurate) exhibits broad antimicrobial properties. Clinical studies have shown that monolaurin prevents skin and vaginal infections and slows the growth of a range of bacteria, fungi, molds, and viruses (Cai et al., 2011). Laboratory studies have shown that monolaurin can weaken HIV-1 viruses. This substance is also used as a nontraditional preservative in food products (Zhang et al., 2009).

Monolaurin, dilaurin, trilaurin, and water are produced during the esterification of glycerol with lauric acid. For this conversion, heterogeneous chemical catalysis can exert the most profound effect on intensifying the process and improving the selectivity of the desired product, i.e., monolaurin, thereby enabling multiple industrial applications (Zhang et al., 2009). Acidic resins and zeolites with small pore diameters (<0.8 nm) have been used for such applications. However, the small pore diameter makes these resins unfavorable for synthesis reactions involving bulky molecules, such as fatty acids. Acidic resins present good catalytic activity, but are highly susceptible to swelling in organic solvents and unstable at elevated reaction temperatures (>150°C) (Pouilloux et al., 1999).

Many important acid-catalyzed processes, such as alkylation, isomerization, and esterification reactions, have been studied in recent years (Hello et al., 2014; Hoo and Abdullah, 2014; Nie et al., 2014; Li et al., 2014; Mekala et al., 2013; Thiruvengadaravi et al., 2012; Hamouda et al., 2000). In general, monoglycerides can be synthesized by direct esterification of glycerol with fatty acid in the presence of an acidic catalyst at low temperature (90–120°C) (Hoo and Abdullah, 2014). Sophisticated synthesis methods and post-synthesis modification techniques could provide porous materials with pore sizes that are finely tuned according to the molecular sizes of the desired key products (Kärger et al., 2009). Zirconia is an attractive catalyst support for high-temperature applications because of its high thermal and mechanical stabilities (With et al., 2010). Sulfated zirconia (SZ) presents considerable potential as a strong solid acid catalyst for these reactions (Kärger et al., 2009; With et al., 2010). The active site of SZ consists of polysulfate species comprising three or four oligomers with two ionic bonds of S–O–Zr. SZ possesses both strong Bronsted and Lewis sites depending on the preparation conditions. According to previous studies (Davis et al., 1994), catalyst activity may be affected by the initial calcination and final catalyst treatment in the preparation process. The acidic nature of SZ can vary with slight changes in the preparation methods. Therefore, identification of a nanosized SZ with high surface area and pore volume is necessary. Moreover, the preparation of SZ supported on a mesoporous silica

Address correspondence to Ahmad Zuhairi Abdullah, School of Chemical Engineering, Universiti Sains Malaysia, Engineering Campus, 14300 Nibong Tebal, Penang, Malaysia. E-mail: chzuhairi@usm.my

material, such as MCM-41 (Mobil Composition of Matter No. 41), γ-Al_2O_3, or SBA-15 (Santa Barbara Amorphous type material) which could produce catalysts with superior performance (Garg et al., 2009).

Despite showing high catalytic activity, the application of SZ is limited because of its relatively small surface area and low pore volume. However, SBA-15, which is a mesoporous molecular sieve bearing a large surface area with adjustable pore size volume, can be combined with SZ. This combination could markedly enhance catalytic activity and properties such as acidity, surface area, pore uniformity, and pore-diameter adjustability (Degirmenci et al., 2009). The SBA-15 structure is also highly suitable for impregnation with heteroatoms, such as aluminum, iron, titanium, zirconium, and chromium (With et al., 2010; Garg et al., 2009).

Mesoporous Zr-SBA-15 is receiving considerable attention because Zr-incorporated mesoporous materials can act both as good catalysts and good catalyst supports, with acidic properties for various acid-catalyzed reactions (With et al., 2010). Zr-SBA-15 can be synthesized by one-pot synthesis or under the assistance of urea (Du et al., 2009). The material exhibits excellent hydrothermal stability in both boiling water and 100% steam treatment. Crystalline zirconia is necessary for the formation of strong acidic sites that can be characterized by wide-angle X-ray diffraction (XRD). Du et al. (2009) observed the absence of these crystalline structures in their XRD analysis, but the catalyst remained to show good catalytic activity for esterification and transesterification reactions. Garg et al. (2009) also studied the acidity and catalytic activities of various SZ SBA-15 catalysts. These catalysts are prepared by urea hydrolysis method with various loadings of highly dispersed zirconium (10–50 wt.%). Highly encouraging results have been reported, and the high catalytic activity is attributed to high surface area and mesosized internal pores.

The present work aimed to examine the selective catalytic conversion of lauric acid to monolaurin over a modified SZ-based mesoporous catalyst, SZSBA-15, and to optimize this conversion through the preparation conditions of the modified catalyst. Emphasis was placed on catalyst preparation conditions, including zirconia loading and reflux time, as well as on characterization of the prepared catalysts. Successful incorporation of SZ into SBA-15 at a suitable loading was verified. The structural properties of the obtained materials were elucidated by various approaches. Catalyst performance was demonstrated through a reaction between lauric acid and glycerol. The important reaction parameters included lauric acid conversion and selectivity to monolaurin.

Materials and Methods

Materials

Glycerol (99%) and triblock co-polymer Pluronic 123 (P123) were purchased from Sigma-Aldrich, Malaysia. Lauric acid (99.9%), tetraethyl orthosilicate (TEOS), H_2SO_4 (97%), and HCl (37%) were purchased from Merck. Zirconium oxychloride (99.8%) and urea (99%) were purchased from Fischer. All chemicals were used without further purification. Deionized water (resistivity 18.2 MΩ · cm) was used throughout this work.

Catalyst Preparation

The mesoporous silica SBA-15 material was synthesized according to the method of Garg et al. (2009). Approximately 4 g of P123 was initially dissolved in 30 ml of distilled water and 120 ml of 2 M HCl at room temperature. The solution was heated to 60°C, and 8.5 g of TEOS was added then to the solution. Afterward, the mixture was rapidly stirred at 1000 rpm for 30 min until a precipitate was produced. The stirring rate was then decreased to 120 rpm, and the mixture was kept under this condition for 20 h. After transferring the contents into a polyethylene (PE) bottle and aging at 80°C for 48 h in an oven under a static condition, the solution was allowed to cool to room temperature. The solid product was then filtered, washed with deionized water, dried in air at room temperature, and further dried at 100°C for 12 h. Finally, calcination was carried out in static air at 300°C for 30 min and 550°C for 6 h with a gradual increase in temperature at 1°C/min to obtain pure SBA-15.

After the SBA-15 material was successfully synthesized, SZ SBA-15 (SZSBA-15) catalysts were prepared. For 16% and 27% zirconia loadings over SBA-15, 2 g of SBA-15 (evacuated at 120°C for 4 h at 5°C/min) was added to a solution of 0.58–1.16 g of zirconium oxychloride ($ZrOCl_2 \cdot 8H_2O$) and 1.08 g of urea in 120 ml of distilled water. The mixture was refluxed under constant stirring at 90°C and pH 8 for 3–8 h. Afterward, the products (ZrO_2SBA-15) were filtered, washed with distilled water, dried in air at 100°C for 24 h, and then calcined in air at 550°C for 6 h with a gradual temperature increase of 5°C/min. The obtained solids were subjected to sulfation with 1 N of H_2SO_4 (15 ml/g) at room temperature for 3 h. The resultant solids were filtered, dried at 100°C, and calcined in air at 550°C for 3 h, with a gradual temperature increase of 5°C/min to obtain SBA-15 immobilized with SZ (SZSBA-15). Table I provides the synthesis conditions of each catalyst.

Characterization of Catalysts

The phases and structural properties (i.e., unit size, orientation, and defect structure) of SBA-15 and SZSBA-15

Table I. Catalysts synthesized in this work with respective synthesis conditions

Sample	Mass of $ZrOCl_2 \cdot 8H_2O$ (g)	Loading (wt.%)	Reflux time (h)
SBA-15	–	–	–
SZSBA-15 (1)	0.58	16	5
SZSBA-15 (2)	0.58	16	3
SZSBA-15 (3)	0.58	16	8
SZSBA-15 (4)	1.16	27	5
SZSBA-15 (5)	1.16	27	3
SZSBA-15 (6)	1.16	27	8

catalysts were analyzed by XRD. The diffraction patterns were obtained within the (2θ) range of 0.3–5°, with a step size of 0.01°. The specific surface areas of the catalysts were obtained using an adsorptive curve and calculations through the Brunauer–Emmett–Teller (BET) method. Pore volume (VP) was determined by nitrogen adsorption tests at a relative pressure of 0.98; pore-size distributions were obtained using the Barrett–Joyner–Halenda (BJH) model applied to the adsorption isotherm data. The mean diameter of the mesopores for each calcined solid (DP) corresponded to the maximum pore-size distribution. Micropore area (Sμ) was estimated using the t-Harkins correlation and Jura (t-plot) method. Nitrogen adsorption–desorption isotherms were obtained using a Micromeritics ASAP 2020 surface area and porosity analyzer. Prior to any measurement, the samples were degassed ($P < 10–1$ Pa) at 270°C for 6 h.

Scanning electron microscopy (SEM) offered sample images with superior spatial resolution and depth of focus. SEM images were captured using EDX at an operating voltage range of 0.1–30 kV. In the EDX analysis, Mn Kα was the energy source operated at 15 kV accelerating voltage. The SEM and EDX analyses were performed using the Oxford Instrument model 7573 Deben Research PCD Beam Blanker JEOL SEM system.

Catalytic Activity

The catalytic activity of the heterogeneous catalysts was tested through a solvent-free esterification of glycerol. Typically, a three-necked flask, as a batch reactor, was first placed on a stirring-heating mantle equipped with a temperature controller. Approximately 0.025 mol of lauric acid and 0.102 mol of glycerol were mixed in the reactor to yield a lauric acid-to-glycerol molar ratio of 4.0 (Hermida et al., 2011). The reaction mixture was then heated to 160°C, and 0.7 g of SZSBA-15 catalyst was added to the reaction vessel. One neck of the reactor was dedicated to a thermocouple and another neck was connected to a vacuum pump. After immediately applying a reduced pressure of 500 mmHg, the mixture was stirred for 6 h. A Hewlett Packard 5890A Series II gas chromatograph with a capillary column (15 m × 0.32 mm × 0.10 μm CP Sil 5CB) was used to analyze the mono-, di-, and trilaurin formed in the reaction product mixture. The calculation method proposed by Hermida et al. (2011) was used to determine the conversion of lauric acid conversion and selectivities.

Results and Discussion

Characterization of Catalysts

Results of the small-angle XRD analysis of SBA-15 and SZSBA-15 catalysts are shown in Figure 1. The XRD patterns were recorded at $2\theta = 0.3–1.2°$. Most samples exhibit a single intense reflection at a 2θ angle of around 0.6–0.7°, as in the case for typical SBA-15 materials, and this reflection is generally related to a regular pore size and an ordered pore arrangement (Hoang et al., 2010; Garg et al., 2009). This stucture was close to that of SBA-15 which exhibited a hexagonal orderly structure with a relatively intense peak at around $2\theta = 0.68°$, as reported in the literature (Jin et al., 2004). However, the diffraction of (110) and (200) reflection peaks could not be detected. The shift in the 100 reflection toward a lower value may depend on silica restructuring during adsorption. Moreover, with the increase in pore size, the (100) reflection slightly shifts to the left and the values of 2θ decreases (Sayari and Jaroniec, 2002; Garg et al., 2009). Therefore, the prepared catalyst was confirmed to be a SBA-15 type mesoporous material.

This pattern was similar to that of RuB/Sn-modified SBA-15 reported by Luo et al. (2007). This observation suggested minimal changes in the mesoporous structures of SBA-15 after functionalization. However, the characteristic peak of SZSBA-15 diffraction patterns shifted to slightly lower values of 2θ, indicating that sulfated addition of zirconia induced only minor changes in the cell unit paramater of SBA. This phenomenon may be due to the physical deposition of SZ on the pore wall of SBA-15 with crystal sizes smaller than the size of the channels of this mesoporous material (Garg et al., 2009).

SEM analyses of the synthesized parent SBA-15 and SZSBA-15 were also performed to observe the transformation of SBA-15 after urea hydrolysis to prepare SZSBA-15. The surface morphologies of the parent SBA-15 and SZSBA-15 are shown in Figure 2. The SEM image of SBA-15 shown in Figure 2(a) revealed that its structure consisted of well-defined wheat-like macro-structure aggregates, with numerous rope-like domains having a uniform size of 1–2 μm. This observation was similar to that of the SBA-15 samples synthesized by other researchers (Margolese et al., 2000; Liu et al., 2004; Mirji et al., 2006; Mazaj et al., 2009; Hermida et al., 2010), thereby indicating the successful synthesis of SBA-15 material in the present study.

After acid funtionalization to produce SZ SBA-15, a similar surface morphology was observed, as shown in Figure 2(b)–(f). This observation suggested the incorporation of SZ in the internal walls of SBA-15 channels. These

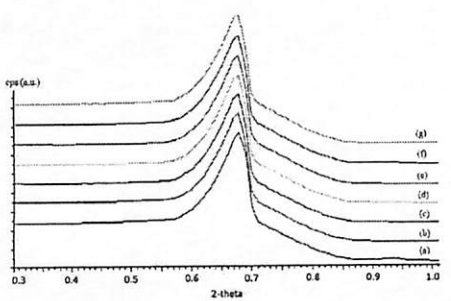

Fig. 1. XRD patterns of (a) SBA-15, (b) SZSBA-15(1), (c) SZSBA-15(2), (d) SZSBA-15(3), (e) SZSBA-15(4), (f) SZSBA-15(5), and (g) SZSBA-15(6) catalysts.

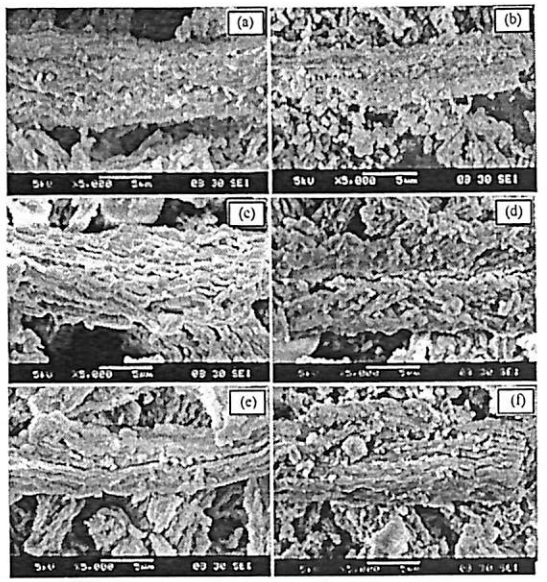

Fig. 2. SEM images of (a) SBA-15, (b) SZSBA-15(1), (c) SZSBA-15(3), (d) SZSBA-15(4), (e) SZSBA-15(5), and (f) SZSBA-15(6) catalysts.

SEM images indicated the stability of SBA-15 mesopores; the structure was definitely retained after acid funtionalization. A significant amount of SZ was deposited onto the external surface of SZSBA-15, as proven by the EDX results (Table II). Therefore, SZ was mainly deposited onto the internal surface of the SBA-15 particles. This result agreed well with XRD results. In SBA-15 materials, internal mesopore areas usually constitute about 70–80% of the total surface area (Garg et al., 2009; Du et al., 2009). Therefore, the ability to accommodate high loading of active metals was clearly the advantage of the SBA-15 material over other small-pore materials.

EDX analysis was also conducted to determine the elemental composition of SZ-incorporated SBA-15 surface. The elemental compositions are summarized in Table II. EDX analysis on SBA-15 revealed the presence of silica atom (Si) at 52.3 wt.% or 38.4 at.% and oxygen atom at 47.7 wt.% or 61.6 at.%. Meanwhile, SZSBA-15(6), SZSBA-15(4), and SZSBA-15(1) indicated the presence of zirconium atom at 19.2, 11. 9, and 10.41 wt.%, respectively. This observation suggested the successful incorporation of SZ into SBA-15. SZSBA-15(6) showed the highest content of zirconium atom at 5.1 at.%. Meanwhile, SZSBA-15(3) and SZSBA-15(5) showed relatively low zirconium contents. SZSBA-15(3) showed 4.7 wt.% or 1.1 at.% zirconia loading, whereas SZSBA-15(5) only contained 1.3 wt.% or 0.30 at.%, which was the lowest zirconium loading recorded among all the synthesized catalysts. This result indicated that low amounts of the metal precursor and short reflux time were unfavorable toward high metal loading. Meanwhile, the effect of low precursor amount was easily understood, and reflux duration was interestingly found to be critical in promoting higher zirconia loading in SBA-15.

The synthesis variables for SZSBA-15(3) were 0.58% zirconium oxyhydrochloride loading and 8 h of reflux time, whereas those for SZSBA-15(5) were 1.16% zirconium oxyhydrochloride loading and 3 h of reflux time. Meanwhile, the same parameters for SZSBA-15(4) were 1.16 g of zirconium oxyhydrochloride and 5 h of reflux time, whereas those for SZSBA-15(6) were 1.16 g of zirconium oxyhydrochloride and 8 h of reflux time. Both catalysts contained high amount of SZ; however, the position of SZ deposition on SBA-15 could also influence catalyst performance. A relationship was observed between zirconium oxyhydrochloride loading and reflux time, which could affect the performances of the catalysts in the esterification reaction (With et al., 2010; Davis et al., 1994). Thus, EDX analysis revealed the successful incorporation of a zirconium atom into the parent SBA-15 using the proposed functionalization method.

Table II. Elemental composition of catalysts used in this work based on EDX results

	SBA-15		SZSBA-15(1)		SZSBA-15(3)		SZSBA-15(4)		SZSBA-15(5)		SZSBA-15(6)	
Element	wt%	atm%	wt%	atm%	wt%	atm%	wt%	atm%	wt%	atm%	wt%	atm%
S	-	-	3.5	2.3	1.2	0.8	1.5	1.0	0.5	0.3	1.9	1.5
O	47.7	61.6	51.0	68.4	48.6	64.0	41.1	58.9	49.6	63.8	38.4	58.4
Si	52.3	38.4	35.1	26.8	45.5	34.2	45.5	37.1	48.6	35.6	40.4	35.0
Zr	-	-	10.4	2.5	4.7	1.1	11.9	3.0	1.3	0.3	19.2	5.1
Total	100	100	100	100	100	100	100	100	100	100	100	100

Selected samples from each category in Table II, including SBA-15, SZSBA-15(2), SZSBA-15(4), and SZSBA-15(6), were also tested for surface characteristics. The nitrogen adsorption–desorption isotherms of the parent SBA-15 and those of SZ-functionalized SBA-15 catalysts are shown in Figure 3. The isotherm characteristics of the parent SBA-15 and all other modified materials showed a type-IV isotherm, which implied an ordered mesoporous structure with a relatively narrow pore distribution (With et al., 2010). The general pattern of the parent SBA-15 was retained, with vertically offset curves at partial pressures of about 0.5, similar to the isotherms of SBA-15 reported by Cai et al. (2011). However, except for SZSBA-15(4), the functionalized SBA-15 samples showed reduced amount of adsorbed nitrogen, suggesting reduced surface areas.

SZSBA-15(2) and SZSBA-15(6) both showed similar characteristics to the parent SBA-15. These characteristics included drastic increases in the amount adsorbed at a partial pressure of 0.6, with horizontal offsets at 200 cm^3/g STP. Meanwhile, SZSBA-15(4) presented a significantly higher adsorbed amount, with vertically offsets at about 700 cm^3/g STP, and further increased to about 1250 cm^3/g STP. This result suggested significant variations in the internal surface areas with different pore characteristics and consistent with the data in Table III, indicating that SZSBA-15(4) had the highest total surface area among all studied catalysts.

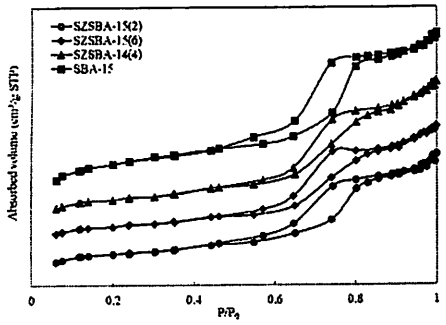

Fig. 3. N_2 adsorption–desorption isotherm of SBA-15, SZSBA-15(2), SZSBA-15(4), and SZSBA-15(6) catalysts.

SBA-15 with a surface area of 599 m^2/g and average pore size of 53.5 Å was found to be a mesoporous material. After functionalizing SBA-15, SZSBA-15 catalysts were observed to possess a larger average pore diameter than that of the parent SBA-15 material. Moreover, the functionalized catalysts showed both lower mesopore and micropore areas than that of the parent SBA-15. SZ was found to be mainly incorporated into the wall of the silica rather than in the pores or the channels, and the sulfonic acid groups were grafted on the mesoporous surface (Zheng et al., 2005). Increasing the surface area of functionalized catalysts is prepared by immobilization of sulfonated zirconia (SZ) to SBA-15 structure. These results propose that restructuring of the hexagonal structures occurred during the preparation of these catalysts, causing a significant decrease in micropore structures. For the intended reaction, i.e., esterification of lauric acid with glycerol, a mesoporous area was generally desirable.

The pore-distribution curves of SBA-15, SZSBA-15(2), SZSBA-15(4), and SZSBA-15(6) are shown in Figure 4. These curves were plotted using the BJH method applied to the desorption data. The diameter of the mesopores for each calcined solid (DP) satisfactorily corresponded to the maximum point of pore-size distribution in the figure. In this case, SZSBA-15(4) exhibited the largest peak at 66.8 Å, but showed the smallest mean diameter of mesopores. Other catalysts, namely, SBA-15, SZSBA-15(2), and SZSBA-15(6) showed maximum peaks at 68, 66, and 67 Å, respectively. These materials showed two regions of pore sizes, suggesting that the internal pores were mostly mesosized, whereas micropores could be mainly contributed by interstices between SZ crystals and, less importantly, between SBA-15 particles.

Based on the data in Table III, SBA-15 presented a total surface area of 599 m^2/g. The total surface area of modified SZSBA-15(2) and SZSBA-15(6) significantly decreased from 599 m^2/g to 314 m^2/g and 333 m^2/g, respectively. This table also clearly shows that, after the incorporation of SZ over SBA-15, the total surface area of SZSBA-15(4) increased from 599 m^2/g to 890 m^2/g. This finding can be attributed to the microporosity created between SZ crystals. Meanwhile, the total pore volume of SZSBA-15(2) and SZSBA-15(6) experienced a corresponding decrease from 0.801 cm^3/g to 0.502 cm^3/g and 0.530 cm^3/g, respectively. At the same time, that of SZSBA-15(4) increased from 0.801 cm^3/g to 1.792 cm^3/g. The modified SZSBA-15 catalysts, except for SZSBA-15(4), presented the total surface area and total pore volume in the same order of magnitude

Table III. Surface characteristics of SBA-15, SZSBA-15(2), SZSBA-15(4), and SZSBA-15(6) catalysts

Catalyst	Total surface area (m^2/g)[a]	Micropore area (m^2/g)[b]	Mesopore area (m^2/g)	Average pore diameter (Å)[a]	Total pore volume (cm^3/g)[a]
SBA-15	599	121	478	53.5	0.801
SZSBA-15(2)	314	37	277	63.9	0.502
SZSBA-15(4)	344	46	298	62.4	0.586
SZSBA-15(6)	333	33	300	63.7	0.530

[a]Based on BET equation (S_{BET}).
[b]Based on t-plot method.

as that reported by Garg et al. (2009). This observation led to the same argument stating that the incorporated SZ should be mainly located at the mesoporous channel of SBA-15.

The data in Table III also suggest that the micropore areas of SZSBA-15(2) and SZSBA-15(6) were significantly lower than that of the parent SBA-15. However, the mesopore diameter of SZSBA-15(2) and SZSBA-15(6) increased from 53.5 Å to 63.9 Å and 63.7 Å, respectively. This finding agreed with the XRD results. Moreover, the mesopore area of the same modified catalysts, SZSBA-15(2) and SZSBA-15(6), also increased from 80% of the parent SBA-15 to 88% and 90%, respectively, in terms of the amount of mesopore area in the total surface area. This finding indicated that the post-synthesis functionalization method managed to improve the quality of the mesoporous structure of SBA-15, as reported by Hermida et al. (2010) in the case of sulfonic acid-functionalized SBA-15.

Meanwhile, the mesopore diameter and mesopore area in the total surface area of SZSBA-15(4) were 80.5 Å and 38%, respectively. Notably, SZSBA-15(4) possessed a significantly greater micropore area than SBA-15. This result suggested that the micropores contributed more surface area than the mesopores. This finding was an undesirable consequence of SBA-15 funtionalization for catalytic purposes, as in this case, because catalytic performance in the esterification reaction may be affected. Although the amount of zirconia over

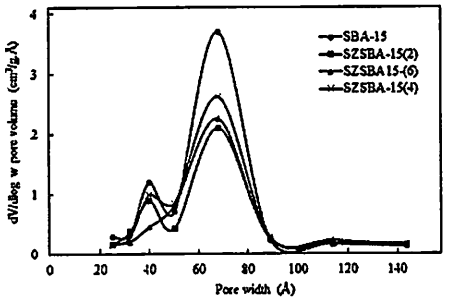

Fig. 4. Pore size distribution curve of SBA-15, SZSBA-15(2), SZSBA-15(4), and SZSBA-15(6) catalysts.

SZSBA-15(4) was sufficiently high (Table II), no zirconia deposition was observed in the SEM images (Figure 2). This result suggested satisfactory incorporation within mesopores and possibly within micropores in the pore walls of SBA-15 (With et al., 2010).

Catalytic Performance

The conversion of lauric acid, selectivities to monolaurin, dilaurin, and trilaurin, and yield of monolaurin over SBA-15 and modified SZSBA-15 after 6 h of reaction at 160°C are shown in Table IV. Despite SBA-15 being a neutral material, the reaction involving SBA-15 led to a lauric acid conversion of 60%. This result clearly indicated that lauric acid actually served as an autocatalyst in this reaction. The small pore size would pose certain geometric limitations to the reactant, as well as to the product (da Silva-Machado et al., 2000). Superacidity catalysts with small particle sizes (<100 nm), such as lead oxide, cobalt chloride, sulfated iron oxide, zinc chloride, and tin chloride, were found to present activation energies in the range between 68 and 78 kJ/mol. However, reaction without catalyst and merely in the presence of fatty acid, which can act as autocatalyst, reported to be 89 kJ/mol (Hermida et al., 2011). The existence of solid acid catalysts was observed to cause a reduction in the energy barrier for monoglyceride production from oleic acid. In addition, further reduction could be attained via a catalyst with mesopore structures, because the monoglyceride would be formed in the internal pores of the catalyst.

However, in the presence of acidic catalysts, the selectivities to mono-, di-, and trilaurin improved. The selectivity to monolaurin was invariably higher than that to dilaurin and trilaurin for all catalysts. Therefore, the attachment of another lauric acid to monolaurin was relatively difficult because of steric hindrance. In the present work, the results of SZSBA-15(1) and SBA-15 catalysts were compared with the corresponding data tested under the same conditions as reported by Hermida et al. (2010). Based on the data in this table, SZSBA-15(2) showed the highest monolaurin yield, the highest conversion of lauric acid, and the highest selectivity to monolaurin. The yield of monolaurin was measured to be 79.1% at 94.9% lauric acid conversion, with 83.4% selectivity to monolaurin. Meanwhile, SZSBA-15(5) yielded a high conversion of 83.4%, but selectivity to monolaurin was measured to be merely 52.9%, which was lower than those of SZSBA-15(2) and SZSBA-15(6). These findings could be correlated with the pore-size distribution of

Table IV. Conversion of lauric acid, products selectivity, and yield of monolaurin for different catalysts

Sample code	Conversion, %	Selectivity, %			Yield, %
		Monolaurin	Dilaurin	Trilaurin	
SZSBA-15(1)[a]	62.00	67.00	N/A	N/A	41.5
SZSBA-15(2)	94.88	83.42	5.61	1.79	79.1
SZSBA-15(3)	64.75	45.30	24.37	1.99	29.3
SZSBA-15(4)	29.51	17.65	15.13	17.36	52.0
SZSBA-15(5)	83.02	52.39	21.25	1.70	43.5
SZSBA-15(6)	73.81	77.93	9.61	0.95	57.5
SBA-15[a]	60.00	40.00	N/A	N/A	24.0

[a]Result obtained from Hermida et al. (2010).

the catalyst. SZSBA-15(2) and SZSBA-15(6) presented higher mesopore area and total surface area than SBA-15. Furthermore, SZSBA-15(6) showed the highest zirconium (Zr) loading based on EDX analysis results.

Despite its high total surface area, SZSBA-15(4) showed the lowest conversion and selectivity values (29.5% and 17.7%, respectively) among all studied catalysts. Notably, the zirconium content of SZSBA-15(4) was the second highest among all catalysts. Therefore, the catalytic activity in this reaction was strongly governed by molecular-sieving effects. In this case, high microporosity in the catalyst was considered to be the contributing factor. Modified catalyst SZSBA-15(2) showed good behavior for producing a high amount of monolaurin with a high conversion of lauric acid in comparison with all other catalysts. According to a previous study (Freitas et al., 2010), the highest selectivity of monolaurin achieved using lipase as catalyst is only 62.9%. Except for SZSBA-15(4), the other modified SBA-15 catalyst obtained higher selectivity to monolaurin than that of the enzyme within 6 h of reaction time. This finding showed the advantage of heterogeneous catalysts in promoting the formation of the desired product. Modified catalysts SZSBA-15(2) and SZSBA-15(5) also showed better performances than previously reported aluminium- and zirconium-containing mesoporous molecular sieve materials (AlZrMMS-H), which recorded to present 40% conversion and 80% selectivity to monolaurin.

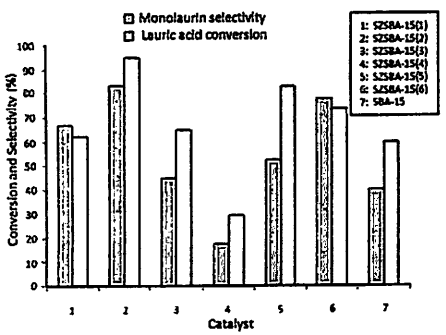

Fig. 5. Lauric acid conversion and selectivity to monolaurin for SBA-15 and modified SBA-15 catalysts.

Lauric acid conversion and selectivity to monolaurin were also correlated with reflux time and zirconium loading, as shown in Figure 5 and Table IV. Figure 5 clearly shows that 16 wt.% SZSBA-15 catalyst showed higher efficiency for the selective conversion of lauric acid than 27 wt.% SZSBA-15. Hence, 16 wt.% SZSBA-15 catalyst was preferred over 27 wt.% SZSBA-15 based on the overall average results of conversion, selectivity, and yield of the prepared modified SZSBA-15 catalyst. Thus, larger mesopores allowed for the undesirable subsequent esterification reactions on monolaurine to di- and tri-laurin.

The conversion of lauric acid and selectivity of monolaurin for functionalized SBA-15 catalyst prepared at different reflux times and $ZrOCl_2 \cdot 8H_2O$ loading are shown in Table IV. The highest conversion and selectivity were observed for 16 wt.% SZBA-15 after 3 h of reflux time. Meanwhile, increasing the reflux time from 3 h to 8 h caused a gradual reduction in selectivity toward monolaurin. Besides, with more than 27 wt.% SZSBA-15 catalyst, the highest conversion of lauric acid was obtained for the sample after 3 h of reflux time. However, 27 wt.% SZSBA-15 exhibited the highest monolaurin selectivity after a reflux time of 8 h. This finding could lead to the conclusion that the reflux time of 3 h was more suitable for the preparation of 16 and 27 wt.% SZSBA-15 catalysts. A long reflux time was deemed to be detrimental to catalytic properties and was associated with the surface properties of the functionalized catalysts. In conclusion, the duration of reflux time significantly affected the activity and properties of catalysts.

From the obtained results, we can conclude that these results are comparable with those of other results reported in the literature for this reaction using different type of catalysts. In the present study, a high monolaurin selectivity of 83.4% was achieved at 94.9% conversion of lauric acid in the esterification of glycerol and lauric acid over SZ-loaded SBA-15 catalyst. Uniformed SBA-15 catalysts functionalized with 12-tungstophosphorus acid (HPW) were synthesized and used in the esterification of glycerol and lauric acid to monolaurate. A monolurin yield of 50% was obtained at a lauric acid conversion of 70% after 6 h at 160°C over 20 wt.% HPW catalyst (Hoo and Abdullah, 2014). The esterification of glycerol by lauric acid using aluminium and zirconium containing mesoporous MMS-H materials at 150°C for 18 h was studied by Sakthivel et al. (2007). A high conversion of 93% with 48% selectivity toward monolaurin was achieved.

Conclusions

SZ was successfully incorporated into the internal mesopores of SBA-15. Reaction behaviors with respect to the conversion of lauric acid and good selectivity to monolaurin were successfully elucidated and correlated with the properties of the mesoporous catalysts. SZSBA-15(2) catalysts resulted in the highest monolaurin yield of 79.1%. SZSBA-15 catalyst required 3 h of reflux time and 16 wt.% zirconium oxychloride loading to provide this yield. Characterizations of SZSBA-15 catalysts showed the successful incorporation of SZ over SBA-15 modified catalysts, with improved properties, such as larger mesopore surface area, lower micropore area, and higher zirconia content. After the incorporation of SZ, the mesoporous structure of the SBA-15 support was retained, and the performance of SZSBA-15 was found to be clearly better than that of the parent SBA-15. A high conversion of lauric acid (94.9%) and good selectivity to monolaurin (83.4%) were achieved within 6 h at a lauric acid-to-glycerol molar ratio of 4.0 and at 160°C.

Funding

A Research University (RU) grant (814144) and a Sciencefund (613381) are gratefully acknowledged for the support of this work.

References

Cai, Y., Li, H., Du, B., Yang, M., Li, Y., Wu, D., Zhao, Y., Dai, Y., and Wei, Q. (2011). Ultrasensitive electrochemical immunoassay for BRCA1 using BMIM.BF4-coated SBA-15 as labels and functionalized graphene as enhancer, *Biomaterials*, 32, 2117–2123.

da Silva-Machado, M., Cardoso, D., Pérez-Pariente, J., and Sastre, E. (2000). Esterification of lauric acid with glycerol using modified zeolite beta as catalyst. *Stud. Surf. Sci. Catal.*, 130, 3417–3422.

Davis, B. H., Keogha, R. A., and Srinivasana, R. (1994). Sulfated zirconia as a hydrocarbon conversion catalyst, *Catal. Today*, 20, 219–256.

Degirmenci, V., Yilmaz, A., and Uner, D. (2009). Selective methane bromination over sulfated zirconia in SBA-15 catalysts, *Catal. Today*, 142, 30–33.

Du, Y., Sen, L., Yonglai, Z., Faisal, N., Yanyan, J., and Feng-Shou, X. (2009). Urea-assisted synthesis of hydrothermally stable Zr-SBA-15 and catalytic properties over their sulfated samples, *Micropor. Mesopor. Mat.*, 121, 185–193.

Freitas, L., Ariela, V. P., Julio, S. C. D., Gisella, M. Z., and Heizir, C. F. D. (2010). Enzymatic synthesis of monoglycerides by esterification reaction using *Penicillium camembertii* lipase immobilized on epoxy SiO_2-PVA composite, *J. Mol. Catal. B: Enzym.*, 65, 87–90.

Garg, S., Kapil, S., Muthu, K. G., Rajaram, B., Kinga, G. M., Gupta, J. K., Sharma, L. D., and Murali, D. G. (2009). Acidity and catalytic activities of sulfated zirconia inside SBA-15, *Catal. Today*, 141, 125–129.

Hamouda, L. B., Ghorbel, A., and Figueras, F. (2000). Study of acidic and catalytic properties of sulfated zirconia prepared by sol-gel process: influence of preparation conditions, *Stud. Surf. Sci. Catal.*, 130, 971–976.

Hello, K. M., Adam, F., and Ali, T. H. (2014). A solid sulfonic acid catalyst for the solvent free alkylation of phenol, *J. Taiwan Inst. Chem. Eng.*, 45(1), 134–142.

Hermida, L., Abdullah, A. Z., and Mohamed, A. R. (2011). Synthesis of monoglyceride through glycerol esterification with lauric acid over propyl sulfonic acid post-synthesis functionalized SBA-15 mesoporous catalyst, *Chem. Eng. J.*, 174, 668–676.

Hermida, L., Abdullah, A. Z., and Mohamed, A. R. (2010). Post synthetically funtionalized SBA-15 with organosulfonic acid and sulfated zirconia for esterification of glycerol to monoglyceride, *J. Appl. Sci.*, 10, 3199–3206.

Hoang, v. D., Dang, T. P., Dinh, Q. K., Nguyen, H. P., and Vu, A. T. (2010). The synthesis of novel hybrid thiol-functionalized nanostructured SBA-15. *Adv. Nat. Sci.: Nanosci. Nanotechnol.*, 1, 1–6.

Hoo, P. Y., and Abdullah, A. Z. (2014). Direct synthesis of mesoporous 12-tungstophosphoric acid SBA-15 catalyst for selective esterification of glycerol and lauric acid to monolaurate, *Chem. Eng. J.*, 250, 274–287.

Jin, H., Qingyin, W., and Wenqin, P. (2004). Preparation and conductivity of tungstovanadogermanic heteropoly acid supported on mesoporous silicate SBA-15. *Mater. Lett.*, 58, 3657–3660.

Kärger, J., Cool, J. P., Coppens, M. O., Jones, D., Kapteijn, F., Reinoso, F. R., Stöcker, M., Theodorou, D., Vansant, E. F., and Weitkamp, J. (2009). Benefit of microscopic diffusion measurement for the characterization of nanoporous materials, *Chem. Eng. Technol.*, 32, 1494–1502.

Li, Q., Tao, W., Li, A., Zhou, Q., and Shuang, C. (2014). Poly (4-vinylpyridine) catalyzed isomerization of maleic acid to fumaric acid, *Appl. Catal. A: Gen.*, 484, 148–153.

Liu, Y. M., Yong, C., Nan, Y., Wei-Liang, F., Wei-Lin, D., Shi-Run, Y., He-Yong, H., Kang-and Nian, F. (2004). Vanadium oxide supported on mesoporous SBA-15 as highly selective catalysts in the oxidative dehydrogenation of propane, *J. Catal.*, 224, 417–428.

Luo, G., Shirun, Y., Minghua, Q., and Kangnian, F. (2007). RuB/Sn-SBA-15 catalysts: preparation, characterization and catalytic performance in ethyl lactate hydrogenation, *Appl. Catal. A*, 332, 79–88.

Margolese, D., Melero, J. A., Christiansen, S. C., Chmelka, B. F., and Stucky, G. D. (2000). Direct syntheses of ordered SBA-15 mesoporous silica containing sulfonic acid groups, *Chem. Mater.*, 12, 2448–2459.

Mazaj, M., Stevens, W. J. J., Logar, N. Z., Ristic, A., Tušar, N. N., Arcon, I., Daneu, N., Meynen, V., Cool, P., Vansant, E. F., and Kaucic, V. (2009). Synthesis and structural investigations on aluminium-free Ti-beta/SBA-15 composite, *Micropor. Mesopor. Mat.*, 117, 458–465.

Mekala, M., Thamida, S. K., and Goli, V. R. (2013). Pore diffusion model to predict the kinetics of heterogeneous catalytic esterification of acetic acid and methanol, *Chem. Eng. Sci.*, 104, 565–573.

Mirji, S. A., Halligudi, S. B., Sawant, D. P., Patil, K. R., Gaikwad, A. B., and Pradhan, S. D. (2006). Adsorption of toluene on Si(100)/SiO_2 substrateand mesoporous SBA-15, *J. Colloid. Surf. A*, 272, 220–226.

Nie, G., Zou, J.-J., Feng, R., Zhang, X., and Wang, L. (2014). HPW/MCM-41 catalyzed isomerization and dimerization of pure pinene and crude turpentine, *Catal. Today*, 234, 271–277.

Pouilloux, Y., Abro, S., Vanhove, C., and Barrault, J. (1999). Reaction of glycerol with fatty acids in the presence of ion-exchange resins: preparation of monoglycerides, *J. Mol. Catal. A*, 149, 243–254.

Sakthivel, A., Nakamura, R., Komura, K., and Sugi, Y. (2007). Esterification of glycerol by lauric acid over aluminium and zirconium containing mesoporous molecular sieves in supercritical carbon dioxide medium, *J. Sup. Fluids*, 42, 219–225.

Sayari, A., and Jaroniec, M. (2002). *Nanoporous Materials III, Proceedings of the 3rd International Symposium on Nanoporous Materials*, Elsevier Science, Amsterdam, Netherlands.

Thiruvengadaravi, K. V., Nandagopal, J., Baskaralingam, P., Sathya Selva Bala, V., and Sivanesan, S. (2012). Acid-catalyzed esterification

of karanja (*Pongamia pinnata*) oil with high free fatty acids for biodiesel production, *Fuel*, 98, 1–4.
With, P., Heinrich, A., Lutecki, M., Fichtner, S., Böhringer, B., and Gläser, R. (2010). Zirconia with defined particle morphology and hierarchically structured pore system synthesized via combined exo- and endotemplating, *Chem. Eng. Technol.*, 33, 1712–1720.
Zhang, H., Wei, H., Cui, Y., Zhao, G., and Feng, F. (2009). Antibacterial interactions of monolaurin with commonly used antimicrobials and food components, *J. Food Sci.*, 74(7), 418–427.
Zheng, Y., Su, X., Zhang, X., Wei, W., and Sun, Y. (2005). Functionalized mesoporous SBA-15 silica with propylsulfonic groups as catalysts for esterification of salicylic acid with dimethyl carbonate, *Stud. Surf. Sci. Catal.*, 156, 205–212.

of karanja (*Pongamia pinnata*) oil with high free fatty acids for biodiesel production, *Fuel*, 98, 1–4.
With, P., Heinrich, A., Lutecki, M., Fichtner, S., Böhringer, B., and Gläser, R. (2010). Zirconia with defined particle morphology and hierarchically structured pore system synthesized via combined exo- and endotemplating, *Chem. Eng. Technol.*, 33, 1712–1720.
Zhang, H., Wei, H., Cui, Y., Zhao, G., and Feng, F. (2009). Antibacterial interactions of monolaurin with commonly used antimicrobials and food components, *J. Food Sci.*, 74(7), 418–427.
Zheng, Y., Su, X., Zhang, X., Wei, W., and Sun, Y. (2005). Functionalized mesoporous SBA-15 silica with propylsulfonic groups as catalysts for esterification of salicylic acid with dimethyl carbonate, *Stud. Surf. Sci. Catal.*, 156, 205–212.

Energy Sources, Part A: Recovery, Utilization, and Environmental Effects, 37:1747–1755, 2015

ISSN: 1556-7036 print/1556-7230 online
DOI: 10.1080/15567036.2011.631968

Response Surface Methodology for Simulation of Ultrasonic-assisted Biodiesel Production Catalyzed by SrO/Al_2O_3 Catalyst

H. Mootabadi[1] and A. Z. Abdullah[1]

[1]*School of Chemical Engineering, Universiti Sains Malaysia, Penang, Malaysia*

Ultrasound-assisted transesterification of palm oil by SrO/Al_2O_3 catalyst was investigated. Effects reaction time (10–50 min), alcohol to oil molar ratio (3:1–15:1), catalyst loading (0.5–2.5 wt%) and ultrasonic amplitude (15–95%) were studied. Response surface methodology was employed to evaluate and optimize the process. Interactions among the variables and the response were elucidated. The model was accurate with less than 5% error. 80.2% of biodiesel yield was achieved at a methanol to oil ratio of 9.2, 1.6 wt% of catalyst, 30.2 min of reaction time, and 69.7% of ultrasonic amplitude power.

Keywords: biodiesel production, optimization, simulation, SrO/Al_2O_3 catalyst, ultrasound

INTRODUCTION

Compared to conventional homogeneous catalysts, heterogeneous catalysts have many advantages in biodiesel production process but they are usually subject to poor catalytic activity (Santos et al., 2009). The use of ultrasonic energy for biodiesel production has become an area of interest to solve this problem (Mootabadi et al., 2010; Santos et al., 2009). Due to poor miscibility, the reaction between oil and alcohol only occurs in the interface (Mootabadi et al., 2010). Conventionally, vigorous mechanical stirring or agitation is used to enhance the interfacial area between the two phases (Salamatinia et al., 2010). Ultrasonic energy provides great interest by two means. It can produce a homogeneous mixture of the reactants to improve mass transfer and heating effects created by ultrasonic irradiation can further accelerate the reaction.

Response surface methodology (RSM) is a mathematical-based technique that is useful for analyzing the effects of several independent variables on the response. A key component of RSM is response surface design (Ryan, 2007). One of the most common designs in RSM studies used for fitting a second-order model is the central composite design (CCD). This design might be used because of its ability to run consecutively. It predicts linear interaction as well as curvature effects between process variables (Montgomery, 2001).

The main aim of this study is to characterize the effects of ultrasonic energy in the presence of alumina-supported strontium oxide as heterogeneous catalysts. In this study, the data obtained from

Address correspondence to Dr. A. Z. Abdullah, School of Chemical Engineering, Universiti Sains Malaysia, Nibong Tebal, Penang 14300, Malaysia. E-mail: chzuhairi@eng.usm.my

Color versions of one or more of the figures in the article can be found online at www.tandfonline.com/ueso.

Downloaded by [Universiti Sains Malaysia] at 18:54 21 July 2015

the experimental work by varying one factor at a time were fitted to the central composite design and the overall trend was characterized while the accuracy of the models developed was simultaneously evaluated.

MATERIALS AND METHODS

Reactants and Catalyst

Commercial palm oil (Vesawit, Malaysia) was purchased from a local store while an analytical grade methanol supplied by Thermo Fisher Scientific Inc. (USA). Reference standards, such as methyl myristate, methyl palmitate, methyl oleate, methyl stearate, and methyl linoleate, were obtained from NuChek Prep. Inc., Australia. Strontium carbonate ($SrCO_3$) was supplied by ACROS Corporation (USA) while gamma alumina was supplied by Nanostructured & Amorophous Materials Inc. (USA). A strontium oxide catalyst supported on γ-alumina was prepared using a wet impregnation method Initially, 10 g of $SrCO_3$ was mixed with 50 ml of HNO_3 in order to prepare an aqueous solution of $Sr(NO_3)_2$. Commercial γ-Al_2O_3 (157 m^2/g) was then added to the solution followed by drying in a rotary evaporator at 70°C for 12 h. The supported SrO/Al_2O_3 catalyst was then calcined in a furnace at 500°C for 5 h.

Experimental Setup

The ultrasound-assisted transesterification reaction was carried out in a 500-ml three-neck glass batch reactor vessel equipped with an ultrasonic transducer and probe, a condenser, a stirrer, and a thermocouple thermometer. The ultrasonic reactions were performed using a Branson (USA) ultrasonic processor (20 kHz) with a full power of 200 W (100%). Details of the experimental setup are available elsewhere (Mootabadi et al., 2010). The alcohol to oil molar ratios were varied between 3:1 and 15:1 while the catalyst loadings were varied in the range of 0.5–2.5 wt%. The amplitude of the ultrasonic processor was varied between 15 to 95%. The biodiesel analysis was performed by means of a gas chromatograph (Perkin-Elmer Series Clarus 500) with a capillary column (Nucol, 50 m × 50 μm).

Application of Response Surface Methodology

The data obtained from the experimental runs as mentioned above were fitted to a central composite design for the application of response surface methodology. The Design Expert (Version 6.0.7, StatEase, Inc., USA) software was used for regression and graphical analyses of the data obtained. The ranges and the designated levels of the variables investigated in this study are given in Table 1. The general quadratic equation model for predicting the optimal point is expressed by Eq. (1):

$$Y = \beta_0 + \sum_{i=1}^{k} \beta_i X_i + \sum_{i=1}^{k} \beta_{ii} X_i^2 + \sum_{i=1} \sum_{j=i+1} \beta_{ij} X_i X_j + \varepsilon, \quad (1)$$

where Y is the response calculated by model (dependent variables), β_0 is the constant coefficient, β_i is coefficient for the linear effect, β_{ii} is the coefficient for the quadratic effect, while β_{ij} stands for the coefficient for the cross-product effect. In Eq. (1), X_i, X_j are the variables corresponding to factors (independent variables) and ε is the error.

TABLE 1
Coded and Actual Values of Variables Used in the Experimental Design

Factor		Coded Levels of Variables				
		-α	-1.00	0	1.00	+α
Time, min	A	10	20	30	40	50
Catalyst weight ratio, wt%	B	0.5	1.0	1.5	2.0	2.5
Alcohol to oil molar ratio	C	3	6	9	12	15
Ultrasonic amplitude	D	15	35	55	75	95

RESULTS AND DISCUSSION

Model Fitting and Statistical Analysis

The biodiesel yields obtained from the experiments using SrO/Al_2O_3 as the catalyst were found to vary from 41.6 to 80.3%, depending on the experimental conditions. These results provide evidence that ultrasound-assisted intensified the transesterification process and yields higher than 80% could be obtained in just about 40 min. Similar yields were reported to be only achieved in about 120 min using a conventional stirring reactor (Georgogianni et al., 2009). Transesterification of vegetable oil and methanol is known to be a mass-transfer controlled reaction (Meher et al., 2006). As such, emulsification effects between the liquid reactants were indeed beneficial in accelerating the reaction. The biodiesel yield developed a second-order polynomial equation (Eq. (2)) as below:

$$Y = 77.79 + 4.49A + 2.33B + 3.71C + 7.18D - 2.91A^2 - 1.324B^2 - 5.54C^2 - 5.29D^2 + 2.20CD. \quad (2)$$

The second-order response function relates to Y, which is the response for biodiesel yield, to A, which is the coded value of reaction time, B is the coded value of catalyst mass ratio, C is the coded value of methanol to oil ratio, and D is the coded value of amplitude of ultrasonic processor. A positive sign in front of the terms indicates synergistic effect while a negative sign indicates antagonistic effect. The equation shows that the yield of palm oil fatty acid methyl ester (FAME) followed a quadratic trend for the four transesterification process variables studied. The parity plot between the experimental versus predicted data using Eq. (2) for the biodiesel yield and the responses suggested that the regression model equation provided a very accurate description of the experimental data. The predicted values match the observed values reasonably well within the ranges of experimental conditions, with an R^2 value of 0.95. This result suggested the applicability and reliability of the equation in representing the reaction over these wide ranges of experimental conditions.

Statistical analysis obtained from the analysis of variance (ANOVA) for the response surface reduced quadratic model suggested that the model F-value was 44.55. The value of "$P > F$" for the models is less than 0.05 to indicate that it is significant. The result shows that the terms in the model indeed have a significant effect on the response. The value of $P < 0.0001$ indicates that there is only about 0.01% chance that a "model F-value" will occur due to noise. Values greater than 0.0500 indicate that the model terms are not significant.

The model showed insignificant values for the two-level interaction between term A (reaction time) and term B (catalyst mass ratio), two-level interaction between term A and term C (methanol to oil ratio), two-level interaction between term A and term D (amplitude of ultrasonic processor), two-level interaction between terms B and C, and two-level interaction between terms B and D, while the other model terms were significant. Therefore, A, B, C, D, A^2, B^2, C^2, D^2, and CD are proven to be significant model terms to affect the biodiesel yield. Interactions between other variables were insignificant in the ranges tested. The "Lack of Fit F-value" of 2.48 implies that it is not significant relative to the pure error. Therefore, there is a 16.1% chance that a "Lack of Fit F-value" this large could occur due to noise. Insignificant lack of fit is considered as a good indication that the model can fit.

The null hypothesis was also tested to prove that the model is applicable. The null hypothesis is rejected if F-statistic is too big. In order to have a lack-of-fit sum of squares, one should observe more than one value of the response variable for each value of the set of predictor variables (Salamatinia et al., 2010). The replicates at the center points indicated more than one value for the response in the same conditions. The insignificancy of the lack of fit implies that the experimental data observed can satisfactorily fit the model.

Influence of Individual Effect

The individual effects of A, B, C, and D towards biodiesel yield based on Eq. (2) can be graphically seen in Figures 1a–1d. As noted in Figure 1a, generally there is an upward trend for SrO/Al_2O_3 catalyst with the increase in the reaction time reaching a plateau at a reaction time of about 35 min. There are no reports found in the literature on SrO/Al_2O_3 as the catalyst for transesterification for comparison. Yet the use of alumina as a support in a conventional stirring reactor system has been reported by several researchers (Li et al., 2007). Generally, reaction times of longer than 1 h are needed for the biodiesel yield to reach the plateau. As such, it can be concluded that the reaction time in this work was cut nearly in half.

In general, the reaction time significantly dropped using ultrasonification compared to the reported results. A reaction time of 4 h has been reported for transesterification of *Nannochloropsis oculata* microalga's lipid to biodiesel using Al_2O_3-supported CaO and MgO catalysts. Al_2O_3-supported alkali and alkali earth metal oxides for transesterification of palm kernel oil and coconut oil have been reported to achieve the highest yield at a reaction time of about 3 h (Benjapornkulaphong et al., 2009). Whereas the decrease in the reaction time could be contributed by the difference between the catalysts used, the main reason for this phenomenon could be attributed to the ultrasonic effect. Ultrasonication apparently enhanced the extent of mixing between the reactants to allow a larger interface area for contact and mass transfer. The same results were earlier found in the authors' previous research using unsupported SrO as the catalyst in which the reaction time decreased significantly compared to the conventional stirred reactor system (Mootabadi et al., 2010). Reduction in the time is undeniably an important factor that can reduce the overall biodiesel production costs.

Effects of the catalyst mass ratio on biodiesel yield for the SrO/Al_2O_3 catalyst are illustrated in Figure 1b. Biodiesel yield increased moderately with the increase in the catalyst mass ratio. This upward trend slowed down after 1.5 wt% of catalyst loading reaching a biodiesel yield of around 76%. It should be noted that only a minor increase in the biodiesel yield was achieved when increasing the catalyst mass ratio from 1.5 to 2 wt%. This amount of catalyst was significantly low as compared to the results reported for Al_2O_3-supported alkali and alkali earth metal oxides for transesterification of palm kernel oil and coconut oil (10 and 15–20 wt% catalyst to oil ratio, respectively) (Benjapornkulaphong et al., 2009). The reduction in the catalyst loading could be partly attributed to the larger surface area of the supported catalyst. However, the intensified reaction rate due to ultrasonication was deemed to be the reason for this improvement. It was also reported that when potassium loaded on alumina was used as the catalyst at a loading of 6.5%, the conversion of soybean oil reached 87% in 7 h of time (Xie et al., 2007). Thus, higher reaction rate in this work brought about the desired effects in terms of lower catalyst requirement and shorter reaction time.

Downloaded by [Universiti Sains Malaysia] at 18:54 21 July 2015

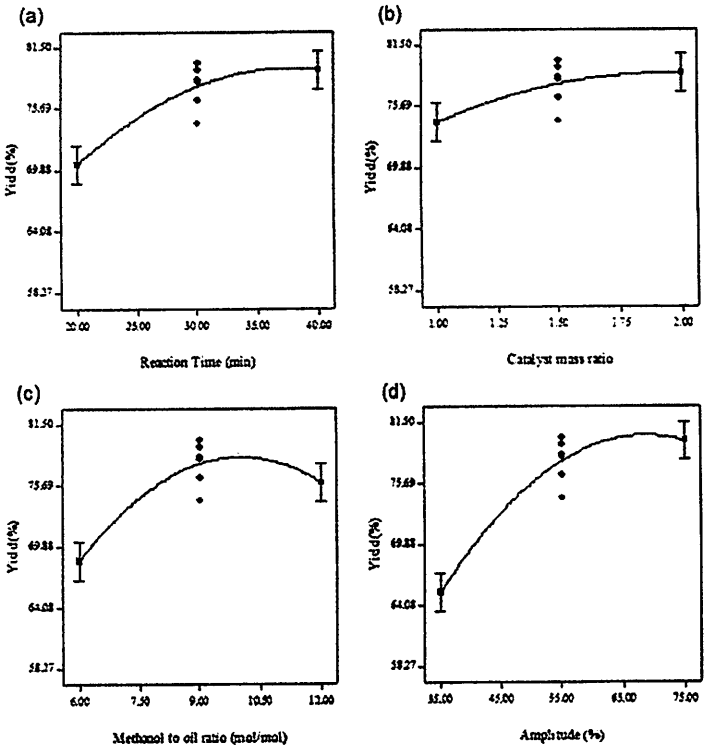

FIGURE 1 The individual effect of (a) reaction time, (b) catalyst mass ratio, (c) methanol to oil ratio and (d) amplitude of ultrasound towards biodiesel yield.

Figure 1c shows the effects of methanol to oil molar ratio on biodiesel yield. As can be observed, the biodiesel yield increased with the increase in the methanol to oil molar ratio from 6:1 to almost 9:1. The yield remained nearly constant at around 76% and beyond this ratio, the biodiesel yield dropped significantly. Thus, the best condition for the yield was found to be a ratio of around 9:1.

Comparing these results with those reported by other researchers, it could be concluded that ultrasonification in the transesterification reaction could reduce the amount of methanol needed to be used. A methanol to soybean oil molar ratio of 15:1 at a reaction time of 7 h was reported by Xie et al. (2007). There are some reports available in the literature showing lower molar ratios in very high reaction times but in the end the reaction reached lower yields. For example, Eu_2O_3/Al_2O_3 was reported to catalyze the transesterification of soybean oil at a methanol to oil ratio of 6:1, reaching a conversion of only 63% in 8 h (Li et al., 2007). Thus, ultrasonication could provide a better mixing affect, which improved the contact between the reactants. Consequently, a

significant reduction in the amount of the methanol needed would be achieved to make the process more environmentally friendly and it also can reduce the production cost, which is of great industrial concern.

Another variable that could influence the reaction is the amplitude of the ultrasonic processor. In this study, the effect is illustrated in Figure 1d. By increasing the ultrasonic amplitude, a sharp increase was observed in the biodiesel yield. The yield reached a peak at amplitudes between 65–70% and dropped slightly afterwards.

Transesterification is a reversible reaction and a drop at high amplitudes could be attributed to the ultrasonic force to promote reverse reaction. The optimum predicted point occurred at around 70% of amplitude of the ultrasonic processor. The high improving effect of ultrasonic was clearly obvious in the transesterification process. However, the main factor that contributed to the improvement was the high mixing affects by ultrasonication.

Interactions between Variables

Equation (2) suggests the presence of interactions between methanol to oil ratio (C) and amplitude of ultrasonic processor (D). Therefore, it is of great interest to further characterize the interactions in the range of process variables studied. Based on the value of the coefficient of C^2 and D^2, it was also noted in the individual effects of the parameters that amplitude and the ratio demonstrated a more varying trend as compared to the other two variables. The contour and three-dimensional plots for the interaction between the methanol to oil ratio and amplitude of ultrasonic processor towards biodiesel yield are shown in Figures 2a and 2b, respectively.

When the transesterification process was carried out at 35% of ultrasonic amplitude, the biodiesel yield was only about 63%. However, the biodiesel yield increased with increasing ultrasonic amplitude to 65% and remained almost constant up to an amplitude of 70%. Afterwards, a decrease in the yield was observed as the amplitude was increased towards its high level (75%). This observation was consistent with earlier findings using unsupported catalysts (Mootabadi et al., 2010; Salamatinia et al., 2010). This was also the exact phenomenon that was discussed in the individual analysis of the parameters. The same trend was shared for the whole range of methanol to oil ratios studied (6:1 to 12:1). However, the optimum ultrasonic amplitude for the highest yield shifted towards a higher range of methanol to oil ratio as noted in Figure 2. Thus, the behavior of the system in terms of these two variables achieved high yields with slightly lower than the higher level of these two variables.

The optimum methanol to oil molar ratio is much influenced by the system configuration, reaction volume, type of catalyst (homogeneous or heterogeneous), operating pressure, etc. Generally, molar ratios of about 6:1 have been reported for a mechanically mixed homogeneous catalytic system (Meher et al., 2006), while heterogeneous systems require a slightly higher ratio due to slower reaction rate (Liu et al., 2007; Xie et al., 2007). A high ratio is needed to shift the equilibrium in the reversible reaction towards the products (Meher et al., 2006). However, an excessive level of methanol in the system will bring the dilution effect to the limiting reactant, i.e., the vegetable oil (Liu et al., 2007). However, it can be seen that ultrasonication reduced the requirement for methanol in the reaction. This could be attributed to the accelerated reaction caused by ultrasonication so that less methanol was needed.

In the model equation, the amplitude of ultrasonic processor (D) was the major regression variable affecting the response (greatest coefficients), while this variable had a significant interaction with methanol to oil ratio (C). The regression coefficients are 7.18 and 3.71 for both individual effects, respectively. Kawashima et al. (2009) reported that supported metal oxides catalysts, such as CaO-CeO_2 and $CaZrO_3$ catalysts, could achieve 60% of biodiesel yield in 2 h with a magnetically stirred system. By using ultrasonic energy, higher yields of biodiesel could be achieved in just 30 min.

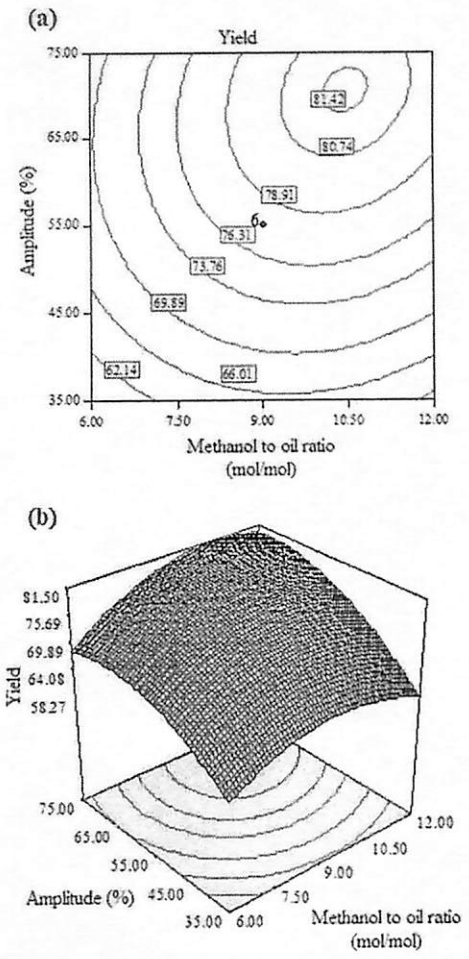

FIGURE 2 Contour and three dimensional plots for the effect of methanol to oil ratio and ultrasonic amplitude towards biodiesel yield.

Optimization of Process Parameters

The successful use of computer-based RSM to optimize the parameters affecting the reaction in various transesterification systems have been reported by other researchers (Salamatinia et al., 2010; Santos et al., 2009). In this study, optimization of the biodiesel production process using a numerical feature of the Design Expert 6.0.6 software was performed to search for optimum conditions to get the maximum biodiesel yield using SrO/Al_2O_3 as the catalyst. The goal for all variables should be in the tested range in order to determine the maximum yield of biodiesel (response). The ranges were decided based on reported results, own experiences, as well as some process economical considerations.

TABLE 2
Results of Experiments Conducted at Optimum Conditions as Obtained from DOE

Solution	*A*	*B*	*C*	*D*	*Predicted Value, %*	*Experimental Value, %*
2	39.11	2.18	10.73	66.55	83.6	81.3
6	36.14	1.58	11.90	72.16	82.3	78.9
8	30.26	1.63	9.20	69.68	81.2	80.2

Altogether 10 solutions for the optimum conditions were generated by the software according to the order of suitability. The three solutions were then chosen for further process studies to evaluate the validity of the statistical experimental strategies by comparing with experimental data. The experimental values obtained for biodiesel yield were found to be quite close (within 2.23% mean error) to those predicted values obtained through RSM as shown in Table 2. These results confirmed the predictability of the model in the experimental conditions used. For the optimization of process parameters in the transesterification process, it is observed that the optimal set of process variables are 69.7% of ultrasonic amplitude, 9.20 mol/mol for the methanol to oil ratio, 1.63 wt% for the catalyst loading, and 30 min for reaction time to about give 81% of biodiesel yield.

CONCLUSIONS

By employing response surface methodology in the ultrasound-assisted transesterification process, the existence of interactions among the factors and the results were successfully elucidated. A mathematical model was developed and it was able to accurately predict the biodiesel yield at any point in the range of the variables with a high level of significance (>99.99%). The coefficient of determination was found to be 95.25. The optimum conditions were obtained at 9.2 for the methanol to oil ratio, 1.6 wt% for the catalyst loading, 30.2 min for the reaction time, and 69.7% for the ultrasonic amplitude to give the best biodiesel yield of 80.2%.

REFERENCES

Benjapornkulaphong, S., Ngamcharussrivichai, C., and Bunyakiat, K. 2009. Al_2O_3 supported alkali and alkali earth metal oxides for transesterification of palm kernel oil and coconut oil. *Chem. Eng. J.* 145:468–474.

Georgogianni, K. G., Katsoulidis, A. P., Pomonis, P. J., and Kontominas, M. G. 2009. Transesterification of soybean frying oil to biodiesel using heterogeneous catalysts. *Fuel Process. Technol.* 90:671–676.

Kawashima, A., Matsubara, K., and Honda, K. 2009. Acceleration of catalytic activity of calcium oxide for biodiesel production. *Bioresour. Technol.* 100:696–700.

Li, X., Lu, G., Guo, Y., Wang, Y., Zhang, Z., and Liu, X. 2007. A novel solid superbase of Eu_2O_3/Al_2O_3 and its catalytic performance for the transesterification of soybean oil to biodiesel. *Catal. Commun.* 8:1969–1972.

Liu, X., He, H., Wang, Y., and Zhu, S. 2007. Transesterification of soybean oil to biodiesel using SrO as a solid base catalyst. *Catal. Commun.* 8:1107–1111.

Meher, L. C., Sagar, D. V., and Naik, S. N. 2006. Technical aspects of biodiesel production by transesterification—A review. *Renewable Sustainable Energy Rev.* 10:248–268.

Montgomery, D. C. 2001. *Design and Analysis of Experiments*, 5 Ed. New York: John Wiley & Sons.

Mootabadi, H., Salamatinia, B., Bhatia, S., and Abdullah, A. Z. 2010. Ultrasonic-assisted biodiesel production process from palm oil using alkaline earth metal oxides as the heterogeneous catalysts. *Fuel* 89:1818–1825.
Ryan, T. P. 2007. *Modern Experimental Design*. Hoboken, NJ: John Wiley & Sons.
Salamatinia, B., Mootabadi, H., Bhatia, S., and Abdullah, A. Z. 2010. Optimization of ultrasonic-assisted heterogeneous biodiesel production from palm oil: A response surface methodology approach. *Fuel Process. Technol.* 91:441–448.
Santos, F. F. P., Rodrigues, S., and Fernandes, F. A. N. 2009. Optimization of the production of biodiesel from soybean oil by ultrasound assisted methanolysis. *Fuel Process. Technol.* 90:312–316.
Xie, W., Peng, H., and Chen, L. 2007. Transesterification of soybean oil catalyzed by potassium loaded on alumina as a solid-base catalyst. *Appl. Catal., A* 300:67–74.

UNIVERSITI SAINS MALAYSIA

Pejabat Pendaftar

Office of The Registrar

Kampus Kejuruteraan
(Engineering Campus)
Universiti Sains Malaysia
14300 Nibong Tebal
Pulau Pinang, Malaysia
Tel : 04-5995999
www.usm.my

Our Ref. : USM/KKJ. 9/5

Date : 2 November 2012

Dr. Shazia Sultana
Biofuel & Biodiversity Lab.
Department of Plant Sciences
Quaid-i-Azam University
Islamabad
Pakistan - 45320

Dear Dr. Shazia Sultana,

APPOINTMENT AS POST-DOCTORAL FELLOW

I am pleased to inform you that Universiti Sains Malaysia has agreed to your appointment as a Post-Doctoral Fellow as prescribed below :

i. Honorarium	:	MYR6,173.47 per month
ii. Duration	:	One(1) year commencing from the date you report for duty
iii. Project Coordinator	:	**Associate Professor Ahmad Zuhairi Abdullah,** School of Chemical Engineering.
iv. Project Title	:	"Application of Ultrasonic Irradiation Technology for Biodiesel Production from Non-edible Oil"

2. The above appointment shall be subjected to the University rules and regulations as prescribed from time to time.

3. **Medical Benefits :** During your period of appointment, you may seek medical attention for yourself only at the University's Wellness Centre (*Pusat Sejahtera*)/HUSM. However should you require further medical attention in any other hospital, kindly take note that all expenses will be borne by you. You are advised to take up a medical insurance in Malaysia paid by yourself.

4. **Passage Assistance:** The University will provide you with return air passage assistance once during your period of appointment from your permanent/current place of residence whichever is lower to Penang. You can make arrangement for a Malaysia Airlines (MAS) economy class air ticket on the most direct and cheapest route and reimbursement claims will be process after you report for duty. Return air passage will be provided upon the completion of your attachment with the University.

5. The appointment is also subjected to the following conditions:-

(a) The necessary Employment Pass is approved and obtained from the Immigration Department. Please fill in the necessary forms and return to this office as soon as possible.

(b) You are medically certified to be fit. You are required to undergo a medical examination (on your own expenses) and submit the report which is attached herewith direct to this office.

International Journal of Green Energy (2015) 12, 1066–1075
Copyright © Taylor & Francis Group, LLC
ISSN: 1543-5075 print / 1543-5083 online
DOI: 10.1080/15435075.2014.891220

Taylor & Francis
Taylor & Francis Group

Distaff Thistle Oil: A Possible New Non-Edible Feedstock for Bioenergy

MUSHTAQ AHMAD[1,2], SHAZIA SULTANA[1,2], LEE KEAT TEONG[1], AHMAD ZUHAIRI ABDULLAH[1], HALEEMA SADIA[2], MUHAMMAD ZAFAR[2], TAIBI BEN HADDA[3], MUHAMMAD AQEEL ASHRAF[4], and RASOOL BAKHSH TAREEN[5]

[1]*School of Chemical Engineering, University of Sains Malaysia, Nibong Tebal, Penang, Malaysia*
[2]*Biofuel Lab. Department of Plant Sciences, Quaid-i-Azam University, Islamabad, Pakistan*
[3]*Laboratoire Chimie Matériaux, Faculté des Sciences d'Oujda, Université Mohammed Premier, Oujda, Morocco*
[4]*Department of Geology, University of Malaya, Malaysia*
[5]*Department of Botany, University of Baluchistan, Pakistan*

The present work examines the production of biodiesel from distaff thistle (Carthamus lanatus L.) using alkali catalyzed transesterification. The low acid value (0.14 mg KOH/g) and free fatty acid (FFA) contents (2.81%) of distaff thistle oil (DTO) determined prior to transesterification indicated that the pretreatment of raw oil with acid is not required for biodiesel synthesis. The optimum operating reaction conditions of methanol to oil molar ratio (5:1), catalyst concentration (0.64%) and temperature (60°C) were applied during the transesterification to obtain the highest biodiesel yield of 97%. We have determined various fuel properties of distaff thistle oil biodiesel (DTOB) including kinematic viscosity (5.85@ 40°C c St), acid value (0.14 mg KOH/g), density (0.8980@40°C Kg/L), cetane number (50), flash point (126°C), cloud point (10°C), pour point (15°C) and distillation characteristics (358 @ 90% recovery °C). The values of fuel properties were found to be comparable with mineral diesel and in agreements with ASTM biodiesel standards. In addition to this, the synthesized fatty acid methyl esters (FAMEs) were confirmed and characterized by Gas chromatography-Mass spectroscopy (GC-MS), Fourier transform-Infra red (FT-IR), ^{1}H NMR (Nuclear magnetic resonance) and ^{13}C NMR analyses. Our results conclude that DTO appears to be an acceptable new non-edible oil feedstock for biodiesel industry.

Keywords: Non-edible oil, distaff thistle plant, biodiesel, fuel properties, FAMEs characterization

Introduction

Synthesis and use of biodiesel as an alternate fuel using transesterification of vegetable oils, animal fats and used frying oil mainly consisting of triglyceride converting into the corresponding mono-alkyl esters has increased significantly in recent years. In addition, the advantages of biodiesel as compared to petro-diesel may include reduction in exhaust emissions, improved biodegradability, inherent lubricity, higher flash point, and domestic origin (Knothe, Krahl, and Van Gerpen 2005).

However, many questions arise concerning the raw material used for synthesis of biodiesel and its cost. It is only during 2008 the very peaks of the oil spike that biodiesel was able to approach the cost of petro-diesel. Of this cost, about 60–85% comes from the feedstock. Legitimate concerns have also been raised about the possible effect of using vegetable oils for fuel on food prices (Trostle 2008). Capacity expansion may lead to a decrease in the availability of land for food crops along with the overall negative effect on climate change. The enormous demand for diesel fuel dwarfs the available supply of vegetable oils. The global production of palm, soybean, rapeseed, sunflower, peanut, cottonseed, palm kernel, coconut, linseed, maize, safflower and olive oil (the top 12 vegetable oils) in 2006 was about 125 600 000 metric tons. In contrast, the total consumption of diesel fuel by the transportation industry in the same year was about 693 000 000 metric tons. Thus, even if all of the vegetable oils produced in the world in 2006 were converted to biodiesel, this would fill only about 18% of the total demand in the same year for the transportation industry alone. It is necessary that feedstock production must increase dramatically if biodiesel is to have any real positive impact to solve the energy crises. The issues of an alternative feedstock has been studied and reviewed recently from several different viewpoints (Canakci and Sanli 2008; Moser 2009).

A considerable amount of research has been conducted on alternative feedstock for biodiesel production mainly using non-edible oils seeds including castor bean, pongame, jatropha, tiger nut oil, safflower, wild safflower, etc. (Ugheoke at al. 2007; Ahmad et al. 2009; Sadia et al. 2013). However in all these investigations, every effort has been made to make the feedstock acceptable while to best of our knowledge by reviewing literature,

Address correspondence to Shazia Sultana, School of Chemical Engineering, University of Sains Malaysia, Nibong Tebal, Penang, Malaysia, 14300 and Biofuel Lab. Department of Plant Sciences, Quaid-i-Azam University, Islamabad, Pakistan 45320. E-mail: shaziaflora@hotmail.com
Color versions of one or more of the figures in the article can be found online at www.tandfonline.com/ljge.

Original article

Nutrient and mineral assessment of edible wild fig and mulberry fruits

Haleema Sadia[1], Mushtaq Ahmad[1,2], Shazia Sultana[1,2*], Ahmad Zuhairi Abdullah[2], Lee Keat Teong[2], Muhammad Zafar[1], Asghari Bano[1]

[1] Dep. Plant Sci., Quaid-i-Azam Univ., Islamabad, 45320, Pakistan, shaziaflora@hotmail.com

[2] School Chem. Eng., Univ. Saina Malaysia, 14300, NibongTebal, Penang, Malaysia

* Correspondence and reprints

Received 18 April 2013
Accepted 23 July 2013

Fruits, 2014, vol. 69, p. 1–8

DOI: 10.1051/fruits/2014006
www.fruits-journal.org

Resumen Español, p. 8

Nutrient and mineral assessment of edible wild fig and mulberry fruits.

Abstract – Introduction. Edible wild plants are nature's gift to mankind. Considering the growing need to identify alternative bio-nutritional sources, some underutilized species of figs (*Ficus carica* L., *F. palmata* Forssk., *F. racemosa* L.) and mulberries (*Morus alba* L., *M. nigra* L, *M. laevigata* Wall.) of the family Moraceae were evaluated as wild edible fruits to study their nutritive and mineral composition in order to prioritize their edibility for indigenous people. **Materials and methods.** The major proximal components (moisture, ash, lipids, proteins, fibers and carbohydrates) were determined by standard AOAC methods. The concentration of various minerals (K, Ca, Mg and Na) and trace elements (Fe, Mn, Zn, Cu and Ni) were recorded by using an atomic absorption spectrophotometer. **Results.** Our results indicated a range of moisture contents from 17.82–80.37 g·100 g^{-1} (fresh weight basis) in *F. carica-M. laviegata*; protein, 6.31–13.50 g·100 g^{-1} (dry weight basis) in *F. glomerata-M. alba*; crude fats, 1.02–2.71 g·100 g^{-1} in *F. palmate-F. glomerata*; carbohydrates 69.47–75.58 g·100 g^{-1} in *M. alba-M. nigra*; and fiber 7.63–17.81 g·100 g^{-1} in *M. laviegata-F. palmate*, respectively. The significantly highest energy value was computed in *M. laviegata* (367.7 kcal·100 g^{-1}). Moreover, sufficient quantities of essential elements were found in all the studied materials. The highest levels of N [(0.24 ± 0.07) mg·g^{-1}] and Fe [(1.43 ± 0.42 mg·g^{-1}] were found in *M. laviegata*; Na [(1.92 ± 0.11 mg·g^{-1}] and Mg [(6.92 ± 0.37 mg·g^{-1}] in *F. palmate*; and K [(17.21 ± 0.03 mg·g^{-1}] in *F. glomerata*. Significant variation existed among the selected species in all the nutritional parameters. **Conclusion.** According to our results, fig and mulberry fruits are recommended for commercial-scale production for the green industry to overcome food crises as they are potential food sources, particularly *Morus laviegata* and *Ficus palmata*, with rich nutritional attributes and mineral profiles.

Pakistan / *Morus* / *Ficus* / fruits / proximate composition / mineral content

Évaluation des nutriments et des ressources minérales des fruits de figuiers et de mûrier sauvages comestibles.

Résumé – Introduction. Les plantes sauvages comestibles sont un don que fait la nature à l'humanité. Considérant le besoin croissant d'identifier de nouvelles sources de bio-nutrition, certaines espèces sous-utilisées de figuiers (*Ficus carica* L., *F. palmata* Forssk., *F. racemosa* L.) et de mûriers (*Morus alba* L., *M. nigra* L, *M. laevigata* Wall.) de la famille des Moraceae ont été évaluées en tant que fruits sauvages comestibles pour étudier leur composition nutritive et minérale afin de prioriser leur consommation auprès des populations autochtones. **Matériel et méthodes.** La composition globale des fruits étudiés (humidité, cendres, lipides, protéines, fibres et glucides) a été déterminée par utilisation de méthodes AOAC standards. La concentration en divers minéraux (K, Ca, Mg et Na) et en oligo-éléments (Fe, Mn, Zn, Cu et Ni) a été déterminée en utilisant un spectrophotomètre d'absorption atomique. **Résultats.** Nos résultats ont révélé une gamme de teneurs en humidité de 17,82–80,37 g·100 g^{-1} (poids frais) pour *F. carica-M. laviegata* ; en protéines, de 6,31–13,50 g·100 g^{-1} (poids sec) pour *F. glomerata-M. alba* ; en graisses brutes, de 1,02–2,71 g·100 g^{-1} pour *F. palmate-F. glomerata* ; en glucides, de 69,47–75,58 g·100 g^{-1} pour *M. alba-M. nigra* ; en fibres, de 7.63–17,81 g·100 g^{-1} pour *M. laviegata-F. palmate*, respectivement. Une valeur énergétique significativement élevée a été calculée pour *M. laviegata* (367,7 kcal·100 g^{-1}). En outre, des quantités non négligeables d'éléments essentiels ont été trouvées chez toutes les espèces étudiées. Les plus hauts niveaux de N [(0,24 ± 0,07) mg·g^{-1}] et Fe [(1,43 ± 0,42 mg·g^{-1}] ont été trouvés dans *M. laviegata* ; de Na [(1,92 ± 0,11 mg·g^{-1}] et Mg [(6,92 ± 0,37 mg·g^{-1}], dans *F. palmate* ; et K [(17,21 ± 0,03 mg·g^{-1}], dans *F. glomerata*. Des variations significatives sont apparues entre les espèces étudiées pour tous les éléments nutritionnels. **Conclusion.** Selon nos résultats, les fruits de figuiers et de mûriers devraient être recommandés à l'échelle d'une production commerciale pour l'industrie verte afin de surmonter les crises alimentaires en tant que source potentielle en alimentation quotidienne, particulièrement les fruits de *Morus laviegata* et *Ficus palmata* qui ont de riches propriétés nutritionnelles et profils minéraux.

Pakistan / *Morus* / *Ficus* / fruit / composition globale / teneur en éléments minéraux

International Journal of Green Energy (2015) 12, 447–452
Copyright © Taylor & Francis Group, LLC
ISSN: 1543-5075 print / 1543-5083 online
DOI: 10.1080/15435075.2013.841165

Taylor & Francis
Taylor & Francis Group

Optimization of Biodiesel Production from *Carthamus Tinctorius* L. *CV*.Thori 78: A Novel Cultivar of Safflower Crop

MUSHTAQ AHMAD[1,2], LEE KEAT TEONG[1], SHAZIA SULTANA[1,2], INAM ULLAH KHAN[2], AHMAD ABDULLAH ZUHAIRI[1], MUHAMMAD ZAFAR[2], and FAYYAZ-UL HASSAN[3]

[1]*School of Chemical Engineering, Universiti Sains Malaysia, Nibong Tebal, Malaysia*
[2]*Department of Plant Sciences, Quaid-i-Azam University, Islamabad, Pakistan.*
[3]*Department of Agronomy, PMAS-Arid Agriculture University, Rawalpindi, Pakistan*

In the present work, the potential of novel cultivar of safflower seed crop with highest 52% oil contents is evaluated for the first time as a feedstock for biodiesel synthesis. The specific aim of this study was to optimize the transesterification process for maximum biodiesel yield using different parameters and to evaluate its fuel compatibility with mineral diesel. Fatty acid methyl esters (FAMEs) of safflower oil were produced by standard transesterification process using potassium hydroxide (KOH) as catalyst. Optimum biodiesel yield of 98% achieved at 65°C, 5:1 methanol: oil molar ratio, 0.32 g catalyst concentration, and reaction time of 80 min. The kinematic viscosity@ 40°C (cSt), flash point, sulfur contents (wt%), pour point and cloud point of pure safflower oil biodiesel (SOB) were found to be 5.32 mm^2/s, 80°C, 0.00041%, –9°C and –11°C, respectively. These together with other fuel parameters were in accordance with ASTM standards. The results obtained indicate that SOB appears to be the potential feedstock for biodiesel production and can be used as an alternate source of fuel in diesel engines.

Keywords: Biodiesel, Optimization, Variables, Novel cultivar, Safflower oil, Fuel properties

1. Introduction

Currently, the petroleum fuel, diesel, and natural gas resources are depleting rapidly due to their high consumption by the fast population growth and technology in world (Ahmad et al. 2007). The world is now looking for alternate sources of renewable energies like biomass, solar, and wind that are environmentally friendly (Patil and Deng 2009). In various forms of biomass energy, the biodiesel is considered to be one of the good option for its use in transport industry as substitute of diesel fuel. While in current scenario, the biodiesel mainly comes from edible oil feedstock which create problems like increased cost of edible oils, biodiesel, and non-availability of edibles to poor nations which increase world poverty level high (Gui, Lee, and Bhatia 2008; Kansedo, Lee, and Bhatia 2009). Meanwhile the scientists, agriculturists, policy makers, and industrialists are in search to explore alternate source of raw material for biodiesel synthesis e.g., non-edible oil seeds or edible oil seeds with surplus production with multipurpose usage. Non-edible oil seed resources possess high adaptability toward the waste land with sustained high yield of oil with lower cost production (Hirsinger 1989; Kumar et al. 2007). Among these, safflower plant with high seed oil contents is considered to be one of the good options as an alternate feed-stock material for biodiesel production (Vilatersana et al. 2000).

Safflower plant belongs to the family Asteraceae and is branched herb with flower heads containing 15 to 20 seeds per head. This crop is native to arid part of the world with deep taproot system which enables it to thrive in such environments. It is cultivated mainly on marginal land since ancient times for dye extraction form its flowers and ornamental purposes (Pourdad and Mohamadi 2008). According FAO report, the total area in the world for safflower cultivation is estimated to be about 814,000 ha (Fan, Burton, and Austic 2010), production is about 600,000 tons per year (Gyulai 1996) and among 20 cultivated countries India contributes 210,000 million tones and Mexico 212,765 million tone which is more than half of the world's total production (Mohamadi et al. 2007). The safflower is investigated recently as one of the optional crop for biodiesel production at global perspectives which shows promising results for the biodiesel production (Rashid and Anwar, 2008). This oil seed crop has been reported to constitute 96–99% linoleic acid, oleic acid, palmatic acid, and stearic acid of the total fatty-acids contents (Cosge, Gurbuz, and Kiralan 2007; Mohammad et al. 2008). In current scenario the agriculturists, farmers, breeders, and industrialists are in search of new oil seed crops as raw material for biodiesel production. In addition, researchers are developing certain new crops with high oil content just for the production of biodiesel. Therefore, it would be very useful to look for new raw sustainable materials for biodiesel production that do not involve the use of cereals. In this regard, various cultivars of oil seed crops are introduced in different parts of the world for this

Address correspondence to Shazia Sultana, School of Chemical Engineering, Universiti Sains Malaysia, Nibong Tebal, 14300, Malaysia and Department of Plant Sciences, Quaid-i-Azam University, Islamabad, 45320, Pakistan. E-mail: shazia@qau.edu.pk

Applied Energy 113 (2014) 660–669

Contents lists available at ScienceDirect

Applied Energy

journal homepage: www.elsevier.com/locate/apenergy

Experimental analysis of di-functional magnetic oxide catalyst and its performance in the hemp plant biodiesel production

Kifayat Ullah [a,b,*], Mushtaq Ahmad [a,c], Shazia Sultana [a,c], Lee Keat Teong [c], Vinod Kumar Sharma [b], Ahmad Zuhairi Abdullah [c], Muhammad Zafar [a], Zahid Ullah [a]

[a] Biofuel & Biodiversity Lab, Department of Plant Sciences, Faculty of Biological Sciences, Quaid-i-Azam University, 45320 Islamabad, Pakistan
[b] ENEA/ICTP Research Centre Trisaia, 75026 Rotondella, MT, Italy
[c] School of Chemical Engineering, Universiti Sains Malaysia, Nibong Tebal 14300, Penang, Malaysia

HIGHLIGHTS

- Di-functional magnetic oxide catalyst preparation for hemp oil biodiesel synthesis.
- Catalyst re-usability & characterization via XRD, TG–DTA, SEM & VSM analyses.
- Reduction of FFA contents 47.15–1.01 mg KOH/g through esterification.
- Maximum of 92.16% biodiesel yield under optimized operating conditions.
- Application of GC–MS, FT–IR & NMR techniques for biodiesel characterization.

ARTICLE INFO

Article history:
Received 27 September 2012
Received in revised form 26 June 2013
Accepted 7 August 2013

Keywords:
Hemp oil
Di-functional magnetic catalyst
Fatty acid methyl ester
Re-usability
Stability

ABSTRACT

This paper reports a study on the performance assessment of di-functional magnetic Fe–Ca oxide catalyst in biodiesel production using hemp oil. In situ co-precipitation procedure was used for synthesis of di-functional magnetic solid base catalyst. The resultant catalyst had good magnetic property with relatively high saturation magnetism (45.6 emu/g) and the reused catalyst status is quite functional. The catalyst was characterized using various techniques including XRD, TG–DTA, SEM and VSM. The produced biodiesel was characterized and conformed by GC/MS, NMR and FT/IR. The synthesis of biodiesel was carried out at constant temperature (60 °C), reaction time (2 h) oil alcohol molar ratio (1:6), agitation (600 rpm) and catalyst concentration (2.25%) w/w. The maximum biodiesel yield was achieved 92.16% using di-functional magnetic Fe–Ca oxide catalyst.

1. Introduction

Energy and, in particular the clean energy, is certainly an important scientific topic that needs special attention by the scientific community worldwide and, more so, in the context of the developing countries. Many developing countries rely primarily on biomass resources to fulfill their energy needs in some context (e.g. palm oil in Malaysia and sugar cane in Brazil).

Currently, biofuels are gaining considerable public and scientific attention, driven by factors such as oil price hikes, the need for increased energy security, concern over greenhouse gas emissions using fossil fuels, etc. Meantime, the major challenge faced by biofuel industry in world is the competition with food crops as the main raw feedstock used currently is the edibles. The world is now looking for non-edible feedstock for this industry and similarly valorization of agro-waste from bio-based industry, is believed to be the promising raw material for the countries' building a sustainable bio-based industry for tomorrow. In continuity of such efforts to explore alternative non-edible oil feedstock for biodiesel production, in this study, we have focused on hemp seed oil to be used as potential raw feedstock for biodiesel synthesis using heterogeneous solid catalyst.

The use of a heterogeneous catalyst for transesterification of triglycerides to fatty acid methyl esters (FAMEs) by methanol enables its simple isolation from the reaction mixture and good quality yield. The hemp filtered oil after transesterification reaction considered to be compatible with petro-diesel based on fuel properties as discussed in previous literature. Development of di-functional catalysts (capable of performing two or more distinct conversions) involved in moving from plant to product without sacrificing

* Corresponding author at: Biofuel & Biodiversity Lab, Department of Plant Sciences, Faculty of Biological Sciences, Quaid-i-Azam University, 45320 Islamabad, Pakistan. Tel.: +92 3339328026.

0306-2619/$ - see front matter © 2013 Elsevier Ltd. All rights reserved.
http://dx.doi.org/10.1016/j.apenergy.2013.08.023

International Journal of Green Energy, 11: 280–291, 2014

ISSN: 1543-5075 print / 1543-5083 online
DOI: 10.1080/15435075.2013.772520

THE PRODUCTION, OPTIMIZATION, AND CHARACTERIZATION OF BIODIESEL FROM A NOVEL SOURCE: *Sinapis alba* L.

Shazia Sultana[1,2], Aneela Khalid[2], Mushtaq Ahmad[1,2], Ahmad Abdullah Zuhairi[1], Lee Keat Teong[1], Muhammad Zafar[2], and Fayyaz ul Hassan[3]

[1]*School of Chemical Engineering, Universiti Sains Malaysia, Nibong Tebal, Penang, Malaysia*
[2]*Biofuel Laboratory, Department of Plant Sciences, Quaid-i-Azam University, Islamabad, Pakistan*
[3]*Department of Agronomy, PMAS Arid Agriculture University, Rawalpindi, Pakistan*

In this study, biodiesel is prepared from Sinapis alba L. oil commonly known as white mustard through transesterification of the crude oil with methanol in the presence of NaOH as catalyst. Optimum conditions for the reaction were established to achieve maximum biodiesel yield of 92% at 6:1 molar ratio (methanol to oil), by using 0.5 g of NaOH, reaction temperature 65°C, and reaction time 75 minutes. Sinapis alba oil biodiesel (SAOB) was testified by using various fuel properties such as kinematic viscosity at 40°C (5.45 cSt), density at 15°C (0.8721 kg/L), acid number (0.242 mg KOH/gm), flash point (90°C), cloud point (−10°C), pour point (−13°C), and sulfur contents (0.00432%). Based on these findings, it is stated that SAOB can be used as alternative fuel in diesel engines.

Keywords: *Optimization; Characterization; Biodiesel;* Sinapis alba

INTRODUCTION

The significance of energy cannot be denied by the humanity as it is a vital input for social and economic development especially after the induction of the industrial revolution in the late 18th and early 19th century. In current era of energy crisis and shortage of petroleum fuel, the world is looking for alternative resources like biofuel. The production of biofuel is anticipated to rise gradually in the coming few decades (Fukuda, Kondo, and Noda 2001). Biodiesel is currently seeking massive attention in different countries all around the globe because of its ecofriendly nature, renewability, non-toxicity, availability, better gas emissions, and its biodegradability. Biodiesel is preferred because it has higher flash point, ultra-low sulfur concentration, better lubricating efficiency, and better cetane number (Joshi and Pegg 2007; Demirbas 2009a,b).

Address correspondence to Muhammad Zafar, Biofuel Laboratory, Department of Plant Sciences, Quaid-i-Azam University, Islamabad, 45320 Pakistan. E-mail: catlacatla@hotmail.com

UNIVERSITI SAINS MALAYSIA

Tarikh : 9 Mac 2015

Bahagian Penyelidikan dan Inovasi
Division of Research and Innovation

Memorandum

Universiti Sains Malaysia
Aras 6, Bangunan Canselori
11800, USM Pulau Pinang, Malaysia
T : (6)04-653 3108/3178/3988/5019
F : (6)04-656 6466/8470
: (6)04-653 2350
L : www.research.usm.my
www.usm.my

Profesor Dr. Ahmad Zuhairi Abdullah
Pusat Pengajian Kejuruteraan Kimia
Universiti Sains Malaysia
Kampus Kejuruteraan

Tuan,

KEPUTUSAN PERMOHONAN SKIM GERAN PENYELIDIKAN TRANSDISIPLINARI (TRGS) FASA 2/2014

TAJUK PROGRAM : ***PRODUCTION OF VALUABLE CHEMICALS FROM CRUDE GLYCEROL USING CATALYTIC AND BIOCHEMICALS METHODS***
JUMLAH PROJEK : **3**
JUMLAH PERUNTUKAN : **RM755,600.00 (KESELURUHAN PROGRAM)**

Dengan segala hormatnya perkara di atas adalah dirujuk.

2. Tahniah diucapkan di atas kejayaan tuan memperolehi geran TRGS Fasa 2/2014 di bawah Kementerian Pendidikan Malaysia (KPM) sebagai **Ketua Program** seperti tajuk di atas. Berikut ialah butiran penting berkaitan projek beserta nombor akaun untuk rujukan dan tindakan oleh pihak tuan.

Ketua Program	Profesor Dr. Ahmad Zuhairi Bin Abdullah	PTJ	Pusat Pengajian Kejuruteraan Kimia
Penyelidik bersama	1. Profesor Dr. Farook Adam 2. Prof. Madya Dr. Mohd Roslee Othman 3. Dr. Melati Khairuddean	PTJ	1. Pusat Pengajian Sains Kimia 2. Pusat Pengajian Kejuruteraan Kimia 3. Pusat Pengajian Sains Kimia
No. Akaun	**203 / PJKIMIA / 6762001**		
Tajuk Projek	*Mesoporous Composite Catalyst for Conversion of Purified Crude Glycerol to Lactic Acid*		
Tempoh Projek	36 bulan	Jumlah Peruntukan	**RM311,200.00**
Tarikh Mula	1 Februari 2015	Tarikh Tamat	31 Januari 2018

TRANSESTERIFICATION OF CRUDE JATROPHA OIL BY ULTRASOUND-ASSISTED PROCESS IN THE PRESENCE OF HETEROPOLYACID BASED CATALYSTS

ALI SABRI BADDAY

UNIVERSITI SAINS MALAYSIA
2013

TRANSESTERIFICATION OF CRUDE JATROPHA OIL BY ULTRASOUND-ASSISTED PROCESS IN THE PRESENCE OF HETEROPOLYACID BASED CATALYSTS

by

ALI SABRI BADDAY

Thesis submitted in fulfillment of the requirements
for the degree of
Doctor in Philosophy

August 2013

TRANSESTERIFICATION OF CRUDE JATROPHA OIL BY ULTRASOUND-ASSISTED PROCESS IN THE PRESENCE OF HETEROPOLYACID BASED CATALYSTS.

ABSTRACT

The current research work research work focused on the investigation of FAME production from high FFA and water content crude Jatropha oil through an ultrasound-assisted process. The ultrasonic energy was invested to overcome the barrier of poor contact between the oil and methanol due to the immiscible nature of them reducing the required reaction time and temperature. New heterogeneous acid catalysts based on heteropoly acid were synthesized, characterized and used in the transesterification reaction. Tungstophosphoric acid (TPA) was immobilized on activated carbon (AC) and gamma alumina (Al) or converted to its cesium (Cs) salt to improve its resistance against the solubility in the polar reaction media. Different TPA loadings on the supports and various molar ratios of cesium to TPA were studied and characterized. TPA20-AC, TPA25-Al and Cs salt with molar ratio of 1.5 were used in the investigation of the optimum reaction conditions with the aid of design of experiments software (DOE). Four reaction variables including reaction time (10-50 min), reactants molar ratio (5:1-25:1), ultrasonic amplitude (30-90 %) and catalyst amount (2.5-4.5 w/w oil) were chosen and optimized to generate thorough understanding on the behavior of the system under ultrasonic conditions. The catalysts were also investigated for possible reusability and leaching phenomenon under ultrasonic conditions. The reactions were mostly heterogeneous in nature and the TPA supported on Al and Cs salt catalysts showed minimal reduction in the activity after three successive reaction runs under the optimum

reaction conditions. The catalyst of Cs showed the activity of ~ 90% of FAME yield and the greatest potential of reusability within a reaction temperature of 65 ^{O}C in just 34 min. The catalysts were further investigated for transesterification of different non-edible oils and tested in high FFA and water content systems and they generally showed promising results. The reaction kinetics was investigated and the tracing of FFA and water contents during the reaction course proved that the catalysts were able to accelerate both esterification of FFA and transesterification of triglycerides simultaneously.

ACID-BASE BIFUNCTIONALIZED HYDROTALCITE CATALYST FOR BIODIESEL PRODUCTION FROM WASTE COOKING OIL USING ULTRASOUND-ASSISTED REACTOR SYSTEM

MOHD.RAZEALY ANUAR

UNIVERSITI SAINS MALAYSIA
2016

ACID-BASE BIFUNCTIONALIZED HYDROTALCITE CATALYST FOR BIODIESEL PRODUCTION FROM WASTE COOKING OIL USING ULTRASOUND-ASSISTED REACTOR SYSTEM

by

MOHD.RAZEALY ANUAR

Thesis submitted in fulfillment of the requirements

for the degree of

Doctor in Philosophy

May 2016

ACID-BASE BIFUNCTIONALIZED HYDROTALCITE CATALYST FOR BIODIESEL PRODUCTION FROM WASTE COOKING OIL USING ULTRASOUND-ASSISTED REACTOR SYSTEM

ABSTRACT

Fossil fuel depletion is a current worrisome problem. In tandem with such problem, research on advanced technology for biodiesel production is of global concern. Currently, research on biodiesel production from non-edible oils is gaining popularity. However, non-edible oils such as waste cooking oil contain high amount of free fatty acid (FFA) and moisture. Besides, the use of conventional mechanical stirring method is not efficient and often requires longer reaction time. Thus, this research work is focused on the development of an advanced catalytic fatty acid methyl ester (FAME) production from waste cooking oil using an ultrasound-assisted system. Hydrotalcite (HT) catalyst prepared using combustion method was employed with some structural modification in order to develop acid-base bifunctionalized HT. The acid-base bifunctionalized HT was meant to be beneficial in conducting simultaneous transesterification and esterification reaction. The use of ultrasound-assisted system might overcome the emulsification and mass transfer limitations due to immiscibility of oil and alcohol. Hence, reaction time could be significantly shortened. Two important parameters to synthesize MgAl based HT i.e. calcination temperature (550 °C–850 °C) and fuel type (saccharose, glucose and fructose) were particularly investigated. Alteration on MgAl based HT structure was done by introducing second divalent metals (nickel, copper and zinc). The amphoteric properties of these transition metals successfully resulted in bifunctional acid-base

properties of HT. The structural, crystallinity, surface morphology, thermal decomposition, bonding characteristics and acid strength of the synthesized HT were elucidated by several characterization techniques. The dependence of HT's characteristics on the synthesis parameters and correlations with their catalytic performance under ultrasound condition were successfully studied. The MgAl based HT catalyst prepared using saccharose and calcined at 650 °C showed high biodiesel yield (about 76.45 %) in just 60 minutes in the presence of low ultrasound amplitude (~11 kHz). Meanwhile, HT introduced with 10 % nickel demonstrated the highest FAME yield of about 86.84 % in just 60 minutes. The simultaneous transesterification and esterification reactions were evidently demonstrated by carrying out the FFA test reaction. The FAME yield was found to increase due to the esterification of FFA to FAME. The HT catalyst synthesized was highly stable which was capable to perform several cycles of reaction with significantly low total FAME reduction (4.52 %) and with no significant leaching of active component. The optimization study successfully demonstrated effects of 4 independent reaction variables i.e. reaction time (30-90 min), methanol to oil ratio (7:1-23:1), amplitude (40-60 %) and catalyst amount (0.06-0.08 g catalyst/ g oil). A quadratic model is generated with 95.84 % of confidence level. The most reasonable optimum parameters with the smallest error (1.15 %) are identified. The quality of the obtained FAME was evaluated which conform to the ASTM D6751 and EN 14214 specifications. Lastly, kinetic study was also investigated and the apparent activation energy for the simultaneous transesterification and esterification reactions (73.11 kJ/mol) is lower than that of transesterification reaction (81.16 kJ/mol) to indicated accelerated reaction.